



UNIVERSITÀ  
DEGLI STUDI  
FIRENZE

# DOTTORATO DI RICERCA IN SCIENZE CHIMICHE

CICLO XXX

COORDINATORE Prof. Piero Baglioni

**Molecular, Macromolecular and Nanostructured Antioxidants**

Settore Scientifico Disciplinare CHIM/06

**Dottorando**

Dott. Lorenzo Tofani

**Tutore**

Prof. Stefano Menichetti

**Coordinatore**

Prof. Baglioni Piero

Anni 2014/2017



Compounds numbering restart for each chapter; each compound (c) number is preceded by the number of the chapter (ch) in which it is reported (e.g. **ch2-c3** indicates compound number 3 of chapter 2). All numbers relative to the same compound, when it appears in different chapters, are reported in the experimental section.

### List of Abbreviations

ATP	adenosine triphosphate
AuNPs	gold nanoparticles
AVEC	ataxia with vitamin E deficiency
BDE	bond dissociation enthalpy
BDE (OH)	bond dissociation enthalpy of the O-H bond
BHA	butyl hydroxy anisole
BHT	butyl hydroxy toluene
BnBr	benzyl bromide
BOP	(Benzotriazol-1-yloxy)tris(dimethylamino)phosphonium hexafluorophosphate
CB-A	chain-breaking acceptord
CB-D	chain-breaking donors
CoN3	<i>turbobeads click</i>
CoNH2	<i>turbobeads amine</i>
CoNPs	cobalt nanoparticles
CuAAC	Copper (I) catalyzed azide-alkyne cycloaddition
DBBA	3,5-di- <i>tert</i> -butyl-4-hydroxybenzyl acrylate
DCM	dichloromethane
DMAP	4-(Dimethylamino)pyridine
DMF	dimethylformamide
DMSO	dimethyl sulfoxide
ESI-MS	Electron Spray Ionization-Mass Spectroscopy
GMA	glycidyl methacrylate

HALS	hindered amine light stabilizers
HOBt	1-Hydroxybenzotriazole hydrate
IHB	Intramolecular Hydroge Bond
kinh	inhibition rate constant of the reaction $R-OH+R-OO \rightarrow R-O+ROOH$
LDPE	low-density polyethylene
MAO	methylaluminoxane
MNPs	metallic nanoparticles
MR	molar ratio
MRI	magnetic resonance imaginng
MS	molecular sieves
MS	mass spectrometry
NBO	Natural Bond Orbital
NMR	nuclear magnetic resonance
NMs	nanomaterials
PD	peroxyde decomposers
Pht	phthalimide
PhtNSCl	phthalimide sulfenyl chloride
PMC	2,2,5,7,8-pentamethylchroman-6-ol
<i>p</i> -TsOH	<i>para</i> -toluenesulfonic acid
rAOs	reactive antioxidants
RB	reactive blending
rpm	revolutions per minute
$S_EAr$	electrophilic aromatic substitution
SOD	superoxide dismutase
SOMO	single occupied molecular orbital
SPIONs	superparamagnetic iron oxide nanoparticles
T101	trigonox 101



TFA	trifluoroacetic acid
THF	tetrahydrofuran
TIBA	triisobutylaluminium
TLC	thin layer chromatography
TMSOTf	trimethylsilyl trifluoromethanesulfonate
TsCl	tosyl chloride
TTP	Tocopherol Transfer Protein
$\alpha$ -TOH	$\alpha$ -Tocopherol

## Index

1 Introduction.....	1
1.1 References.....	10
2 Vitamin E-like molecular antioxidants.....	12
2.1 Introduction.....	12
2.2 Results and discussion.....	22
2.2.1 Synthesis of phenolic derivatives.....	23
2.2.2 Synthesis of ortho-hydroxy-N-thiophthalimide derivatives.....	27
2.2.3 Synthesis of benzo[b][1,4]oxathiine derivatives.....	28
2.2.4 Transposition reaction of benzo[b][1,4]oxathiine derivatives.....	30
2.2.5 Antioxidant activity of dihydro- and benzo[b]thiophenes.....	43
2.2.6 Binding affinity of $\alpha$ -TTP for benzo[b]thiophenes.....	44
2.3 Experimental Section.....	48
2.4 References.....	77
3 Polymeric antioxidants.....	82
3.1 Introduction.....	82
3.2 Non-releasing antioxidants for polyolefins stabilization.....	109
3.2.1 Non-releasing polymeric antioxidants.....	110
3.3 Results and Discussion.....	116
3.3.1 Synthesis of BHT-like comonomers for the copolymerization with polyolefins.....	116
3.3.2 Synthesis of BHT-like comonomers for the reactive blending.....	124
3.4 Terpolymeric antioxidant additives.....	127
3.4.1 Introduction.....	127
3.4.2 Ethylene/1-hexene/16 terpolymers.....	130

3.4.2.1 Synthesis and characterization .....	130
3.4.2.2 Blends with the LDPE matrix.....	132
3.4.2.3 Thermal and thermo-oxidative stability tests.....	132
3.4.2.4 Thermo-ageing tests.....	134
3.4.3 Ethylene/Norbornene/16 terpolymers .....	135
3.4.3.1 Synthesis and characterization .....	135
3.4.3.2 Blends with the COC matrix.....	137
3.4.3.3 Thermal and thermo-oxidative stability tests.....	137
3.4.3.4 Thermo-ageing tests.....	140
3.5 Experimental section.....	141
3.6 References .....	154
4. Free Radical grafting of reactive antioxidants on polyethylene.....	164
4.1 Introduction.....	164
4.2 Results and Discussion .....	172
4.2.1 Characterization of UF-AO and grafting on polyethylene (PE) .....	172
4.2.2 Long-term thermo-oxidative stability studies. ....	184
4.2.3 Grafting in the presence of a reactive coagent.....	190
4.3 Experimental section.....	195
4.4 References .....	196
5. Nanostructured antioxidants.....	198
5.1 Introduction.....	198
5.2 Results and Discussion .....	203
5.2.1 Synthesis of antioxidant derivatives for the functionalization of gold nanoparticles (AuNPs).....	203
5.2.2 Synthesis of antioxidant derivatives for the functionalization of superparamagnetic iron oxide nanoparticles (SPIONs) .....	213

5.2.3 Synthesis of antioxidant derivatives for the functionalization of cobalt nanoparticles (CoNPs).....	220
5.2.3.1 Evaluation of the antioxidant activity of CoNPs-AntiOx.....	229
5.2.4 Conclusions and possible applications .....	231
5.3 Experimental Section .....	233
5.4 References .....	257
6. Conclusions.....	267

## Abstract

During the past decades, the key role of Reactive Oxygen Species (ROS) in different pathologies has been indicated to take part to many physiological and pathological processes including aging, cancer, neurodegenerative and cardiovascular diseases. The role of ROS is not delimited inside living organisms, but affects also synthetic polymers limiting their commercial use. Indeed, common polymers like polyolefins are subjected to deterioration by oxygen-promoted oxidative processes both during processing and end-use conditions. In biological systems the detrimental action of free radicals is continuously balanced by the action of specific enzymes and dietary antioxidants able in transforming ROS in non-oxidant species. The oxidative degradation of polymers is generally prevented or retarded by adding low concentration (0.05-0.5 wt%) of antioxidants, such as hindered phenols or amines and organo-phosphorous compounds. However, when pro-oxidant species overwhelm antioxidant defenses, oxidative stress and oxidative degradation take place in biological systems and polymers, respectively. The research of new antioxidants with an improved efficacy respect to the already used is then very important and was the central topic of this PhD thesis. In Chapter 1 the oxidation phenomena and the most important antioxidants, both natural and synthetic ones, are briefly introduced. In Chapter 2 is reported our work concerning the preparation and evaluation of the antioxidant activity of 7-hydroxy dihydrobenzo[*b*]thiopenes and 7-hydroxy benzo[*b*]thiopenes developed by both the structure of Vitamin E and that of sulfur containing antioxidants previously synthesized by our research group. Part of this work was published in the journal *Organic Letters* (*Organic Lett.* 2016, 18, 5464-5467). In Chapter 3 is described the use of polymeric antioxidants, obtained from the copolymerization of a polymerizable antioxidant with appropriate monomers, as better stabilizing additives (respect to low molecular weight molecular antioxidants) for polyolefins. This work was also published on the *Polymer Degradation and Stability* journal (*Polym. Degrad. Stab.* 2017, 144, 167-175). In the same chapter it is also reported the synthesis of new antioxidant derivatives suitable for the preparation of polymeric antioxidants through copolymerization reactions or reactive blending. The stabilization of polyolefins is also the subject of Chapter 4, where are reported the outcomes of my work in the research group of professor S. Al-Malaika at the Aston University, Birmingham (UK), that was focused on the direct linking of a phenolic antioxidant on polyethylene through grafting reactions. Finally, in Chapter 5 is described the modification of commercially available molecular antioxidants (Trolox, Catechin and BHT) for the preparation of metallic nanostructured antioxidants (Au,  $\gamma$ -Fe<sub>2</sub>O<sub>3</sub>, Co) in order to reduce their toxicity in biomedical applications, for the treatment of stress related pathologies and as additives for ether solvents stabilization.

## 1 Introduction

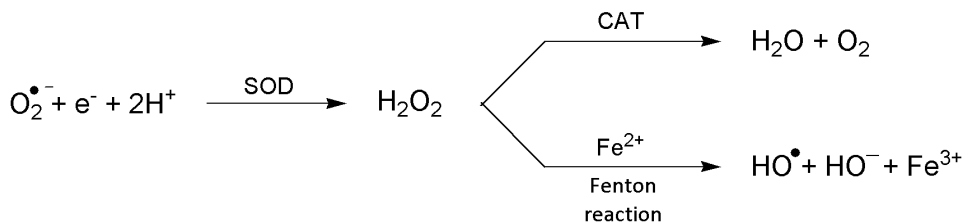
Life of aerobic organisms requires molecular oxygen. All the energy for life and reproduction is produced in mitochondria through reactions that involve the reduction of  $O_2$ . Evolution from anaerobic to aerobic metabolism increased the quantity of fruitful energy derived from the oxidation of food, and the wider amount of endogenous ATP has brought to the development of complex multicellular organisms. Oxygen is then an essential molecule for vital processes but, at the same time, it is an oxidant potentially noxious for living organisms and all the organic matter. Indeed, oxygen is responsible for the degradation of drugs, foods and beverages, the aging of plastics and paints and many other processes. A central role in these dangerous effects is played by a family of products called Reactive Oxygen Species (ROS) that are generated from the partial reduction of oxygen.<sup>1</sup> Their formation occurs under the action of different sources like UV or ionizing radiations, in the presence of various chemicals including transition metals and many xenobiotics, but also by enzymes or electron leakage in the course of metabolic pathways.<sup>2</sup>

The term "ROS" includes not only oxygen-centred radicals such as  $O_2^{\bullet-}$  (superoxide anion),  $ROO^{\bullet}$  (peroxyl radical) and  $HO^{\bullet}$  (hydroxyl radical), but also non-radical oxidants, such as  $H_2O_2$  (hydrogen peroxide),  $O_2^*$  (singlet oxygen), and  $HClO$  (hypochlorous acid) in turn capable of forming radical species. In living beings, free radicals and ROS are natural byproducts of the normal metabolism and play also an important role in cell signalling, homeostasis and many biochemical transformations. Typically, the generation of ROS in biological systems starts with the reduction of molecular oxygen ( $O_2$ ) to the superoxide anion (Scheme 1).<sup>3</sup>



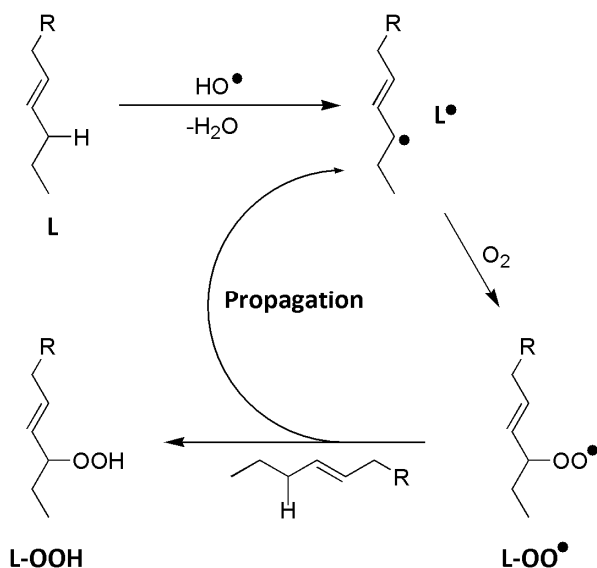
### Scheme 1

Superoxide anion is one of the products of metabolism of different intracellular sources. The mitochondrial electron transport chain is generally considered as the most important source of  $O_2^{\bullet-}$ , but the latter is also produced with the normal activity of several enzymes like NADPH oxidases and xanthine oxidase.<sup>1,4</sup> The superoxide anion is not extremely reactive itself but is the source, either directly or through enzyme or metal-catalysed processes, of several other ROS. For example, Superoxide Dismutase (SOD) catalyses the conversion of the superoxide anion to hydrogen peroxide ( $H_2O_2$ ) which, in turn, is decomposed to water and oxygen by catalase (CAT) (Scheme 2). Alternatively, hydrogen peroxide can react with  $Fe^{2+}$  leading to the formation of hydroxyl radicals through the so-called Fenton reaction.



**Scheme 2**

Hydroxyl radical is one of the most reactive oxidant species formed in biological systems able to react at a diffusion-controlled rate with almost all molecules in living cells. Hence, after  $\text{HO}^\bullet$  is formed in vivo, it damages whatever it is generated next to, before it could migrate at any significant distance within the cell. This leads to damage at proteins, DNA and lipids.<sup>5</sup> One of the principal targets of  $\text{HO}^\bullet$  and other ROS are the polyunsaturated fatty acids of cell membranes whose oxidation, generally labelled as lipid peroxidation, is particularly dangerous because it proceeds as a chain reaction with major damage. Lipid peroxidation is an auto-oxidation reaction activated by a radical species that abstracts a hydrogen atom from an activated C-H bond forming a carbon-centred radical ( $\text{L}^\bullet$ ). The latter rapidly reacts with  $\text{O}_2$  to give a peroxy radical ( $\text{L-OO}^\bullet$ ), able to cleave another C-H bond generating a hydroperoxide ( $\text{L-OOH}$ ) and a new  $\text{L}^\bullet$ , responsible of the propagation of the radical chain reaction (Scheme 3).<sup>6</sup>



**Scheme 3**

ROS are not always noxious to biological environments. In macrophages and neutrophils, for example, the NADPH oxidase complex generates  $\text{O}_2^{\bullet-}$  and  $\text{H}_2\text{O}_2$  to destroy pathogens and prevent serious diseases. Over the past years, several proofs emerged concerning the implication of ROS as signalling molecules to regulate

biological and physiological process.<sup>7-9</sup> Toxicological problems arise when there is an excess of ROS concentration respect to the activity of all of those antioxidant systems that keep them under control.<sup>10</sup> This state of redox disequilibrium, labelled as 'oxidative stress', seems involved in many dangerous diseases such as neurodegeneration, cardiovascular injury, mutation of healthy cells into cancerous ones, and many others.<sup>11,12</sup>

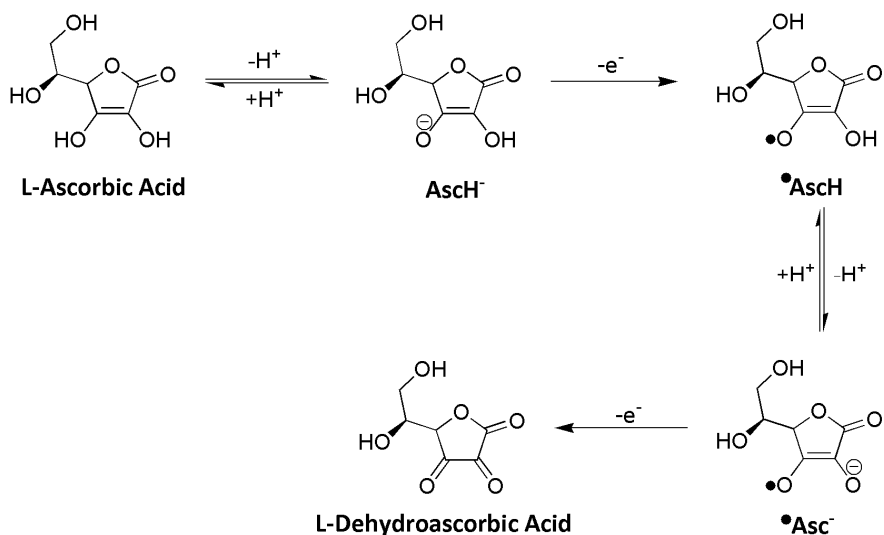
Antioxidant systems are able to neutralise the potentially injurious effects of ROS when their concentration is out of control. Among the several definitions proposed for antioxidants, a broad one defines an antioxidant as "any substance that, even when present at lower concentrations than the oxidizable substrate, significantly delays or prevents substrate oxidation".<sup>1</sup> The oxidative stress generation is prevented by the action of endogenous and exogenous antioxidant defences that keep under control the ROS level preventing their accumulation in biological tissues.

The set of endogenous defences is mainly composed by enzymatic antioxidants such as superoxide dismutase [SOD], catalase [CAT] and glutathione peroxidase [GPx]. Each of these proteins have the ability to prevent biological damages through the neutralization of high toxic radicals. In addition to enzymes, low-molecular weight free radical scavengers operate at biological level. For example, glutathione (GSH) and other endogenic thiols represent an efficient defence being able of scavenging various reactive species with formation of safe products.

Exogenous defences involve mainly small organic molecules introduced in the organism through diet and characterized by antioxidant and radical scavenger activity. Among them, vitamins are surely the most important ones: ascorbic acid (vitamin C),  $\beta$ -carotenes (vitamin A), tocopherols (vitamin E), and flavonoids (vitamin P) are the main antioxidant nutrients introduced with the diet.<sup>5</sup> They have different characteristics, mechanism of action and targets, and represent the most important exogeneous defence against ROS. It has been widely demonstrated that the actual protective action of these small organic molecules is enhanced if they can operate in a synergic way by transforming a highly oxidant species into a harmless one through a series of redox reactions with a decrescent potential. For this reason, a variegated diet, rich in antioxidants, is the best method that assists the endogenous defences to maintain the concentration of free radicals in tissues under control avoiding oxidative stress and correlated pathologies. Considering the biological importance of exogenous antioxidants, the knowledge of their mechanism of action, physicochemical properties and structure activity relationships (SAR) is at the centre of in-depth researches.

For example, L-ascorbic acid, or its oxidized form L-dehydroascorbic acid, is the active component of Vitamin C, probably the most important hydrophilic antioxidant. It has an effective reducing activity against superoxide radical anion, hydrogen peroxide, hydroxyl radical, singlet oxygen, and reactive nitrogen oxide.<sup>3</sup>

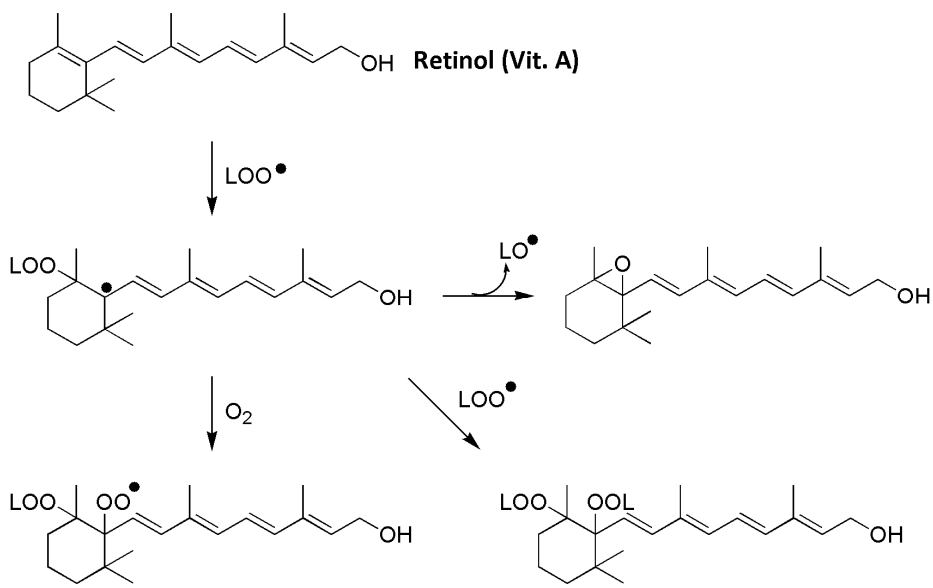




**Scheme 4**

The radical scavenger activity of L-Ascorbic acid is a multi-step mechanism that starts from the formation of the ascorbate anion (**Asch<sup>-</sup>**) and the subsequent oxidation to the ascorbyl radical (**•Asch**). The latter is deprotonated to the monodehydroascorbyl radical (**•Asc<sup>-</sup>**) and finally further oxidized to L-Dehydroascorbic acid (Scheme 4).<sup>13</sup>

Vitamin A included at least 12 different forms characterized by the  $\beta$ -ionone moiety. The main responsible for the antioxidant activity of Vitamin A is its free-alcohol form, retinol, that interrupts lipid peroxidation by quenching the lipid peroxy radicals (LOO<sup>•</sup>) with the mechanism depicted in Scheme 5.<sup>14,15</sup>



**Scheme 5**

Vitamin E occurs naturally in eight different forms:  $\alpha$ ,  $\beta$ ,  $\gamma$ ,  $\delta$ - tocopherol and  $\alpha$ ,  $\beta$ ,  $\gamma$ ,  $\delta$ - tocotrienol (Figure 1).<sup>16</sup> All of them bear a chromanol ring and a long aliphatic side chain, saturated in Tocopherols (phytyl chain) while it is unsaturated in Tocotrienols (isoprenoid chain).

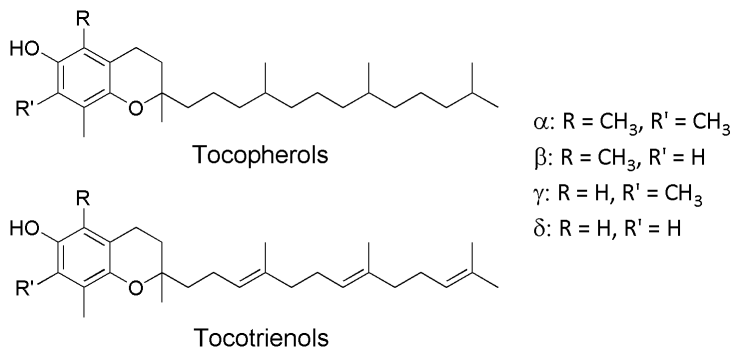
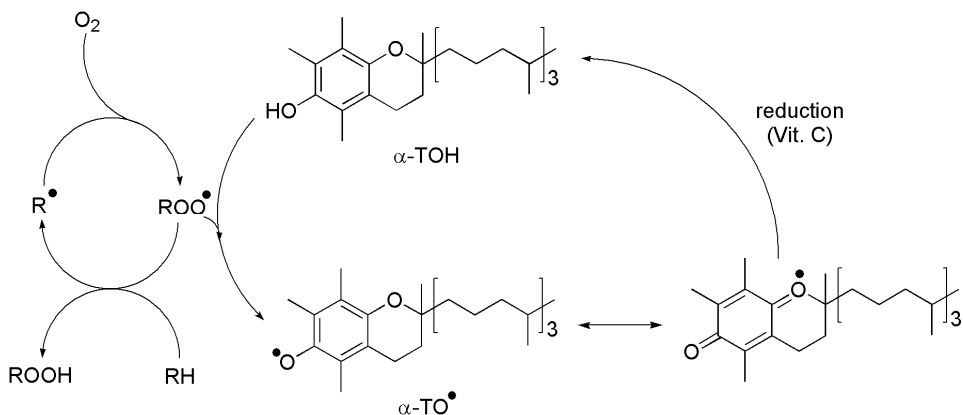


**Figure 1**

The main component of vitamin E,  $\alpha$ -Tocopherol ( $\alpha$ -TOH, R=R'=CH<sub>3</sub>), is the most powerful lipophilic antioxidant known in nature, and has a key role in the prevention of oxidative stress in biological tissues. Its activity is mainly addressed to the protection of cell membranes by protecting their main component, *i.e.* the polyunsaturated phospholipids.<sup>17</sup> The peroxy radicals (ROO<sup>\*</sup>) generated during the polyunsaturated phospholipids oxidation are quenched as hydroperoxides (ROOH) by the donation of a

hydrogen atom from the phenolic OH of  $\alpha$ -TOH which, in turn, is converted in a relatively stable  $\alpha$ -tocopheroxyl radical ( $\alpha$ -TO $\cdot$ ) (Scheme 6).<sup>18</sup>



**Scheme 6**

Thus,  $\alpha$ -Tocopherol is able to interrupt the propagation of the oxidative chain reaction in phospholipids, justifying its ability as 'chain-breaking antioxidant'. Actually, the reactivity of  $\alpha$ -TOH is more complex and each molecule of the antioxidant is able to trap two equivalents of peroxy radicals, with the formation of  $\alpha$ -TOH quinonoid by-products.<sup>19</sup> The simultaneous presence of other endogenous antioxidants like ubiquinol or vitamin C has a positive effect on the antioxidant activity of  $\alpha$ -TOH because they can regenerate the phenolic form from  $\alpha$ -TO $\cdot$ .<sup>20,21</sup>

Vitamin P includes a list of compounds denominated flavonoids, characterized by the 2-phenylchromane skeleton and a polyphenolic structure.<sup>22-24</sup> Some member of this family of powerful antioxidants is reported in Figure 2.

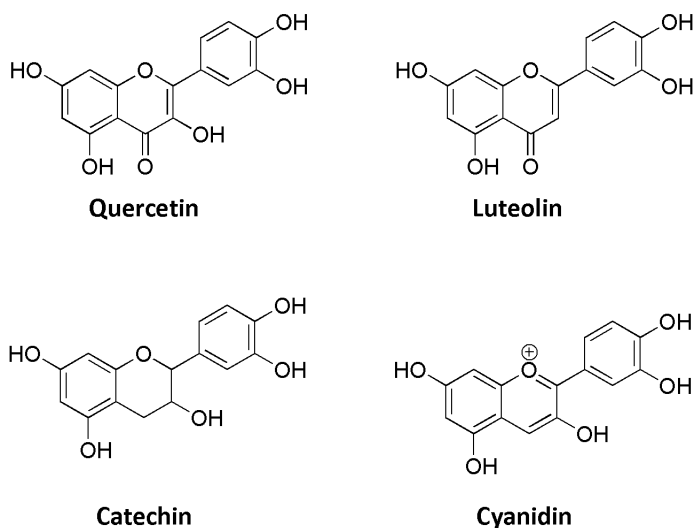
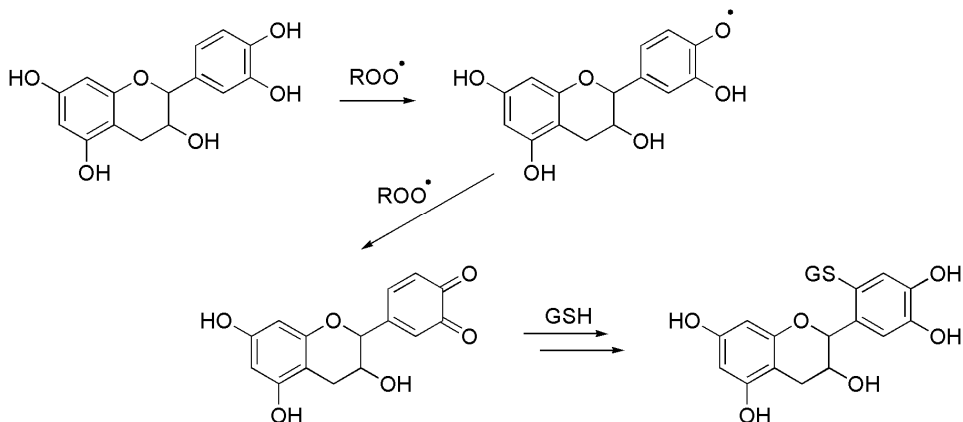


**Figure 2**

Like tocopherols, flavonoids are chain-breaking antioxidants able to reduce peroxy radicals into hydroperoxides with a mechanism depicted in Scheme 7 with Catechin as a model.



**Scheme 7**

The quenching of the first  $\text{ROO}^\bullet$  leads to the formation of a semiquinonic radical derivative which, in turn, is able to react with another peroxy radical. Therefore, each molecule of Catechin traps two equivalents of  $\text{ROO}^\bullet$ , as seen for  $\alpha$ -TOH.<sup>25</sup> Unfortunately, the *ortho*-thioquinone formed in the last step is relatively unstable and can react with endogenous nucleophiles, such as the sulfydryl groups of glutathione (GSH), to give toxicologically non-innocent adducts. On the other hand, the antioxidant activity of flavonoids is not limited to the quenching of peroxy radicals. Indeed, they

can complex metal ions like  $\text{Cu}^+$  and  $\text{Fe}^{2+}$  (Figure 3) preventing their participating in red-ox processes able to generate ROS like the Fenton reaction.<sup>26-29</sup>

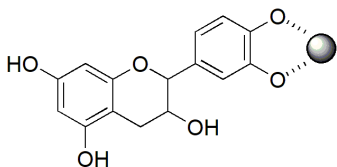


**Figure 3**

Another recognized property of this family of antioxidants is the prevention against cardiovascular diseases. The exact mechanism of this effect has not been well elucidated, but is demonstrated by the low incidence of cardiovascular diseases in populations that associate a high intake of animal fats with foods rich in polyphenols like red wine, red fruits and tea (*i.e.* the “French paradox”).<sup>30</sup>

The oxidative degradation of atmospheric oxygen and related ROS it is not limited to biological systems but concerns the ‘organic’ materials overall. Well known consequences of oxidative reactions are the degradation of mechanical, aesthetic and electrical properties of polymers,<sup>31</sup> the loss of flavour and development of rancidity in foods,<sup>32</sup> and the increase in viscosity, acidity and formation of insoluble materials in lubricants.<sup>33</sup> Indeed, molecular antioxidants are generally added to all those systems that can undergo oxidative degradation to prevent or retard these unavoidable and undesired processes. For this purpose, synthetic antioxidants are mostly used instead of natural ones because they are easy to synthesize and cheap in price. Many compounds are used as additives to enhance the stability of food to various manufacturing conditions as well as to prevent the oxidation during storage for prolonging the shelf life.<sup>34</sup> Synthetic antioxidants are added to synthetic polymers in order to protect these materials against degradation during both the processing and the end use.<sup>35</sup> Also gasoline and jet engine fuels require the addition of antioxidants because they undergo oxidative degradation processes during the storage that determine the oxidation of their unsaturated components into undesired products.<sup>36</sup> Several types of synthetic antioxidants have been developed, starting in most cases from the structure of natural ones with the aim to optimize their ability to quench the oxidation processes. Some of the most important are reported in Figure 4.

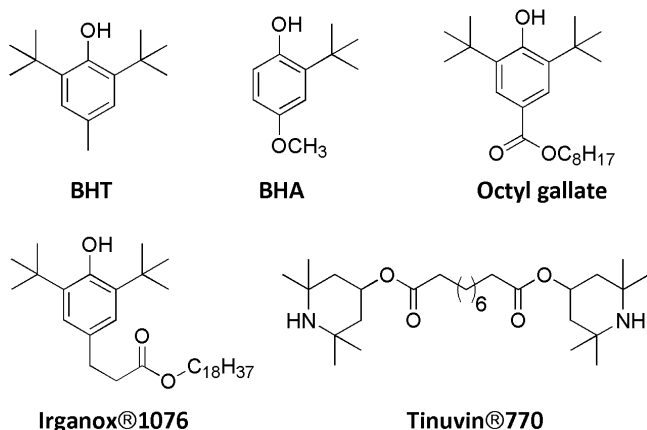


**Figure 4**

The development of these molecules has been useful not only for their direct application in human activities but also to have a better knowledge of their mechanisms of action, to use them as standard systems for the evaluation of antioxidant activity of new compounds, and for the research of innovative antioxidant molecules characterized by an increased efficacy. Indeed, despite a huge number of innovative antioxidants has been developed, traditional molecules like  $\alpha$ -TOH and 2,6-di-*tert*-butylated phenols have not been replaced yet and still represent the first choice for many applications. The problem is the difficulty in outperforming the traditional antioxidants both in terms of antioxidant performance and of production costs. This point is particularly important because  $\alpha$ -TOH and 2,6-di-*tert*-butylated phenols are not without shortcomings, and this fact limits their possible applications in medicinal chemistry, biology, and material science. Better antioxidants could be useful for the treatment of stress-related pathologies, the increasing of food shelf life, the delay of synthetic polymers degradation or their use in high demanding engineering and biomedical applications. Considering that each system liable of oxidative degradation is characterized by different properties (physical state, chemical composition, surrounding conditions, *etc*) and undergoes this process in a typical way, the application of a tailor-made method for the development of new antioxidants would give better results. This means that the strength of an antioxidant is not only related to its pure chemical reactivity with ROS but also to other factors like the solubility and the persistence in the medium, its localization close to the regions of ROS production, the synergism with other active species, and many others. The structure modification of traditional antioxidant moieties is a preferred way for developing new molecules and, for this goal, a mechanistic knowledge of their structure-activity relationship is fundamental in order to improve the efficacy of these systems. At the same time, the exploration of innovative research fields like supramolecular chemistry is an attractive way for achieving new properties that are otherwise unreachable with molecular systems.

The preparation of molecular antioxidants developed by the knowledge of structure-activity relationship and the development of macromolecular and nanostructured systems has been the base of this PhD thesis. Together with the synthesis of these systems, also the characterization of the antioxidant properties and the discussion of the results are reported.

## 1.1 References

- (1) Halliwell, B.; Gutteridge, J. M. C. *Free Radicals in Biology and Medicine*, 5th ed.; Halliwell, B., Gutteridge, J. M. C., Eds.; Oxford University Press: London, 2015.
- (2) Potterat, O. *Curr. Org. Chem.* **1997**, *1* (4), 415–440.
- (3) Carocho, M.; Ferreira, I. C. F. R. *Food Chem. Toxicol.* **2013**, *51*, 15–25.
- (4) Turrens, J. F. *J. Physiol.* **2003**, *552*, 335–344.
- (5) Nimse, S. B.; Pal, D. *RSC Adv.* **2015**, *5*, 27986–28006.
- (6) Girotti, A. W. *J. Free Radic. Biol. Med.* **1985**, *1*, 87–95.
- (7) Ray, P. D.; Huang, B. W.; Tsuji, Y. *Cell. Signal.* **2012**, *24*, 981–990.
- (8) Schieber, M.; Chandel, N. S. *Curr. Biol.* **2014**, *24*, R453–R462.
- (9) Holmström, K. M.; Finkel, T. *Nat. Rev. Mol. Cell Biol.* **2014**, *15*, 411–421.
- (10) Finkel, T.; Holbrook, N. J. *Nature* **2000**, *408*, 239–247.
- (11) Li, N.; Xia, T.; Nel, A. E. *Free Radic. Biol. Med.* **2008**, *44*, 1689–1699.
- (12) Pham-Huy, L. A.; He, H.; Pham-Huy, C. *Int. J. Biomed. Sci.* **2008**, *4*, 89–96.
- (13) Ruiz, J. J.; Aldaz, A.; Domínguez, M. *Can. J. Chem.* **1977**, *55*, 2799–2806.
- (14) Tesoriere, L.; Arpa, D. D.; Re, R.; Livrea, M. A. *Arch. Biochem. Biophys.* **1997**, *343*, 13–18.
- (15) Samokyszyn, V. M.; Marnett, L. J. *Free Radic. Biol. Med.* **1990**, *8*, 491–496.
- (16) Wang, X.; Quinn, P. J. *Prog. Lipid Res.* **1999**, *38*, 309–336.
- (17) Leng, X.; Kinnun, J. J.; Marquardt, D.; Ghefli, M.; Kucerka, N.; Katsaras, J.; Atkinson, J.; Harroun, T. A.; Feller, S. E.; Wassall, S. R. *Biophys. J.* **2015**, *109*, 1608–1618.
- (18) Engin, K. N. *Mol. Vis.* **2009**, *15*, 855–860.
- (19) Liebler, D. C.; Burr, J. A.; Philips, L.; Ham, A. J. *Anal. Chem.* **1996**, *236*, 27–34.
- (20) Niki, M. *Am. J. Clin. Nutr.* **1991**, *54*, 1119S–1124S.
- (21) Retsky, K. L.; Freeman, M. W.; Frei, B. *J. Biol. Chem.* **1993**, *268*, 1304–1309.

- (22) Middleton Jr, E.; Kandaswarni, C. *The Flavonoids Advances in Research Since 1986*; Harborne, J. B., Ed.; Chapman & Hall: London, 1994.
- (23) Bohm, B. A. *Introduction to Flavonoids*; Harwood Academic Publishers: Amsterdam, 1998.
- (24) Dixon, R. A.; Ferreira, D. *Phytochemistry* **2002**, *60*, 205–211.
- (25) Mochizuki, M.; Yamazaki, S.; Kano, K.; Ikeda, T. *Biochim. Biophys. Acta* **2002**, *1569*, 35–44.
- (26) Hynes, M. J.; Ó Coinceanainn, M. J. *Inorg. Biochem.* **2001**, *85*, 131–142.
- (27) Mira, L.; Fernandez, M. T.; Santos, M.; Rocha, R.; Florêncio, M. H.; Jennings, K. R. *Free Radic. Res.* **2002**, *36*, 1199–1208.
- (28) Khokhar, S.; Owusu Apenten, R. K. *Food Chem.* **2003**, *81*, 133–140.
- (29) Treml, J.; Smejkal, K. *Compr. Rev. Food Sci. Food Saf.* **2016**, *15*, 720–738.
- (30) Sun, A. Y.; Simonyi, A.; Sun, G. Y. *Free Radic. Biol. Med.* **2002**, *32* (4), 314–318.
- (31) Billingham, N. C. *Mater. Sci. Technol.* **2013**, 469–507.
- (32) Carocho, M.; Barreiro, M. F.; Morales, P.; Ferreira, I. C. F. R. *Compr. Rev. Food Sci. Food Saf.* **2014**, *13*, 377–399.
- (33) Rasberger, M. In *Chemistry and Technology of Lubricants*; Mortier, R. M., Orszulik, S. T., Eds.; Springer: Dordrecht, 1997; pp 98–143.
- (34) Berdahl, D. R.; Nahas, R. I.; Barren, J. P. In *Oxidation in foods and beverages and antioxidant applications*; Decker, E. A., Elias, R. J., McClements, D. J., Eds.; Elsevier, 2010; pp 272–320.
- (35) Solera, P. J. *Vinyl Addit. Technol.* **1998**, *4*, 197–210.
- (36) Groysman, A. In *Corrosion in Systems for Storage and Transportation of Petroleum Products and Biofuels*; Springer: Dordrecht, 2014; pp 23–32.



## 2 Vitamin E-like molecular antioxidants

### 2.1 Introduction

In the last decades big efforts have been done to investigate the structural properties responsible of the vitamin E antioxidant properties. The synthesis of new compounds with equal or better activity than  $\alpha$ -Tocopherol ( $\alpha$ -TOH) has been studied as well, taking into consideration the requirements of good bioavailability, solubility and absence of toxicity.<sup>1</sup> To reach this goal, the structure of the tocopheroxyl radical that is formed by the reaction of  $\alpha$ -TOH with peroxy radicals has been examined in depth, focusing on all the stereo-electronic features responsible for its stabilization. An essential role is played by the endocyclic oxygen since the constraining inside the chromanic ring forces its p-type lone pair to be nearly perpendicular to the aromatic plane hence parallel to the semi-occupied p-orbital of the phenoxyl radical (Figure 1).<sup>2,3</sup>

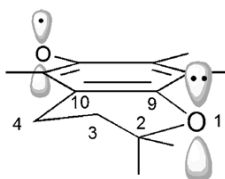
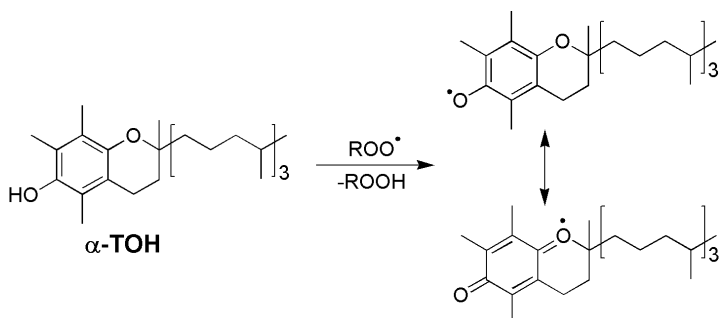


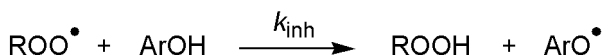
Figure 1

The result of this orientation is a favourable overlap between the p-orbitals of the two oxygen atoms that allows an excellent stabilization of the phenoxyl radical through conjugative electron delocalization (Scheme 1).



Scheme 1

One of the most important parameters used to calculate the antioxidant activity of  $\alpha$ -TOH and other natural or synthetic antioxidants is the inhibition constant ( $k_{inh}$ ) i.e. the kinetic constant of the reaction between a radical-chain phenolic inhibitor (ArOH) and peroxy radicals ( $ROO^\bullet$ ), hence a high  $k_{inh}$  indicates a strong chain-breaking activity.



This parameter is strictly related to the Bond Dissociation Enthalpy of the O-H bond (BDE (OH)) of the antioxidant that is cleaved during the inhibition reaction.<sup>4</sup> The almost linear correlation between  $\log k_{\text{inh}}$  and BDE allows to acquire one parameter knowing the other. For example,  $\alpha$ -TOH has a  $k_{\text{inh}} = 3.2 \times 10^6 \text{ M}^{-1}\text{s}^{-1}$  and a BDE of  $78.2 \text{ kcal mol}^{-1}$ .<sup>3,5</sup>

Among the factors influencing BDE, the nature and position of substituents on the phenolic aromatic ring are crucial. The -OH is overall a good electron-donor group but, after the interaction with  $\text{ROO}^\bullet$ , the loss of a hydrogen atom reverses its characteristics being  $\text{-O}^\bullet$  a potent electron-withdrawing group. The ideal substituent should be able of weakening the ArO-H bond facilitating the homolytic cleavage (high  $k_{\text{inh}}$  and low BDE) while stabilizing the phenoxyl radical ( $\text{ArO}^\bullet$ ). The lower is the BDE of the ArO-H the better is the antioxidant activity of the phenol. To have a thermodynamically favoured ArO-H bond breaking, the BDE of the phenolic antioxidant should be smaller than the BDE of the hydroperoxide  $\text{ROOH}$ .<sup>6</sup> Figure 2 shows the correlation among BDE of the phenolic ArO-H bond and the effect of electron-donor (EDG) and electron-withdrawing (EWG) groups on the aromatic ring.

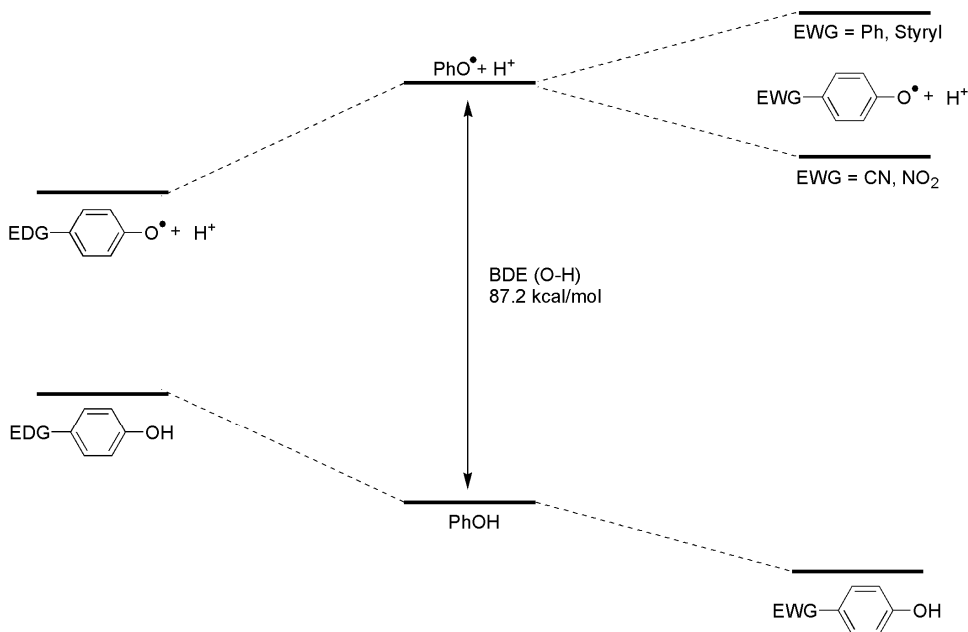


**Figure 2<sup>6</sup>**

Due to the aforementioned opposite electronic character of ArO-H and ArO<sup>•</sup>, the presence of an EDG on the right position of the aromatic ring has a dual positive effect because both destabilizes the ground state (ArOH) and stabilizes its corresponding radical (ArO<sup>•</sup>), thus reducing the energy difference between the two species (Figure 2, left). Exactly the opposite occurs with phenols bearing EWGs (Figure 2, right) even though, in the case of the phenoxyl radical, depending on the type of substituent there is a small increase or decrease of the stability that anyway is not so relevant.<sup>7</sup> As a

result with electron-withdrawing groups the overall BDE increases and  $k_{inh}$  decreases, thus depleting the antioxidant activity of the system.

The analysis of the four tocopherols existing in nature is in agreement with Figure 2. The antioxidant activity increases with the number of EDG methyl substituents.  $\alpha$ -TOH is fully methylated and, confirming the positive contribute of EDG to BDE and  $k_{inh}$ , is the most active tocopherol of Vitamin E.  $\beta$ - and  $\gamma$ -TOH, bearing two methyl groups, have a similar behaviour being both worse than  $\alpha$ -TOH, while  $\delta$ -TOH with just one methyl is the worst (Figure 3).<sup>4</sup>

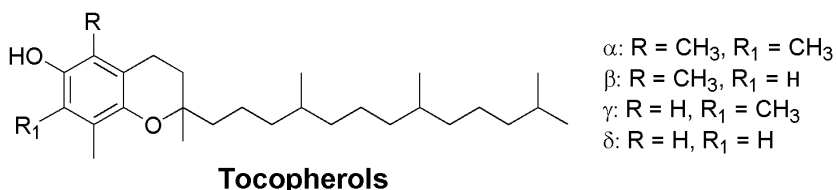


**Figure 3**

However, the electronic behaviour of the substituents is not the only aspect that influences the magnitude of the antioxidant activity. Among many other, the ability of intramolecular hydrogen bond (IHB) formation with *ortho* substituents has a great importance. In phenols bearing substituents able to establish an IHB (like alkoxy groups) there is a stabilization of the ground state hence an increasing of the BDE. For example, the BDE(OH) increases of 3 kcal mol<sup>-1</sup> from 4- to 2-methoxyphenol due to the IHB that stabilizing the ground state of phenol disfavours the H<sup>•</sup> transfer (Figure 4).<sup>6</sup>

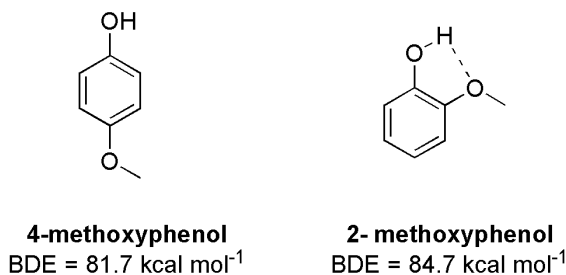


**Figure 4**

Another important factor that contributes to the antioxidant activity is the structural conformation. In  $\alpha$ -TOH the endocyclic oxygen stabilizes the phenoxyl radical due to the correct orientation of its p orbital, *i.e.* nearly perpendicular to the aromatic plane (Figure 1). In 4-methoxy-2,3,5,6-tetramethylphenol (Figure 5) the same situation cannot occur since the steric hindrance of the methyls that, preventing the planarity of the O-CH<sub>3</sub> group with the aryl ring, prevents the stabilization of the ArO<sup>•</sup> group by conjugation. Indeed, the BDE(OH) of 4-methoxy-2,3,5,6-tetramethylphenol is 2.6 kcal mol<sup>-1</sup> higher than  $\alpha$ -TOH.<sup>6</sup>

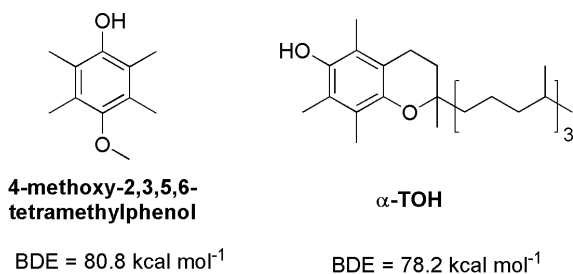


**Figure 5**

The role of conformational issues is confirmed considering that passing from a six-membered heterocyclic system, the chromane ring of α-TOH, to a five membered one, a benzo[*b*]dihydrofuran, there is an increase of the corresponding  $k_{inh}$  (Figure 6)<sup>8</sup> since a better orbital overlapping of the lone pair of the furanic oxygen with the phenoxyl radical is caused by the increased rigidity of the five membered ring.

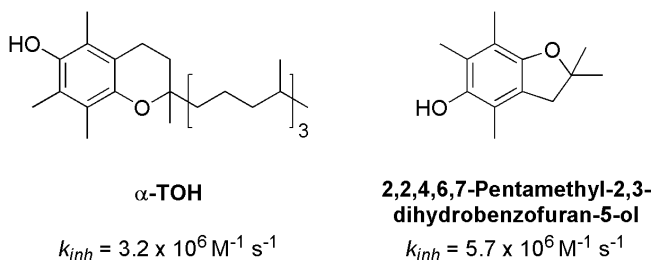
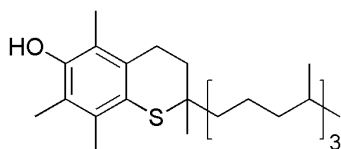


**Figure 6**

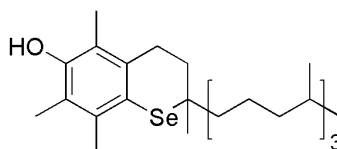
Among the several modifications of the α-TOH skeleton,<sup>9</sup> some of the most important are the insertion of alkyl or aryl substituents at the *ortho* or *meta* position of the phenolic OH,<sup>10,11</sup> the contraction of the hexacyclic structure of the chromanol ring to a dihydrofuranic pentacyclic structure,<sup>8</sup> and insertion of an additional OH on phenolic ring to form the catechin moiety.<sup>1</sup> Another active area of research is the introduction of further active groups on the skeleton of α-TOH in order to add additional antioxidant activities. This is the case of heavy chalcogens (sulfur, selenium and tellurium) that in their divalent state are able to act as efficient hydroperoxides decomposers,<sup>12</sup> thus chalcogen-substituted phenols have been found to possess both chain-breaking and peroxide decomposing activities.<sup>13</sup>

Introduction of chalcogen atoms into the chroman ring typically causes a decrease of the radical scavenger activity. Indeed, both all racemic 1-thio-<sup>14</sup> and 1-seleno-<sup>15</sup> α-tocopherol analogues showed a good ability of quenching peroxy radicals but slightly lower than that of α-TOH (Figure 7).



**1-thio- $\alpha$ -tocopherol**

$$k_{inh} = 1.3 \times 10^6 \text{ M}^{-1} \text{ s}^{-1}$$

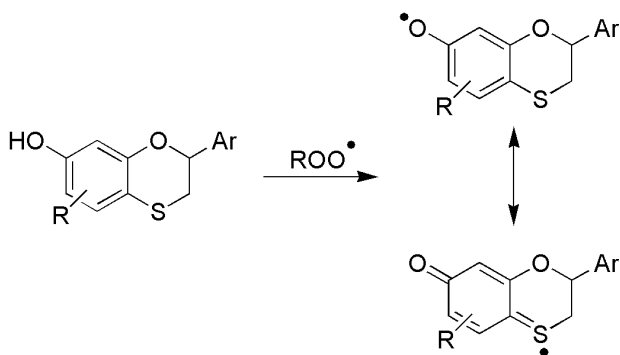


**1-seleno- $\alpha$ -tocopherol**

$$k_{inh} = 1.2 \times 10^6 \text{ M}^{-1} \text{ s}^{-1}$$

**Figure 7**

Analogous results were obtained in our research groups with the preparation of  $\alpha$ -tocopherol like 4-thiaflavanes reported in Scheme 2,<sup>16</sup> which, in turn, corroborate that chalcogens, like sulfur or selenium, participate to the stabilization of *para* phenoxy radicals without matching the ability of an oxygen atom (Scheme 2).



**Scheme 2**

On this light, the efforts for the research of new Vit. E-like molecules characterized by an improved radical scavenger activity led our research group to the preparation of 6-hydroxyl-4-thiaflavanes (Figure 8), where the relative *para* position between the OH and the endocyclic oxygen groups is maintained.<sup>17</sup>

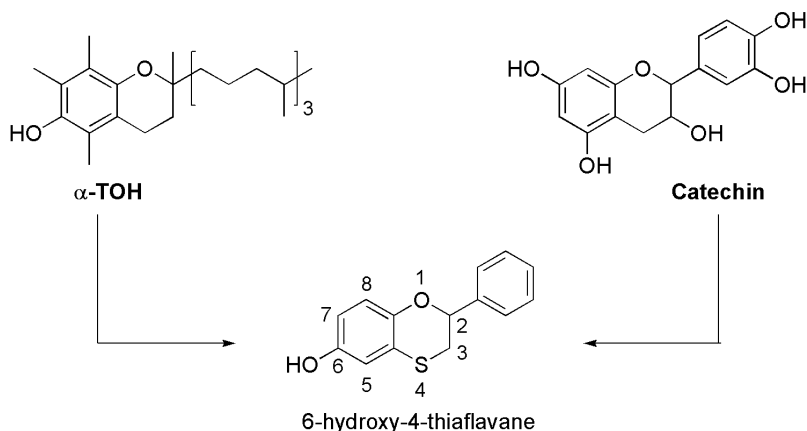
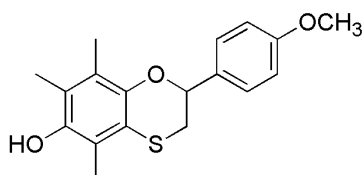


**Figure 8**

It has been possible to synthesize phenolic antioxidants containing critical portions of the skeleton of the two most important families of natural antioxidants, flavonoids and tocopherols (see Chapter 1), and the potential hydroperoxide decomposing activity of divalent sulfur. The best performances were obtained with derivative **1**, characterized by a BDE(OH) and a  $k_{inh}$  very similar, yet slight lower, than those of  $\alpha$ -TOH (Figure 9).



**1**

$$k_{inh} = 1.3 \times 10^6 \text{ M}^{-1} \text{ s}^{-1}$$

$$\text{BDE} = 78.9 \text{ kcal mol}^{-1}$$

**Figure 9**

The worse reactivity towards peroxy radicals of thiachromanols respect to the corresponding chromanols was ascribed to the change in the molecular shape caused by insertion of a sulfur atom into the framework of vitamin E. The excellent radical scavenger activity of  $\alpha$ -TOH is related to the planarity of the chromanol ring. The introduction of the sulfur atom into chromanol induces a great flexibility of the ring, thus a deviation from planarity and a worse stabilization of the phenoxy radical (Figure 10).

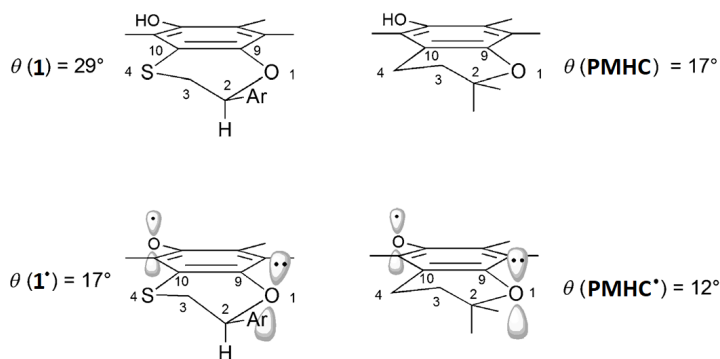


**Figure 10**

Actually, the enhancement of the calculated dihedral angle  $\theta$  (C10-C9-O1-C2) passing from the phenoxyl radical of  $\alpha$ -TOH ( $12^\circ$ ) to that of 4-thiaflavanes ( $17^\circ$ ) is small but sufficient to induce the measured loss of antioxidant activity.

The behaviour was confirmed with the synthesis of  $\alpha/\beta/\gamma/\delta$ -4-thiatocopherols **2a-d** (Figure 11) that differ from the corresponding  $\alpha$ -TOH just for the substitution of a  $\text{CH}_2$  group with a divalent sulfur and showed, overall, a very good antioxidant activity yet a  $k_{inh}$  smaller than those of the corresponding  $\alpha/\beta/\gamma/\delta$ -TOH.<sup>18</sup>

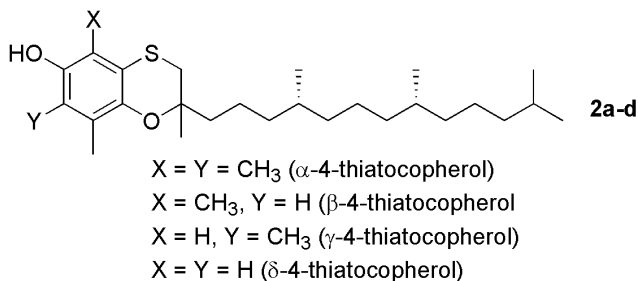


**Figure 11**

The optimization of the antioxidant activity of hydroxy-substituted 4-thiaflavanes continued with the preparation of 5-hydroxy-4-thiaflavane derivatives reported in Figure 12, characterized by the *ortho* position of the sulfur atom respect to the phenolic OH, that showed an outstanding radical scavenger activity with values of  $k_{inh}$  and BDE(OH) identical or very similar to that of  $\alpha$ -TOH.<sup>19</sup>

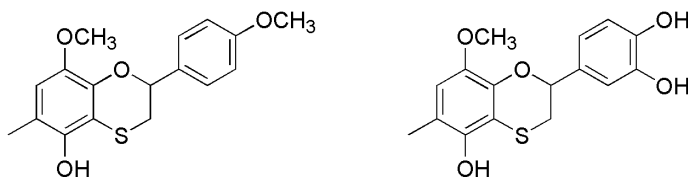


**Figure 12**

In these derivatives, the mutual position between the phenolic OH and the chromanic oxygen is different than in  $\alpha$ -TOH. The chromanic oxygen is in *meta* to the phenolic OH then the stabilization of the phenoxyl radical is mainly due to the *para* methoxy group and the *ortho* divalent sulfur. The latter stabilizes as expected the phenoxyl radical by conjugation due to its electron-donating nature, moreover and more importantly it is unable to give a strong IHB with the phenolic OH. Indeed, in the case of sulfur the IHB requires a defined conformation with the substituent on sulfur and the aromatic ring perpendicular each other. Being the sulfur part of the benzofused heterocycle such conformation cannot be reached as well as the corresponding stabilization of the phenol ground state that is adverse to the antioxidant activity (Figure 13, right). Differently, when the sulfur atom is in a system where is free to rotate (Figure 13, left), a solid IHB is formed with the corresponding increase of the BDE(OH) and decrease of the  $k_{inh}$ .<sup>20</sup>

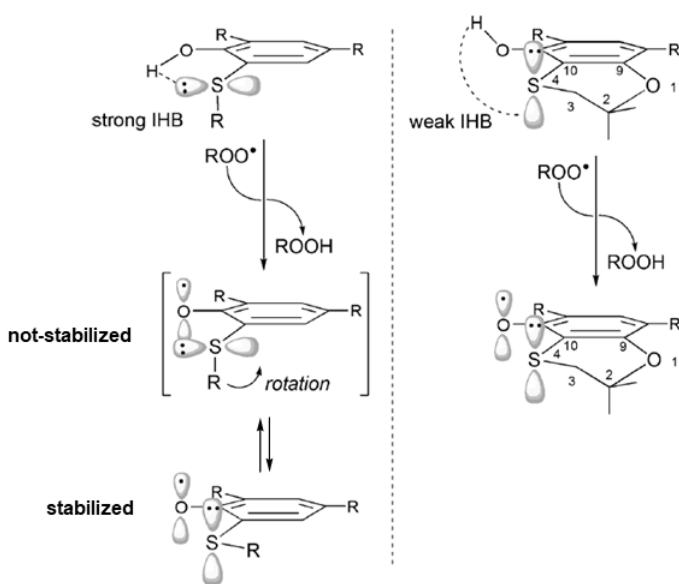


**Figure 13**

The skeleton of 5-hydroxy-4-thiaflavanes is different from that of tocopherols then analogous conformational considerations are impossible. In these systems (Figure 13) the dihedral angle  $\theta$  (C10-C9-O1-C2) is higher than in chromanols but it does not lead to a destabilization of the phenoxyl radical because the oxygen is in *meta* respect to the OH and then it is only negligibly involved in its stabilization. The dihedral angle that has to be considered in 5-hydroxy-4-thiaflavanes is the one containing the sulfur (C9-C10-S4-C3) because the latter, being in *ortho* to the phenolic OH, is more involved in the stabilization of the phenoxyl radical. As depicted in Figure 13 (right) the C3 is almost coplanar with the phenolic ring and, consequently, the C9-C10-S4-C3 dihedral angle is very small ( $2-8^\circ$ ) thus allowing a better conjugation between the aromatic ring and the



p-type lone pair of the sulfur atom. These results suggested that an endocyclic benzo-fused sulfide sulfur was an ideal *ortho* substituent for the development of highly effective chain-breaking antioxidants.

This research continued preparing two new families of compounds, namely 7-hydroxybenzo[*b*]dihydrothiophenes and 9-hydroxy-2,3-dihydrobenzo[*de*]thiochromenes, that showed an excellent radical scavenger activity (Figure 14).<sup>21</sup>

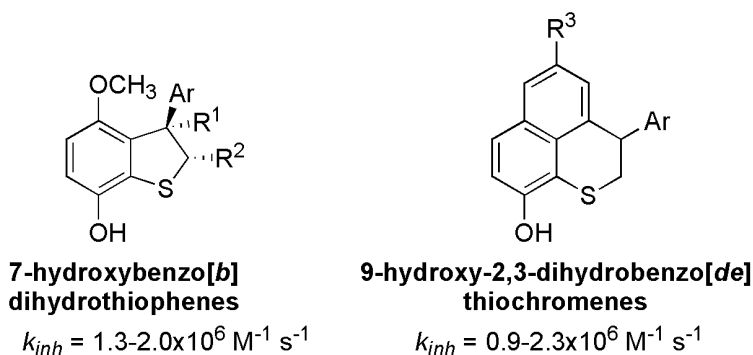


**Figure 14:** Ar = 4-methoxyphenyl; R<sub>1</sub> = H or CH<sub>3</sub>; R<sub>2</sub> = H or CH<sub>3</sub>; R<sub>3</sub> = H or OCH<sub>3</sub>.

Despite the different skeleton, these new derivatives were characterized by the same structural motif of 5-hydroxyl-4-thiaflavanes, *i.e.* an endocyclic sulfide sulfur in *ortho* to the phenolic OH that was responsible for their optimal antioxidant properties. Indeed, measured  $k_{inh}$  of these compounds resulted to be only slightly lower (up to  $2.3 \times 10^6 \text{ M}^{-1} \text{ s}^{-1}$ ) than reference  $\alpha$ -TOH ( $3.2 \times 10^6 \text{ M}^{-1} \text{ s}^{-1}$ ).

Also in this case the excellent antioxidant performance of these derivatives was ascribed to the almost planarity of the benzofused system that allows an effective stabilization of the phenoxyl radical by the endocyclic sulfide sulfur being the p-type orbital on sulfur and the semi-occupied p orbital of Ar-O nearly parallel. Additionally, also in this case the IHB is very weak as confirmed by FT-IR studies (Figure 15).

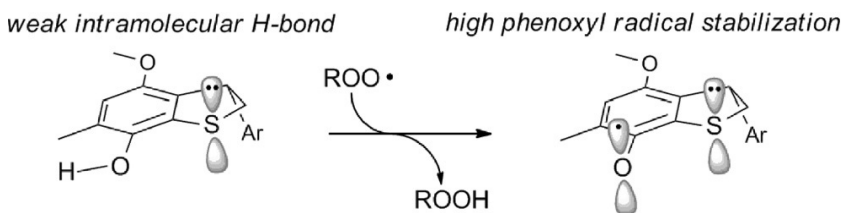
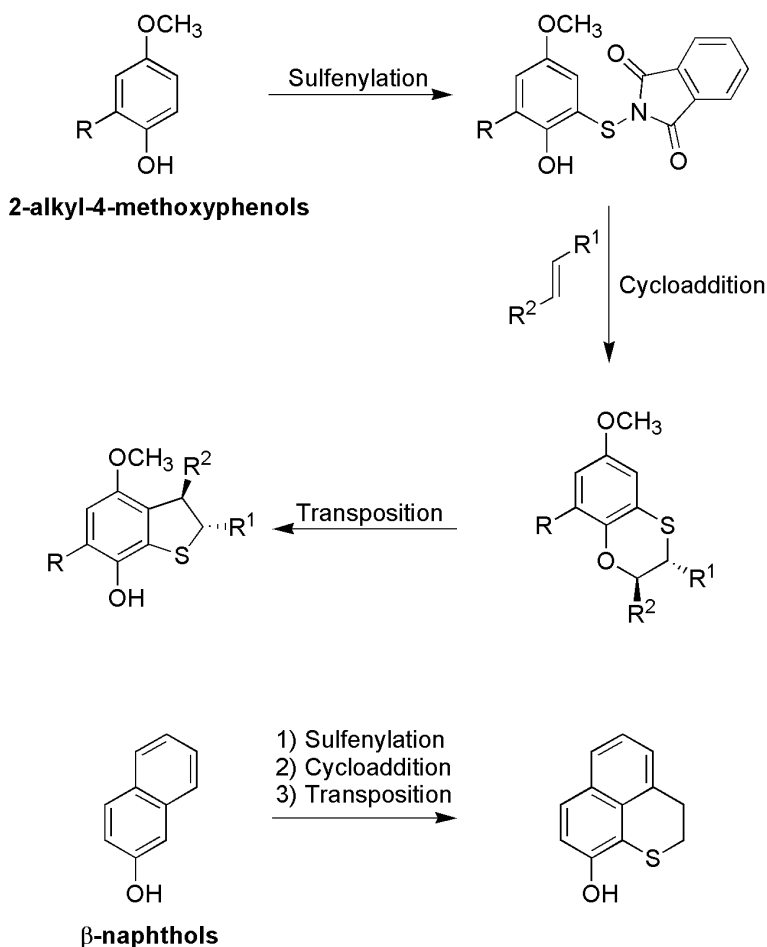


**Figure 15:** Ar = 4-methoxyphenyl

For the synthesis of these derivatives, commercially available 2-alkyl-4-methoxyphenols or  $\beta$ -naphthols were sulfenylated and then converted into a 1,4-benzo[*b*]oxathiine through a hetero Diels-Alder reaction with the appropriate alkene (Scheme 3). An acid

promoted transposition of the benzo[*b*]oxathiine allowed to obtain 7-hydroxybenzo[*b*]dihydrothiophenes or 9-hydroxy-2,3-dihydrobenzo[*de*]thiochromenes depending on the starting material used.



**Scheme 3**

The last step of this synthetic route, *i.e.* the transposition reaction, will be discussed in detail in the next section. The derivatives obtained, despite did not match the radical scavenger activity of α-tocopherol, showed excellent antioxidant properties that are related to three structural characteristics already discussed:

- The presence of EDG groups on the phenolic ring reduces its stability in the ground state thus facilitating the cleavage of the O-H bond. EDG groups also allow the stabilization of the corresponding EWG phenoxyl radical;
- The endocyclic sulfide sulfur in *ortho* to the phenolic OH, stabilizes the phenoxyl radical because of the favourable interaction between its p-type lone

pair and the semi-occupied p orbital of the oxygen radical. The latter interaction is particularly important as a consequence of the almost planarity of the benzodihydro[*b*]thiophene system.

- The sulfide sulfur inserted in a five or a six-membered ring prevents the formation of a strong IHB and the stabilization of the phenol.

During my PhD work we capitalized on all these findings for the preparation of innovative sulfur containing molecular polyphenolic antioxidants.

## 2.2 Results and discussion

Our work was based on the idea of synthesizing highly effective antioxidants by combining in the same structure two motifs that are responsible for an efficient radical scavenger activity (Figure 16):

- The chroman moiety of  $\alpha$ -TOH, characterized by the endocyclic oxygen in *para* to the phenolic OH.
- A dihydrothiophene ring benzofused to the phenolic cycle so as to have the endocyclic sulfide sulfur in *ortho* to the OH.

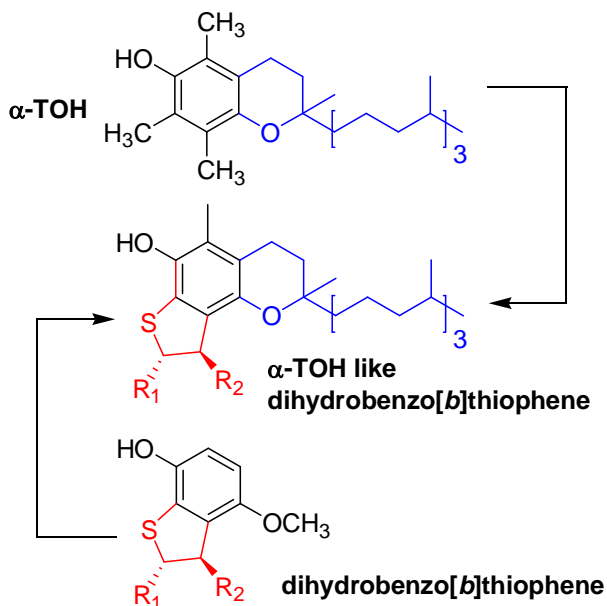
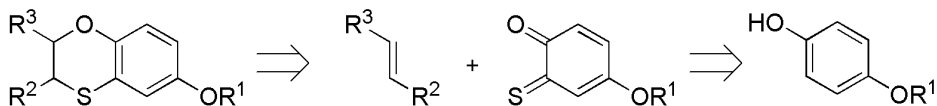


Figure 16

The synthetic way we followed was the acid promoted transposition described in **section 2.1** (Scheme 3) that allows to convert 1,4-benzo[*b*]oxathiines into dihydrobenzo[*b*]thiophenes. It was then necessary to prepare appropriate 1,4-benzo[*b*]oxathiines. These derivatives can be obtained through a hetero Diels-Alder reaction between an electron rich alkene and an *ortho*-thioquinone which is prepared,

in turn, starting from a *ortho*-hydroxy-*N*-thiophthalimide deriving from a proper substituted phenol (Scheme 4).



**Scheme 4**

### 2.2.1 Synthesis of phenolic derivatives

The first step was the preparation of phenolic derivatives with a tocopherol like structure (A), a long alkoxy chain (B) or a dihydrofuran group (C) to use as starting materials (Figure 17).

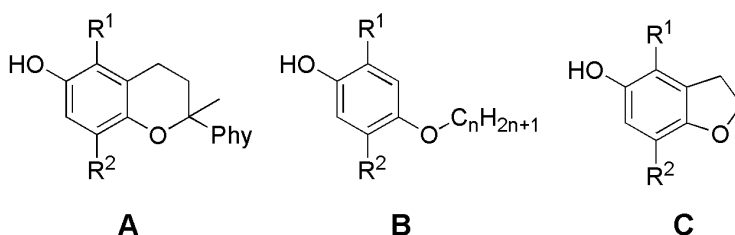
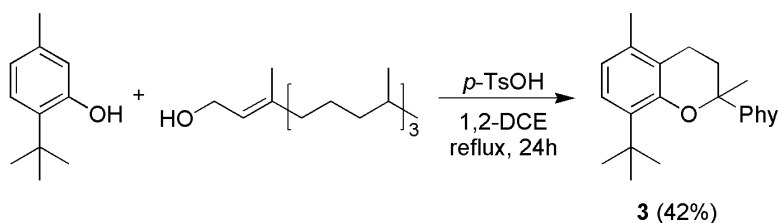


**Figure 17:** R<sup>1</sup> = alkyl; R<sup>2</sup> = H or *tert*-butyl.

The nature and position of the substituents R<sup>1</sup> and R<sup>2</sup> are particularly important. R<sup>1</sup> is in a position that constrains the sulfenylation on the unique unsubstituted *ortho* OH position; R<sup>2</sup> should be H or a removable group because it is the position where the new C-S bond is formed during the acid promoted transposition.

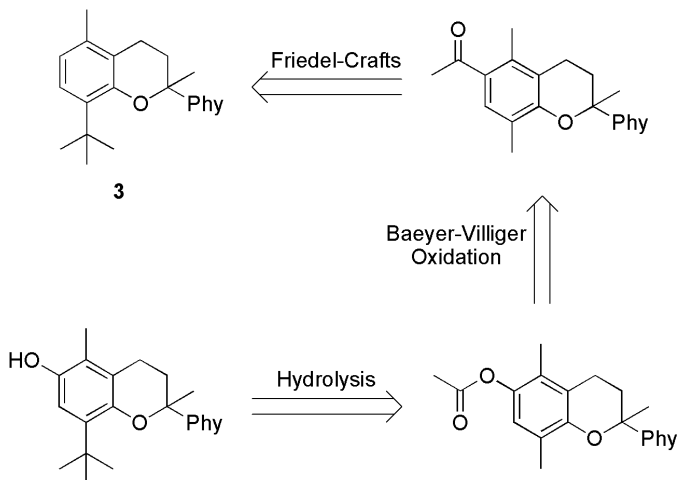
#### *Synthesis of Tocopherol-like phenols (A)*

For the synthesis of a phenol with a Tocopherol-like structure we started from the construction of the chromanol ring. Phytol was reacted with 2-*tert*-Butyl-5-methylphenol (3 equiv) in the presence of 0.05 equiv of *para*-toluenesulfonic acid (*p*-TsOH), allowing the isolation of the chroman derivative **3** in 42% yield (Scheme 5).<sup>22</sup>



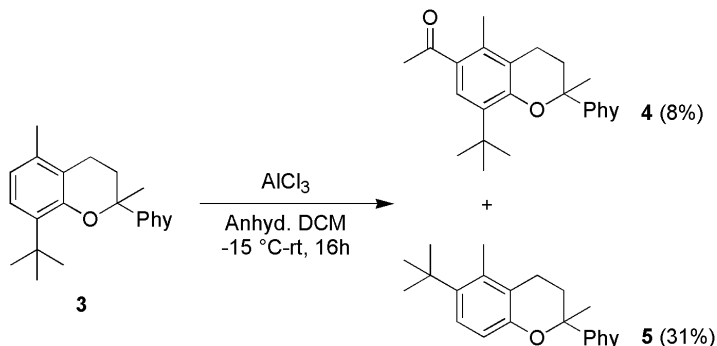
**Scheme 5:** Phy = phytol

Despite a hydroxylation on the C6 position of **3** would have been a direct way for obtaining the desired phenol, this option was discarded. A direct hydroxylation of an aromatic ring requires the use of strong acids for the generation of an electrophilic oxygen from  $\text{H}_2\text{O}_2$ <sup>23</sup> but, under these conditions, chromans are generally unstable and undergo ring opening.<sup>24</sup> A three steps alternative synthetic route constituted by: 1) the Friedel-Crafts acylation of **3**; 2) a Baeyer-Villiger transposition with the formation of an acetyl ester; 3) the hydrolysis of the ester (Scheme 6) was envisaged.



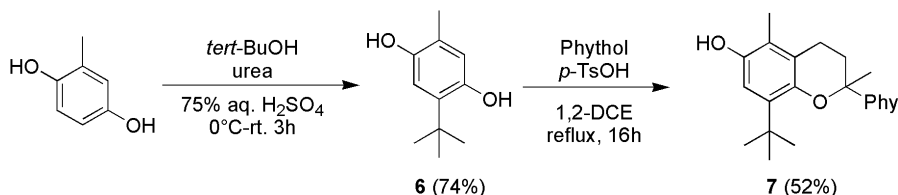
**Scheme 6**

The Friedel-Crafts acylation of **3** with acetyl chloride was done using  $\text{AlCl}_3$  as catalyst.<sup>25</sup> Unfortunately, the alkylarylketone **4** was obtained in very low yield (8%) because, under the acid conditions used, the retro-alkylation/alkylation of the *tert*-butyl group took place giving derivative **5** as the main product (Scheme 7).



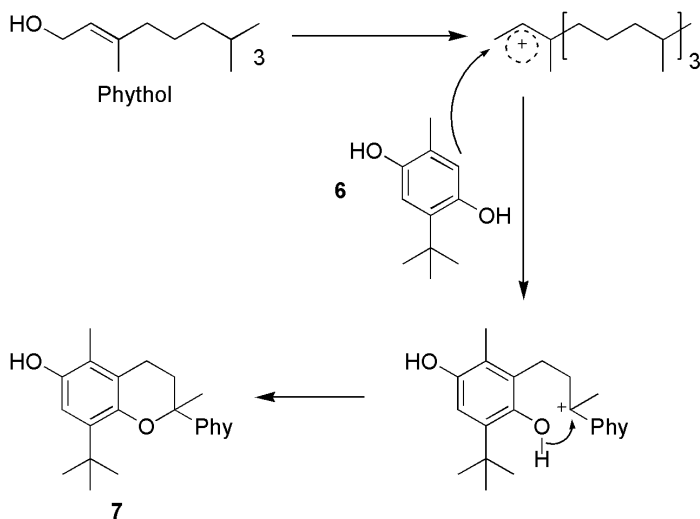
**Scheme 7**

Thus, we decided to use a methylhydroquinone as starting material and to introduce, in sequence, the *tert*-butyl group and the phytol substituted chroman moiety (Scheme 8).



**Scheme 8**

*tert*-Butylation was carried out with *tert*-butanol in the presence of urea<sup>25</sup> to give 2-*tert*-butyl-4-methylphenol **6** in 74% yield. This was converted into the desired Tocopherol-like phenol **7** using phytol and *p*-TsOH acid (0.005 equiv) in 1,2-DCE (Scheme 8). Despite the presence in **6** of two hydroxyl groups with a free adjacent position, hence two different chroman derivatives possibly formed, compound **7** was the unique isomer obtained (Scheme 9). The sensitivity of the ring closure to steric hindrance suggests a stepwise mechanism where: 1) the first step is an intermolecular electrophilic attack by the phenolic ring to the allylic cation derived from phytol; 2) the second step is an intramolecular cyclization (Scheme 9).

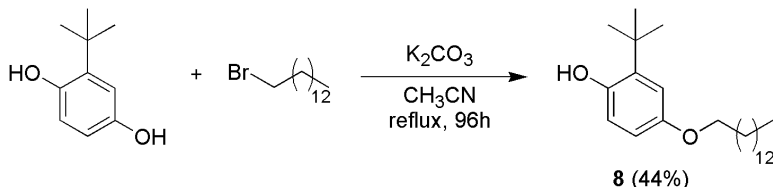


**Scheme 9**

#### Synthesis of phenols with a non-phytylic long alkoxy lateral chain (**B**)

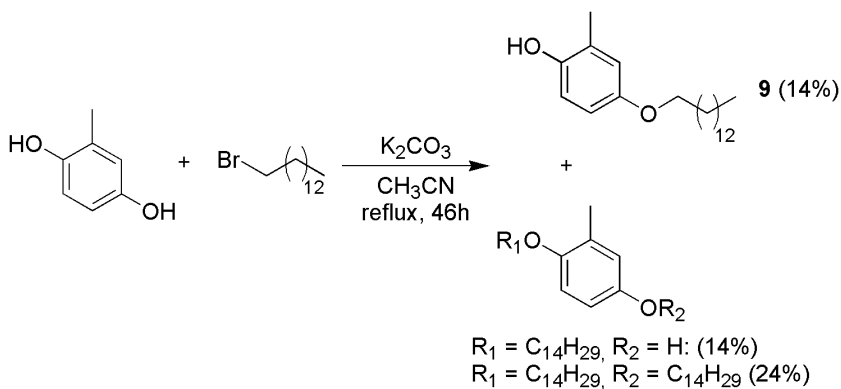
Two different phenols characterized by a long alkylate chain in *para* to the phenolic OH were prepared. Both of them were obtained in a single step. The first was synthesized through a Williamson reaction of *tert*-butylhydroquinone with 1-bromotetradecane in the presence of  $\text{K}_2\text{CO}_3$  as base (Scheme 10). The alkylation occurred preferentially on

the C4 OH, allowing the isolation of **8** as the major product with a tiny lower amount of the corresponding *bis*-alkylated product.



**Scheme 10**

The second phenol derivative **9** was synthesized by an analogue Williamson reaction of 1-bromotetradecane with methylhydroquinone (Scheme 11). In this case, the yield of the desired product **9** was quite low because of the poor steric hindrance differentiation around the two hydroxyl groups. The major product was the *bis*-alkylated (24%), while both mono-alkylated were isolated in roughly 14% yield.



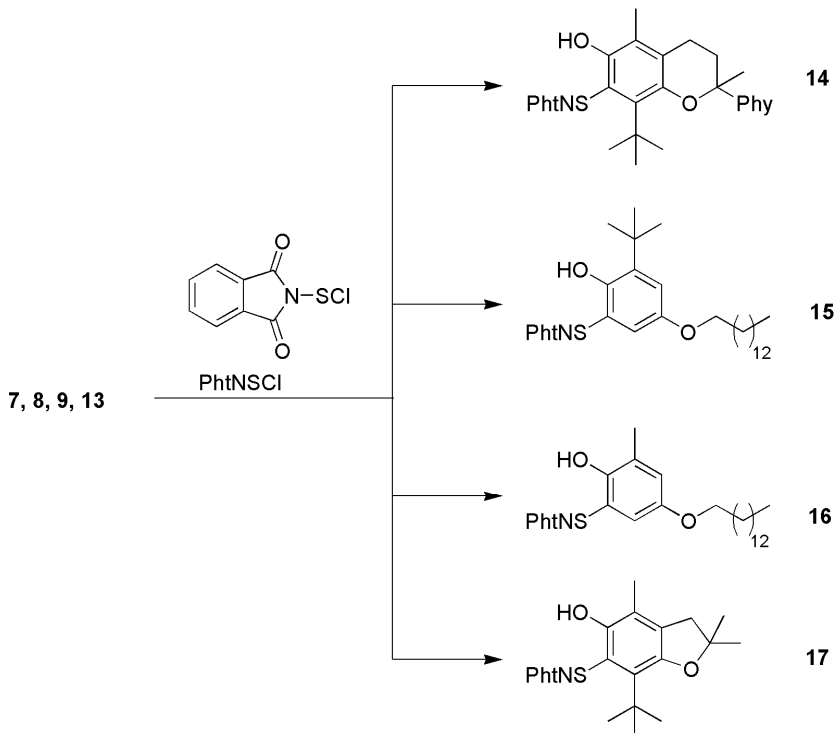
**Scheme 11**

The preparation of **9** was also achieved using a different synthetic way (Scheme 12). 3-Methylphenol was alkylated with 1-bromotetradecane and the resulting ether **10** was acylated using acyl chloride. The following Baeyer-Villiger oxidative transposition allowed the conversion of the ketone **11a** to the corresponding acetyl ester **12** which, in turn, was hydrolysed in the final step achieving the desired phenol **9**. Unfortunately, the overall yield of this procedure was low (11%) because of the concomitant formation, in the second step, of the *ortho*-OR acylated regioisomer **11b** (ratio **11a/11b** : 1/1).





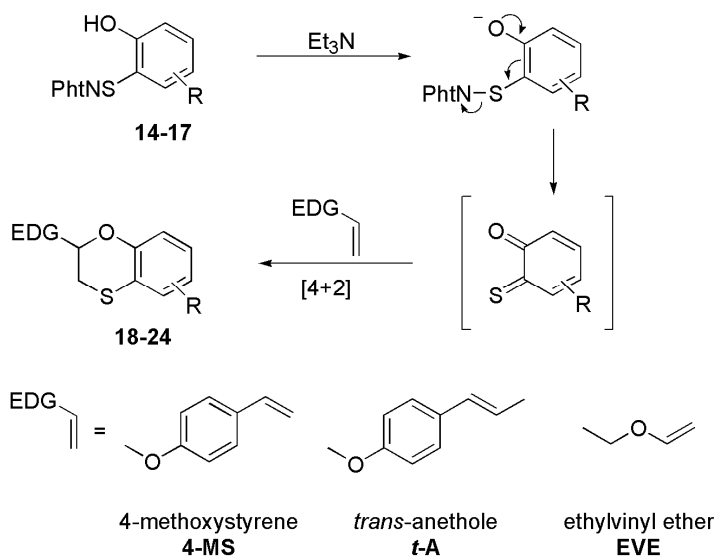
desired *ortho*-hydroxy-*N*-thiophthalimides **14**, **15**, **16** and **17** were obtained in quantitative yield and used in the next step without any purification (Scheme 14).



Scheme 14

### 2.2.3 Synthesis of benzo[*b*][1,4]oxathiine derivatives

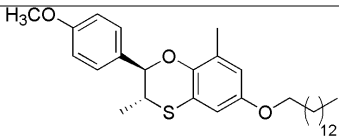
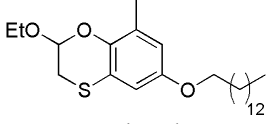
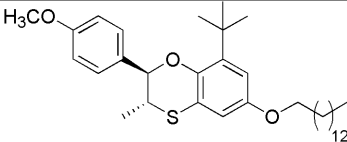
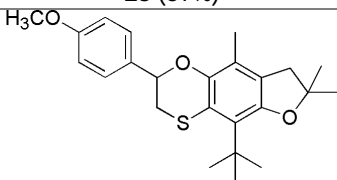
In the presence of tertiary amines, *ortho*-hydroxy-*N*-thiophthalimides are transformed into the corresponding *ortho*-thioquinones which, in turn, take part to an inverse electron demand hetero Diels-Alder reaction with electron-rich alkenes.<sup>27</sup> Derivatives **14-17** were transformed into the corresponding thioquinones with triethylamine (TEA) and allowed to react with 4-methoxystyrene (4-MS), *trans*-anethole (*t*-A) or ethylvinyl ether (EVE) (Scheme 15) to obtain the expected benzo[*b*][1,4]oxathiines **18-24** reported in Table 1.



**Scheme 15**

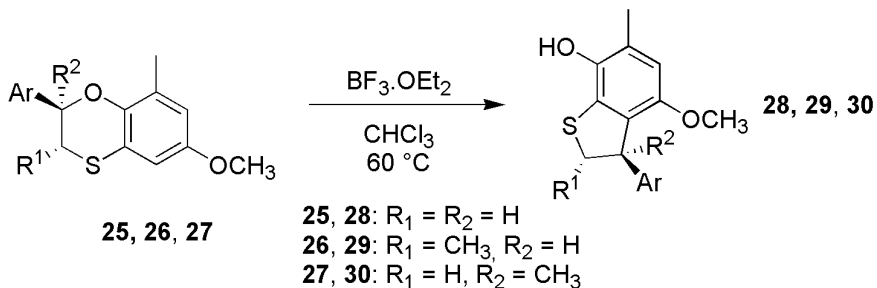
**Table 1:** Reactions performed at 60 °C in a 0.1 M solution of the *ortho*-hydroxy-N-thiophthalimide in  $\text{CHCl}_3$ .

Substrate	Dienophile (equiv)	Time (h)	Product (yield %)
<b>14</b>	4-MS (3)	24	 <b>18 (72%)</b>
<b>14</b>	<i>t</i> -A (2 equiv)	24	 <b>19 (28%)</b>
<b>16</b>	4-MS (3)	19	 <b>20 (36%)</b>

16	<i>t</i> -A (2)	22	 <b>21 (37%)</b>
16	EVE (10)	17	 <b>22 (53%)</b>
15	<i>t</i> -A (2)	96	 <b>23 (37%)</b>
17	4-MS (3)	16	 <b>24 (59%)</b>

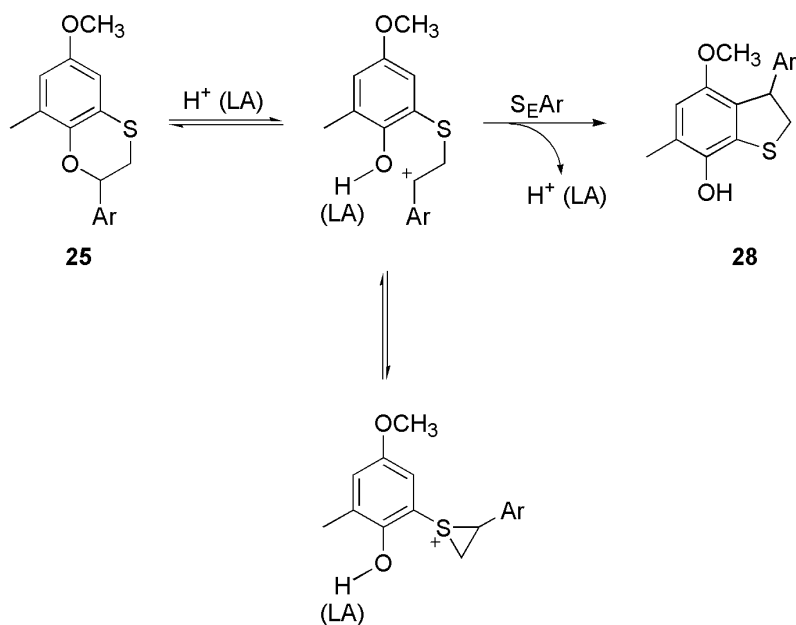
## 2.2.4 Transposition reaction of benzo[*b*][1,4]oxathiine derivatives

Recently, we reported<sup>21</sup> a synthetic procedure that, starting from benzo[*b*][1,4]oxathiines **25**, **26**, and **27** allowed to obtain 7-hydroxy dihydrobenzo[*b*]thiophenes **28**, **29**, and **30** (Scheme 16).



**Scheme 16:** Ar = 4-methoxyphenyl

These derivatives showed an excellent radical scavenger activity, with  $k_{inh}$  ranging from 1.4-1.6 x 10<sup>6</sup> M<sup>-1</sup> s<sup>-1</sup> (slightly lower than  $\alpha$ -TOH,  $k_{inh}$  = 3.2 x 10<sup>6</sup> M<sup>-1</sup> s<sup>-1</sup>). Their formation is the result of an acid promoted transposition with the mechanism depicted in Scheme 17 for the derivative **25**.



**Scheme 17;** Ar = 4-methoxyphenyl

In the first step an acid-catalysed ring-opening of the benzo-fused oxathiine ring occurs with the formation of a benzylic carbocation reasonably in equilibrium with a thiiranium ion.<sup>28–35</sup> In the second step, an intramolecular  $\text{S}_E\text{Ar}$  takes place leading to the closing of the dihydrobenzo[*b*]thiophene ring.

During my PhD, studying this reaction in more details, we discovered that, under the conditions used (3 equiv of  $\text{BF}_3 \cdot \text{OEt}_2$  in  $\text{CHCl}_3$  at 60 °C see Scheme 16), the transposition of the benzo[*b*]oxathiine **27** ( $\text{R}^1 = \text{H}$ ,  $\text{R}^2 = \text{CH}_3$ ), besides the expected derivative **30**, allowed the isolation of benzo[*b*]thiophene **31** in 16% yield (Figure 18).

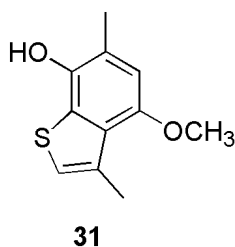
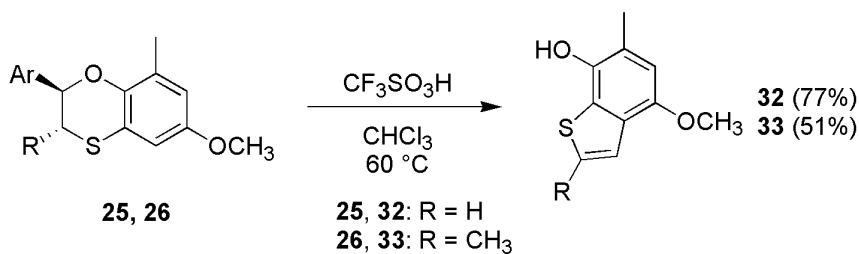


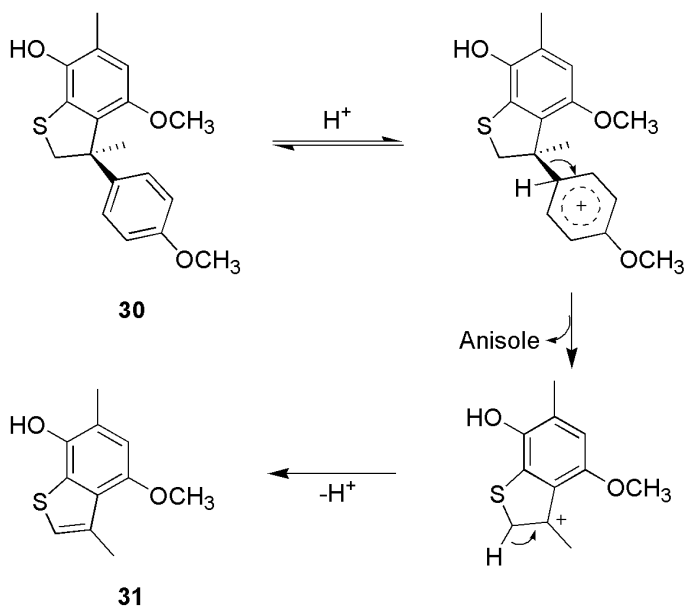
**Figure 18**

Reacting **27** under harsher acid conditions (1 equiv of  $\text{CF}_3\text{SO}_3\text{H}$ ) and longer reaction time allowed the formation of **31** as the unique product in 46% yield. The reaction showed to be quite general since repeating the same procedure on **25** and **26**, the benzo[*b*]thiophenes **32** and **33** were isolated in 77% and 51% yield respectively (Scheme 18).



**Scheme 18:** Ar = 4-methoxyphenyl

The unexpected formation of derivatives **31**, **32** and **33** can be explained considering an acid promoted retro-alkylation (from the anisole ring)<sup>36</sup> with elimination of a benzo[b]oxathiine cation, followed by a deprotonative aromatization process (Scheme 19). Thus, the more stable the intermediate cation the easier will be the process and in the case of **27** even using  $\text{BF}_3 \cdot \text{OEt}_2$  it was possible to promote the formation of the corresponding tertiary carbocation while for benzo[*b*]oxathiines **25** and **26** the formation of a less stable secondary carbocation required harsher acid conditions (triflic acid).



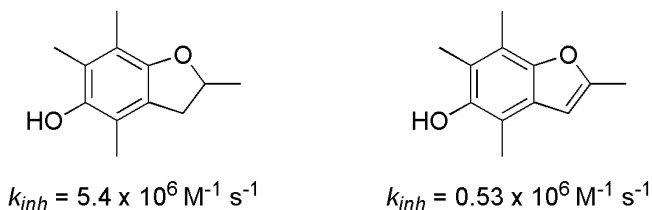
**Scheme 19**

Beside the appeal of such synthetic procedure, the most surprisingly characteristic of benzo[*b*]thiophenes **31**, **32** and **33** was their excellent radical scavenger activity. Indeed, measured  $k_{inh}$  of these derivatives were higher than those of the corresponding dihydrobenzo[*b*]thiophenes and actually better than that of  $\alpha$ -TOH itself (Table 2).

**Table 2:**  $k_{inh}$  values of dihydro- and benzo[*b*]thiophenes.

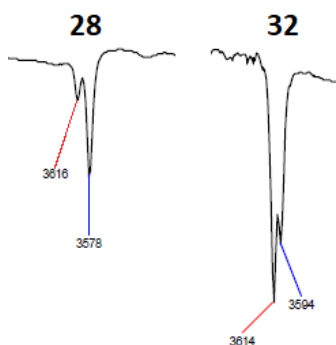
Dihydrobenzo[ <i>b</i> ] thiophenes	$k_{inh}$ ( $10^6 \text{ M}^{-1} \text{ s}^{-1}$ )	Benzo[ <i>b</i> ] thiophenes	$k_{inh}$ ( $10^6 \text{ M}^{-1} \text{ s}^{-1}$ )
<b>28</b>	1.5	<b>32</b>	5.0
<b>29</b>	1.4	<b>33</b>	5.9
<b>30</b>	1.6	<b>31</b>	3.3

These results were apparently inconsistent with literature data because the aromatization of similar derivatives like 2,3-dihydrobenzofuran-5-ols leads to a decrease of about one order of magnitude of the  $k_{inh}$  values (Figure 19).<sup>14</sup>



**Figure 19**

In benzo[*b*]furanols there is a breakdown of the antioxidant activity because, despite the enhanced planarity, the aromatization decreases the electron-donating ability of the endocyclic oxygen atom and then the stabilization of the phenoxyl radical. Consistent with these findings, and considering the aromatic character of thiophenes vs furanes, for the derivatives **31**, **32** and **33**  $k_{inh}$  values at least one order of magnitude lower than those of the dihydrobenzo[*b*]thiophenes **30**, **28** and **29** were expected. On the contrary, opposite results were obtained, with  $k_{inh}$  values of the benzo[*b*]thiophenes up to four times higher than those of the corresponding dihydro precursors. To rationalise this result, at least in part, we can consider the lower capacity of the benzo[*b*]thiophenes to give IHB respect to dihydrobenzo[*b*]thiophenes. In fact, FT-IR spectra demonstrated for derivative **32** (Figure 20) a free O-H stretching ( $3614 \text{ cm}^{-1}$ ) more intense than that involved in IHB. Instead, in dihydrobenzo[*b*]thiophene **28** the stretching of O-H involved in IHB ( $3578 \text{ cm}^{-1}$ ) is predominant.

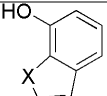


**Figure 20:** Enlargement of the FTIR spectra of **28** (left) and **32** (right).

This can be explained considering the previous consideration on IHB strength and relative conformation of the *ortho*-sulfur containing substituent related with the complete planarity of aromatic benzo[*b*]thiophenes. However, these arguments are not enough to justify data reported in Table 2 and additional effects responsible for the extra stabilization of the phenoxyl radical involving the sulfur atom have to be envisioned. The issue was deeply studied by determining through theoretical calculations the BDE(OH) of these benzofused phenols.<sup>37,38</sup> Benzo[*b*]thiophenes **32** and **33** showed identical BDE(OH) values (74.6 kcal mol<sup>-1</sup>) that were 3.2 kcal mol<sup>-1</sup> lower than **28** and **29** (77.8 kcal mol<sup>-1</sup>) and 1.0 kcal mol<sup>-1</sup> lower than 2,2,5,7,8-pentamethylchroman-6-ol (PMC), an analogous of  $\alpha$ -TOH used to simplified theoretical calculations. Benzo[*b*]thiophenes seem thus actually characterized by a better radical scavenger activity than dihydrobenzo[*b*]thiophenes both in terms of calculated BDE(OH) and experimental kinetic results. To further deepen the matter the same theoretical calculations were done to determine the BDE(OH) of parent 5- and 7-hydroxybenzo-fused five membered heterocycles containing O, S, and Se atoms (Table 3).

**Table 3:** Calculated ArO-H BDE and Most Positive  $\sigma$ -Hole Electrostatic Potentials on S and Se atom

Substrate	BDE <sup>a</sup>			$V_{s,max}^{a,b}$ ArOH / ArO <sup>•</sup>	
	X=O	X=S	X=Se	X=S	X=Se
	79.5	81.1	81.9	24 / 44	32 / 47
	84.2	84.7	84.9	37 / 50	41 / 54
	84.3	83.3	83.4	26 <sup>c</sup> / 38	31 <sup>c</sup> / 41

	84.3	82.1	82.6	36 <sup>c</sup> / 44	40 <sup>c</sup> / 48
---	------	------	------	----------------------	----------------------

<sup>a</sup>kcal/mol. <sup>b</sup>Calculated on an isodensity surface corresponding to 0.005 au by Multiwfn software.<sup>38</sup> <sup>c</sup>Relative to the most stable conformer with the O-H bond pointing opposite to S or Se atom, as shown in Figure 29. See the experimental section for details.

5-Hydroxy derivatives had a behaviour that is in accordance with literature data. In these systems, characterized by the *para* position of the endocyclic heteroatom respect to the phenolic OH, the aromatization has a negative impact on the BDE(OH), in particular for furans. Instead, the opposite result was observed with 7-hydroxy derivatives, where the endocyclic heteroatom is in *ortho* to the phenolic OH. With these systems, with the aromatization if the heteroatom is oxygen the BDE does not change while if it is sulfur or selenium, it decreases. Analogous results were obtained by the measurement of the enthalpy differences ( $\Delta H$ ) among the phenoxyl radicals. With all the heteroatoms, *ortho*-dihydroradicals are less stable than *para* radicals (up to 3.6 kcal mol<sup>-1</sup> for dihydrofurans, Figure 21, A), while *ortho* "heteroatomic" radicals are more stable than *para* radicals (more than 3 kcal mol<sup>-1</sup> for thiophenes and selenophenes, Figure 21, B).

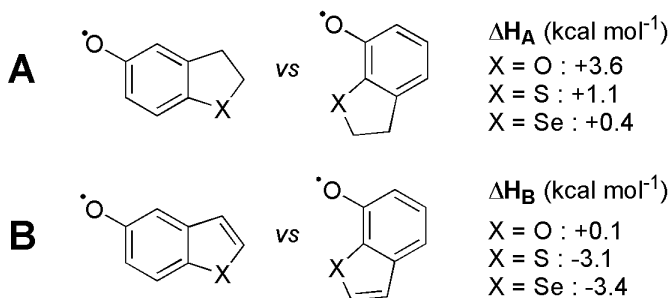


**Figure 21**

These outcomes suggested the presence of some intramolecular interaction between an electron-deficient area on the surface of the covalently bonded chalcogen (S or Se) and the negative surface of the O atom<sup>39</sup> that leads to the stabilization of the phenoxyl radical. This interaction was found thanks to the analysis of the electrostatic potential surfaces of the benzothiophene phenoxyl radical (Figure 22), that revealed the presence of  $\sigma$ -holes<sup>40,41</sup> as two regions of positive potential along the outer side of the carbon-chalcogen  $\sigma$ -bonds.



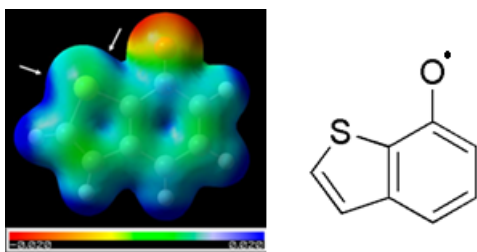


**Figure 22:** Molecular electrostatic potential showing the  $\sigma$ -hole position (blue, positive potential; red, negative potential).

As demonstrated by the quantitative analysis of electrostatic potential surfaces (Table 3), there is an enhancement of the  $\sigma$ -hole magnitude when:

- 1) The atomic number of the chalcogen increases ( $O \rightarrow S \rightarrow Se$ ).
- 2) The system is aromatic.
- 3) Phenoxy radicals are considered instead of phenols.

In the electrostatic potential map of 7-hydroxy-benzo[*b*]thiophene radical (Figure 22)  $\sigma$ -holes are indicated by the arrows. It is then possible that the extra stabilization of the  $ArO^{\bullet}$  in benzo[*b*]thiophenes is due to a noncovalent interaction between the negative electronic density of the oxygen centred phenoxy radical and the sulfur  $\sigma$ -hole. Instead, if we take in consideration the 7-hydroxy-benzo[*b*]furan radical, its electrostatic potential map reveals the absence of the  $\sigma$ -hole around the endocyclic oxygen due to its higher electronegativity respect to sulfur (Figure 23). The absence of the  $\sigma$ -hole in the 7-hydroxy-benzo[*b*]furan radical explains the missing effect of extra stabilization of the radical and the low antioxidant activity of these systems.

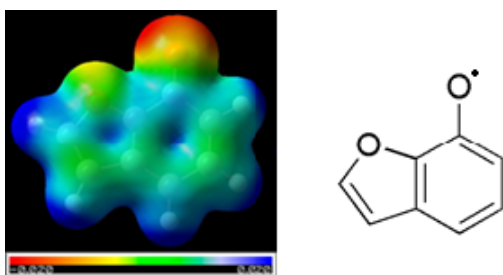


**Figure 23**

The high radical scavenger activity of benzo[*b*]thiophenes seems to be related to a noncovalent sulfur-oxygen interaction that stabilizes its phenoxy radical form. The occurrence of this type of interactions has been demonstrated in different domains like the rationalization of the receptor-drug binding<sup>42,43</sup> or the preferred conformation of polythiophenes in organic electronic devices.<sup>44-48</sup> However, to the best of our knowledge, the stabilization of a phenoxy radical intermediate has not been reported

yet. Actually, the alignment between the  $\sigma$ -hole and the oxygen lone pair is not optimal in our systems for an oxygen-sulfur noncovalent interaction. However, in support of our argument, several examples of “directionally unfavourable” intramolecular interactions are reported in literature<sup>42–48</sup> and NBO (Natural Bond Orbital) perturbation theory analysis revealed a weak interaction between an oxygen lone pair and the  $\sigma^*$ <sub>(S-C2)</sub> in the 7-benzothiophenoxyl radical (0.16 and 0.18 kcal/mol for  $\alpha$  and  $\beta$  spin sets, respectively). This interaction is absent in the 7-benzofuranoxyl radical. Additionally, an oxygen-sulfur  $\sigma$ -hole interaction is also present when approaching parent phenoxyl radical and thiophene, a simplified intermolecular model that we investigated to support our hypothesis (Figure 24).

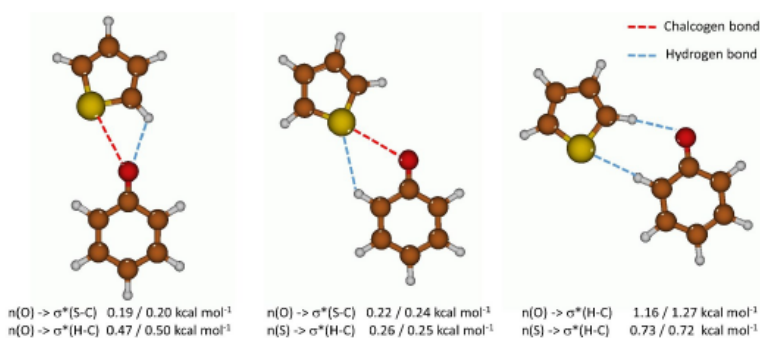


**Figure 24:** Occurrence of H-bonds and chalcogen bonds in the intermolecular model. The interaction energy was obtained by NBO perturbation theory analysis. The geometries were obtained by performing a relaxed energy surface in which the contact angle between S and O atoms (C-O...S) was fixed at 180, 120 and 90 degrees.

All of these data suggest that the high  $k_{inh}$  and low BDE(OH) of 7-hydroxybenzothiophenes can be also ascribed to the formation of a sulfur-oxygen chalcogen bond. This interaction ensures an efficient stabilization of the phenoxyl radical without stabilizing, at the same time, the parent phenol (Figure 25).

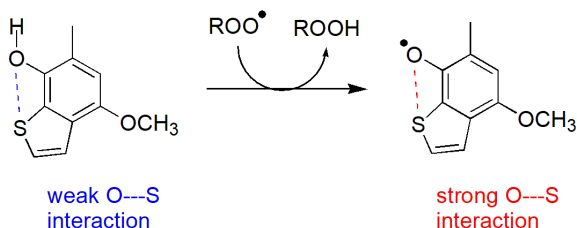
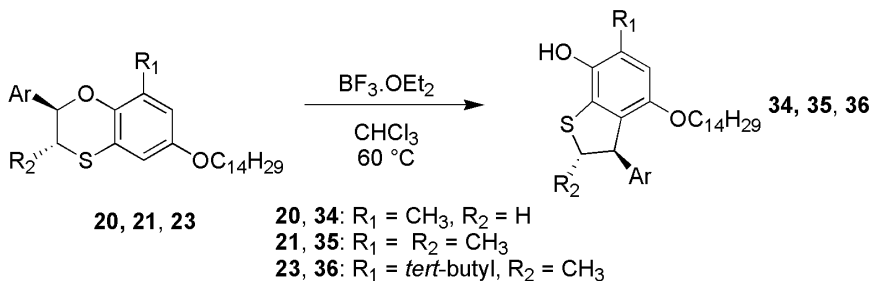


**Figure 25**

The transposition of benzo[*b*][1,4]oxathiines **25–27** to the dihydrobenzo[*b*]thiophenes **28–30** and the subsequent aromatization to the benzo[*b*]thiophenes **31–33** gave interesting results both for the usefulness of the synthetic procedure and the excellent

antioxidant activity of the obtained compounds. Benzo[*b*][1,4]oxathiines **18-24** were then used for the preparation of the corresponding dihydro- and benzo[*b*]thiophenes in order to evaluate their radical scavenger activity.

The reaction of derivatives **20**, **21** and **23** with  $\text{BF}_3 \cdot \text{OEt}_2$  (3 equiv) in  $\text{CHCl}_3$  at  $60^\circ\text{C}$  (Scheme 20) gave the corresponding dihydrobenzo[*b*]thiophenes **34**, **35**, and **36**, respectively, in moderate to good yields (45-63%, Table 4).



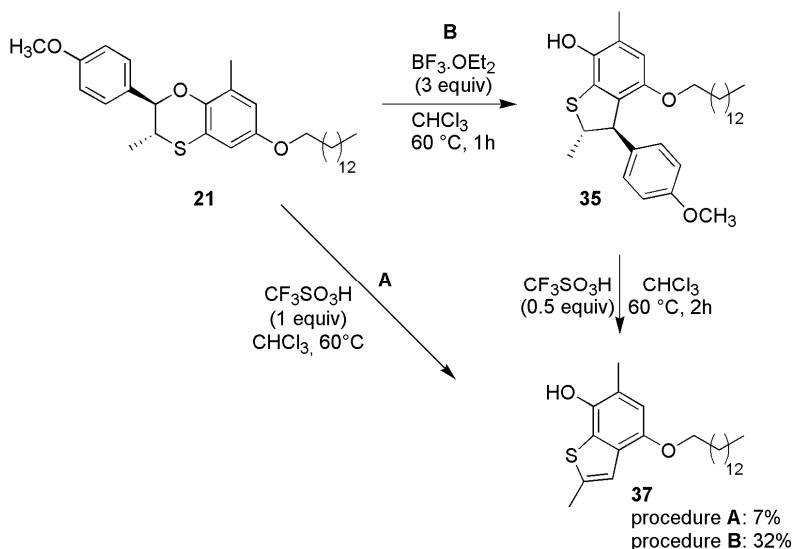
**Scheme 20:** Ar = 4-methoxyphenyl.

**Table 4:** Transposition reactions of benzo[*b*][1,4]oxathiines **20**, **21**, and **23** in a chloroformic solution of  $\text{BF}_3 \cdot \text{OEt}_2$  (3 equiv) at  $60^\circ\text{C}$ .

Substrate	Time	Product (yield %)
<b>20</b>	2h30'	 <b>34 (53%)</b>
<b>21</b>	1h	 <b>35 (63%)</b>
<b>23<sup>a</sup></b>	30h	 <b>36 (45%)</b>

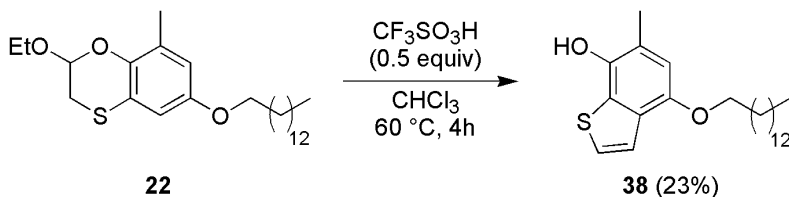
<sup>a</sup> 6 equiv of  $\text{BF}_3 \cdot \text{OEt}_2$  were used.

The attempts of direct transformation of benzo[*b*][1,4]oxathiines **20**, **21**, and **23** to the corresponding benzo[*b*]thiophenes using  $\text{CF}_3\text{SO}_3\text{H}$  as catalyst failed due to the harsher acid conditions that led to the degradation of starting materials. Only in the case of **21** it was possible to obtain the desired derivative **37**, even though in very low yield (7%, Scheme 21 procedure **A**). Derivative **37** was obtained with a better overall yield (32%) performing the two reactions, *i.e.* the transposition with  $\text{BF}_3 \cdot \text{OEt}_2$  (3 equiv) of **21** and the retro-alkylation/deprotonative aromatization with  $\text{CF}_3\text{SO}_3\text{H}$  (0.5 equiv), in separate steps (Scheme 21 procedure **B**).



### Scheme 21

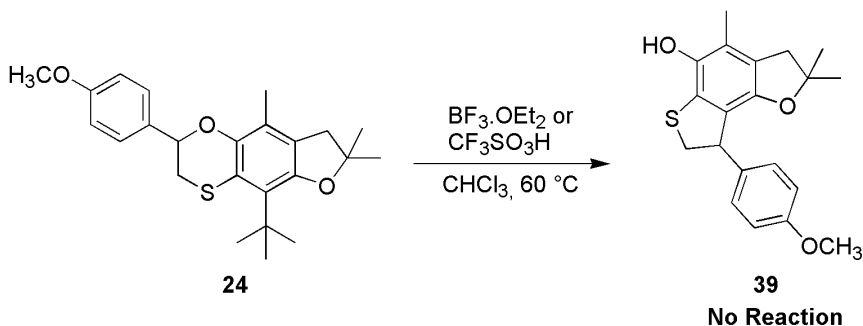
This two-steps synthetic approach did not work for benzo[*b*][1,4]oxathiines **20** and **23**. However, the direct synthesis of the benzo[*b*]thiophene **38** that would have been obtained from **20** was achieved in 23% yield using as starting material the derivative **22** with 0.5 equiv of  $\text{CF}_3\text{SO}_3\text{H}$  (Scheme 22).



### Scheme 22

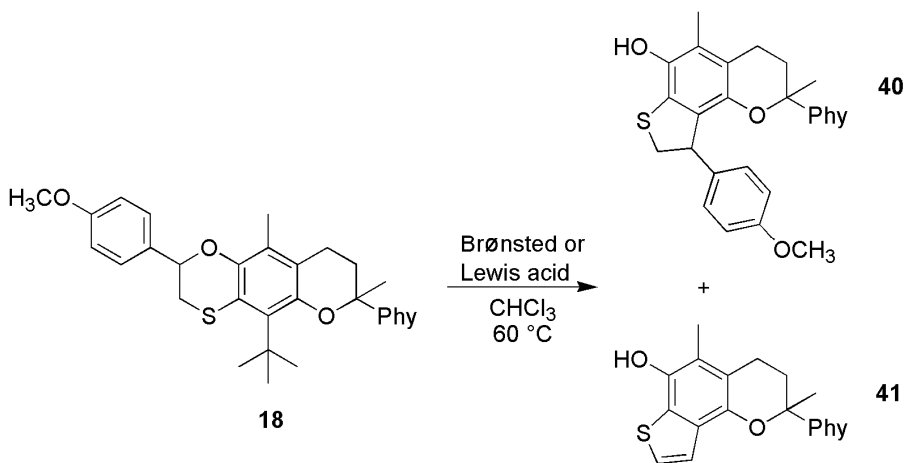
In benzo[*b*][1,4]oxathiines **18**, **19** and **24** a *tert*-butyl group, inserted to ensure the regioselective closure of the chromanic or the dihydrofuranic cycle, was present in the position where the ring closure should occur thus preventing the transposition.

However, we considered the possibility the one-pot procedure used for the transposition could also allow the removal of the *tert*-butyl group, that is labile in acid conditions. Regrettably, reacting derivative **24** under the acid conditions required for the transposition caused extensive decomposition with opening of the dihydrofuranic ring<sup>49</sup> thus preventing the synthesis of dihydrobenzo[*b*]thiophene **39** (Scheme 23).



**Scheme 23**

On the contrary, the chromanic ring of the benzo[*b*][1,4]oxathiine **18** resulted stable under acid conditions and a careful study was done in order to optimize the transposition to the corresponding dihydrobenzo[*b*]thiophene **40** and the subsequent retro-alkylation/deprotonative aromatization to the benzo[*b*]thiophene **41** (Scheme 24 and Table 5).



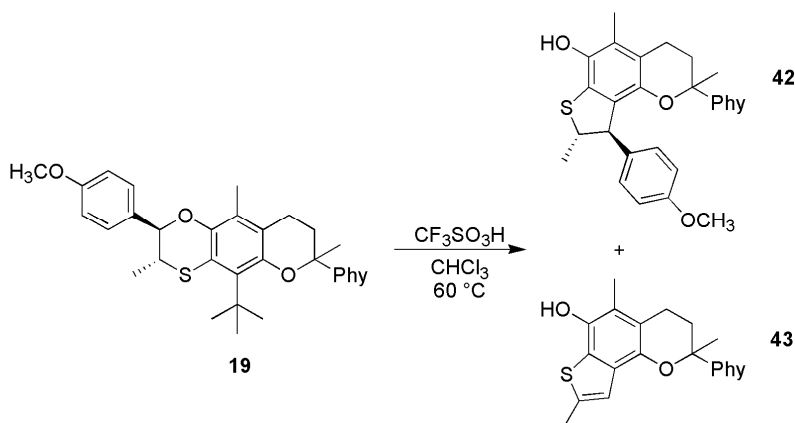
**Scheme 24**

**Table 5:** Transposition reactions of benzo[*b*][1,4]oxathiine **18** in a chloroformic solution of BF<sub>3</sub>.OEt<sub>2</sub> or CF<sub>3</sub>SO<sub>3</sub>H at 60 °C.

Entry	Acid	Equiv	T (°C)	Time	Yield %(40)	Yield %(41)
1	AlCl <sub>3</sub>	1	60	1h30'	-	-
2	BF <sub>3</sub> .OEt <sub>2</sub>	3	25	3h30'	39	-
3	CF <sub>3</sub> SO <sub>3</sub> H	3	60	4h	-	-
4	CF <sub>3</sub> SO <sub>3</sub> H	0.5	60	2h	55	14
5	CF <sub>3</sub> SO <sub>3</sub> H	1	60	1h30'	60	8
6	CF <sub>3</sub> SO <sub>3</sub> H	1	60	2h30'	7	40

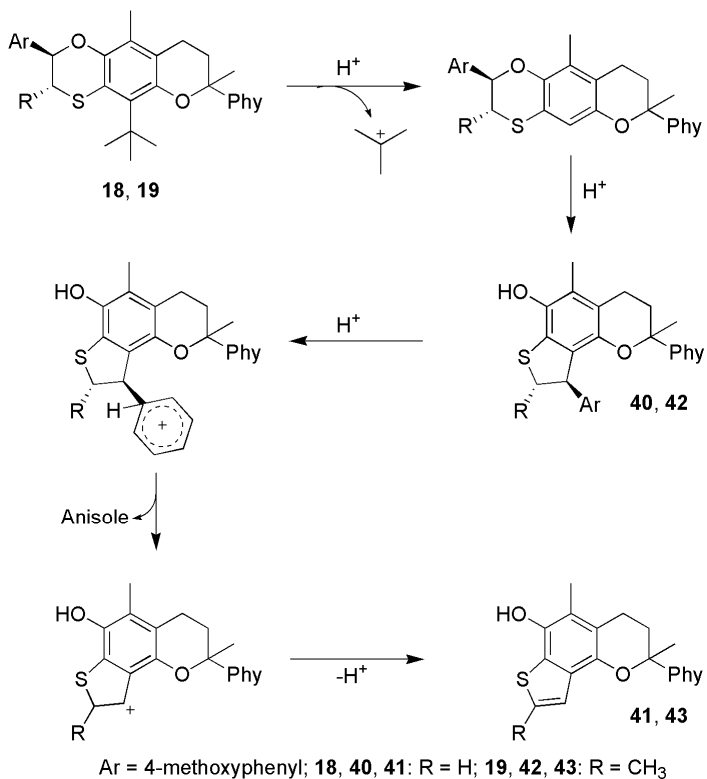
Using AlCl<sub>3</sub> as catalyst (entry 1) the retro-alkylation of the *tert*-butyl group took place but neither the two possible transposition products (**40** and/or **41**) were obtained. With BF<sub>3</sub>.OEt<sub>2</sub> (entry 2) in accordance with the previous reported results both the de-*tert*-butylation and the transposition occurred, and the dihydrobenzo[*b*]thiophene **40** was isolated in 39% yield. Better results were obtained with CF<sub>3</sub>SO<sub>3</sub>H as catalyst. An excess of this acid (entry 3) led to the expected degradation of the chromanic ring of **18**.<sup>24</sup> Instead using CF<sub>3</sub>SO<sub>3</sub>H in substoichiometric amount (entry 4) it was possible to isolate the benzo[*b*]thiophene **41**, even though the major product was still its dehydro-precursor **40**. Similar results were obtained enhancing the amount of the acid to 1 equiv (entry 5). Eventually, using longer reaction time (2h30', entry 6) **41** was achieved in 40% yield.

An analogous sensibility to reaction conditions was observed with the benzo[*b*]oxathiine **19** (Scheme 21). Using the same conditions (1 equiv of CF<sub>3</sub>SOH in CHCl<sub>3</sub> at 60 °C), the dihydrobenzo[*b*]thiophene **42** was the unique product isolated after 2h in 56% yield. Longer reaction times (3h30') allowed the isolation of the benzo[*b*]thiophene **43** as unique product in 38% yield (Scheme 25).



**Scheme 25**

The acid catalysed transposition of benzo[*b*]oxathiines **18-23** allowed to prepare the dihydrobenzo[*b*]thiophenes **34, 35, 36, 40,** and **42** and the benzo[*b*]thiophenes **37, 38, 41** and **43** that were investigated for their antioxidant properties, as it will be discussed in the next section. The preparation of these products was possible through a one-pot procedure where all of the steps are catalysed by the acid conditions used (Scheme 26).



**Scheme 26**

The general mechanism of this reaction is constituted, for the benzo[*b*][1,4]oxathiines containing a *tert*-butyl group in the position where the ring closure occurs, by five consecutive electrophilic events.

The first step catalysed by the acid conditions is the removal of the *tert*-butyl group. Afterwards, the ring opening of the benzoxathiine ring is possible after the interaction between its endocyclic oxygen and a Brønsted or Lewis acid, and the following ring closure leads to the formation of a dihydrobenzo[*b*]thiophene. In the next step the anisyl group is protonated with the formation of a relatively stable carbocation that is eliminated through a retro S<sub>E</sub>Ar. Finally, a deprotonative aromatization leads to the formation of the benzothiophene ring. Actually, it is not possible to know if the de-*tert*-

butylation foreruns the ring opening or conversely, however both cases do not influence the right progression of the transposition reaction.

### 2.2.5 Antioxidant activity of dihydro- and benzo[*b*]thiophenes

The radical scavenger activity of the synthesized benzo[*b*]thiophenes and dihydrobenzo[*b*]thiophenes was evaluated by the measurement of their  $k_{inh}$ . These measures were done by determining the ability of these molecules to inhibit the thermally initiated autooxidation of styrene, that is kinetically comparable to that of polyunsaturated fatty acids, and were carried out by the research group of Dr. R. Amorati of the University of Bologna. These experiments were done in an apparatus that measures the variation of oxygen concentration thus allowing to plot its consumption over time (see experimental section for details).

Diagrams obtained for derivatives **40**, **41**, **42** and **43** are reported in Figure 26. In the presence of good antioxidants, substrate oxidation and oxygen consumption were much slower than in their absence, and a clear inhibition period was observed.

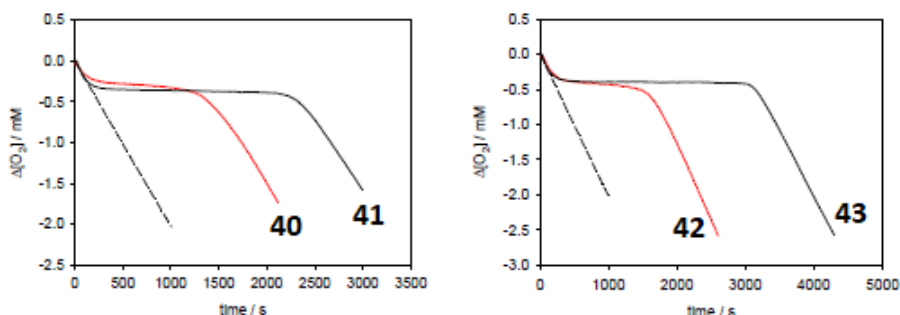


**Figure 26:** Oxygen consumption during the autooxidation of styrene in chlorobenzene initiated by AIBN at 30°C without inhibitors (dashed) or in the presence of **40** (5.2  $\mu$ M) and **41** (8.2  $\mu$ M); (left) **42** (5.0  $\mu$ M) and **43** (7.6  $\mu$ M) (right).

It was possible to calculate the rate constants for the reaction with  $ROO^*$  radicals ( $k_{inh}$ ) because the rate of  $O_2$  consumption during the inhibition period is inversely dependent on  $k_{inh}$  and the concentration of the antioxidant. From the length of the inhibition period were obtained the values of  $n$ , *i.e.* the number of  $ROO^*$  radicals trapped by each antioxidant molecule. Resulting data are reported in Table 6, together with those of reference  $\alpha$ -TOH and dihydro- and benzo[*b*]thiophenes **28**, **29**, **32** and **33**.



**Table 6:** Reactivity towards peroxy radicals ( $k_{inh}$ ) of dihydrobenzo[*b*]thiophenes and benzo[*b*]thiophenes.

Dihydrobenzo[ <i>b</i> ]thiophene	$k_{inh}$ ( $10^6 \text{ M}^{-1} \text{ s}^{-1}$ )	n	Benzo[ <i>b</i> ]thiophene n	$k_{inh}$ ( $10^6 \text{ M}^{-1} \text{ s}^{-1}$ )	
<b>28</b>	1.5	1.9	<b>32</b>	5.0	1.9
<b>29</b>	1.4	2.1	<b>33</b>	5.9	1.7
<b>40</b>	3.2	1.5	<b>41</b>	7.4	1.6
<b>42</b>	2.9	1.9	<b>43</b>	9.8	1.9
<b>34</b>	1.8	1.8	<b>38</b>	5.2	1.9
<b>35</b>	1.6	1.9	<b>37</b>	6.3	1.8
<b>36</b>	1.2	1.9	<b><math>\alpha</math>-TOH</b>	3.2	2

All of the products showed a rate inhibition constant of the same order of magnitude of  $\alpha$ -TOH, confirming that the presence of an endocyclic sulfide sulfur in *ortho* to the phenolic OH is responsible for a good antioxidant activity. In all the cases the benzo[*b*]thiophenes resulted to be best free radical scavengers than their dihydro-parent analogous, with  $k_{inh}$  values at least 2 times higher. As expected, the chromanic and the thiophenic rings fused together in the right position ensure an outstanding antioxidant activity. Among the prepared derivatives, the best proved to be those containing the chromanol moiety of vitamin E. Indeed, the  $k_{inh}$  values of **41** ( $7.4 \times 10^6 \text{ M}^{-1} \text{ s}^{-1}$ ) and **43** ( $9.8 \times 10^6 \text{ M}^{-1} \text{ s}^{-1}$ ) are up to three times higher than the reference  $\alpha$ -TOH. Instead, benzo[*b*]thiophenes with an alkoxy lateral chain (**38** and **37**) are better antioxidants than  $\alpha$ -TOH but did not match **41** and **43**. Concerning the structure-activity relationship inside each type of derivatives, in the series of benzo[*b*]thiophenes the presence of a methyl substituent in *ortho* to the thiophenic sulfur causes an increase of the antioxidant activity (**32** vs **33**, **41** vs **43** and **38** vs **37**). Instead, in the series of dihydrobenzo[*b*]thiophenes the same modification is responsible for a modest decrease of  $k_{inh}$  values (**28** vs **29**, **40** vs **42** and **34** vs **35**). The less strong antioxidant among the dihydrobenzo[*b*]thiophene derivatives is **36**, characterized by the presence of a *tert*-butyl group adjacent to the phenolic OH instead of a methyl. However, also in this case the decrease of  $k_{inh}$  is modest.

### 2.2.6 Binding affinity of $\alpha$ -TTP for benzo[*b*]thiophenes

Derivatives **34-43** were synthesized with the aim to obtain antioxidants with a radical scavenger activity comparable or even superior to that of  $\alpha$ -TOH, the most powerful liposoluble antioxidant known in nature. Considering the structure of benzo[*b*]thiophenes **41** and **43**, characterized by the presence of the chromanol moiety of  $\alpha$ -TOH (Figure 27), it was then interesting to evaluate if they were recognized by the  $\alpha$ -tocopherol transfer protein ( $\alpha$ -TTP).

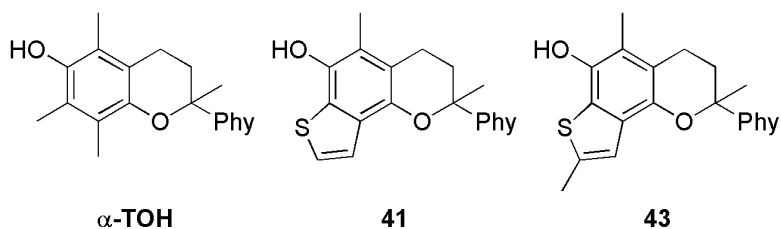


**Figure 27**

$\alpha$ -TTP is responsible for the incorporation of  $\alpha$ -TOH into nascent VLDL in living organisms.<sup>50</sup> The activity of this protein maintains the normal plasma concentration of the antioxidant and a pathology called ataxia with vitamin E deficiency (AVEC) has been associated to a mutation of the  $\alpha$ -TTP.<sup>51</sup> Several residues of tryptophan are present in the hydrophobic pocket close to the residues reported to be involved in  $\alpha$ -TOH binding, then the quenching of their fluorescence can be used to measure the binding affinity of a ligand in terms of dissociation constant ( $K_d$ ).<sup>52</sup> The binding affinity of derivatives **41** and **43** with  $\alpha$ -TTP was studied by fluorescent titration experiments in collaboration with Professor G. Caminati (Department of Chemistry 'Ugo Schiff', University of Florence).

All-*rac*- $\alpha$ -TOH was used as reference ligand in order to have a coherent comparison with our transposition products, all obtained as diastereoisomeric mixtures of racemates. Experimental results showed that the addition of either **41** or **43** leads to a sharp decrease of the intrinsic tryptophan fluorescence at 340 nm of the  $\alpha$ -TTP (Figure 28, left), and the magnitude of fluorescence quenching is function of ligand concentration (Figure 28, right). These diagrams showed that all the ligands exhibit a similar quenching behaviour in the same concentration range.

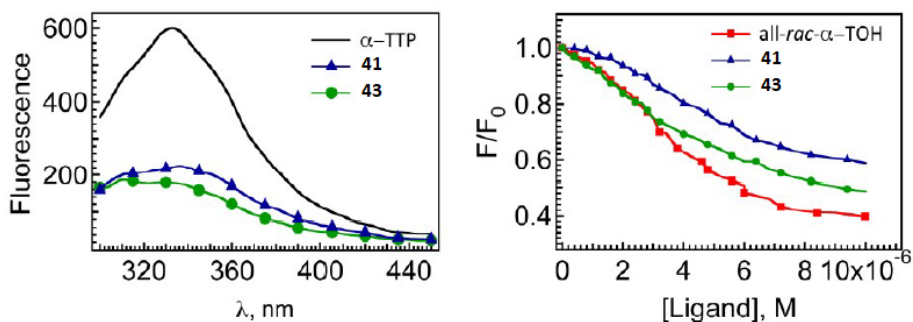


**Figure 28:** (Left) Fluorescence emission spectra of  $\alpha$ -TTP in SET Buffer alone (solid line) and after the addition of 10  $\mu$ M **41** (triangles) and **43** (circles) at 293 K. (Right) Relative fluorescence intensity decrease of  $\alpha$ -TTP fluorescence as a function of ligand concentration: *all-rac*- $\alpha$ -TOH (squares), **41** (triangles), and **43** (circles). In all samples,  $\alpha$ -TTP concentration was 0.2  $\mu$ M, excitation wavelength was  $\lambda = 280$  nm.

Experimental data were fitted with an equation (see experimental section) that allowed to calculate the  $K_d$  of each ligand. Due to the known dependence of  $K_d$  on experimental conditions, the affinities of the ligands were also expressed as dissociation constant ratios (R) with respect to the  $K_d$  of the reference all-*rac*- $\alpha$ -TOH. The values of  $K_d$  and R are reported in Table 7.

**Table 7:** Dissociation constant  $K_d$  for all-*rac*- $\alpha$ -TOH, for the synthesized ligands **41** and **43**. Literature results for (R,R,R)- $\alpha$ -TOH and  $\alpha$ -TOH-NBD are reported for comparison.

Ligand	$K_d$ (M)	R <sup>a</sup>
(R,R,R)- $\alpha$ -TOH <sup>53</sup>	$3.6 \times 10^{-8} \pm 0.5 \times 10^{-8}$	-
$\alpha$ -TOH-NBD <sup>54</sup>	$8.5 \times 10^{-9} \pm 6.3 \times 10^{-9}$	-
all- <i>rac</i> - $\alpha$ -TOH	$1.53 \times 10^{-5} \pm 0.17 \times 10^{-5}$	1
<b>41</b>	$2.77 \times 10^{-5} \pm 0.16 \times 10^{-5}$	1.8
<b>43</b>	$1.18 \times 10^{-5} \pm 0.07 \times 10^{-5}$	0.8

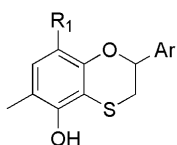
<sup>a</sup> R =  $K_d$  (ligand) /  $K_d$  (all-*rac*- $\alpha$ -TOH).

The experimentally determined dissociation constants of the TTP complex with ligands **41** and **43** resulted to be of the same order of magnitude of that of the model ligand all-*rac*- $\alpha$ -TOH. Resulting R values shows that in the case of **43** the binding affinity of this compound is even superior to that of all-*rac*- $\alpha$ -TOH.

These results demonstrate that the insertion of an unsubstituted (**41**) or a 2-methyl-substituted benzo[*b*]thiophene (**43**) moiety in the  $\alpha$ -TOH skeleton does not negatively affect its ability to be recognized by the  $\alpha$ -TTP, thus opening to the use of these systems in biomedical applications.

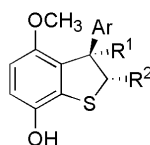
### Conclusions

The synthesis and characterization of sulfur containing phenolic antioxidants with a tocopherol-like activity is one of the main topics of our research group. A common element of the products developed is the presence of an endocyclic sulfide sulfur in *ortho* to the phenolic OH. Several of these products showed an antioxidant performance slightly lower or equal to that of  $\alpha$ -TOH (Figure 29).



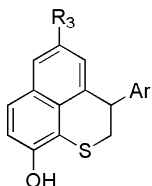
**5-hydroxy-4-thiaflavanes**

$$k_{inh} = 1.2\text{-}3.4 \times 10^6 \text{ M}^{-1} \text{ s}^{-1}$$



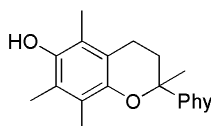
**7-hydroxybenzo[b]dihydrothiophenes**

$$k_{inh} = 1.3\text{-}2.0 \times 10^6 \text{ M}^{-1} \text{ s}^{-1}$$



**9-hydroxy-2,3-dihydrobenzo[de]thiochromenes**

$$k_{inh} = 0.9\text{-}2.3 \times 10^6 \text{ M}^{-1} \text{ s}^{-1}$$



**$\alpha$ -TOH**

$$k_{inh} = 3.2 \times 10^6 \text{ M}^{-1} \text{ s}^{-1}$$

**Figure 29**

The planarity of these bicyclic system and the absent formation of a strong IHB between the sulfur atom and the phenolic OH is responsible for the stabilization of the phenoxyl radical without stabilizing the ground state of the phenol, hence the optimal antioxidant activity. During my PhD, we found that benzo[*b*][1,4]oxathiines can be transformed into 7-hydroxy-dihydro- and 7-hydroxybenzo[*b*]thiophenes by two consecutive acid promoted transpositions. For selected derivatives the whole transformation occurs through five consecutive electrophilic events carried out 'one-pot'. Unexpected results were obtained for 7-hydroxybenzo[*b*]thiophenes which, in opposition with the literature data available for the corresponding benzofuranes, showed an excellent radical scavenger activity. We explained these outcomes by the presence of a noncovalent interaction between the ArO<sup>•</sup> group and the sulfur  $\sigma$ -hole that is responsible for an extra stabilization of the phenoxyl radical. As a result, there is a relevant lowering of the BDE(OH) and increasing of the  $k_{inh}$  in all the benzo[*b*]thiophenes prepared. The best performance was obtained with those derivatives bearing the chromanol ring of  $\alpha$ -TOH fused to the benzo[*b*]thiophene moiety like **41** and **43** reported in Figure 30.

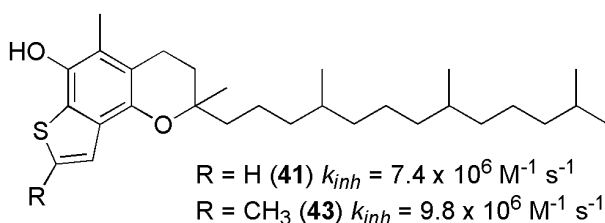


**Figure 30**

These two derivatives, obtained from the corresponding benzo[*b*]oxathiines through an elegant one-pot procedure constituted by five consecutive electrophilic transformations, showed  $k_{inh}$  values up to three times higher than the reference natural antioxidant  $\alpha$ -TOH as well as the ability of being perfectly recognized by  $\alpha$ -TTP.

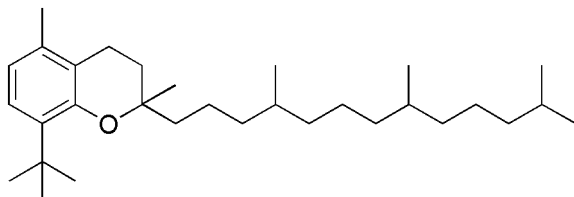
## 2.3 Experimental Section

$^1\text{H}$  and  $^{13}\text{C}$  NMR spectra were recorded with Varian Gemini 200 or Varian Mercury Plus 400, using as solvent:  $\text{CDCl}_3$  using the reference at 7.26 ppm of the residue of chloroform in  $^1\text{H}$  NMR spectrum and at 77.0 ppm in the  $^{13}\text{C}$ -NMR. FT-IR spectra were recorded with FT Infrared Spectrometer 1600 Perkin-Elmer in  $\text{CCl}_4$  or  $\text{CDCl}_3$  solutions. GC-MS spectra were recorded with a QMD 100 Carlo Erba. ESI-MS spectra were recorded with a JEOL MStation JMS700. Melting points were measured with Melting Point Buchi 510 and are uncorrected. All the reactions were monitored by TLC on commercially available precoated plates (silica gel 60 F 254) and the products were visualized with acidic vanillin solution. Silica gel 60 (230–400 mesh) was used for column chromatography. Commercial available reagents and catalysts were used as obtained from freshly open container without further purifications. Dry solvents were obtained by Pure Solv Micro.  $\text{CHCl}_3$  was washed 10 times with deionized water, dried on anhydrous  $\text{CaCl}_2$ .  $\text{Et}_3\text{N}$  was distilled over  $\text{KOH}$ , dried on anhydrous  $\text{CaCl}_2$ .  $\alpha$ -Tocopheryl Transferase ( $\alpha$ -TTP) was purchased from CusAb (purity >90%, SDS-PAGE). EDTA, Tris-HCl and KCl used for the preparation of SET Buffer (1 mM EDTA, 50 mM Tris-HCl, 250 mM sucrose and 100 mM KCl) were obtained from Merck (EDTA) and Sigma-Aldrich (Tris-HCl and KCl), and used as received. All-*rac*- $\alpha$ -TOH was obtained from Sigma-Aldrich and used without further purification. Ethanol (95%) was purchased Sigma-Aldrich. Milli-Q water (Millipore, USA) was used for all samples.

### 2.3.1 Synthesis

Derivatives **3**, **4**, **7**, **14**, **18**, **19**, **21**, **23**, **35**, **36**, **40**, **41**, **42**, **43**, have been obtained as diastereoisomeric mixtures. For some of them in the  $^1\text{H}$  NMR spectra we can distinguish two main diastereoisomeric species, thus we described their signals as sum of diastereoisomers (SoD).

8-*tert*-Butyl-2,5-dimethyl-2-(4,8,12-trimethyl-tridecyl)-chroman (**3**)



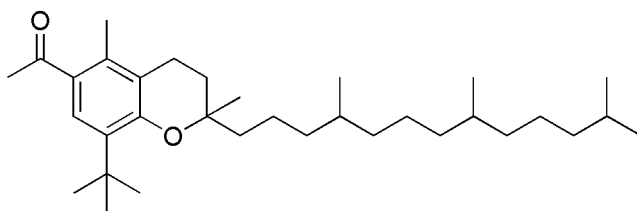
To a solution of 2-*tert*-Butyl-5-methylphenol (4920 mg, 30 mmol) in DCE (35 mL) were added phytol (2.5 mL, 10 mmol) and *para*-toluensulfonic acid (100 mg, 0.53 mmol), then the mixture was left under magnetic stirring for 1h at room temperature. Subsequently the reaction mixture was stirred for 22h at reflux temperature ( $T = 80^\circ\text{C}$ ),

then poured into saturated aqueous  $\text{NH}_4\text{Cl}$  solution (200 mL) and the crude reaction products were extracted using petroleum ether (3 x 100 mL). The combined organic solution was washed with water (100 mL) and then dried over anhydrous  $\text{Na}_2\text{SO}_4$ . After removing the drying agent by filtration, the solvent was evaporated *in vacuo*. The crude reaction mixture was purified by silica-gel column chromatography using petroleum ether as eluent to isolate the product **3** (1840 mg). Yield: 42%.

$^1\text{H NMR}$  (400 MHz,  $\text{CDCl}_3$ )  $\delta$  7.08 (d,  $J = 7.9$  Hz, 1H), 6.70 (d,  $J = 7.9$  Hz, 1H), 2.67 (t,  $J = 6.2$  Hz, 2H), 2.23 (s, 3H), 1.91–1.56 (m, 8H), 1.42 (s, 9H), 1.42–1.11 (m, 18H), 0.93–0.89 (m, 12H).

$^{13}\text{C NMR}$  (100 MHz,  $\text{CDCl}_3$ )  $\delta$  152.4, 135.4, 134.9, 123.8, 120.1, 119.9, 75.4, 41.2, 39.4, 37.7, 37.5, 37.4, 37.3, 34.6, 32.8, 32.7, 30.6, 30.5, 29.9, 28.0, 24.8, 24.5, 23.2, 22.6, 21.3, 20.6, 19.7, 19.0.

1-[8-*tert*-Butyl-2,5-dimethyl-2-(4,8,12-trimethyl-tridecyl)-chroman-6-yl]-ethanone (**4**)

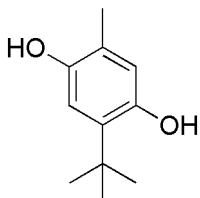


Acetyl chloride (70 mg, 0.89 mmol) was added dropwise to a stirred suspension of aluminum chloride (151 mg, 1.13 mmol) in anhydrous dichloromethane (7 mL) at  $-15^\circ\text{C}$  under nitrogen atmosphere. After 1h of stirring, a solution of **3** (357 mg, 0.81 mmol) in dichloromethane dry (0.5 mL) was added dropwise. After stirring for 16h the reaction mixture was poured into ice-water. The organic layer was diluted with HCl 0.5M (40 mL), then extracted with dichloromethane (3 x 50mL). The combined organic layers were washed with a saturated aqueous  $\text{NaHCO}_3$  solution (40 mL), with water twice (2 x 40 mL) and then dried over anhydrous sodium sulfate. After removal of the solvent, the residue was purified by silica-gel column chromatography using at first petroleum ether as eluent, and then a mixture of petroleum ether and dichloromethane 1:1 to isolate the product **4** (30 mg). Yield: 8%.

$^1\text{H NMR}$  (200 MHz,  $\text{CDCl}_3$ )  $\delta$  7.50 (s, 1H), 2.67 (t,  $J = 6.7$  Hz, 2H), 2.55 (s, 3H), 2.37 (s, 3H), 1.89–1.79 (m, 2H), 1.39 (s, 9H), 1.28–1.10 (m, 24H), 0.88–0.85 (m, 12H).

$^{13}\text{C NMR}$  (100 MHz,  $\text{CDCl}_3$ )  $\delta$  202.0, 155.3, 136.3, 134.5, 129.8, 126.0, 121.2, 76.5, 41.0, 39.4, 37.6, 37.5, 37.4, 37.3, 34.6, 32.8, 32.7, 31.3, 30.6, 30.5, 29.7, 28.0, 24.8, 24.4, 23.2, 22.7, 21.2, 20.9, 19.7, 16.0.

2-*tert*-Butyl-5-methyl-benzene-1,4-diol (**6**)



Under stirring, urea (6 g, 100 mmol) and *tert*-butyl alcohol (7.4 g, 99 mmol) were added to 75% H<sub>2</sub>SO<sub>4</sub> (100 mL) slowly at room temperature. After 2h30' 2-*tert*-butyl-5-methyl hydroquinone (10 g, 80 mmol) was added to the reaction mixture at 0-5 °C. After stirring at room temperature for 3h, the reaction mixture was quenched and extracted with ethyl acetate (3×100 mL). The organic layer was washed successively with saturated aqueous sodium bicarbonate (3×100 mL), brine (100 mL) and water (100 mL), then dried over anhydrous sodium sulfate. After removing the drying agent by filtration, the solvent was evaporated *in vacuo* to give the product **6** as a light brown solid (10.6 g). Yield: 74%.

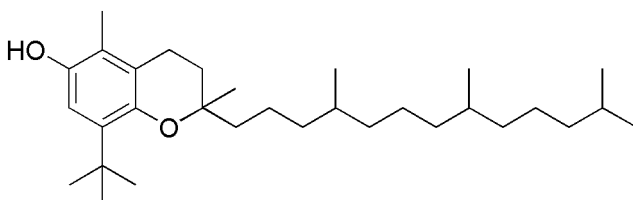
**Mp:** 109-111°C.

**<sup>1</sup>H NMR** (400 MHz, CDCl<sub>3</sub>) δ 6.72 (s, 1H), 6.46 (s, 1H), 4.52 (bs, 1H), 2.16 (s, 3H), 1.38 (s, 9H).

**<sup>13</sup>C NMR** (100 MHz, CDCl<sub>3</sub>) δ 147.7, 147.0, 134.9, 121.7, 118.9, 114.1, 34.2, 29.6, 15.1.

**IR** (CDCl<sub>3</sub>, 0.05M, cm<sup>-1</sup>) ν 3603, 3448, 2961, 2871, 1652, 1515, 1452, 1409, 1176, 1134.

8-*tert*-Butyl-2,5-dimethyl-2-(4,8,12-trimethyl-tridecyl)-chroman-6-ol (**7**)



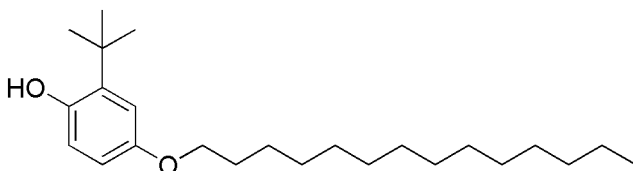
To a solution of 2-*tert*-Butyl-5-methylhydroquinone **6** (1000 mg, 5.55 mmol) in DCE (8 mL) were added phytol (645 μL, 1.85 mmol) and *para*-toluensulfonic acid (3.5 mg, 0.018 mmol), then the mixture was left under magnetic stirring for 1h at room temperature. Subsequently the reaction mixture was stirred for 16h at reflux temperature (T= 80°C), then poured into saturated aqueous NH<sub>4</sub>Cl solution (100 mL) and the crude reaction products were extracted using petroleum ether (3 x 100 mL). The combined organic solution was washed with water (2 x 100 mL) and then dried over anhydrous Na<sub>2</sub>SO<sub>4</sub>. After removing the drying agent by filtration, the solvent was evaporated *in vacuo*. The crude product was purified by silica-gel column chromatography using a mixture of petroleum ether and ethyl acetate 15:1 as eluent. The purified product **7** was obtained as a light brown oil (440 mg). Yield: 52%.

**<sup>1</sup>H NMR** (400 MHz, CDCl<sub>3</sub>) δ 6.65 (s, 1H), 4.27 (bs, 1H), 2.65 (t, *J* = 6.5 Hz, 2H), 2.10 (s, 3H), 1.88–1.42 (m, 9H), 1.36 (s, 9H), 1.32–1.25 (m, 6H), 1.24 (s, 3H), 1.22–1.02 (m, 8H), 0.89–0.85 (m, 12H).

**<sup>13</sup>C NMR** (100 MHz, CDCl<sub>3</sub>) δ 146.5, 145.5, 136.0, 120.8, 119.6, 112.0, 74.7, 41.2, 39.4, 37.7, 37.5, 37.4, 37.3, 34.6, 32.8, 32.7, 30.7, 29.8, 28.0, 24.8, 24.4, 22.9, 22.7, 21.3, 21.2, 19.8, 19.7, 11.0.

**IR** (CDCl<sub>3</sub>, 0.05M, cm<sup>-1</sup>) ν 3607, 2954, 2928, 2968, 2253, 1468, 1410, 1233.

#### 2-*tert*-Butyl-4-tetradecyloxy-phenol (**8**)

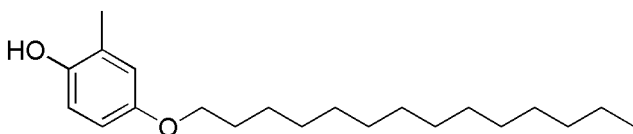


In a Schlenk tube containing 2-*tert*-butyl-hydroquinone (200 mg, 1.2 mmol) and potassium carbonate (166 mg, 1.2 mmol) was added anhydrous CH<sub>3</sub>CN (3 mL) and 1-bromotetradecane (360 μL, 1.2 mmol). The mixture was left under magnetic stirring and heated at reflux under nitrogen atmosphere for 96h. The brown mixture was diluted with H<sub>2</sub>O and extracted with Et<sub>2</sub>O twice. The combined organic layers were washed with water, dried over anhydrous Na<sub>2</sub>SO<sub>4</sub>, filtered and concentrated *in vacuo*. The crude product obtained was purified by silica-gel column chromatography using a mixture of dichloromethane and petroleum ether 1:1 as eluent, to give **8** as a brown oil (190 mg). Yield: 44%.

**<sup>1</sup>H NMR** (200 MHz, CDCl<sub>3</sub>) δ 6.87 (bs, 1H), 6.60–6.59 (m, 2H), 4.50 (bs, 1H), 3.89 (t, *J* = 6.6 Hz, 2H), 1.80–1.69 (m, 2H), 1.49–1.27 (m, 22H), 1.40 (s, 9H), 0.89 (t, *J* = 6.6 Hz, 3H).

**IR** (CDCl<sub>3</sub>, 0.05M, cm<sup>-1</sup>) ν 3601, 2928, 2854.

#### 2-Methyl-4-tetradecyloxy-phenol (**9**)



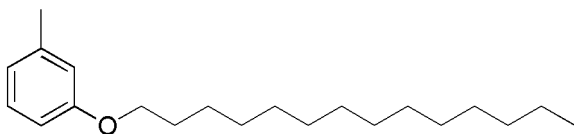
In a two-necked round-bottomed flask containing K<sub>2</sub>CO<sub>3</sub> (1.11 g, 8.06 mmol) and toluhydroquinone (1.00 g, 8.06 mmol) was added anhydrous CH<sub>3</sub>CN (20 mL) previously degassed for 1h with N<sub>2</sub>, and at last was added 1-bromotetradecane (2.2 mL, 8.06 mmol). The reaction mixture was stirred under nitrogen atmosphere at reflux (80°C) and after 46 h was diluted with H<sub>2</sub>O (50 mL) and extracted with diethyl ether (3 x 50 mL). The combined organic layer was washed with brine (3 x 50 mL), dried over anhydrous Na<sub>2</sub>SO<sub>4</sub>, filtered and evaporated *in vacuo*. The crude was purified by silica-gel column chromatography, using a mixture of petroleum ether and ethyl acetate 10:1 as eluent. The purified product **9** was obtained as a light pink solid (370 mg). Yield: 14 %.



**<sup>1</sup>H NMR** (400 MHz, CDCl<sub>3</sub>) δ 6.69–6.67 (m, 2H), 6.63–6.60 (m, 1H), 4.33 (s, 1H), 3.88 (t, *J* = 6.6 Hz, 2H), 2.22 (s, 3H), 1.77–1.70 (m, 2H), 1.47–1.39 (m, 2H), 1.33–1.26 (m, 20H), 0.90–0.86 (m, 3H).

**<sup>13</sup>C NMR** (100 MHz, CDCl<sub>3</sub>) δ 166.3, 153.2, 124.7, 117.4, 115.5, 112.6, 68.6, 31.9, 29.7, 29.6, 29.4 (3 signal for 9 non-equivalent CH<sub>2</sub> groups), 26.1, 22.7, 16.1, 14.1.

#### 1-Methyl-3-tetradecyloxy-benzene (**10**)

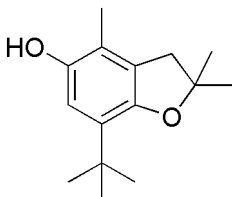


In a Schlenk tube containing *meta*-cresol (14.5 mL, 13.9 mmol) and potassium carbonate (5172 mg, 37.2 mmol) was added anhydrous CH<sub>3</sub>CN (45 mL) and 1-bromotetradecane (11.2 mL, 37.3 mmol). The reaction mixture was left under magnetic stirring and heated at reflux under nitrogen atmosphere for 96h. The mixture was diluted with H<sub>2</sub>O and extracted with Et<sub>2</sub>O twice. The combined organic layers were washed with water, dried over anhydrous Na<sub>2</sub>SO<sub>4</sub>, filtered and concentrated in vacuum. The crude product obtained was purified by silica-gel column chromatography using dichloromethane as eluent, to give **10** as a colourless oil (8520 mg). Yield: 100%.

**<sup>1</sup>H NMR** (400 MHz, CDCl<sub>3</sub>) δ 7.16 (t, *J* = 7.8 Hz, 1H), 6.77–6.70 (m, 3H), 3.94 (t, *J* = 6.6 Hz, 2H), 2.33 (s, 3H), 1.81–1.74 (m, 2H), 1.49–1.42 (m, 2H), 1.37–1.28 (m, 20H), 0.90 (t, *J* = 6.7 Hz, 3H).

**<sup>13</sup>C NMR** (100 MHz, CDCl<sub>3</sub>) δ 159.2, 139.4, 129.1, 121.3, 115.4, 111.3, 67.8, 31.9, 29.7, 29.6, 29.4, 29.3 (4 signals for 9 non-equivalent CH<sub>2</sub>), 26.1, 22.7, 21.5, 14.1.

#### 7-*tert*-Butyl-2,2,4-trimethyl-2,3-dihydro-benzofuran-5-ol (**13**)



To a solution of **6** (500 mg, 2.77 mmol) in DCE (4 mL) were added 2-methyl-2-propen-1-ol (78 μL, 0.92 mmol) and *para*-toluenesulfonic acid (17.6 mg, 0.09 mmol), then the mixture was left under magnetic stirring for 1h at room temperature. Subsequently the reaction mixture was stirred for 18 h at reflux temperature (*T* = 80°C), then poured into saturated aqueous NH<sub>4</sub>Cl solution (100 mL) and the crude reaction products were extracted using petroleum ether (3 x 100 mL). The combined organic solution was washed with water (2 x 100 mL) and then dried over anhydrous Na<sub>2</sub>SO<sub>4</sub>. After removing the drying agent by filtration, the solvent was evaporated *in vacuo*. The crude product

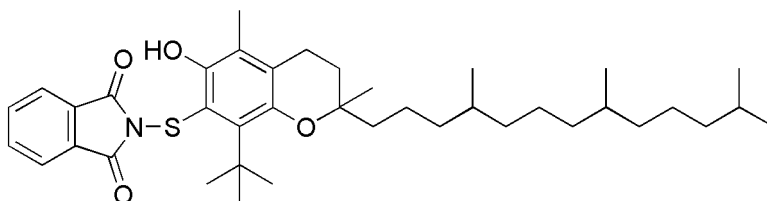
was purified by silica-gel column chromatography using CH<sub>2</sub>Cl<sub>2</sub> as eluent. The purified product **13** was obtained as a light brown oil (160 mg). Yield: 74%.

**<sup>1</sup>H NMR** (400 MHz, CDCl<sub>3</sub>) δ 6.54 (s, 1H), 4.20 (s, 1H), 2.87 (s, 2H), 2.09 (3H), 1.45 (s, 6H), 1.31 (s, 9H).

**<sup>13</sup>C NMR** (100MHz, CDCl<sub>3</sub>) δ 150.5, 146.6, 130.5, 127.7, 118.0, 111.4, 85.4, 42.2, 33.8, 29.1, 28.3, 12.3.

**IR** (CDCl<sub>3</sub>, 0.05M, cm<sup>-1</sup>) ν 3607, 2969, 2244, 1491, 1411, 1391, 1244, 1170, 1148, 1066.

2-[8-*tert*-Butyl-6-hydroxy-2,5-dimethyl-2-(4,8,12-trimethyl-tridecyl)-chroman-7-ylsulfanyl]-isoindole-1,3-dione (**14**)



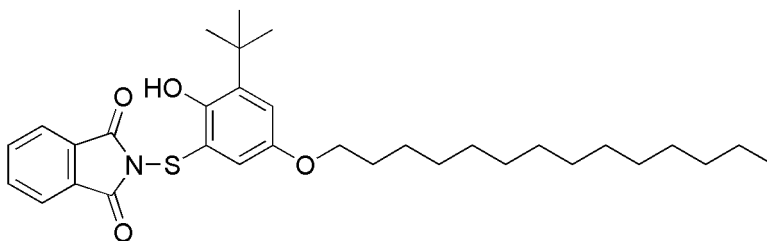
To a solution of **7** (750 mg, 1.63 mmol) in CHCl<sub>3</sub> (20 mL), was added at T = 0°C, dropwise, through a dropping funnel, a solution of PhtNSCI (384 mg, 1.80 mmol) in CHCl<sub>3</sub> (20 mL), and the mixture was stirred at room temperature (reached gradually from T=0°C), under N<sub>2</sub> atmosphere for 25 hours. The reaction mixture was diluted with 100 mL of CH<sub>2</sub>Cl<sub>2</sub>, washed twice with 100 mL (x 2) of a saturated solution of NaHCO<sub>3</sub>, once with water (100 mL). The organic layer was dried over Na<sub>2</sub>SO<sub>4</sub>, filtered, and evaporated *in vacuo*, to yield the desired product **14** as a thick yellow oil that did not require any further purification. Yield: 100%.

**<sup>1</sup>H NMR** (400 MHz, CDCl<sub>3</sub>) δ 7.88-7.84 (m, 2H), 7.73-7.71 (m, 2H), 4.25 (bs, 1H), 2.61 (t, J = 6.3 Hz, 2H), 2.09 (s, 3H), 1.80 (s, 9H), 1.72-1.45 (m, 9H), 1.28-1.22 (m, 11H), 1.15-1.05 (m, 6H), 0.87-0.84 (m, 12H).

**<sup>13</sup>C NMR** (100 MHz, CDCl<sub>3</sub>) δ 168.8 (2C), 149.1, 146.4, 139.2, 134.5 (2C), 132.0 (2C), 126.3, 123.9 (2C), 121.1, 116.4, 75.5, 41.2, 40.1, 39.4, 37.6, 37.5, 37.4, 37.3, 33.1, 32.8, 32.7, 29.8, 28.0, 24.8, 24.4, 22.7, 22.6, 21.8, 21.3, 19.8, 19.7, 12.2.

**IR** (CDCl<sub>3</sub>, 0.05M, cm<sup>-1</sup>) ν 3607, 3405, 2954, 2928, 1784, 1731, 1712, 1469, 1377, 1277.

2-(3-*tert*-Butyl-2-hydroxy-5-tetradecyloxy-phenylsulfanyl)-isoindole-1,3-dione (**15**)



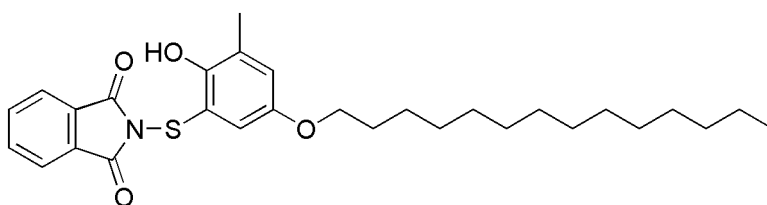
To a solution of **8** (170 mg, 0.47 mmol) in CHCl<sub>3</sub> (4 mL) was added dropwise at 0°C a solution of PhtNSCl (110 mg, 0.52 mmol) and the mixture was left under magnetic stirring for 10 minutes. Then the solution was stirred at room temperature for 16h. The crude mixture was diluted in CH<sub>2</sub>Cl<sub>2</sub> and washed with saturated aqueous NaHCO<sub>3</sub> solution (2 x 50 mL). The organic phases were collected and washed once with H<sub>2</sub>O (100 mL). The organic layer was dried over Na<sub>2</sub>SO<sub>4</sub> and evaporated *in vacuo* to obtain **15** as a yellow solid (230 mg) that did not require any further purification. Yield: 100%.

**<sup>1</sup>H NMR** (400 MHz, CDCl<sub>3</sub>) δ 7.91–7.89 (m, 2H), 7.77–7.75 (m, 2H), 7.24 (d, *J* = 3.1 Hz, 1H), 7.01 (d, *J* = 3.0 Hz, 1H), 3.90 (t, *J* = 6.6 Hz, 2H), 1.76–1.72 (m, 2H), 1.38 (s, 9H), 1.33–1.26 (m, 22H), 0.88 (t, *J* = 6.2 Hz, 3H).

**<sup>13</sup>C NMR** (100MHz, CDCl<sub>3</sub>) δ 168.4 (2C), 151.9, 151.4, 139.1, 134.7 (2C), 132.0, 124.1 (2C), 121.4, 118.4, 118.2, 68.4, 35.4, 31.9, 29.7, 29.6, 29.4 (3 signals for 9 non-equivalent CH<sub>2</sub> groups), 29.3, 26.0, 22.7, 14.1.

**MS (EI)** *m/z* (%): 539 (15.41); 103 (99.25); 146 (95.35); 75 (100.00).

2-(2-Hydroxy-3-methyl-5-tetradecyloxy-phenylsulfanyl)-isoindole-1,3-dione (**16**)

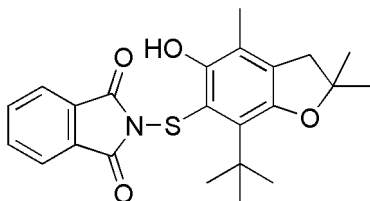


To a solution of **9** (370 mg, 1.15 mmol) in CHCl<sub>3</sub> (15 mL), was added at T = 0°C, dropwise, through a dropping funnel, a solution of PhtNSCl (306 mg, 1.38 mmol) in CHCl<sub>3</sub> (15 mL), and the mixture was stirred at room temperature (reached gradually from T=0°C), under nitrogen atmosphere for 22 hours. The reaction mixture was diluted with 100 mL of CH<sub>2</sub>Cl<sub>2</sub>, washed twice with 100 mL (x 2) of a saturated solution of NaHCO<sub>3</sub>, once with water (100 mL). The organic layer was dried over Na<sub>2</sub>SO<sub>4</sub>, filtered, and evaporated *in vacuo*, to yield the product **16** as a soft beige solid that did not require any further purification. Yield: 100%.

**<sup>1</sup>H NMR** (400 MHz, CDCl<sub>3</sub>) δ 7.90–7.88 (m, 2H), 7.76–7.74 (m, 2H), 7.20–7.18 (m, 1H), 6.85–6.84 (m, 1H), 3.87 (t, *J* = 6.5 Hz, 2H), 2.23 (s, 3H), 1.75–1.70 (m, 2H), 1.46–1.41 (m, 2H), 1.30–1.26 (m, 20H), 0.87 (t, *J* = 6.7 Hz, 3H).

**<sup>13</sup>C NMR** (100 MHz, CDCl<sub>3</sub>) δ 168.5 (2C), 151.4, 134.8 (2C), 131.9 (2C), 127.3, 124.2 (2C), 118.8, 117.2, 115.4, 112.5, 68.7, 31.9, 29.6, 29.5, 29.4, 29.3 (4 signals for 9 non-equivalent CH<sub>2</sub> groups), 26.0, 22.7, 16.8, 14.1.

2-(7-*tert*-Butyl-5-hydroxy-2,2,4-trimethyl-2,3-dihydro-benzofuran-6-ylsulfanyl)-isoindole-1,3-dione (**17**)



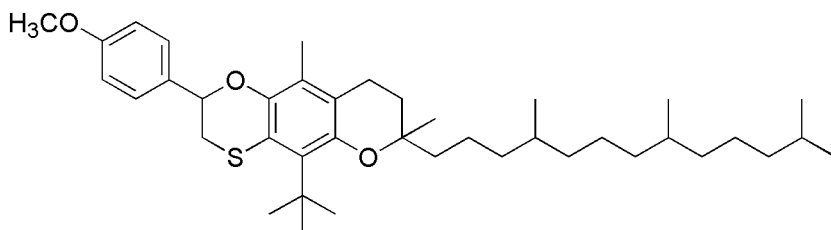
To a solution of **13** (150 mg, 0.64 mmol) in  $\text{CHCl}_3$  (4 mL), was added at  $T = 0^\circ\text{C}$ , dropwise, through a dropping funnel, a solution of PhtNSCI 96% (157 mg, 0.70 mmol) in  $\text{CHCl}_3$  (4 mL). The mixture was stirred at room temperature (reached gradually from  $T=0^\circ\text{C}$ ), under nitrogen atmosphere for 65h. The reaction mixture was diluted with 100 mL of  $\text{CH}_2\text{Cl}_2$ , washed twice with 100 mL (x 2) of a saturated solution of  $\text{NaHCO}_3$ , once with water (100 mL). The organic layer was dried over  $\text{Na}_2\text{SO}_4$ , filtered, and evaporated *in vacuo*, to yield the product **17** as a yellow solid that did not require further purification. Yield: 100%.

**$^1\text{H NMR}$**  (400 MHz,  $\text{CDCl}_3$ )  $\delta$  7.87–7.84 (m, 2H), 7.74–7.72 (m, 2H), 2.84 (s, 2H), 2.07 (s, 3H), 1.75 (s, 9H), 1.43 (s, 6H).

**$^{13}\text{C NMR}$**  (100 MHz,  $\text{CDCl}_3$ )  $\delta$  169.0 (2C), 151.2, 150.4, 134.6 (2C), 133.6, 132.8, 131.9 (2C), 123.9 (2C), 119.4, 115.6, 84.6, 42.3, 39.2, 32.0, 28.2, 13.5.

**IR** ( $\text{CDCl}_3$ , 0.05M,  $\text{cm}^{-1}$ )  $\nu$  3606, 3424, 2928, 2856, 1782, 1732, 1710, 1609, 1468, 1340, 1282, 1221, 1199, 1060.

10-*tert*-Butyl-2-(4-methoxy-phenyl)-6,9-dimethyl-6-(4,8,12-trimethyl-tridecyl)-2,3,7,8-tetrahydro-6H-1,5-dioxo-4-thia-anthracene (**18**)

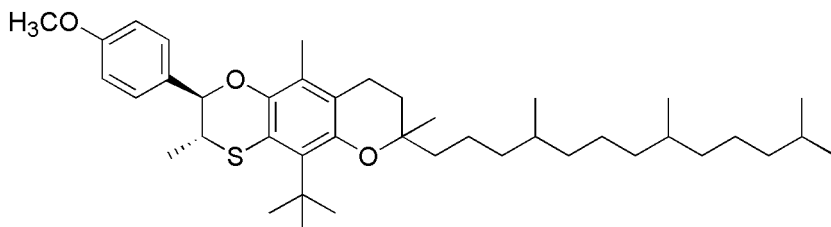


To a solution of **14** (100 mg, 0.16 mmol) in  $\text{CHCl}_3$  (2 mL), was added 4-methoxystyrene (63 mg, 63  $\mu\text{L}$ , 0.47 mmol) and then triethylamine (16 mg, 22  $\mu\text{L}$ , 0.73 mmol) dropwise. The reaction mixture was left stirring at  $60^\circ\text{C}$  for 24 hours, then it was diluted with  $\text{CH}_2\text{Cl}_2$ , washed with  $\text{KOH}$  1M (2 x 20 mL) and water (20 mL). The organic layer was dried over  $\text{Na}_2\text{SO}_4$ , filtered and evaporated *in vacuo*. The crude was purified by silica-gel column chromatography, using a mixture of petroleum ether and  $\text{CH}_2\text{Cl}_2$  3:1 as eluent. The purified product **18** was obtained as an orange oil (70 mg). Yield: 72%.

**<sup>1</sup>H NMR** (400 MHz, CDCl<sub>3</sub>) δ 7.38–7.34 (m, 2H), 6.93–6.90 (m, 2H), 5.24–5.19 (m, 1H), 3.82 (s, 3H), 3.07–2.88 (m, 2H), 2.64–2.59 (m, 2H), 2.06 + 2.05 (s, 3H, SoD), 1.90–1.65 (m, 3H), 1.62 (s, 9H), 1.55–1.06 (m, 23H), 0.88–0.84 (m, 12H).

**<sup>13</sup>C NMR** (100 MHz, CDCl<sub>3</sub>) δ 159.4, 147.6, 144.8, 133.9, 132.2, 127.3, 124.9, 121.0, 118.9, 113.9, 78.6, 75.4, 55.3, 41.0, 40.5, 39.4, 38.6, 37.7, 37.6, 37.4, 35.3, 32.6, 30.6, 30.5, 30.4, 28.0, 24.8, 24.5, 23.4, 23.1, 22.6, 21.4, 19.8, 19.7, 11.9.

10-*tert*-Butyl-2-(4-methoxy-phenyl)-3,6,9-trimethyl-6-(4,8,12-trimethyl-tridecyl)-2,3,7,8-tetrahydro-6H-1,5-dioxo-4-thia-anthracene (**19**)

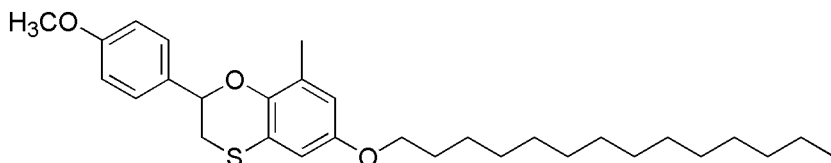


To a yellow solution of **14** (500 mg, 0.79 mmol) in CHCl<sub>3</sub> (10 mL), was added trans-anethole (236 μL, 1.57 mmol) and triethylamine (110 μL, 0.79 mmol), dropwise. The mixture was left under magnetic stirring at reflux (60°C) until complete consumption of the starting reagent; after 24h the dark yellow solution obtained was diluted with CH<sub>2</sub>Cl<sub>2</sub> (40 mL) then washed twice with a 1 M solution of KOH (50 mL) and once with water (50 mL). The organic layer was dried over anhydrous Na<sub>2</sub>SO<sub>4</sub>, filtered and evaporated *in vacuo*. The crude product was purified through silica-gel column chromatography using a mixture of petroleum ether and CH<sub>2</sub>Cl<sub>2</sub> 2:1 as eluent. The purified product **19** was obtained as an amber oil (140 mg). Yield: 28%.

**<sup>1</sup>H NMR** (400 MHz, CDCl<sub>3</sub>) δ 7.27–7.24 (m, 2H), 6.91–6.89 (m, 2H), 4.69 (dd, *J* = 16.5, 9.6, 1H), 3.83 (s, 3H), 3.13–3.03 (m, 1H), 2.62–2.57 (m, 2H), 1.97 (s, 3H), 1.87–1.67 (m, 3H), 1.62 (s, 9H), 1.41–1.36 (m, 4H), 1.30–1.05 (m, 22H), 0.88–0.84 (m, 12H).

**<sup>13</sup>C NMR** (100 MHz, CDCl<sub>3</sub>) δ 159.5, 147.5, 144.9, 132.6, 131.8, 128.2, 124.4, 121.2, 118.7, 113.8, 85.5, 75.3, 55.2, 42.4, 41.1, 40.4, 39.4, 37.7, 37.6, 37.4, 37.3, 32.6, 30.6, 30.5, 30.4, 28.0, 24.8, 24.4, 23.6, 22.7, 22.6, 21.4, 19.8, 19.7, 17.1, 11.9.

2-(4-Methoxy-phenyl)-8-methyl-6-tetradecyloxy-2,3-dihydro-benzo[1,4]oxathiine (**20**)



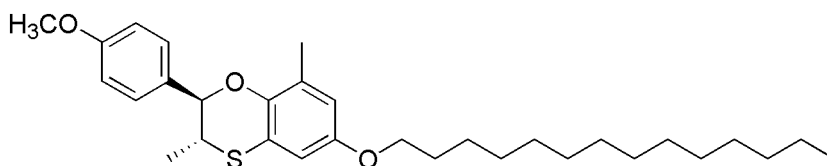
To a solution of **16** (101 mg, 0.20 mmol) in CHCl<sub>3</sub> (2.6 mL) was added 4-methoxystyrene (82 μL, 0.60 mmol) and triethylamine (28 μL, 0.20 mmol), dropwise, then the reaction mixture was stirred at 60°C for 19h. After complete consumption of the starting

material the solution was diluted with CH<sub>2</sub>Cl<sub>2</sub> (40 mL) then washed twice with a 1 M solution of KOH (2 x 25 mL) and once with water (50 mL). The organic layer was dried over anhydrous Na<sub>2</sub>SO<sub>4</sub>, filtered and evaporated *in vacuo*. The crude product was purified by silica-gel column chromatography with a mixture of petroleum ether:CH<sub>2</sub>Cl<sub>2</sub> = 3:1. The purified product **20** was obtained as a white solid (37 mg). Yield: 36%.

**<sup>1</sup>H NMR** (400 MHz, CDCl<sub>3</sub>) δ 7.35 (d, *J* = 8.8 Hz, 2H), 6.94 (d, *J* = 8.8 Hz, 2H), 6.49 (s, 2H), 5.08 (dd, *J* = 9.6, 1.8 Hz, 1H), 3.87 (t, *J* = 6.6 Hz, 2H), 3.83 (s, 3H), 3.22 (dd, *J* = 12.9, 9.6 Hz, 1H), 3.05 (dd, *J* = 12.9, 1.9 Hz, 1H), 2.17 (s, 3H), 1.77–1.70 (m, 2H), 1.44–1.39 (m, 2H), 1.35–1.26 (m, 20H), 0.88 (t, *J* = 6.6 Hz, 3H).

**<sup>13</sup>C NMR** (100 MHz, CDCl<sub>3</sub>) δ 159.5, 152.8, 144.6, 133.0, 128.8, 127.0, 117.0, 114.5, 114.0, 109.2, 68.5, 55.3, 32.3, 31.9, 30.9, 29.7, 29.6, 29.4, 29.3 (4 signals for 9 non-equivalent CH<sub>2</sub> groups), 26.0, 22.7, 16.4, 14.1.

2-(4-Methoxy-phenyl)-3,8-dimethyl-6-tetradecyloxy-2,3-dihydro-benzo[1,4]oxathiine (**21**)

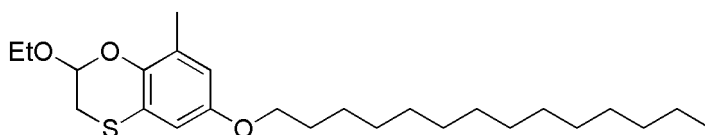


To a solution of **16** (100 mg, 0.20 mmol) in Toluene (3 mL) was added trans-anethole (90 μL, 0.60 mmol) and triethylamine (28 μL, 0.20 mmol), dropwise, then the reaction mixture was stirred at 60°C for 22 hours. After complete consumption of the starting material the solution was diluted with CH<sub>2</sub>Cl<sub>2</sub> (40 mL) then washed twice with a 1 M solution of KOH (2 x 25 mL) and once with water (50 mL). The organic layer was dried over anhydrous Na<sub>2</sub>SO<sub>4</sub>, filtered and evaporated *in vacuo*. The crude product was purified by silica-gel flash chromatography with a mixture of petroleum ether:CH<sub>2</sub>Cl<sub>2</sub> = 3:1 as eluent. The purified product **21** was obtained as a white solid (37 mg). Yield: 37%.

**<sup>1</sup>H NMR** (400 MHz, CDCl<sub>3</sub>) δ 7.28 (d, *J* = 8.6 Hz, 2H), 6.94 (d, *J* = 8.6 Hz, 2H), 6.48 (s, 2H), 4.61 (d, *J* = 8.6 Hz, 1H), 3.87 (t, *J* = 6.6 Hz, 2H), 3.84 (s, 3H), 3.46–3.38 (m, 1H), 2.12 (s, 3H), 1.78–1.71 (m, 2H), 1.45–1.40 (m, 2H), 1.33–1.28 (m, 20H), 1.09 + 1.07 (s, 3H, SoD), 0.91–0.88 (m, 3H).

**<sup>13</sup>C NMR** (100 MHz, CDCl<sub>3</sub>) δ 159.6, 152.9, 144.7, 131.3, 128.4, 128.3, 118.9, 114.2, 113.9, 108.7, 82.5, 68.5, 55.2, 38.9, 31.9, 29.7, 29.6, 29.4 (3 signals for 9 non-equivalent CH<sub>2</sub> groups), 26.0, 22.7, 17.6, 16.5, 14.1.

2-Ethoxy-8-methyl-6-tetradecyloxy-2,3-dihydro-benzo[1,4]oxathiine (**22**)

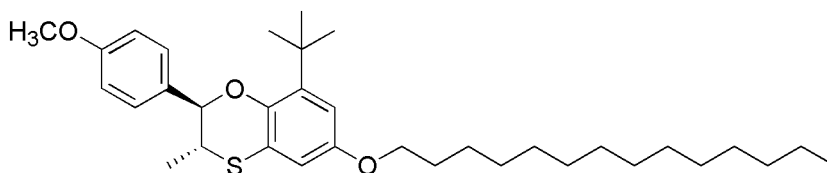


To a solution of **16** (150 mg, 0.30 mmol) in  $\text{CHCl}_3$  (5 mL) was added ethyl vinyl ether (296  $\mu\text{L}$ , 3.00 mmol) and triethylamine (42  $\mu\text{L}$ , 0.30 mmol), dropwise. The reaction mixture was stirred at  $60^\circ\text{C}$  for 17h then it was diluted with  $\text{CH}_2\text{Cl}_2$  (40 mL) then washed twice with a 1 M solution of KOH (2 x 25 mL) and once with water (50 mL). The organic layer was dried over anhydrous  $\text{Na}_2\text{SO}_4$ , filtered and evaporated *in vacuo*. The crude product was purified by silica-gel column chromatography with a mixture of petroleum ether: $\text{CH}_2\text{Cl}_2$  = 3:1 as eluent. The purified **22** product was obtained as a light yellow solid (37 mg). Yield: 53%.

**$^1\text{H}$  NMR** (400 MHz,  $\text{CDCl}_3$ )  $\delta$  6.49–6.45 (m, 2H), 5.34 (dd,  $J$  = 5.0, 2.2 Hz, 1H), 3.97–3.89 (m, 1H), 3.45 (t,  $J$  = 6.6 Hz, 2H), 3.75–3.68 (m, 1H), 3.14 (dd,  $J$  = 12.7, 2.2 Hz, 1H), 3.00 (dd,  $J$  = 12.7, 5.0 Hz, 1H), 2.18 (s, 3H), 1.76–1.69 (m, 2H), 1.44–1.40 (m, 2H), 1.34–1.24 (m, 23H), 0.88 (t,  $J$  = 6.6 Hz, 3H).

**$^{13}\text{C}$  NMR** (100 MHz,  $\text{CDCl}_3$ )  $\delta$  153.0, 141.6, 128.8, 120.7, 117.8, 114.8, 109.2, 94.8, 68.4, 64.1, 31.9, 29.6, 29.4, 29.3 (3 signal for 9 non-equivalent  $\text{CH}_2$  groups), 26.0, 22.7, 16.3, 15.0, 14.1.

8-*tert*-Butyl-2-(4-methoxy-phenyl)-3-methyl-6-tetradecyloxy-2,3-dihydrobenzo[1,4]oxathiine (**23**)



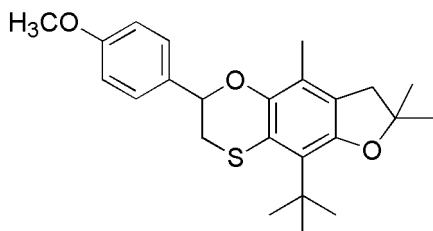
To a solution of **15** (206 mg, 0.40 mmol) in  $\text{CHCl}_3$  (6 mL) was added *trans*-anethol (120  $\mu\text{L}$ , 0.80 mmol) and triethylamine (56  $\mu\text{L}$ , 0.40 mmol). The mixture was left stirring at  $60^\circ\text{C}$  for 96h. Then, the yellow solution obtained was diluted with 100 mL of  $\text{CH}_2\text{Cl}_2$  and washed twice with 125 mL of a 1M solution of KOH and once with 125 mL of  $\text{H}_2\text{O}$ . The organic layer was dried over  $\text{Na}_2\text{SO}_4$  and evaporated *in vacuo*. The crude product was purified by silica-gel column chromatography using a mixture of  $\text{CH}_2\text{Cl}_2$  and petroleum ether 1:1 as eluent. The purified product **23** was obtained as yellow oil (70 mg). Yield: 37%.

**$^1\text{H}$  NMR** (400 MHz,  $\text{CDCl}_3$ )  $\delta$  7.28 (d,  $J$  = 8.8 Hz, 2H), 6.93 (d,  $J$  = 8.8 Hz, 2H), 6.60 (d,  $J$  = 2.9 Hz, 1H), 6.50 (d,  $J$  = 2.9 Hz, 1H), 4.40 (d,  $J$  = 9.1 Hz, 1H), 3.87 (t,  $J$  = 6.6 Hz, 2H), 3.84 (s, 3H), 3.56 (dd,  $J$  = 9.1, 6.6 Hz, 1H), 1.77–1.73 (m, 2H), 1.46–1.42 (m, 2H), 1.36–1.27 (m, 22H), 1.24 (s, 9H), 0.88 (t,  $J$  = 6.6 Hz, 3H).

**$^{13}\text{C}$  NMR** (100 MHz,  $\text{CDCl}_3$ )  $\delta$  159.6, 153.2, 145.9, 141.0, 131.0, 128.3, 120.8, 113.9, 111.2, 107.7, 82.4, 68.4, 55.2, 39.8, 35.0, 31.9, 30.9, 29.7, 29.6, 29.4 (2 signals for 9 non-equivalent  $\text{CH}_2$  groups), 26.1, 22.7, 17.9, 14.1.

**MS (EI)**  $m/z$  (%): 419 (31.29); 148 (100.00).

9-*tert*-Butyl-6-(4-methoxy-phenyl)-2,2,4-trimethyl-2,3,6,7-tetrahydro-1,5-dioxo-8-thia-cyclopenta[*b*]naphthalene (**24**)

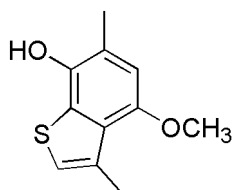


To a solution of **17** (140 mg, 0.34 mmol) in  $\text{CHCl}_3$  (3 mL), was added 4-methoxystyrene (144  $\mu\text{L}$ , 1.02 mmol) and then triethylamine (49  $\mu\text{L}$ , 0.34 mmol) dropwise. The reaction mixture was left stirring at  $60^\circ\text{C}$  for 16h, then it was diluted with  $\text{CH}_2\text{Cl}_2$ , washed with KOH 1M (2 x 20 mL) and water (20 mL). The organic layer was dried over  $\text{Na}_2\text{SO}_4$ , filtered and evaporated *in vacuo*. The crude was purified by silica-gel column chromatography, using a mixture of petroleum ether and  $\text{CH}_2\text{Cl}_2$  2:1 as eluent. The purified product **24** was obtained as colourless oil (80 mg). Yield: 59%.

$^1\text{H NMR}$  (400 MHz,  $\text{CDCl}_3$ )  $\delta$  7.36 (d,  $J = 8.7$  Hz, 2H), 6.93 (d,  $J = 8.7$  Hz, 2H), 5.19 (dd,  $J = 9.2, 3.6$  Hz, 1H), 3.83 (s, 3H), 3.08 (dd,  $J = 12.9, 3.6$  Hz, 1H), 2.99 (dd,  $J = 12.9, 9.2$  Hz, 1H), 2.84 (s, 2H), 2.05 (s, 3H), 1.58 (s, 9H), 1.45 (s, 3H), 1.44 (s, 3H).

$^{13}\text{C NMR}$  (100 MHz,  $\text{CDCl}_3$ )  $\delta$  159.4, 151.3, 145.8, 133.8, 127.2, 126.1, 125.9, 122.8, 119.0, 113.9, 84.2, 77.9, 55.3, 41.9, 37.7, 34.6, 31.7, 28.3, 13.4.

4-Methoxy-3,6-dimethyl-benzo[*b*]thiophen-7-ol (**31**)



To a solution of 6-Methoxy-2-(4-methoxy-phenyl)-2,8-dimethyl-2,3-dihydro-benzo[1,4]oxathiine **27** (60 mg, 0.19 mmol)<sup>21</sup> in dry  $\text{CHCl}_3$  (6 mL)  $\text{CF}_3\text{SO}_3\text{H}$  (29 mg, 0.20 mmol) was added and the mixture heated at  $60^\circ\text{C}$  for 30'. The mixture was diluted with DCM (20 mL), washed twice with saturated  $\text{NaHCO}_3$  and water. The organic phase dried over anhydrous  $\text{Na}_2\text{SO}_4$  and evaporated to dryness to give a crude purified by two consecutive silica gel flash chromatography using DCM for the first and petroleum ether:DCM 1:1 for the second as eluent to give the product **31** as a brown solid. (18 mg, 46%).

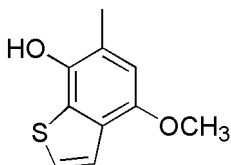
$^1\text{H NMR}$  (400 MHz,  $\text{CDCl}_3$ )  $\delta$  6.80 (d,  $J = 1.2$  Hz, 1H), 6.51 (s, 1H), 4.46 (bs, 1H), 3.85 (s, 3H), 2.56 (d,  $J = 1.2$  Hz, 3H), 2.35 (s, 3H).

$^{13}\text{C NMR}$  (100 MHz,  $\text{CDCl}_3$ )  $\delta$  150.9, 141.7, 134.1, 131.2, 129.2, 119.2, 117.6, 108.3, 55.9, 17.3, 15.6.



IR (CCl<sub>4</sub> 0.05M, cm<sup>-1</sup>) v 3614, 3590, 2925, 2845, 1655, 1614, 1529, 1485, 1464, 1173.

#### 4-Methoxy-6-methyl-benzo[*b*]thiophen-7-ol (**32**)



To a solution of 6-methoxy-2-(4-methoxyphenyl)-8-methyl-2,3-dihydrobenzo[*b*][1,4]oxathiine **25** (60 mg, 0.20 mmol)<sup>21</sup> in dry CHCl<sub>3</sub> (6 mL) CF<sub>3</sub>SO<sub>3</sub>H (30 mg, 0.20 mmol) was added and the mixture heated at 60 °C for 1h. The mixture was diluted with DCM (20 mL), washed twice with saturated NaHCO<sub>3</sub> and water. The organic phase dried over anhydrous Na<sub>2</sub>SO<sub>4</sub> and evaporated to dryness to give a crude purified by silica gel flash chromatography using DCM as eluent to give **32** as a brown solid. (30 mg, 77%).

**Mp:** 95-99°C.

**<sup>1</sup>H NMR** (400 MHz, CDCl<sub>3</sub>) δ 7.43 (d, *J* = 5.6 Hz, 1H), 7.27 (d, *J* = 5.6 Hz, 1H), 6.54 (s, 1H), 4.58 (s, 1H), 3.91 (s, 3H), 2.37 (s, 3H);

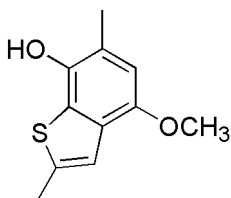
**<sup>13</sup>C NMR** (100 MHz, CDCl<sub>3</sub>) δ 149.1, 141.8, 130.3, 130.0, 124.0, 121.2, 117.8, 107.8, 55.9, 15.7;

**IR** (CCl<sub>4</sub> 0.05M, cm<sup>-1</sup>) 3613, 3594, 3000, 2951, 2934, 2856, 2831, 1662, 1655, 1501, 1463, 1179, 1040.

**MS (EI)** *m/z* (%): 194 (M<sup>+</sup>, 64%).

Anal. Calcd. for C<sub>10</sub>H<sub>10</sub>O<sub>2</sub>S: C, 61.83; H, 5.19; Found: C, 61.67; H, 5.33.

#### 4-Methoxy-2,6-dimethyl-benzo[*b*]thiophen-7-ol (**33**)



To a solution of trans-6-methoxy-2-(4-methoxyphenyl)-3,8-dimethyl-2,3-dihydrobenzo[*b*][1,4]oxathiine **26** (40 mg, 0.13 mmol)<sup>21</sup> in dry CHCl<sub>3</sub> (4 mL) triflic acid (19 mg, 0.13 mmol) was added and the mixture heated at 60 °C for 2h. The mixture was diluted with DCM (20 mL), washed twice with saturated NaHCO<sub>3</sub> and water. The organic phase dried over anhydrous Na<sub>2</sub>SO<sub>4</sub> and evaporated to dryness to give a crude purified by silica gel flash chromatography using DCM/petroleum ether = 1/1 as eluent to give **33** as a brown solid. (14 mg, 51%).

**Mp:** 107-109°C;

**<sup>1</sup>H NMR** (400 MHz, CDCl<sub>3</sub>) δ 7.06 (s, 1H), 6.50 (s, 1H), 4.52 (bs, 1H), 3.87 (s, 3H), 2.56 (s, 3H), 2.34 (s, 3H);

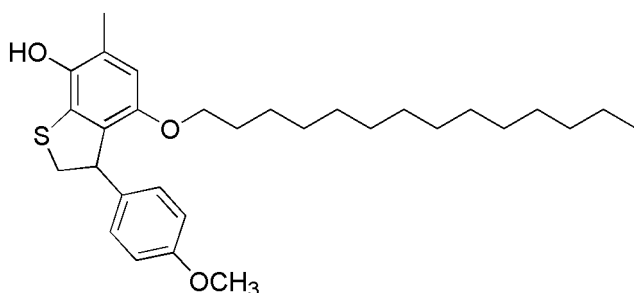
**<sup>13</sup>C NMR** (100 MHz, CDCl<sub>3</sub>) δ 148.2, 141.4, 138.6, 130.6, 129.3, 118.8, 117.0, 108.0, 55.9, 16.1, 15.7;

**IR** (CCl<sub>4</sub> 0.025M, cm<sup>-1</sup>): 3614, 3594, 2921, 2856, 1488, 1464, 1399, 1180, 1050.

**MS (EI)** m/z (%): 208 (M<sup>+</sup>, 94%).

Anal. Calcd. for C<sub>11</sub>H<sub>12</sub>O<sub>2</sub>S: C, 63.43; H, 5.81; Found: C, 63.56; H, 5.88.

3-(4-Methoxy-phenyl)-6-methyl-4-tetradecyloxy-2,3-dihydro-benzo[*b*]thiophen-7-ol  
(**34**)



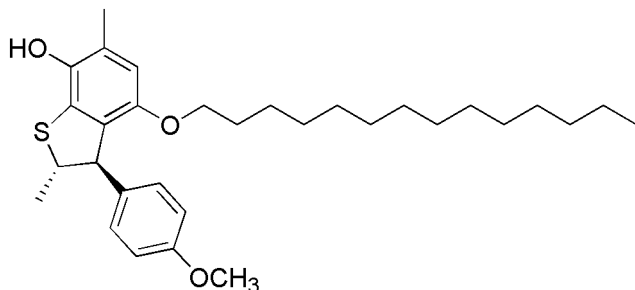
In a round-bottomed flask containing a solution of **20** (30 mg, 0.060 mmol) in CHCl<sub>3</sub> (2.5 mL) was added BF<sub>3</sub>Et<sub>2</sub>O (23 μL, 0.18 mmol); the reaction mixture was left under magnetic stirring at reflux (60°C). Rapidly, the solution changed from colorless to pale yellow. After checking the starting oxathiine was no more detectable on the TLC (2h30') the solution was diluted with CH<sub>2</sub>Cl<sub>2</sub> (20 mL), washed with a saturated aqueous solution of NaHCO<sub>3</sub> (20 mL) and water (20 mL). The organic layer was dried over Na<sub>2</sub>SO<sub>4</sub> then filtered and evaporated *in vacuo*. The crude product was purified by silica-gel column chromatography using before a mixture of petroleum ether and CH<sub>2</sub>Cl<sub>2</sub> 1:2 as eluent. The purified product **34** was obtained as a beige solid (15 mg). Yield: 53%.

**<sup>1</sup>H NMR** (400 MHz, CDCl<sub>3</sub>) δ 7.16 (d, *J* = 8.6 Hz, 2H), 6.78 (d, *J* = 8.6 Hz, 2H), 6.34 (s, 1H), 4.76 (dd, *J* = 8.5, 2.8 Hz, 1H), 4.18 (s, 1H), 3.92 (dd, *J* = 11.1, 8.5 Hz, 1H), 3.81–3.75 (m, 1H), 3.76 (s, 3H), 3.66–3.60 (m, 1H), 3.26 (dd, *J* = 11.1, 2.8 Hz, 1H), 2.23 (s, 3H), 1.52–1.45 (m, 2H), 1.30–1.17 (m, 22H), 0.88 (t, *J* = 6.62 Hz, 3H).

**<sup>13</sup>C NMR** (100 MHz, CDCl<sub>3</sub>) δ 158.3, 149.6, 142.0, 135.4, 130.0, 129.2, 128.1, 124.3, 113.6, 111.5, 68.5, 55.2, 50.3, 42.7, 31.9, 29.71, 29.70, 29.68, 29.66, 29.63, 29.55, 29.4, 29.3, 29.2, 25.8, 22.7, 16.0, 14.1.

**IR** (CDCl<sub>3</sub>, 0.05M, cm<sup>-1</sup>) ν 3603, 2927, 2855, 1609, 1511, 1487, 1468, 1407, 1245, 1179.

3-(4-Methoxy-phenyl)-2,6-dimethyl-4-tetradecyloxy-2,3-dihydro-benzo[*b*]thiophen-7-ol  
(**35**)



In a round-bottomed flask containing a solution of **21** (35 mg, 0.070 mmol) in  $\text{CHCl}_3$  (2.5 mL) was added  $\text{BF}_3 \cdot \text{Et}_2\text{O}$  (26  $\mu\text{L}$ , 0.21 mmol); the reaction mixture was left under magnetic stirring at reflux (60°C). After checking the starting oxathiine was no more detectable on the TLC (1h) the solution was diluted with  $\text{CH}_2\text{Cl}_2$  (20 mL), washed with a saturated aqueous solution of  $\text{NaHCO}_3$  (20 mL) and water (20 mL). The organic layer was dried over  $\text{Na}_2\text{SO}_4$  then filtered and evaporated *in vacuo*. The crude product was purified by silica-gel column chromatography using before a mixture of petroleum ether and  $\text{CH}_2\text{Cl}_2$  1:2 as eluent. The purified product **35** was obtained as a light orange solid (22 mg). Yield: 63%.

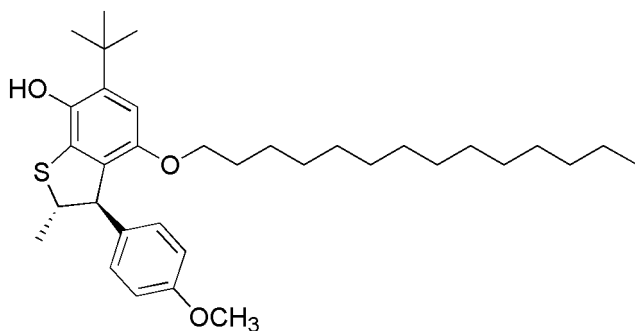
**$^1\text{H NMR}$**  (400 MHz,  $\text{CDCl}_3$ )  $\delta$  7.12 (d,  $J = 8.7$  Hz, 2H), 6.77 (d,  $J = 8.7$  Hz, 2H), 6.35 (s, 1H), 4.32 (d,  $J = 3.1$  Hz, 1H), 4.16 (bs, 1H), 3.80–3.70 (m, 2H), 3.76 (s, 3H), 3.63–3.57 (m, 1H), 2.23 (s, 3H), 1.53 + 1.52 (s, 3H, SoD), 1.48–1.41 (m, 2H), 1.31–1.12 (m, 22H), 0.89 (t,  $J = 6.6$  Hz, 3H).

**$^{13}\text{C NMR}$**  (100 MHz,  $\text{CDCl}_3$ )  $\delta$  158.3, 150.1, 142.1, 135.1, 128.8, 128.3, 128.1, 124.2, 113.6, 111.7, 68.6, 58.9, 55.2, 54.8, 31.9, 29.71, 29.70, 29.68, 29.66, 29.65, 29.55, 29.36, 29.34, 29.23, 25.8, 23.7, 22.7, 16.0, 14.1.

**IR** ( $\text{CDCl}_3$ , 0.05M,  $\text{cm}^{-1}$ )  $\nu$  3571, 2928, 2856, 1610, 1511, 1488, 1468, 1408, 1304, 1245, 1178, 1108, 1036.

**MS (ESI)**:  $m/z$  497.3 [M-H] $^-$ .

6-*tert*-Butyl-3-(4-methoxy-phenyl)-2-methyl-4-tetradecyloxy-2,3-dihydro-benzo[*b*]thiophen-7-ol (**36**)

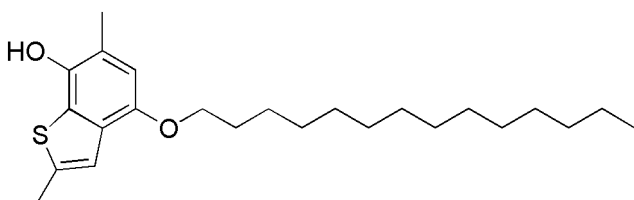


To a solution of the **23** (34 mg, 0.063 mmol) in  $\text{CHCl}_3$  (6 mL) was added  $\text{BF}_3 \cdot \text{Et}_2\text{O}$  (23  $\mu\text{L}$ , 0.19 mmol). The mixture was left under magnetic stirring at  $60^\circ\text{C}$  for 22h. TLC check showed only the presence of the starting cycloadduct, so it was added more  $\text{BF}_3 \cdot \text{Et}_2\text{O}$  (23  $\mu\text{L}$ , 0.19 mmol). The reaction was left for additional 8 hours, then diluted with  $\text{CH}_2\text{Cl}_2$  and washed once with  $\text{H}_2\text{O}$ . The organic layer was dried over  $\text{Na}_2\text{SO}_4$  and concentrated *in vacuo*. The crude was purified by silica-gel column chromatography using before a mixture of petroleum ether and  $\text{CH}_2\text{Cl}_2$  8:1 as eluent to separate the excess of dienophile, then 1:1 to obtain the desired product **36** as an orange solid (15 mg). Yield: 45%.

$^1\text{H NMR}$  (400 MHz,  $\text{CDCl}_3$ )  $\delta$  7.13 (d,  $J = 8.6$  Hz, 2H), 6.79 (d,  $J = 8.6$  Hz, 2H), 6.51 (s, 1H), 4.32 (d,  $J = 3.7$  Hz, 1H), 4.06 (s, 1H), 3.80–3.75 (m, 2H), 3.76 (s, 3H), 3.63–3.58 (m, 1H), 1.53 + 1.51 (s, 3H, SoD), 1.47–1.43 (m, 2H), 1.40 (s, 9H), 1.32–1.14 (m, 22H), 0.88 (t,  $J = 6.6$  Hz, 3H).

$^{13}\text{C NMR}$  (100 MHz,  $\text{CDCl}_3$ )  $\delta$  158.3, 149.7, 142.5, 136.9, 135.0, 129.7, 128.6, 128.3, 113.6, 109.0, 68.7, 59.2, 55.2, 55.1, 34.9, 31.9, 29.7, 29.6, 29.4 (2 signals for 9 non-equivalent  $\text{CH}_2$ ), 25.8, 23.2, 22.7, 14.1.

#### 2,6-Dimethyl-4-tetradecyloxy-benzo[*b*]thiophen-7-ol (**37**)



In a round-bottomed flask containing a solution of **35** (18 mg, 0.036 mmol) was added a solution of  $\text{CF}_3\text{SO}_3\text{H}$  (1.6  $\mu\text{L}$ , 0.018 mmol) in  $\text{CHCl}_3$  (1.2 mL). The reaction mixture was left under magnetic stirring at  $50^\circ\text{C}$  for 40' then, since from the TLC the reaction did not proceed, the solution was heated at reflux ( $60^\circ\text{C}$ ) for other 80'. The solution was then diluted with  $\text{CH}_2\text{Cl}_2$  (20 mL), washed with a saturated aqueous  $\text{NaHCO}_3$  solution (20 mL) and water (20 mL), then dried over anhydrous  $\text{Na}_2\text{SO}_4$  and concentrated *in vacuo*. The crude product was purified by silica-gel column chromatography using a mixture of

petroleum ether and CH<sub>2</sub>Cl<sub>2</sub> 1:1 as eluent. The purified product **37** was obtained as a light brown solid (7 mg). Yield: 50%.

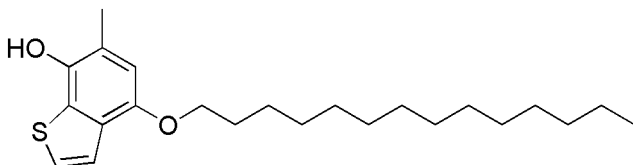
**<sup>1</sup>H NMR** (400 MHz, CDCl<sub>3</sub>) δ 7.08 (s, 1H), 6.50 (s, 1H), 4.45 (bs, 1H), 4.00 (t, *J* = 6.5 Hz, 2H), 2.56 (s, 3H), 2.33 (s, 3H), 1.85–1.78 (m, 2H), 1.52–1.45 (m, 2H), 1.35–1.26 (m, 20H), 0.88 (t, *J* = 6.7 Hz, 3H).

**<sup>13</sup>C NMR** (100 MHz, CDCl<sub>3</sub>) δ 147.8, 141.3, 138.4, 131.1, 129.2, 119.0, 117.0, 109.2, 68.9, 31.9, 29.7, 29.6, 29.5, 29.4 (4 signals for 9 non-equivalent CH<sub>2</sub> groups), 26.2, 22.7, 16.1, 15.7, 14.1.

**IR** (CDCl<sub>3</sub>, 0.05M, cm<sup>-1</sup>) ν 3602, 2928, 2856, 1469, 1277, 1229, 1139, 1039.

**MS (ESI)**: *m/z* 389.3 [M-H]<sup>-</sup>.

6-Methyl-4-tetradecyloxy-benzo[*b*]thiophen-7-ol (**38**)



In a round-bottomed flask containing **22** (20 mg, 0.047 mmol) was added a solution of CF<sub>3</sub>SO<sub>3</sub>H (2 μL, 0.024 mmol) in CHCl<sub>3</sub> (2 mL), very slowly, dropwise; the reaction mixture was left under magnetic stirring at room temperature. After 30', check by TLC showed only the presence of the starting cycloadduct. In order to obtain the transposition product, the oil bath was gradually heated to 30°C (3h) and then to 60°C (1h). The reaction mixture was diluted with CH<sub>2</sub>Cl<sub>2</sub> (20 mL), washed once with a saturated solution of NaHCO<sub>3</sub> (20 mL) and once with H<sub>2</sub>O (20 mL). The organic layer was dried over Na<sub>2</sub>SO<sub>4</sub>, filtered and evaporated *in vacuo*. The crude was purified by silica gel column chromatography, using a mixture of petroleum ether and CH<sub>2</sub>Cl<sub>2</sub> 1:2 as eluent. The purified product **38** was obtained as a light brown solid (4 mg). Yield: 23%.

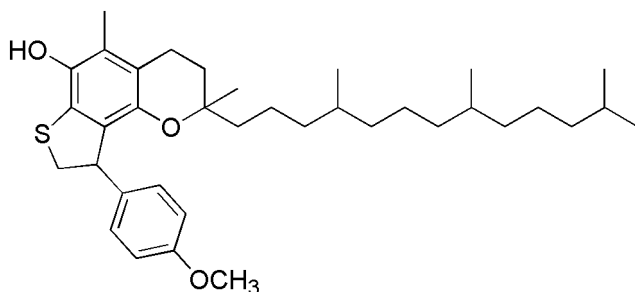
**<sup>1</sup>H NMR** (400 MHz, CDCl<sub>3</sub>) δ 7.44 (d, *J* = 5.8 Hz, 1H), 7.25 (d, *J* = 5.8 Hz, 1H), 6.54 (s, 1H), 4.54 (bs, 1H), 4.04 (t, *J* = 6.5 Hz, 2H), 2.36 (s, 3H), 1.87–1.80 (m, 2H), 1.52–1.46 (m, 2H), 1.26 (bs, 20H), 0.90–0.86 (m, 3H).

**<sup>13</sup>C NMR** (100 MHz, CDCl<sub>3</sub>) δ 148.6, 141.7, 135.0, 134.7, 123.8, 121.4, 117.8, 109.0, 68.9, 31.9, 29.7, 29.6, 29.4 (3 signals for 9 non-equivalent CH<sub>2</sub> groups), 26.2, 22.7, 15.7, 14.1.

**IR** (CDCl<sub>3</sub>, 0.05M, cm<sup>-1</sup>) ν 3602, 2928, 2856, 1466, 1409, 1262, 1099.

**MS (ESI)**: *m/z* 375.2 [M-H]<sup>-</sup>.

9-(4-methoxyphenyl)-2,5-dimethyl-2-(4,8,12-trimethyltridecyl)-3,4,8,9-tetrahydro-2H-thieno[2,3-h]chromen-6-ol (**40**)



To a solution of **18** (50 mg, 0.080 mmol) in  $\text{CHCl}_3$  (2.7 mL) was added  $\text{CF}_3\text{SO}_3\text{H}$  (12 mg, 0.080 mmol) and the reaction mixture at  $60^\circ\text{C}$  for 1h 30min while the initial soft purple colour of the solution turned dark. The solution was so diluted with DCM (40 mL), washed with saturated aqueous  $\text{NaHCO}_3$  solution (40 mL) and water (40mL) then dried over anhydrous  $\text{Na}_2\text{SO}_4$  and concentrated in vacuum. The crude product was purified by silica-gel column chromatography (eluent: petroleum ether/DCM = 1/1 followed by 1/2) to obtain **41** (3 mg, 8%) and **40** as a light brown oil (27 mg, 60%).

$^1\text{H NMR}$  (400 MHz,  $\text{CDCl}_3$ )  $\delta$  7.18–7.15 (m, 2H), 6.78–6.74 (m, 2H), 4.73–4.71 (m, 1H), 4.06 (bs, 1H), 3.94–3.87 (m, 1H), 3.77+3.75 (s, 3H, D1+D2), 3.29–3.23 (m, 1H), 2.56–2.50 (m, 2H), 2.11 (s, 3H), 1.75–1.62 (m, 2H), 1.54–1.01 (m, 24H), 0.88–0.84 (m, 12H).

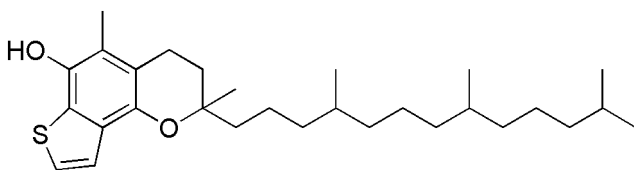
$^{13}\text{C NMR}$  (100 MHz,  $\text{CDCl}_3$ )  $\delta$  158.2, 144.8, 140.9, 135.6, 128.5, 128.2, 126.3, 122.6, 117.7, 113.4, 74.7, 55.1, 50.2, 42.3, 41.2, 39.4, 39.0, 37.6, 37.5, 37.4, 32.8, 32.6, 31.4, 28.0, 24.8, 24.4, 22.7, 22.6, 21.7, 20.7, 19.8, 19.7, 11.4.

$\text{IR}$  ( $\text{CDCl}_3$ , 0.05M,  $\text{cm}^{-1}$ )  $\nu$  3690, 3571, 2868, 2245, 1608, 1510, 1462, 1419, 1245, 1210, 1177.

$\text{MS (ESI)}$ :  $m/z$  565.4  $[\text{M-H}]^-$ .

Anal. Calcd. for  $\text{C}_{36}\text{H}_{54}\text{O}_3\text{S}$ : C, 76.27; H, 9.60; Found: C, 76.44; H, 9.84.

2,5-dimethyl-2-(4,8,12-trimethyltridecyl)-3,4-dihydro-2H-thieno[2,3-h]chromen-6-ol (**41**)



When the above described reaction was kept at  $60^\circ\text{C}$  for 2h 30min the usual work-up and column chromatography (eluent: petroleum ether;DCM = 1/1 followed by 1/2) allowed to isolate **40** (11 mg, 7% yield) and **41** as a light yellow oil (50 mg, 40% yield).

**<sup>1</sup>H NMR** (400 MHz, CDCl<sub>3</sub>) δ 7.41 (d, *J* = 5.5 Hz, 1H), 7.21 (d, *J* = 5.5 Hz, 1H), 4.45 (bs, 1H), 2.69 (t, *J* = 6.5 Hz, 2H), 2.24 (s, 3H), 1.95–1.82 (m, 2H), 1.30–1.09 (m, 24H), 0.87–0.84 (m, 12H).

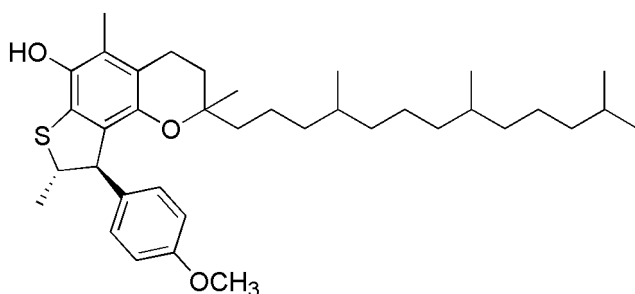
**<sup>13</sup>C NMR** (100 MHz, CDCl<sub>3</sub>) δ 143.4, 140.5, 129.7, 127.8, 123.2, 121.3, 117.5, 115.0, 75.3, 39.8, 39.4, 37.6, 37.5, 37.4, 37.3, 32.8, 32.7, 31.5, 28.0, 24.8, 24.4, 22.7, 22.6, 21.1, 20.8, 19.7, 19.6, 11.4.

**IR** (CDCl<sub>3</sub>, 0.05M, cm<sup>-1</sup>) ν 3746, 3595, 2936, 2242, 1503, 1456.

**MS (ESI)**: *m/z* 457.2 [M-H]<sup>-</sup>.

Anal. Calcd. for C<sub>29</sub>H<sub>46</sub>O<sub>2</sub>S: C, 75.93; H, 10.11; Found: C, 76.23; H, 10.28.

9-(4-methoxyphenyl) -2,5,8-trimethyl-2-(4,8,12-trimethyltridecyl) -3,4,8,9-tetrahydro-2H-thieno[2,3-*h*] chromen-6-ol (**42**)



To a solution of **19** (30 mg, 0.048 mmol) was added a solution of triflic acid (7 mg, 0.048 mmol) in CHCl<sub>3</sub> (1.6 mL) and the reaction mixture at 60°C for 2h min while the solution changed from dark yellow to purple. The solution was diluted with DCM (40 mL), washed with saturated aqueous NaHCO<sub>3</sub> solution (40 mL) and water (40 mL), dried over anhydrous Na<sub>2</sub>SO<sub>4</sub> and concentrated in vacuum. The crude was purified by silica-gel column chromatography (eluent: petroleum ether/DCM = 1/1 followed by 1/2) to obtain **42** as a light brown oil (15 mg, 56%).

**<sup>1</sup>H NMR** (400 MHz, CDCl<sub>3</sub>) δ 7.14–7.11 (m, 2H), 6.77–6.74 (m, 2H), 4.28 (bs, 1H), 4.03 (bs, 1H), 3.77+3.75 (s, 3H, D1+D2), 3.73–3.69 (m, 1H), 2.60–2.47 (m, 2H), 2.12 (s, 3H), 1.73–1.58 (m, 4H), 1.53+1.51 (s, 3H, D1+D2), 1.43–1.02 (m, 22H), 0.88–0.84 (m, 12H).

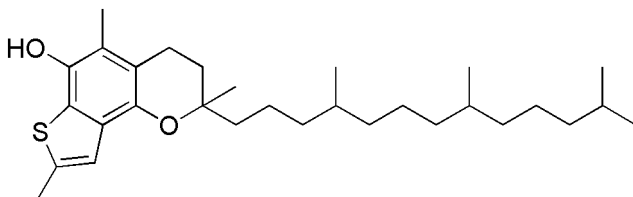
**<sup>13</sup>C NMR** (100 MHz, CDCl<sub>3</sub>) δ 158.2, 145.3, 140.9, 135.6, 128.2, 127.5, 125.5, 122.5, 117.7, 113.4, 74.6, 59.0, 55.1, 54.4, 41.0, 39.4, 38.7, 37.5, 37.4, 37.3, 32.8, 32.5, 31.5, 28.0, 24.8, 24.5, 22.7, 22.6, 21.6, 21.5, 20.6, 19.7, 19.6, 11.4.

**IR** (CDCl<sub>3</sub>, 0.05M, cm<sup>-1</sup>) ν 3572, 2929, 2869, 2244, 1610, 1511, 1463, 1421, 1378, 1245.

**MS (ESI)**: *m/z* 579.4 [M-H]<sup>-</sup>.

Anal. Calcd. for C<sub>37</sub>H<sub>56</sub>O<sub>3</sub>S: C, 76.50; H, 9.72; Found: C, 76.61; H, 9.58.

2,5,8-trimethyl-2-(4,8,12-trimethyltridecyl)-3,4-dihydro-2H-thieno[2,3-h]chromen-6-ol  
(**43**)



When the above described reaction was kept at 60 °C for 3h 30min the usual work-up and column chromatography (eluent: petroleum ether/DCM = 2/1) allowed the isolation of **43** as a brown glassy (18 mg, 38% yield).

**<sup>1</sup>H NMR** (400 MHz, CDCl<sub>3</sub>) δ 7.05 (s, 1H), 4.35 (bs, 1H), 2.66 (t, *J* = 6.6 Hz, 2H), 2.55 (s, 3H), 2.21 (s, 3H), 1.92–1.81 (m, 2H), 1.32–1.20 (m, 12H), 1.29 (s, 3H), 1.16–1.02 (m, 9H), 0.88–0.84 (m, 12H).

**<sup>13</sup>C NMR** (100 MHz, CDCl<sub>3</sub>) δ 142.5, 140.1, 137.8, 130.0, 127.1, 119.0, 116.6, 115.0, 75.1, 39.9, 39.4, 37.6, 37.5, 37.4, 37.3, 32.8, 32.7, 31.5, 28.0, 24.8, 24.5, 23.7, 22.7, 22.6, 21.1, 19.7, 19.6, 16.1, 11.3.

**IR** (CDCl<sub>3</sub>, 0.05M, cm<sup>-1</sup>) ν 3602, 2978, 2968, 1462, 1414, 1379, 1276, 1205.

**MS (ESI)**: *m/z* 471.3 [M-H]<sup>-</sup>.

Anal. Calcd. for C<sub>30</sub>H<sub>48</sub>O<sub>2</sub>S: C, 76.22; H, 10.23; Found: C, 76.34; H, 9.99.

### 2.2.1 Chain-breaking antioxidant activity

The chain-breaking antioxidant activity of the title compounds was evaluated by studying the inhibition of the thermally initiated autoxidation of styrene in chlorobenzene. Styrene was percolated twice on an alumina column before use, AIBN was recrystallized from methanol. Solvents of the highest purity grade were used as received. Autoxidation experiments were followed by measuring the O<sub>2</sub> consumption by using a gas-uptake recording apparatus. In a typical experiment, an air-saturated mixture of styrene in chlorobenzene (50% v/v) containing AIBN (5 × 10<sup>-2</sup> M) was equilibrated with the reference solution containing also an excess of 2,2,5,7,8-pentamethyl-6-chromanol (α-TOH) in the same solvent at 30°C. After equilibration, a concentrated solution of the antioxidant was injected into the sample flask (final concentration from 5 × 10<sup>-6</sup> to 5 × 10<sup>-5</sup> M), and the oxygen consumption in the sample was measured. From the slope of the oxygen consumption during the inhibited period, *k<sub>inh</sub>* values were obtained by using the equation [1], while the *n* coefficient was determined by the length of the inhibited period (*T<sub>inh</sub>*) by using the equation [2] and [3].<sup>55</sup>

$$\Delta[\text{O}_2]_t = -k_p/k_{inh} [\text{styrene}] \ln(1-t/T_{inh}) \quad [1]$$



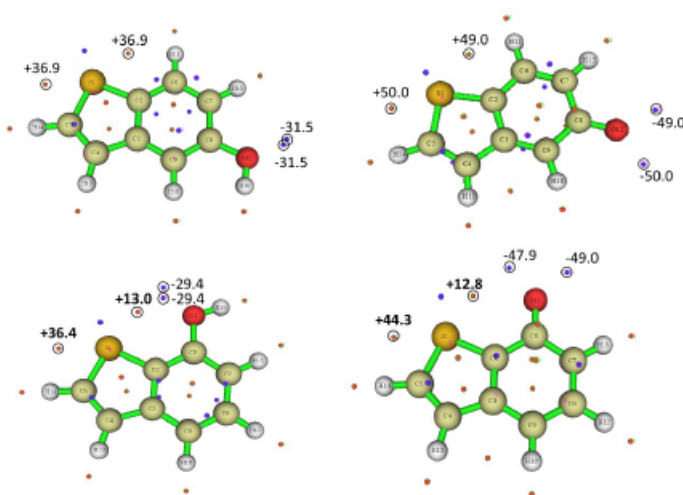
$$n = R_i T_{\text{inh}} / [\text{antioxidant}] \quad [2]$$

$$R_i = 2 [\alpha\text{-TOH}] / T_{\text{inh}} \quad [3]$$

The  $k_p$  values (the propagation rate constant of the oxidizable substrate) of styrene at 303° is 41 M<sup>-1</sup> s<sup>-1</sup>. The value of  $R_i$  (the speed in the production of radicals by the initiator) was determined by using  $\alpha$ -TOH ( $n=2$ ) as a reference.

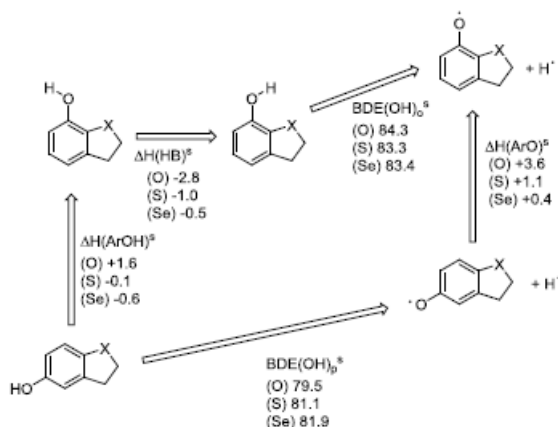
### 2.3.2 Theoretical calculations

Geometries and frequencies were calculated in the gas phase at the M062X/aug-cc-pVDZ level of theory. Geometry minima were checked for the absence of imaginary frequencies. The enthalpies at 298 K were computed at the stationary points from frequency calculations. Bond dissociation enthalpies (BDE) of the phenolic O-H were computed by using the isodesmic approach. It consists in calculating the enthalpy difference between the investigated compound and unsubstituted phenol, and by combining this value with the experimental BDE(OH) of phenol (86.7 kcal/mol).<sup>56,57</sup> Calculations were performed by using Gaussian09/E.01 suite of programs.<sup>58</sup> The structure of compounds **28** and **29** was simplified by removing the substituents on the pentaatomic ring, while that of  $\alpha$ -TOH by removing the phetyl tail (see Tables below). Electrostatic potential surfaces were generated by Gauss View 3.0. Surface quantitative analysis performed by the Multiwfn software, freely available at <https://multiwfn.codeplex.com>. In para isomers,  $\sigma$ -holes are on the outer sides of the Ar-X and of the C-X bonds, and have identical  $V_{s,\text{max}}$  (within 1%) (see for instance Figure 31). In ortho isomers, because of the proximity of the -O<sup>\*</sup> group, it was possible to quantify only the  $\sigma$ -hole on the outer side of the Ar-X bond. Natural bond orbital (NBO) perturbation theory analysis was performed by using NBO version 3 as implemented in Gaussian 09.

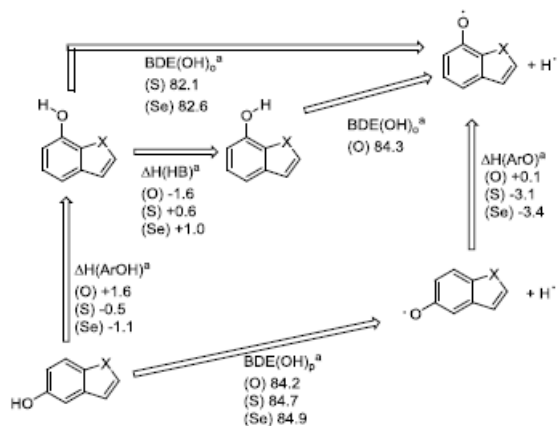


**Figure 31:** Output obtained from the surface quantitative analysis, showing maxima and minima relevant for the formation of a chalcogen bond. As exemplified in this

figure, in 5-hydroxy derivatives (upper) the couples of  $\sigma$ -holes on the chalcogen atom, and the electrostatic potentials of the oxygen lone pairs are essentially identical. In 7-hydroxy derivatives the proximity between the S and O atoms causes the sigma-hole that points toward the O-atom to be smaller in magnitude, as effect of the electrostatic interaction between the two groups.

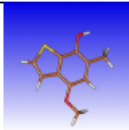
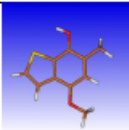
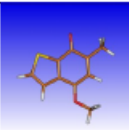
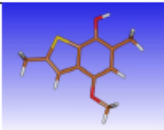
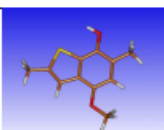
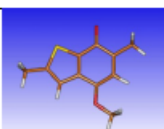


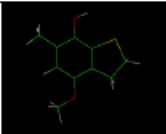
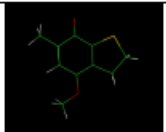
**Figure 32:** Bond dissociation enthalpy (BDE) of the phenolic O-H bond, enthalpy difference between the para and ortho isomers, and H-bond strength for saturated hydroxy-benzo fused five membered heterocycles (all data are in kcal/mol). For comparison, the BDE(OH) of unsubstituted phenol is 86.7 kcal/mol.



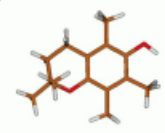
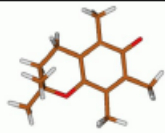
**Figure 33:** Bond dissociation enthalpy (BDE) of the phenolic O-H bond, enthalpy difference between the para and ortho isomers, and H-bond strength for aromatic hydroxy-benzo fused five membered heterocycles (all data are in kcal/mol). For comparison, the BDE(OH) of unsubstituted phenol is 86.7 kcal/mol.

## Calculation

Compound 32		Sum of electronic and thermal Enthalpies (Hartree)
phenol, conformation away		-935.373706
phenol, conformation toward		-935.373221 (less stable by 0.3 kcal/mol than away conformation)
radical		-934.756332
Compound 33		Sum of electronic and thermal Enthalpies (Hartree)
phenol, conformation away		-974.646387
phenol, conformation toward		-974.646114 (less stable by 0.17 kcal/mol than away conformation)
radical		-974.029065

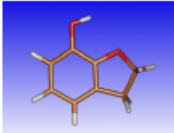
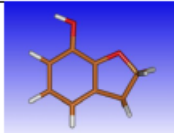
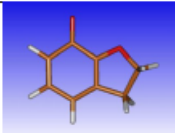
Compounds 28 and 29		Sum of electronic and thermal Enthalpies (Hartree)
phenol, conformation toward		-936.553333
radical		-935.931066

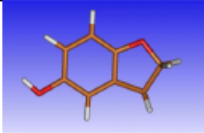
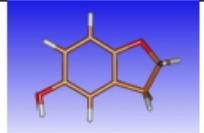
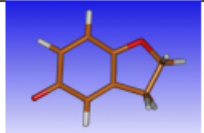
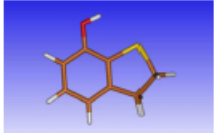
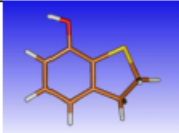
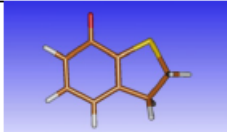
$\alpha$ -TOH Sum of electronic and thermal Enthalpies

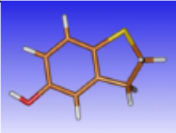
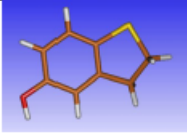
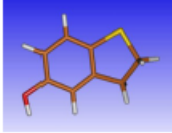
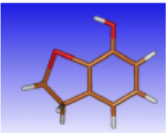
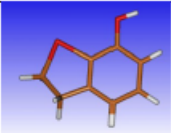
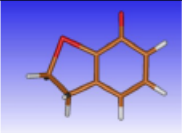
phenol		-695.472553
radical		-694.853622

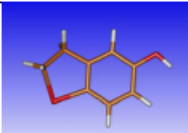
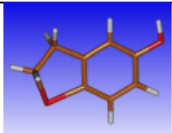
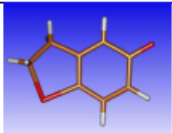
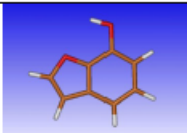
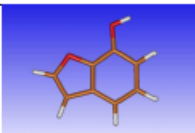
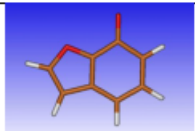
7-hydroxy  
dihydrobenzo[b]furan

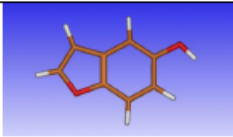
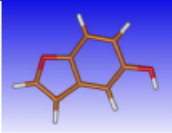
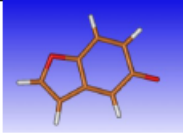
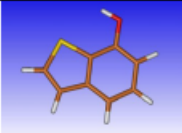
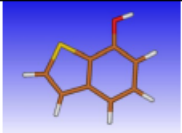
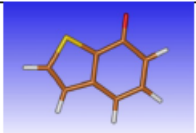
Sum of electronic and thermal Enthalpies

phenol, conformation toward		-459.837279 (more stable by 2.8 kcal/mol than away conformation)
phenol, conformation away		-459.832794
radical		-459.204572

5-hydroxy dihydrobenzo[b]furane		Sum of electronic and thermal Enthalpies
phenol, conformation 1		-459.835352
phenol, conformation 2		-459.834926
radical		-459.210314
7-hydroxy dihydrobenzo[b]thiophene		Sum of electronic and thermal Enthalpies
phenol, conformation toward		-782.821432 (more stable by 0.99 kcal/mol than away conformation)
phenol, conformation away		-782.819857
radical		-782.190333

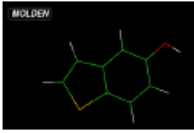
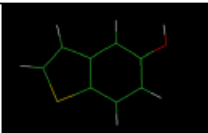
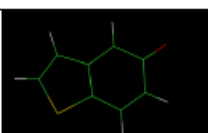
5-hydroxy dihydrobenzo[b]thiophene		Sum of electronic and thermal Enthalpies
phenol, conformation 1		-782.819719
phenol, conformation 2		-782.819352
radical		-782.192085
7-hydroxy dihydrobenzo[b]selenophene		Sum of electronic and thermal Enthalpies
phenol, conformation toward		-2786.202789 (more stable by 0.51 kcal/mol than away conformation)
phenol, conformation away		-2786.201976
radical		-2785.571566

5-hydroxy dihydrobenzo[b]selenophene		Sum of electronic and thermal Enthalpies
phenol, conformation 1		-2786.200995
phenol, conformation 2		-2786.200649
radical		-2785.572187
7-hydroxybenzo[b]furan		Sum of electronic and thermal Enthalpies
phenol, conformation toward		-458.658220 (more stable by 1.6 kcal/mol than away conformation)
phenol, conformation away		-458.655703
radical		-458.025419

5-hydroxybenzo[b]furan		Sum of electronic and thermal Enthalpies
phenol, conformation toward		-458.657961
phenol, conformation away		-458.658178
radical		-458.025621
7-hydroxy benzo[b]thiophene		Sum of electronic and thermal Enthalpies
phenol, conformation toward		-781.641606
phenol, conformation away		-781.642578 (more stable by 0.61 kcal/mol than toward conformation)
radical		-781.013398

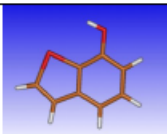
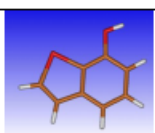
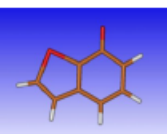


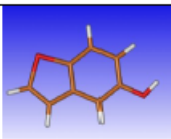
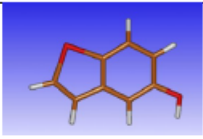
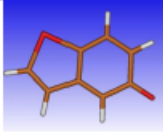
5-hydroxy benzo[b]thiophene Sum of electronic and thermal Enthalpies

phenol, conformation 1		-781.641511
phenol, conformation 2		-781.641821
radical		-781.008529

7-hydroxy  
benzo[b]selenophene

Sum of electronic and thermal Enthalpies

phenol, conformation toward		-2785.019206
phenol, conformation away		-2785.020831 (more stable by 1.0 kcal/mol than toward conformation)
radical		-2784.390908

5-hydroxybenzo[b]selenophene		Sum of electronic and thermal Enthalpies
phenol, conformation 1		-2785.018877
phenol, conformation 2		-2785.019075
radical		-2784.385502

### 2.3.3 Protein binding and localization with the $\alpha$ -tocopherol transfer protein

The binding between  $\alpha$ -TTP and compounds **41** and **43** was studied by means of intrinsic tryptophan fluorescence quenching and the results compared with  $\alpha$ -TTP binding to commercial all-*rac*- $\alpha$ -TOH.

The tryptophan fluorescent residues lie in the hydrophobic pocket close to the residues reported to be involved in  $\alpha$ -TOH binding<sup>51</sup> thus making the  $\alpha$ -TTP intrinsic fluorescence amenable for the determination of the dissociation constant by means of Trp fluorescence quenching.<sup>59</sup> The data reported were analysed with a bimolecular association model as previously described in the literature using equation [4].<sup>60</sup>

$$\frac{F}{F_0} = 1 + \left( \frac{F_b}{F_0} - 1 \right) \left( \frac{P_t + L_t + K_d - \sqrt{(P_t + L_t + K_d)^2 - 4P_tL_t}}{2P_t} \right) \quad [4]$$

Where  $F_0$  is the observed fluorescence emission intensity of the free protein,  $F$  is fluorescence emission intensity of the protein in the presence of the ligand,  $F_b$  is the fluorescence emission of the totally bound protein,  $L_t$  is the total ligand concentration,  $K_d$  is the dissociation constant and  $P_t$  is the total protein concentration.

## 2.4 References

- (1) Hussain, H. H.; Babic, G.; Durst, T.; Wright, J. S.; Flueraru, M.; Chichirau, A.; Chepelev, L. L. *J. Org. Chem.* **2003**, *68*, 7023–7032.
- (2) Burton, G. W.; Le Page, Y.; Cabe, E. J.; Ingold, K. U. *J. Am. Chem. Soc.* **1980**, *102*, 7791–7792.

- (3) Burton, G. W.; Doba, T.; Gabe, E. J.; Hughes, L.; Lee, F. L.; Prasad, L.; Ingold, K. U. *J. Am. Chem. Soc.* **1985**, *107*, 7053–7065.
- (4) *The Encyclopedia of Vitamin E*; Preedy, V. R., Watson, R. R., Eds.; CABI: Wallingford, Oxon (UK), 2007.
- (5) Lucarini, M.; Pedrielli, P.; Pedulli, G. F.; Cabiddu, S.; Fattuoni, C. *J. Org. Chem.* **1996**, *61*, 9259–9263.
- (6) Lucarini, M.; Pedulli, G. F. *Chem. Soc. Rev.* **2010**, *39*, 2106–2119.
- (7) Brigati, G.; Lucarini, M.; Mugnaini, V.; Pedulli, G. F. *J. Org. Chem.* **2002**, *67*, 4828–4832.
- (8) Burton, G. W.; Ingold, K. U. *Acc. Chem. Res.* **1986**, *19*, 194–201.
- (9) Cerecetto, H.; Lopez, G. *Mini-Reviews Med. Chem.* **2007**, *7*, 315–338.
- (10) Mukai, K.; Okabe, K.; Hosose, H. *J. Org. Chem.* **1989**, *54*, 557–560.
- (11) Barclay, L. R. C.; Vinqvist, M. R.; Mukai, K.; Itoh, S.; Morimoto, H. *J. Org. Chem.* **1993**, *58*, 7416–7420.
- (12) Jacob, C.; Giles, G. I.; Giles, N. M.; Sies, H. *Angew. Chemie - Int. Ed.* **2003**, *42*, 4742–4758.
- (13) Malmström, J.; Jonsson, M.; Cotgreave, I. A.; Hammarström, L.; Sjödin, M.; Engman, L. *J. Am. Chem. Soc.* **2001**, *123*, 3434–3440.
- (14) Zahalka, H. A.; Robillard, B.; Hughes, L.; Lusztyk, J.; Burton, G. W.; Janze, E. G.; Kotake, Y.; Ingold, K. U. *J. Org. Chem.* **1988**, *53*, 3739–3745.
- (15) Shanks, D.; Amorati, R.; Fumo, M. G.; Pedulli, G. F.; Valgimigli, L.; Engman, L. *J. Org. Chem.* **2006**, *71*, 1033–1038.
- (16) Menichetti, S.; Aversa, M. C.; Cimino, F.; Contini, A.; Viglianisi, C.; Tomaino, A. *Org. Biomol. Chem.* **2005**, *3*, 3066–3072.
- (17) Amorati, R.; Cavalli, A.; Fumo, M. G.; Masetti, M.; Menichetti, S.; Pagliuca, C.; Pedulli, G. F.; Viglianisi, C. *Chem. - A Eur. J.* **2007**, *13*, 8223–8230.
- (18) Menichetti, S.; Amorati, R.; Bartolozzi, M. G.; Pedulli, G. F.; Salvini, A.; Viglianisi, C. *European J. Org. Chem.* **2010**, 2218–2225.
- (19) Viglianisi, C.; Bartolozzi, M. G.; Pedulli, G. F.; Amorati, R.; Menichetti, S. *Chem. - A Eur. J.* **2011**, *17*, 12396–12404.
- (20) Amorati, R.; Catarzi, F.; Menichetti, S.; Pedulli, G. F.; Viglianisi, C. *J. Am. Chem. Soc.* **2008**, *130*, 237–244.
- (21) Viglianisi, C.; Amorati, R.; Di Pietro, L.; Menichetti, S. *Chem. - A Eur. J.* **2015**, *21*,

- 16639–16645.
- (22) Ishino, Y.; Mihara, M.; Hayakawa, N.; Miyata, T.; Kaneko, Y.; Miyata, T. *Synth. Commun.* **2001**, *31*, 439–448.
- (23) Bjorsvik, H.-R.; Occhipinti, G.; Gambarotti, C.; Cerasino, L.; Jensen, V. R. *J. Org. Chem.* **2005**, 7290–7296.
- (24) *Chromans and tocopherols*; Ellis, G. P., Ed.; John Wiley & Sons, Inc.: Toronto (CAN), 1981.
- (25) Huang, Z.; Cui, Q.; Xiong, L.; Wang, Z.; Wang, K.; Zhao, Q.; Bi, F.; Wang, Q. *J. Agric. Food Chem.* **2009**, *57*, 2447–2456.
- (26) Capozzi, G.; Menichetti, S.; Nativi, C.; Simonti, M. C. *Tetrahedron Lett.* **1994**, *35*, 9451–9454.
- (27) Capozzi, G.; Falciani, C.; Menichetti, S.; Nativi, C. *J. Org. Chem.* **1997**, *62*, 2611–2615.
- (28) Smith, G. H. *Top. Sulfur Chem.* **1977**, *3*, 101.
- (29) Lucchini, V.; Modena, G.; Pasquato, L. *J. Am. Chem. Soc.* **1991**, *113*, 6600–6607.
- (30) Lucchini, V.; Modena, G.; Pasquato, L. *J. Chem. Soc. Chem. Commun.* **1994**, 1565–1566.
- (31) Fachini, M.; Lucchini, V.; Modena, G.; Pasi, M.; Pasquato, L. *J. Am. Chem. Soc.* **1999**, *121*, 3944–3950.
- (32) Gruttadauria, M.; Noto, R. *J. Heterocycl. Chem.* **2001**, *38*, 765–767.
- (33) Rassias, G.; Hermitage, S. A. *Tetrahedron Lett.* **2009**, *50*, 5565–5568.
- (34) Denmark, S. E.; Jaunet, A. *J. Org. Chem.* **2014**, *79*, 140–171.
- (35) Denmark, S. E.; Chi, H. M. *J. Am. Chem. Soc.* **2014**, *136*, 8915–8918.
- (36) Bacci, J. P.; Kearney, A. M.; Van Vranken, D. L. *J. Org. Chem.* **2005**, *70*, 9051–9053.
- (37) Bauza, A.; Alkorta, I.; Frontera, A.; Elguero, J. *J. Chem. Theory Comput.* **2013**, *9*, 5201–5210.
- (38) Lu, T.; Chen, F. *J. Comput. Chem.* **2011**, *33*, 580–592.
- (39) Amorati, R.; Pedulli, G. F.; Valgimigli, L.; Johansson, H.; Engman, L. *Org. Lett.* **2010**, *12*, 2326–2329.
- (40) Politzer, P.; Murray, S.; Clark, T. *Phys. Chem. Chem. Phys.* **2013**, *15*, 11178–11189.

- (41) Murray, J. S.; Lane, P.; Clark, T.; Politzer, P. *J. Mol. Model.* **2007**, *13*, 1033–1038.
- (42) Beno, B. R.; Yeung, K.-S.; Bartberger, M. D.; Pennington, L. D.; Meanwell, N. A. *J. Med. Chem.* **2015**, *58*, 4383–4438.
- (43) Fick, R. J.; Kroner, G. M.; Nepal, B.; Magnani, R.; Horowitz, S.; Houtz, R. L.; Scheiner, S.; Trievel, R. C. *ACS Chem. Biol.* **2016**, *11*, 748–754.
- (44) Turbiez, M.; Frère, P.; Allain, M.; Videlot, C.; Ackermann, J.; Roncali, J. *Chem. - A Eur. J.* **2005**, *11*, 3742–3752.
- (45) Murray, J. S.; Lane, P.; Politzer, P. *Int. J. Quantum Chem.* **2008**, *108*, 2770–2781.
- (46) Fanfrlik, J.; Pràda, A.; Padélková, Z.; Pecina, A.; Machàček, J.; Lepsik, M.; Holub, J.; Ruzicka, A.; Hnyk, A.; Hobza, P. *Angew. Chemie - Int. Ed.* **2014**, *53*, 10139–10142.
- (47) Nziko, V. D. P. N.; Scheiner, S. *J. Org. Chem.* **2015**, *80*, 2356–2363.
- (48) Kremer, A.; Fermi, A.; Biot, N.; Wouters, J.; Bonifazi, D. *Chem. - A Eur. J.* **2016**, *22*, 5665–5675.
- (49) Blanc, A.; Bénéteau, V.; Weibel, J.; Pale, P. *Org. Biomol. Chem.* **2016**, *14*, 9184–9205.
- (50) Arita, M.; Sato, Y.; Miyata, A.; Tanabe, T.; Takahashi, E.; Kayden, H. J.; Arai, H.; Inoue, K. *Biochem. J.* **1995**, *306*, 437–443.
- (51) Min, K. C.; Kovall, R. A.; Hendrickson, W. A. *PNAS* **2003**, *100*, 14713–14718.
- (52) Meier, R.; Tomizaki, T.; Schulze-Briese, C.; Baumann, U.; Stocker, A. *J. Mol. Biol.* **2003**, *331*, 725–734.
- (53) Morley, S.; Panagabko, C.; Shineman, D.; Mani, B.; Stocker, A.; Atkinson, J.; Manor, D. *Biochemistry* **2004**, *43*, 4143–4149.
- (54) Morley, S.; Cross, V.; Cecchini, M.; Nava, P.; Atkinson, J.; Manor, D. *Biochemistry* **2006**, *45*, 1075–1081.
- (55) Ingold, K. U.; Pratt, D. A. *Chem. Rev.* **2014**, *114*, 9022–9046.
- (56) Lucarini, M.; Pedrielli, P.; Pedulli, G. F.; Cabiddu, S.; Fattuoni, C. *J. Org. Chem.* **1996**, *61*, 9259–9263.
- (57) Mulder, P.; Korth, H.-G.; Pratt, D. A.; Dilabio, G. A.; Valgimigli, L.; Pedulli, G. F.; Ingold, K. U. *J. Phys. Chem. A* **2005**, *109*, 2647–2655.
- (58) Frisch, M. J.; Trucks, G. W.; Schlegel, H. B.; Scuseria, G. E.; Robb, M. A.; Cheeseman, J. R.; Scalmani, G.; Barone, V.; Mennucci, B.; Petersson, G. A.; Nakatsuji, H.; Caricato, M.; Li, X.; Hratchian, H. P.; Izmaylov, A. F.; Bloino, J.; Zheng, G.; Sonnenb, D. J. Gaussian 09, Revision E.01, Frisch, M. J.; Trucks, G. W.;

- Schlegel, H. B.; Scuseria, G. E.; Robb, M. A.; Cheeseman, J. R.; Scalmani, G.; Barone, V.; Mennucci, B.; Petersson, G. A.; Nakatsuji, H.; Caricato, M.; Li, X.; Hratchian, H. P.; Izmaylov, A. F.; Bl. Gaussian, Inc., Wallingford CT, 2009, 2009.
- (59) Nava, P.; Cecchini, M.; Chirico, S.; Gordon, H.; Morley, S.; Manor, D.; Atkinson, J. *Bioorg. Med. Chem.* **2006**, *14*, 3721–3736.
- (60) Kane, M. A.; Bright, F. V.; Napoli, J. L. *Biochim. Biophys. Acta* **2011**, *1810*, 514–518.

## 3 Polymeric antioxidants

### 3.1 Introduction

Due to their widespread use in almost all human activities organic polymers have become an unavoidable resource for the humankind. The classification of these products in four major groups is mostly related to their mechanical properties and end use:

- 1) **Plastics:** plastics have replaced metals in lots of applications thanks to their lower weight and better corrosion resistance, as well as for their lower manufacturing energy demand. A further classification of plastics is between *commodity* and *engineering* relative to economic and end use considerations. The first are high-volume and low-cost polymers like polyethylene, polypropylene and polyvinyl chloride and are used almost everywhere above all as disposable items. The latter are low-volume and high-cost polymers like polyamide, polycarbonate and polyphenylene oxide and are characterized by improved mechanical properties and high durability and are used in different markets like transportation, construction, electrical and electronic goods, and industrial machinery.
- 2) **Fibers:** fibers are used in those applications like textiles where high strength and modulus, good elongation and thermal stability are requested. World most used fibers are both natural (cotton and wool) and synthetic (polyester and nylon) polymers.
- 3) **Rubbers:** rubbers (or elastomers) are elastic polymers, in other words systems able to completely recover their original shape after being stretched even to great extent. In the past natural rubber have been the most important natural polymer but nowadays it has been replaced for the most part by synthetic elastomers (nitrile rubber, polybutadiene, styrene-butadiene).
- 4) **Coatings and adhesives:** coatings are mixtures of film-forming materials containing polymers, pigments, solvents, and other additives that are applied as thin films to the object surface for functional and/or decorative purposes. Examples of polymers used in coatings are polyvinyl acetate and polyacrylate esters. Like coatings, adhesives are far more complex than other polymeric materials due to the presence of several additives like solvents, fillers, pigments, and many others. These polymeric materials are able of holding materials together by surface attachment and are extensively used, for example, in the wood industries. Among the most used adhesives are phenol-formaldehyde and urea-formaldehyde polymers.

Market data explain clearly the size of plastics economy,<sup>1</sup> with a 2016 world production of 322 million tons (including thermoplastics, polyurethanes, thermosets, adhesives coatings and sealants) constantly increasing, and a turnover of more than 340 billion euros in 2015 referring to the European Union alone. Polyolefins account for the largest

part of this market. Indeed, most of the plastic demand in European Union is for polypropylene (PP, 19.1%), low density and linear-low-density polyethylene (LD- and LLD-PE, 17.3%), high- and medium-density polyethylene (HD- and MD-PE, 12.1%), and polyvinyl chloride (PVC, 10.1%). On the other side, most important market segments are packaging (39.9%), building and construction (19.7%), automotive (8.9%), and electrical and electronic (5.8%).

The continuous growth in their production and the expansion of their areas of application demands a complete knowledge and command on all of polymers stages like manufacturing processes and service conditions of end use articles. In order to address their physical and chemical properties, synthetic polymers are usually added with a combination of low molecular weight substances like plasticizers, colorants, reinforcing fillers and many others that are generally named as additives. For enhancing the processability are also used processing modifiers like lubricants and thickening agents. Moreover, antioxidants and other stabilizing additives (flame retardants, ultraviolet and heat stabilizers) are added in order to minimize and delay the degradation of these polymers that result from the action of different stress sources like heat, oxygen, light, mechanical stress, pollutants and many others. Due to the complexity and the wide range of degradative influences, both physical and chemical, it's not possible to establish a general stabilizing model that works for all the polymers. Indeed, the type and the amount of protection needed can be very different depending on the nature of the polymer as well as on its manufacturing processes and end-use conditions. This aspect is very important in large tonnage polymers like polyolefins because of their massive and widespread use in lots of commercial applications and the consequent high consumption of stabilizers as compounding ingredients, but also for their increasing use in high demanding engineering and medical applications that require a more efficient stabilization against harsher aggressive conditions.

Polymer degradation is a complex process that takes place both during processing, storage and end use conditions and is related to changes of surface appearance (discoloration, chalking or crazing) and loss of mechanical properties like tensile strength and toughness up to the cracking or breaking of the material. The mechanism of polymer degradation is not unique and several potential routes are possible, both physical and chemical. **Physical degradation** includes all of those factors like thermal effects, physical aging and environmental stress cracking that alter polymer mechanical properties leading to its fracture. The mechanism of these processes is complex and related to alterations of polymer morphology and molecular motions that are consequent to stresses like heating, rapid cooling and solvent swelling.<sup>2</sup> Chemical degradation of polymers is generally related with two main mechanisms, cross-linking and chain scission.



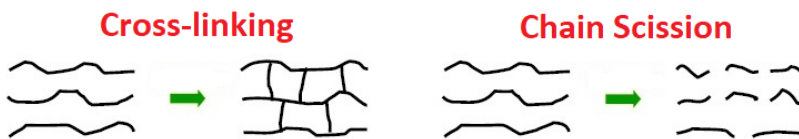


**Figure 1**

The consequences of any chemical degradation reaction are the alteration of mechanical properties, in most cases with the embrittlement of the plastic, and the yellowing or other changes in the appearance. It is worth noting that oxidation reactions have a predominant role in the degradation of polymers like polyolefins and that even the break of only a 1% of polymer C-C bonds can lead to the complete loss of its mechanical properties. It is possible to classify polymers chemical degradation reactions into two main types, thermal and oxidative ones. Thermal degradation includes all of those reactions responsible of polymer failure that take place in the absence of air or radiation. Because during their long-term use polymers are exposed to an oxygen rich environment, oxidative degradation predominates while thermal one is generally absent. Instead when there is a low concentration of oxygen, for example in some processing operations, thermal degradation becomes relevant. It is possible to identify three distinct mechanisms of thermal degradation. The first is the chain scission with depropagation, in other words a depolymerization that decompose the polymer in its monomers. This mechanism is initiated by the thermal scission of polymer backbone bonds with the formation of depropagating monomer radicals. Depropagation takes place when these chain scissions occur above the ceiling temperature, beyond which the equilibrium between the polymer and the monomer shifts towards the latter. The ceiling temperature is characteristic for each polymer and ranges from values close to room temperature to hundreds of Celsius degrees. However, in most cases the chain scission with depropagation leads to a complex mixture of low molecular weight volatile products instead of the pure monomer (Figure 2).

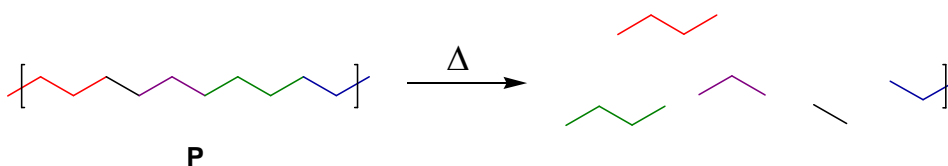


**Figure 2:** P = generic polymer

Indeed, due to the high temperatures involved, depropagation is not the only process and also chain transfer reactions take place. The second mechanism is the random scission without depropagation, where chain breaks do not lead to a significant production of monomers or low molecular weight volatile compounds. Indeed, if the radicals produced after the chain scission are involved in chain transfer and termination reactions too rapidly, the consequence is the impossibility of depropagation to take place. This mechanism can also occur on polymers having functional groups in the main

chain like polyesters and polyamides. Indeed, these functional groups are generally the weakest point of the polymer chain and may undergo scission reactions with a not radical pattern.

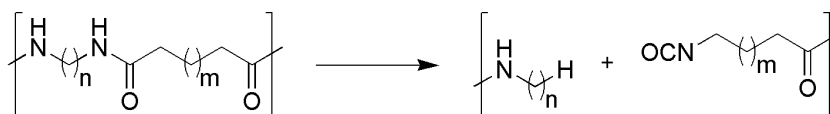


**Figure 3**

The third mechanism of thermal degradation includes all of those chemical reactions that do not cause chain scission. Often this kind of reactions occurs on polymer substituent groups, for example their elimination or their transformation.

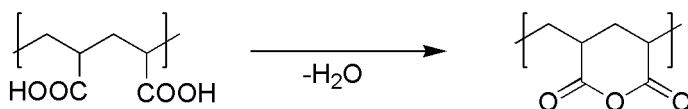
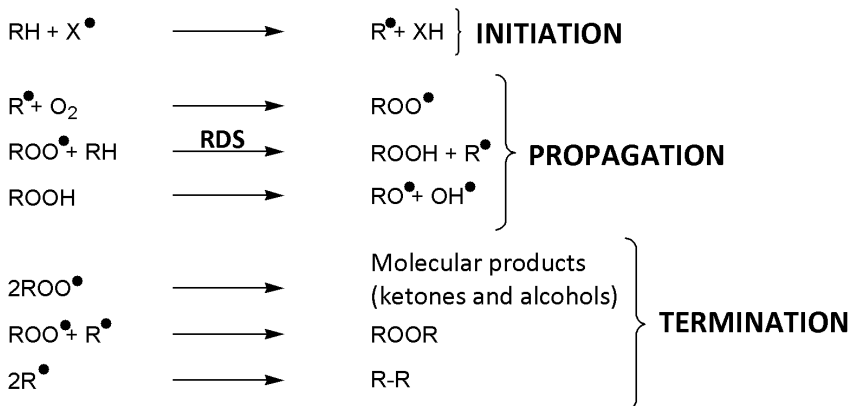


**Figure 4**

These mechanisms of thermal degradation are generally very quick due to the high temperatures involved but are limited to situations of high temperatures and oxygen deficiency like polymer processing and few applications.

Instead, during their lifecycle polymers are mostly in contact with air at mild temperatures. In these conditions the long-term degradation is mainly due to oxidative reactions, the most important chemical process that affects polymers stability. Unlike the mechanisms of thermal degradation previously described, **oxidative degradation** is generally a slow process characterized by a minimal production of volatile compounds and a crucial role played by the oxygen diffusion through the polymer matrix. The basic chemistry of oxidative degradation for most organic polymers is well known and can be described with the cycle of radical reactions that is also typical of the lipid peroxidation in living organisms (Scheme 3, chapter 1), *i.e.* initiation, propagation and termination.



The initiation starts with the formation of a macroalkyl radical  $R^\bullet$  from the reaction between the polymer and a radical source  $X^\bullet$ . The identity of the latter is still unclear but it is generally ascribed to traces of hydroperoxides (ROOH) created during processing that decompose into reactive radical initiators like  $RO^\bullet$  e  $OH^\bullet$  which, in turn, abstract a hydrogen atom from the polymer leading to the formation of the macroalkyl radical  $R^\bullet$ . Many factors are involved in this stage like heat, mechanical stress, light and transition metal impurities. The propagation is a cyclic stage where the macroalkyl radical  $R^\bullet$  reacts with the atmospheric oxygen leading to the formation of an alkylperoxy radical  $ROO^\bullet$  which, in turn, is able to abstract another hydrogen atom from the polymer. The final result of this cycle is the formation of a new macroalkyl radical  $R^\bullet$  that can start a new oxidation process, and of a hydroperoxide ROOH. As seen before, the latter one is unstable and decompose to new radical initiators like  $RO^\bullet$  and  $OH^\bullet$  with a consequent autoacceleration. Indeed, the entire process is generally described as an auto-oxidative cycle because there is a chain reaction that regenerates its own initiators (Figure 5). Macroalkyl radicals  $R^\bullet$  have a very short lifetime because they react very quickly with the atmospheric oxygen. The rate-determining step (RDS) is the subsequent abstraction of a hydrogen atom from the polymer to form a new macroalkyl radical and a hydroperoxide, whose rate depends upon the C-H bond dissociation energy and the stability of the resultant macroalkyl radical.

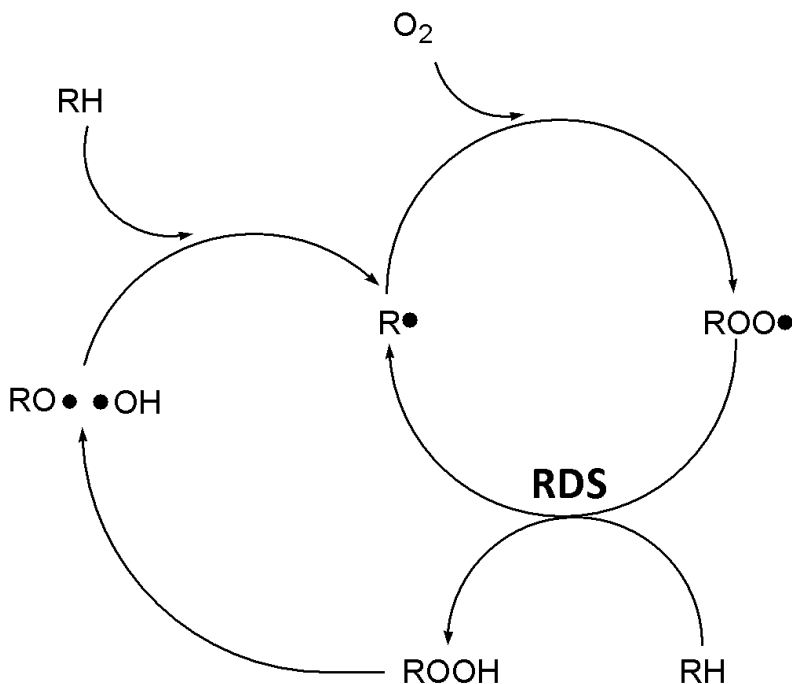


**Figure 5:** Oxidative degradation cycle of polymers.

Several termination reactions are possible depending on the polymer structure and the surrounding conditions. While termination reactions involving alkylperoxyl radicals  $ROO^\bullet$  predominate when there is a normal oxygen pressure, bimolecular termination reactions of  $R^\bullet$  become relevant if there is an oxygen deficiency. The latter mechanism leads to polymer cross-linking, that is one of the two main chemical alterations able to adversely affect polymers mechanical properties (Figure 6,  $O_2$  deficiency).

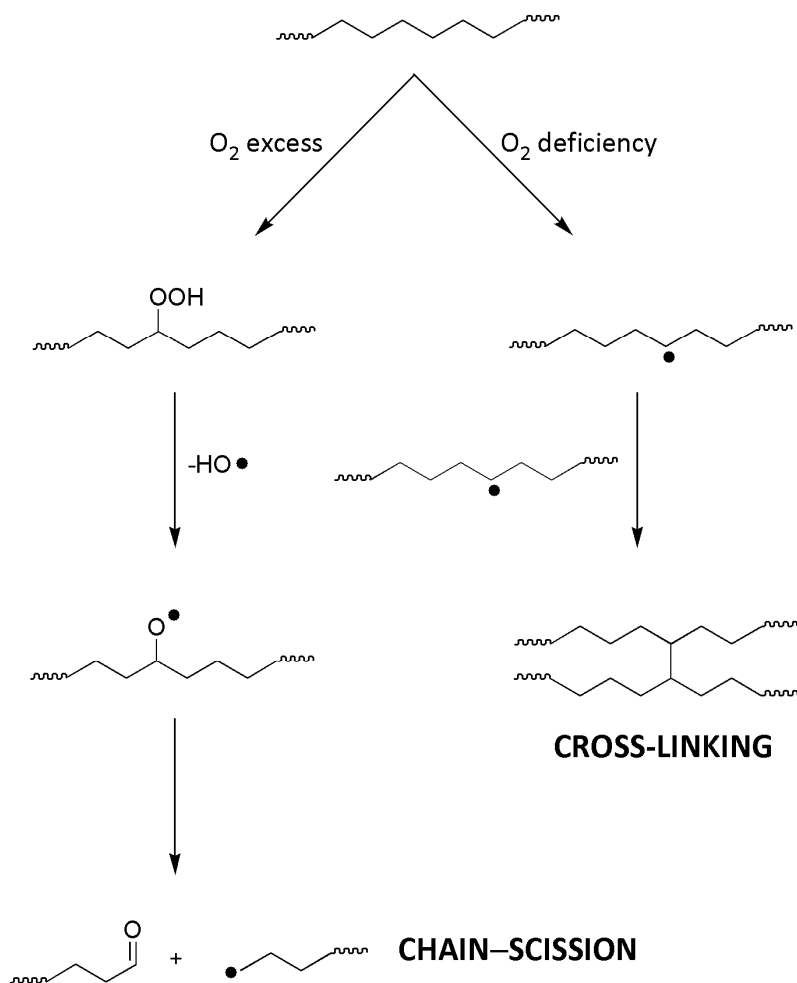


**Figure 6:** Main chemical modifications of polymers during degradation.

The other one is the chain scission caused by a product that arises from hydroperoxides decomposition, the alkyl-peroxyl radical  $RO^\bullet$ . Indeed, these radical species give rise to polymer  $\beta$ -scission reactions resulting in the formation of a carbonyl group and an alkyl radical (Figure 6,  $O_2$  excess). It is worth noting that as a consequence of chain scission aldehydes or ketones are formed and can undergo further oxidizing reactions, thus increasing the polymer photo-sensitivity. The prevalence of chain scission or cross-

linking depends upon polymer structure and surrounding conditions (Figure 7). Under oxygen saturation chain scission prevails in saturated polymers like polyethylene or polypropylene, while in unsaturated rubbers also cross-linking takes place due to double bonds reactivity. In conditions of oxygen deficiency there is a competition between the two degradative mechanisms also in saturated polymers, with the prevalence of chain scission in polypropylene and of cross-linking in polyethylene.

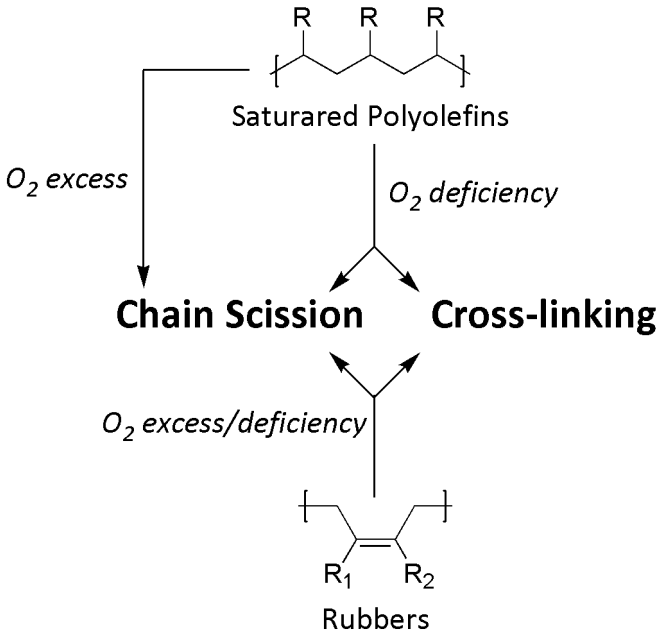


**Figure 7**

As a conclusion of this description, it is possible to identify two main situations under which oxidation takes place:

1. Processing: characterized by a molten state of the polymer, low concentration of oxygen, high shear stress and temperature
2. Service use: characterized by a solid state of the polymer, oxygen saturation, mild temperatures and exposures to stresses like UV, pollutants, etc.

As seen before, the consequences of all of these chemical alterations are both the mechanical failure and the changes in appearance that quickly take place if the polymers are not stabilized somehow. In order to delay these degradation processes that would make unusable most of the modern thermoplastics and rubbers, they are generally added with low molecular weight compounds called stabilizing additives. For most polymers it is possible to identify a typical degradation pattern that depends on its molecular structure and the lifecycle stage (processing, end-use) requiring, as a consequence, the use of specific stabilizing additives. For example, organo-tin compounds and metal carboxylates are used to retard the dehydrochlorination typical

of polyvinyl chloride thermal degradation.<sup>3</sup> However, the oxidative degradation is a process that affects almost all the polymers, then the use of antioxidant additives able to interfere with the auto-oxidative cycle is a general way for their stabilization. Antioxidants may be classified according to their mechanism of action which, in turn, address their action against distinct stages of the polymer auto-oxidative cycle (Figure 8).

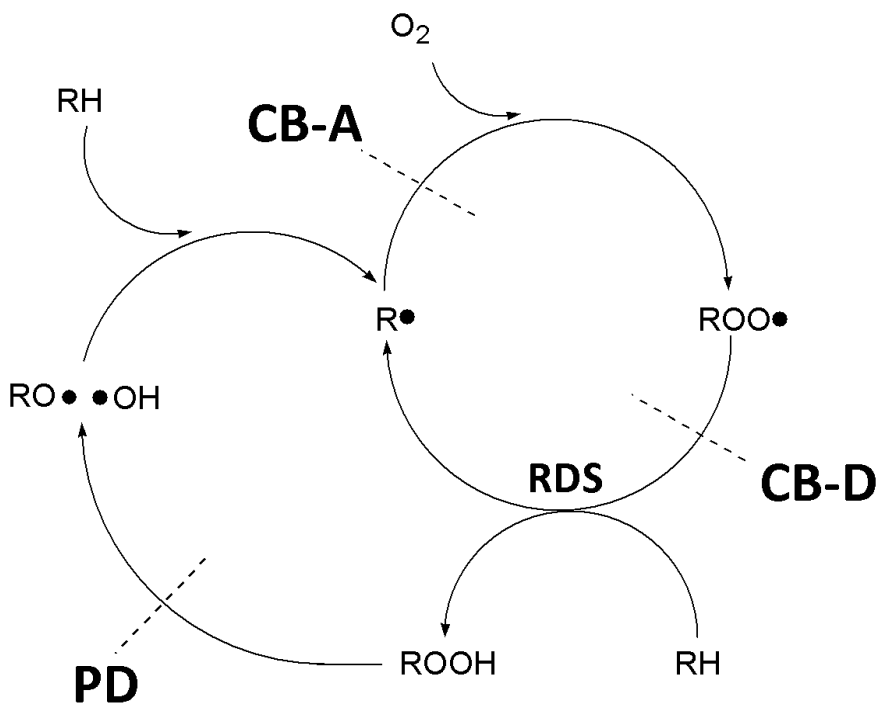
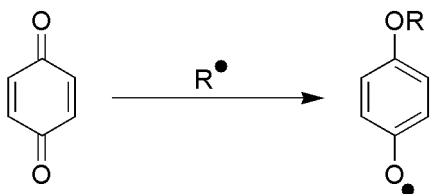


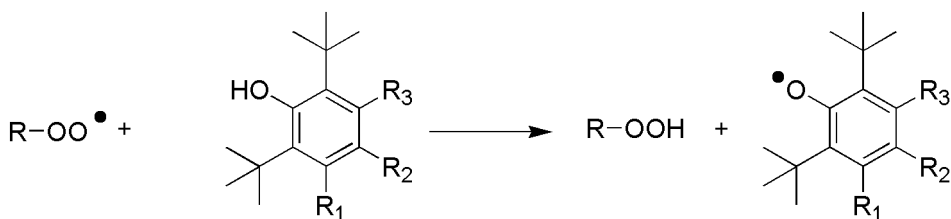
**Figure 8:** Schematic representation of the cyclical oxidation process with the different antioxidant mechanisms.

**Chain-breaking antioxidants** are molecules able to transform the main propagating free-radicals of the oxidative cycle into inert products. These additives are further classified concerning their radical target. Molecules able to trap alkyl radicals  $R^\bullet$  are called chain-breaking acceptors (CB-A) and are useful when there is a low concentration of oxygen. Indeed, they are used as melt stabilizers during processing while are completely useless for end-use stabilization, when it is impossible to compete with oxygen for alkyl radicals. Quinonoid and quinone-type compounds are generally used as processing stabilizers (Scheme 1).



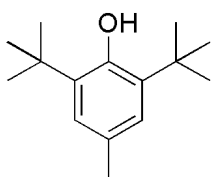
**Scheme 1**

On the other hand, when the polymer is exposed to air, alkylperoxy radicals  $\text{ROO}\cdot$  are the main propagating species. Under these conditions effective antioxidants are those molecules able to suppress alkylperoxy radicals by the donation of a hydrogen atom with the simultaneous formation of a stable non-propagating phenoxyl radical (Scheme 2).

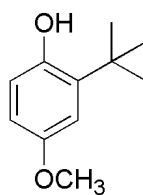


**Scheme 2:**  $\text{R}_1 = \text{R}_2 = \text{R}_3 = \text{H}$  or alkyl

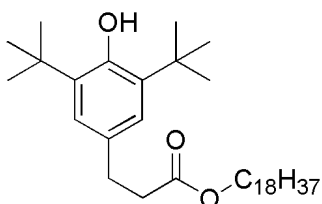
These compounds are called chain-breaking donors (CB-D) and are the most important antioxidant stabilizers during polymer service use, even though they are also used together with CB-A during processing. Most important CB-D antioxidants are sterically-hindered phenols bearing the 2,6-di-*tert*-butylphenol moiety. They trap alkylperoxy radicals by the donation of the phenolic OH hydrogen atom thus leading to the formation of a hydroperoxide and a phenoxyl radical. Actually the chemistry of antioxidants oxidation is quite complex because they generally undergo further reactions depending on their structure and the surrounding conditions.<sup>4</sup> Some of the most important phenolic antioxidants like BHT, BHA,  $\alpha$ -tocopherol (the main component of Vitamin E) and Irganox1076 are depicted in Figure 9.



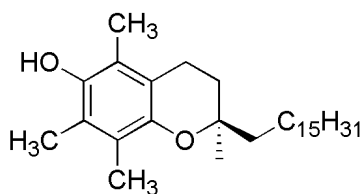
**BHT**



**BHA**



**Irganox®1076**



**$\alpha$ -tocopherol**

**Figure 9**

Their radical scavenger efficacy is related: 1) to the aptitude of the phenolic OH to donate the hydrogen atom, measurable by the BDE(OH); 2) to the stabilization of the resulting phenoxyl radical thanks to the delocalized  $\pi$ -electrons on the aromatic ring. It is possible to identify other two groups of chain-breaking donor antioxidants (Figure 10). The first are molecules based on aromatic amines like Naugard445, characterized by an excellent stabilizing effectiveness but the formation of highly conjugated coloured products limits their use. The second are the hindered-amine stabilizers (HAS) like Tinuvin770, that act as CB-D after the oxidation of the parent hindered amine to the corresponding nitroxide radical, which is the effective antioxidant (Figure 10, down).



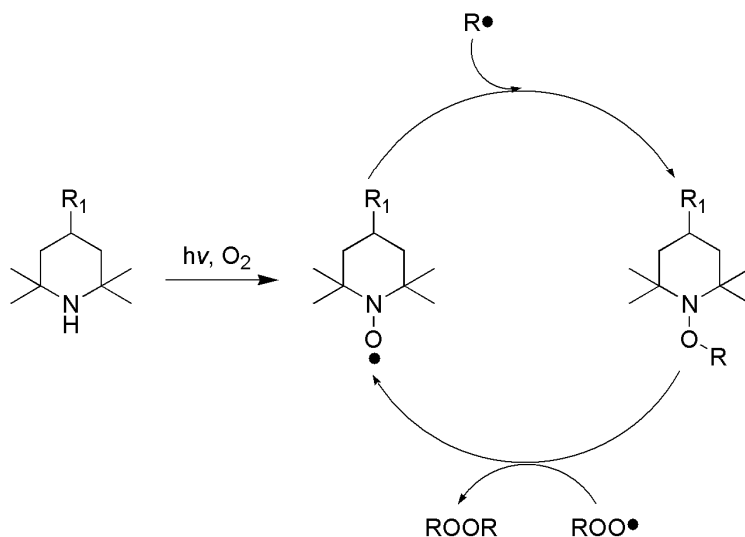
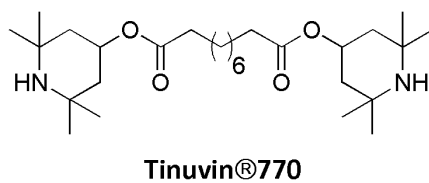
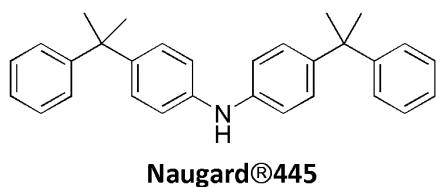
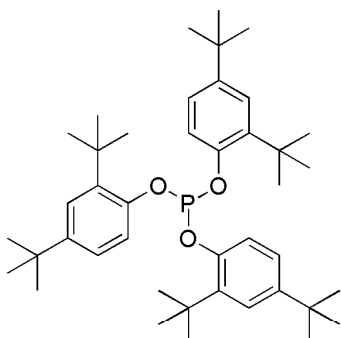
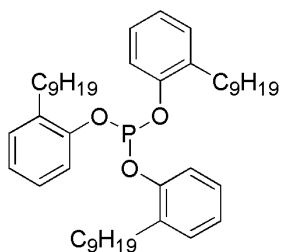


**Figure 10**

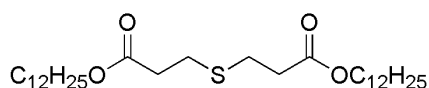
**Peroxide-decomposing (PD) antioxidants** interrupt the auto-oxidative cycle preventing the formation of those initiating radicals like  $RO^\bullet$  and  $OH^\bullet$  that are generated from peroxides decomposition (Figure 8). Indeed, they are also called preventive antioxidants and act by reducing hydroperoxides to alcohols without the formation of radical intermediates.



**Irgafos®168**



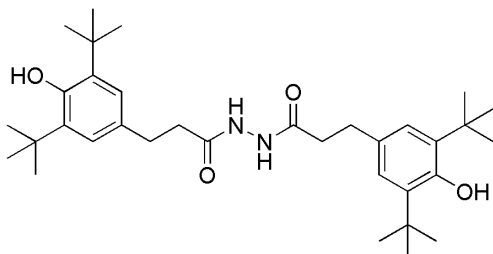
**TNPP**



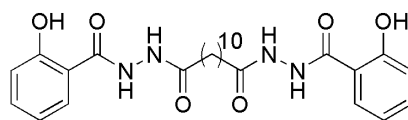
**Dilauryl thiodipropionate**

**Figure 11**

Two main groups of these stabilizers can be identified depending on their mechanism of action, stoichiometric or catalytic. Typical examples of stoichiometric PD are the phosphite esters like Irgafos 168 and tris-nonylphenyl phosphite (TNPP), while several sulfur-containing compounds like dilauryl thiodipropionate act by a catalytic mechanism and are consequently more effective (Figure 11). It has already been mentioned the role of metal impurities in the initiation of polymers degradation, where they act as catalysts for hydroperoxides decomposition. Compounds able to chelate metal ions and then suppress their catalytic activity are then useful stabilizer additives, generally labelled as **metal deactivators**. Often metal deactivators are bifunctional compounds bearing an additional activity, like a chain-breaking or an anti-UV one (Figure 12).



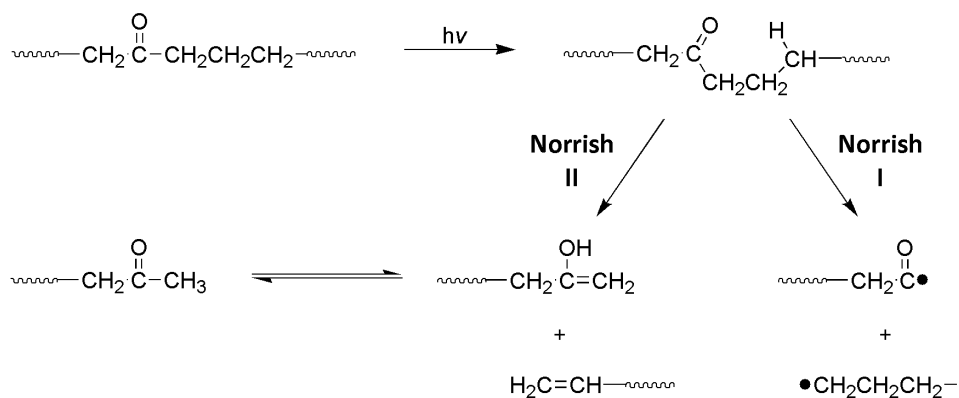
**ADK STAB CDA-10®**



**ADK STAB CDA-6®**

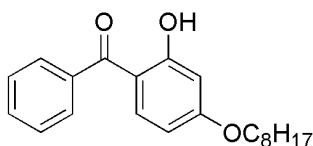
**Figure 12**

Special reference also needs to be made for the photo-degradation because most of the polymers are sensible to the detrimental action of UV light. The latter one is indeed one of the sources able to decompose hydroperoxides to radical species ( $RO\cdot$  e  $OH\cdot$ ), leading to an acceleration of the auto-oxidative cycle. But UV light has moreover a direct action against polymers containing chromophores like carbonyl groups because it causes chain-scission through the so-called Norrish type I and II reactions (Scheme 3).

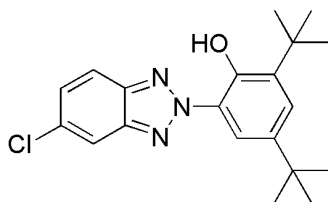


**Scheme 3**

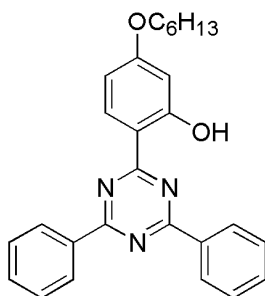
The latter mechanism is characteristic of those polymers where the carbonyl functionality is already present in their repeating unit like polycarbonates, but also polyolefins are subjected to the same degradation process because they undergo a buildup in carbonyl functions during the later stages of thermo-oxidative degradation. To prevent this, polyolefins are generally added with molecules called **UV absorbers** that are able to absorb UV light and dissipate it harmlessly as heat. Among the most known UV absorbers are those bearing the hydroxybenzophenone, benzotriazole or triazine structures (Figure 13).



**CYASORB®UV-531**



**TINUVIN®327**



**TINUVIN®1577**

**Figure 13**

Also, molecules with a different mechanism of action are effective anti-UV. Chain-breaking donor antioxidants stable to UV light are effective photostabilizers because the basic chemistry of polyolefins thermo-oxidation is the same independently from the pathway, thermolysis or photolysis. This is the case of the hindered amine light stabilizers (HALS) that do not absorb the UV light but become powerful chain-breaking antioxidants after the transformation to the corresponding nitroxide radical (Figure 10). Usually the photostabilization of polyolefins is achieved by a synergistic combination of UV absorbers and HALS.

This introductory description of polymers degradation highlights the complexity of the process and consequently of the strategy for their stabilization. It is not possible to identify a unique stabilizing additive able to protect any polymer from all of the several stress sources which they are exposed to. Indeed, an appropriate stabilization is achieved by the use of formulations of different additives depending on polymer structure and conditions of both processing and end-use service. The use of different additives allows not only a defence against the many possible stress sources but also can result in a cooperative effect where the mixture of distinct antioxidants can be more effective than the simple sum of their effects. This phenomenon is called synergism and concern both additives with the same antioxidant mechanism (homosynergism) and those where there is a cooperation between different classes of antioxidants (heterosynergism) like, for example, chain-breaking donors and peroxide-decomposers. Finally, the term autosynergism is used when two or more different antioxidant functions are present in the same molecule.

Up to now, the effectiveness of stabilizing additives has been focused on their ability to interfere with the auto-oxidative cycle in terms of chemical reactivity. In this context it

is also important a mention about the transformation products of the antioxidants because they can preserve a considerable reactivity, antioxidant or pro-oxidant, and lead to changes of polymers surface appearance. For example, aromatic amines are effective chain-breaking donors but the formation of highly coloured polyconjugated products limits their use to those applications where the change of polymer colour is not a problem. As a consequence, the non-colouring properties are one of those essential requirements mandatory in the research of new stabilizing additives. Actually, physical factors are equally important because they influence the compatibility and the persistence of the additive in the polymer.

The compatibility between the polymer and the stabilizer is a measure of the ability of the latter to be uniformly dispersed in the polymer matrix so as to allow an even stabilization. The solubility of the additive in the polymer is the most important physical property that addresses the compatibility between the two components because it determines how much additive can exist in the polymer as a homogeneous solution. If the additive solubility is poor it will lead to phenomena of additive heterogeneous distribution like aggregation or blooming. The additive solubility is in turn related to its persistence in the polymer that, if low, can lead to its physical loss as a consequence of volatilization, migration or extraction. The additive physical loss causes a decrease of its concentration inside the polymer matrix and then the loss of its stabilizing activity. All of these processes take place for all the polymer lifetime depending on both the surrounding conditions and the properties and structures of additives and polymers. Applications where the polymer is subjected to severe conditions like medical devices, high voltage cables and water or oil pipes are the most affected by persistence problems. Also, the sample shape is important because in articles with a high surface to volume ratio like thin films, fibers and coatings the additive physical loss by volatilization or extraction is enhanced.

The compatibility between polymers and additives is strictly related to their respective chemical structure and physical properties. Most of the traditional antioxidant stabilizers are polar low molecular weight compounds and these properties are responsible for two main drawbacks:

- 1) High volatility that facilitates the additive loss by evaporation
- 2) Low solubility in the lipophilic polymer matrix with a resulting increase in additive mobility and loss by migration or extraction

Moreover, the stabilizers migration is of great concern in polymers used for direct human-contact applications like medical implants and food packaging because not just it adversely affects their protective performance but also can represent a toxicological problem.

The increase of the physical persistence of stabilizers in the polymer is therefore a central topic for increasing both their protective performance and health safety. To

achieve this, new antioxidants have been introduced in the last decades maintaining the traditional hindered phenol moiety but with two main modifications:

- 1) The increase of molecular weight to make them less volatile
- 2) The adding of long alkyl chains as substituents on the aromatic cycle in order to enhance their lipophilic nature and then allow a high solubility, a minimal diffusion rate and a homogeneous distribution of the stabilizer in the polymer matrix

The advantages of these two structural modifications on the traditional antioxidant BHT, characterized by high volatility and poor compatibility with polyolefins, are well explained in the commercially available antioxidant labelled as Irganox1076 (Figure 9). This molecule is indeed characterized by a higher compatibility with polyolefins and reduced volatility, with a T-10 (*i.e.* the temperature where a sample exposed to dynamic TGA analysis undergoes a 10% weight loss of its initial mass) of 287 °C clearly better than that of BHT (T-10 = 157 °C).<sup>5</sup> Moreover, while the radical scavenger activity of BHT leads to the undesired formation of highly coloured quinonoid byproducts, the unique byproduct of Irganox1076 is a poorly coloured cinnamate. However, both BHT and Irganox1076 undergo a process called gas fade discoloration that takes place when they are exposed to nitrogen oxides (NO<sub>x</sub>) and other gaseous by-products of fossil fuels combustion. Another shortcoming of Irganox1076 is the presence of only one active function on each molecule and then the necessity of relatively high concentration (in weight) of the stabilizer in the polymer to achieve a satisfactory antioxidant activity. This problem has been overcome with the synthesis of molecules where two or more hindered phenolic moieties are linked together to an aliphatic centre like in Irganox1010 (Figure 14).

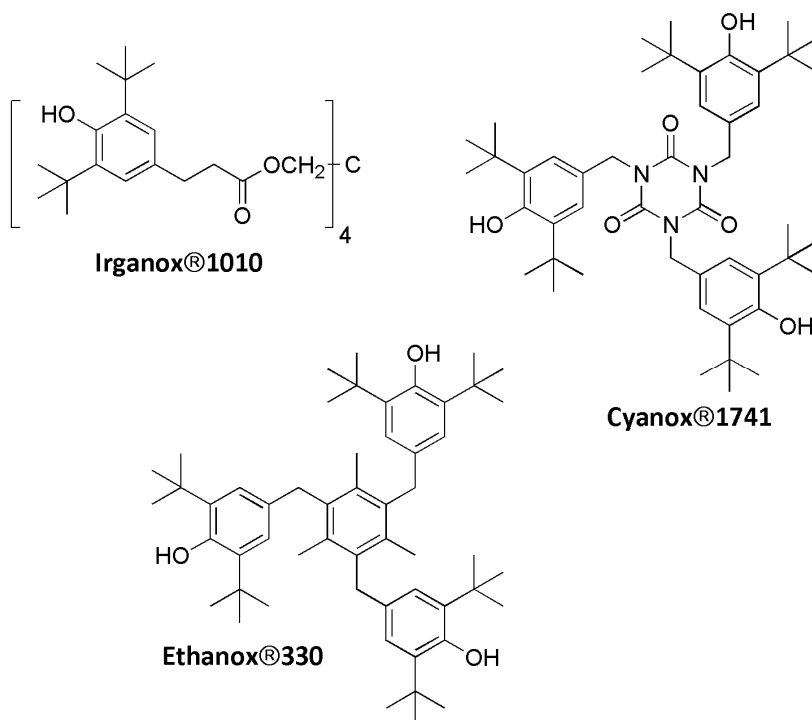
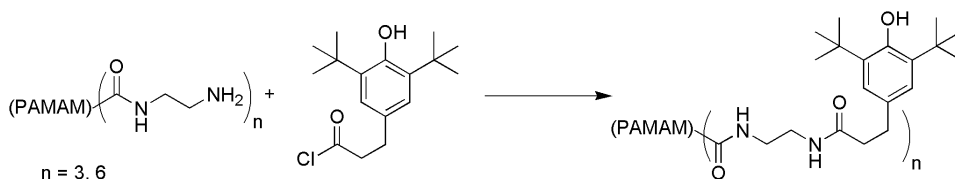


**Figure 14**

These additives have low volatility and high polymer compatibility and, additionally, an increased molar activity that allows the use of lower stabilizer concentrations. However also molecules like Irganox1010 are affected by gas fade discoloration like BHT and Irganox1076. The latter problem can be minimized with the linking of the hindered phenol moieties to an anchoring group that restricts their movement and then their ability to form highly conjugated structures. This goal has been achieved using cyclic groups as anchoring centre like in the commercially available antioxidants Cyanox 1741 and Ethanox 330, that also proved a minimal aptitude to migration.<sup>6</sup> It is important to highlight that an excellent dispersion of the antioxidant inside the polymer matrix does not produce an ideal stabilization. Indeed, well dispersed additives are uniformly distributed across the polymer thickness instead of being concentrated on the polymer surface, where the oxygen concentration is higher and then the oxidation processes are stronger.<sup>7</sup> The ideal antioxidant additive should be highly compatible with the polymer matrix and, at the same time, concentrates itself on the surface.

Molecules like Irganox1010 are characterized by an oligomeric structure and this pattern has been repeated both in industrial and academic research, for example for the synthesis of dendritic antioxidants by the reaction between a suitable hindered phenolic compound and two dendritic derivatives of poly(amidoamine) (PAMAM) used as central linkers (Scheme 4).<sup>8</sup>



**Scheme 4**

The resulting new antioxidant additives were characterized by a molecular weight comparable or even superior of reference compounds, Irganox 1010 and Cyanox 1741, and showed a better protective performance of polyethylene and polypropylene in terms of processing and thermo-oxidative stability. It is also possible to combine the necessity of molecular weight increase with the addition of a different antioxidant function and then obtain a high molecular weight autosynergistic antioxidant bearing both a chain-breaking donor and a peroxide decomposer activity, for example (Figure 15).<sup>9</sup>

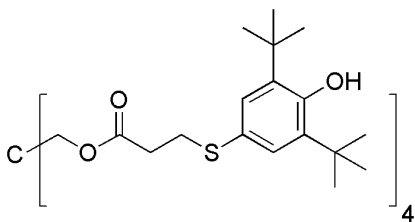


**Figure 15**

A common route followed for the achievement of high molecular weight antioxidants is the use of oligomeric scaffolds suitable for the functionalization with the active moiety (Figure 16). For example polysiloxanes resulted suitable for the functionalization with a hindered phenol antioxidant moiety (polysiloxane-PhOH)<sup>10</sup> or, as in the case of the commercially available Uvasil 2000, with HALS. Another example of an oligomeric additive bearing a stabilizing moiety is the commercially available Chimassorb 944, widely used in the UV protection of polyolefins.<sup>11</sup>



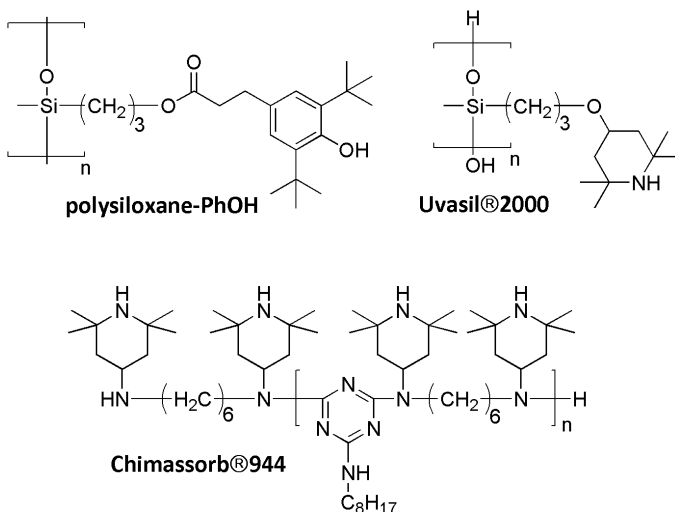


**Figure 16**

The research of new antioxidant additives has examined in depth this concept of increasing the molecular weight and reducing the polarity for a better persistence with the development of polymeric stabilizers, generally labelled also as macromolecular ones. Indeed, the basic idea is that the very high molecular weight and the optimal compatibility consequent to the structural resemblance between the polymer matrix and the polymeric additive can completely delete any volatilization or migration process and broaden also the use to those high demanding applications where the polymer has to withstand very aggressive conditions. It is important to point out that for an actual commercial use polymeric stabilizers have to fulfil some important requirements.<sup>12</sup> Besides the obvious necessity of a satisfactory performance both in terms of molar activity and persistence in the polymer matrix, these additives have to be synthesizable at competitive costs and through industrial customary methods. Moreover, polymeric additives are generally used as masterbatches that are added to unstabilized polymers through a melt blending process and the limited solubility or compatibility can be a serious technical problem when there is a significant difference between the two components in terms of polarity and supramolecular structure. The consequence of the masterbatch limited solubility is the heterogeneity in its distribution inside the polymer matrix that negatively affects the antioxidant performance. It is generally accepted that the answer to this problem is the design of tailor-made polymeric stabilizers whose structure fits as well as possible the one of each host polymer. For this purpose, critical points are also: 1) the relative amount of polar antioxidant moieties in the polymer stabilizer, and 2) its molecular weight that must be relatively low in comparison with that of the host polymer. Literature data suggest that an optimal balance between volatility, compatibility and mobility is achieved with a molecular weight of 3000 to 20000.<sup>13</sup>

**Polymeric additives** can be obtained in several ways depending on how the stabilizing moiety is part of the chain:

- A. A polymerization or copolymerization process is used in order to synthesize a polymeric antioxidant where the active moiety directly constitutes a repeating unit of the polymer backbone or is a pendant group attached to it.
- B. The stabilizing moiety is attached as a pendant group along or at the end of an already existing polymer chain.

A. The preparation of polymeric additives via direct homo- or copolymerization processes is a conventional methodology that requires the use of functional monomers bearing both a stabilizing moiety and a polymerizable function. Since the early '70s methods for preparing hindered phenols with polymerizable groups were reported in several patents.<sup>14-18</sup> If only the functional monomer is used for the polymerization the final product is a homopolymer containing the stabilizing moiety on each repeating unit, instead if a second or more different comonomer are used a copolymer is obtained (Figure 17).

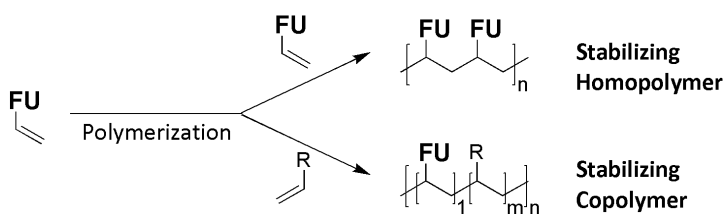


**Figure 17:** FU = Functional Unit

Most of the literature data report the preparation and characterization of homo- and copolymeric antioxidants bearing hindered phenols or HALS as active moieties but the same concepts are true for other types of stabilizers.

Relatively few works are present in literature concerning the synthesis and characterization of homopolymeric additives.

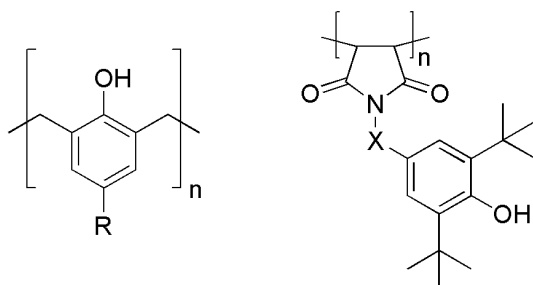
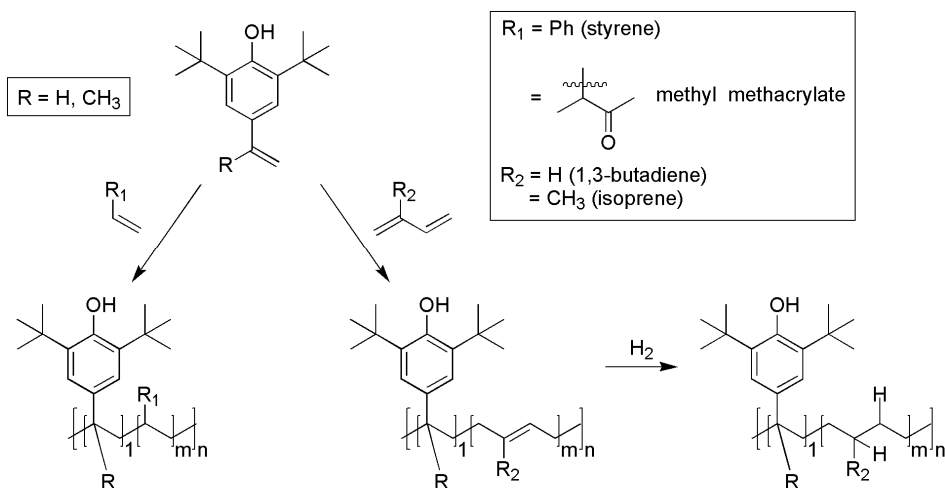


**Figure 18**

As it is clear from their structure two main types of polymeric additives can be obtained, those where the antioxidant moiety is part of the backbone (Figure 18, left) and those where it is a pendant group attached to the main chain (Figure 18, right).

In some of the examples reported a previous modification of commercially available antioxidants is not necessary<sup>19-21</sup>; however in most cases a chemical derivatization of the antioxidant core is mandatory in order to introduce polymerizable groups like maleimide<sup>22</sup> or norbornene.<sup>23,24</sup> Homopolymeric additives are systems with a high molecular weight but also with a significant polarity as a consequence of the high concentration of the antioxidant moiety. They are then characterized by a poor miscibility with polyolefins, rubbers and other nonpolar polymers. In literature is indeed reported that the low performance of homopolymeric stabilizers is related to their poor miscibility with the polyolefin matrix while analogous copolymers are less affected by this problem.<sup>25</sup> Copolymerization allows the introduction, in the polymeric chain of the additive, of monomers that facilitates its dispersion inside the lipophilic polymer matrix. The result are tailor-made polymeric stabilizers that, as mentioned, have a molecular structure similar to that of the host polymer for which they are destined to. First examples of copolymeric antioxidant additives date back to 70s, with some paper and patent reporting the copolymerization of 2,6-di-*tert*-alkyl-4-alkenylphenols with olefinic comonomers like propylene,<sup>26-28</sup> styrene,<sup>29</sup> norbornene,<sup>30</sup> ethylene and 1-octene<sup>27</sup> for the stabilization of saturated polyolefins or with mixtures of dienes and vinylic comonomers<sup>31-33</sup> for the stabilization of rubbers. Noteworthy and explicative is the work of Grosso and Vogl, that reported the copolymerization of 2,6-di-*tert*-butyl-4-vinylphenol and 2,6-di-*tert*-butyl-4-isopropenylphenol with styrene, methyl methacrylate, 1,3-butadiene, and isoprene (Scheme 5).<sup>34,35</sup> The polymeric antioxidants resulted from the copolymerization with 1,3-butadiene and isoprene were used as masterbatches and blended with the corresponding diene homopolymers,<sup>36</sup> proving a better effectiveness in long-term protection compared to low molecular weight antioxidants as demonstrated by oxygen-uptake studies. Similar results were obtained after the hydrogenation of the unsaturated copolymers (Scheme 5) and their blending with polyethylene and polypropylene.



**Scheme 5**

In literature are present works concerning the synthesis and copolymerization of benzotriazole<sup>37-41</sup> and HALS<sup>42</sup> derivatives with different olefinic monomers for the preparation of polymeric UV stabilizers.

A limitation to the applicability of the works so far reported is that most commercial polyolefin materials are produced using Ziegler-Natta type catalysts but the latter are incompatible with phenolic or other polar monomers due to the poisoning effect of the oxygen (or other heteroatoms) on the catalytic system,<sup>43</sup> then the insertion of the functional monomer in good yields was achieved by the use of other methods unsuitable for industrial production like radical<sup>31-33,37,39,40,42</sup> or ring-opening metathesis polymerization<sup>30</sup>. Actually, the insertion of phenolic monomers with Ziegler-Natta catalysts is possible but only with some precaution<sup>43,44</sup> like increasing the steric hindrance about the heteroatom, enhancing the distance between the double bond and the heteroatom<sup>26</sup> or protecting the latter with aluminium reagents in stoichiometric amount<sup>28,44-46</sup> (Figure 19).

**Pretreating the functional monomer  
with a protecting group (trialkylaluminium)**

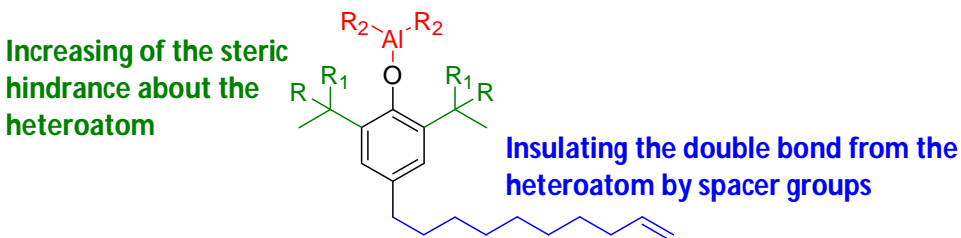
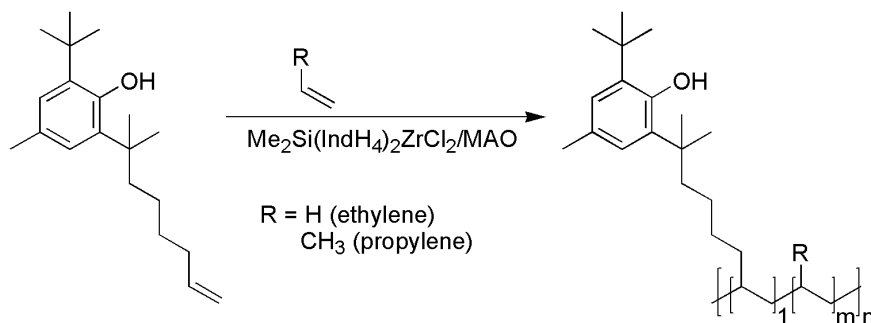


**Figure 19:** Techniques for maintaining (at least in part) the activity of Ziegler-Natta catalyst in the presence of comonomers bearing heteroatoms.

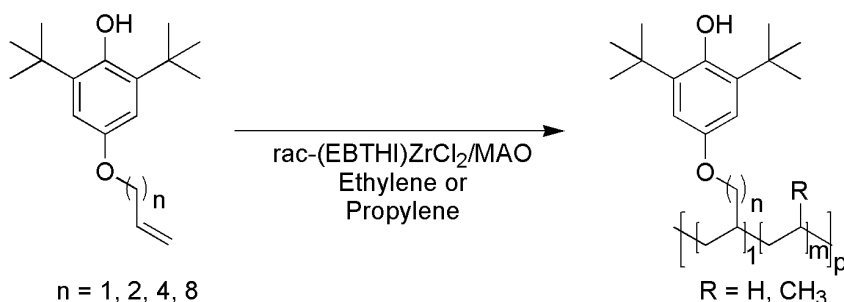
However, most of these precautions are narrow in scope, expensive and copolymers obtained using Ziegler-Natta catalysts are generally characterized by an heterogeneous insertion of the antioxidant comonomer in the main backbone that results in a not uniform stabilization.<sup>43</sup> A breakthrough in this field are the works of Wilén and coworkers that in two papers reported the successful copolymerization in high yields of phenolic alkenyl monomers with propylene<sup>47</sup> and ethylene<sup>48</sup> using homogeneous catalysts based on group IV metallocene/methylaluminoxane (MAO) systems (Scheme 6).



**Scheme 6**

Noteworthy, these works showed that metallocene type catalysts are not just able to incorporate bulky polar monomers without being poisoned, but their catalytic activity is even increased by the presence of the phenolic stabilizer. The authors suggested that the high catalytic activity was due to the phenolic comonomer that acts “as a large weakly coordinating anion which stabilizes the cationic polymerization centre”.<sup>47</sup> Polymers obtained using metallocene catalysts are characterized by a narrower molecular weight distribution and a more homogeneous distribution of the stabilizer comonomers compared to Ziegler-Natta ones. Analogous results were obtained with polymerizable  $\alpha$ -Tocopherol like<sup>49</sup> and hindered amine light stabilizers,<sup>50-52</sup> even if the efficiency for the incorporation of the polar comonomers proved to be strongly dependent on their structure.

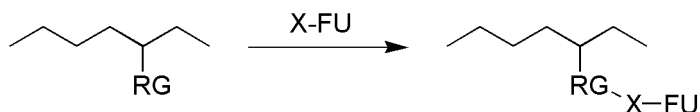
The demonstrated synthetic capability of metallocene type catalysts for the copolymerization of polar comonomers in tunable amounts with  $\alpha$ -olefins was the starting point of our research for the preparation of antioxidant polymeric stabilizers.<sup>53</sup> We reported the preparation of 2,6-di-*tert*-butyl-4-alkoxyphenol derivatives<sup>53,54</sup> bearing a terminal double bond as polymerizable group and their copolymerization with ethylene or propylene (Scheme 7).<sup>55,56</sup>



### Scheme 7

These polymeric additives were used as masterbatches in the melt-blending with additive free commercial polyolefins and proved a better performance compared to analogous polymers stabilized with the molecular antioxidant BHA (Figure 9) both in terms of thermo-oxidative stability and non-migration character. Similar results were obtained using an antioxidant comonomer bearing a norbornene group as polymerizable function.<sup>57-59</sup>

**B.** Polymeric antioxidants can also be obtained by the direct functionalization of an existing polymer. This approach requires the use of a polymer chain, commercially available or synthesized to the purpose, able to chemically bind the active compound (X-FU) thanks to the reactive groups (RG) located along the polymer chain. Examples of appropriate reactive sites are reported in Figure 20.<sup>60</sup>



### FU

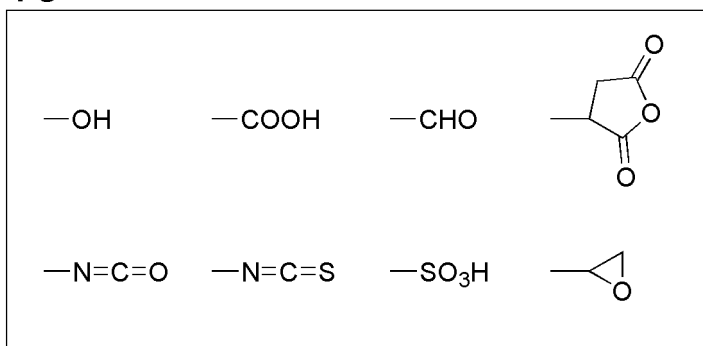
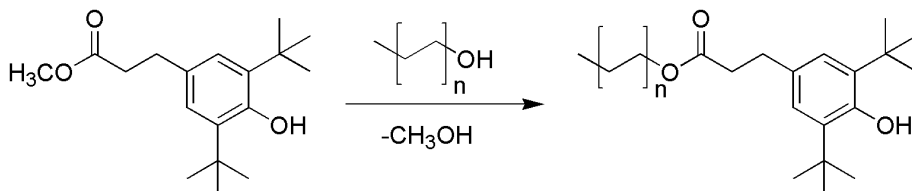


**Figure 20:** RG = Reactive Groups; FU = Functional Unit

Because of the cost and ease of preparation, polymers and copolymers bearing maleic anhydride as reactive site are among the most used for the functionalization with both HALS<sup>61-63</sup> and hindered phenolic stabilizers.<sup>64,65</sup> In literature there are also examples of the use as reactive polymers of ethylene-ethyl or methyl acrylate copolymers,<sup>66</sup>

polyorganosiloxanes,<sup>67</sup> styrene-chloromethyl styrene copolymer<sup>68</sup> and hydroxylated polypropylene.<sup>69</sup> A similar approach is the use of oligomers or low molecular weight polymers characterized by reactive chain ends (living polymers) that can be used for the endcapping with a suitable antioxidant derivative, e.g. the work of Zhang and coworkers that reported the preparation of endcapped polyethylene antioxidants prepared by the transesterification reactions between methyl 3-(3,5-di-*tert*-butyl-4-hydroxyphenyl)propionate and hydroxyl-terminated polyethylenes (Scheme 8).<sup>70</sup>



**Scheme 8**

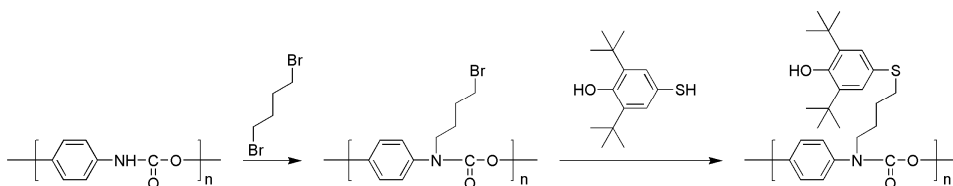
However, the use of functionalized polymers appears to be narrow in scope because of some technological problems connected to the removal of byproducts, undesirable side effects related to the presence of residual unreacted sites on the polymer chain and, concerning endcapped polymers, the small amount of antioxidant moieties that can be incorporated for each polymer chain.<sup>60</sup>

Up to now we have discussed the preparation and use of polymeric stabilizers which may be blended with unstabilized polymers but the latter ones can also be age protected by the direct chemical linking of a low molecular weight additive on their chain. The result is a sort of self-stabilized polymer characterized by an age resistant portion that is not extractable because covalently linked to the main backbone. Self-stabilized polymers can be prepared by some of the ways that we have already discussed for the preparation of polymeric additives, *i.e.* the stabilizing moieties can be incorporated into the polymer backbone as a monomer in a copolymerization process or linked as a pendant group on an existing functionalized polymer. In the first case the same concepts used for polymeric additives can take into account, first of all the use of traditional additives bearing a polymerizable function. In an exhaustive review by Kuczkowski and Gillick are reported a list of patents and papers concerning the synthesis of polymerizable amine and phenolic antioxidants and their use for the preparation of self-stabilizing rubbers.<sup>72</sup> Some explicative works extracted from this review is the copolymerization of N-(4-anilinophenyl)methacrylamide, N-(4-anilinophenyl)maleamic acid or N-(4-anilinophenyl)maleimide with butadiene and acrylonitrile for the preparation of stabilized nitrile rubber,<sup>73,74</sup> and the use of *m*-hydroxy- $\alpha$ -alkylstyrene derivatives for the preparation of different stabilized rubbers<sup>75</sup>.

Concerning the preparation of self-stabilized polyolefins through the copolymerization with a hindered phenol, we have already mentioned the papers of Wilén and coworkers using metallocene type catalysts.<sup>47,48</sup> However the use of this method for the preparation of self-stabilized polyolefins would require to change the customary Ziegler-Natta heterogeneous catalysts used nowadays for the industrial synthesis of

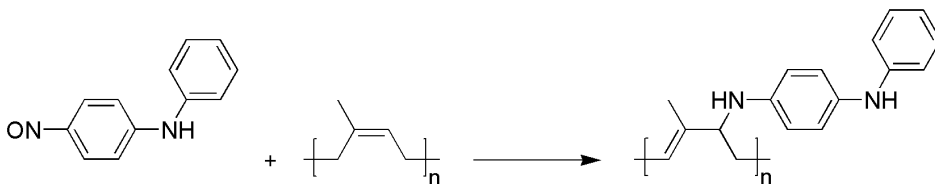
polyolefins to metallocene ones because only the latter are able to incorporate polar bulky comonomers in high yields.

The direct linking of the stabilizer to an existing polymer seems to be preferable, at least in part, because the introduction of the stabilizing additive takes place in a separate step from the polymer synthesis. Most common commercial polymers like rubbers and polyolefins do not contain on their chains reactive sites easily accessible for the binding like hydroxyl, carboxylic acid, succinic anhydride or other groups<sup>60</sup> then their insertion requires a high cost-performance modification of their backbone. This strategy is then worthwhile only in some niche application, for example the bounding of 2,6-di-*tert*-butyl-4-mercaptophenol on polyurethane after its bromobutylation so as to obtain a stabilized polymer for cardiovascular devices (Scheme 9)<sup>76</sup>.



**Scheme 9**

However, alternative and successful ways for the direct functionalization of conventional rubbers and polyolefins with stabilizing additives using customary operations have been achieved. In the aforementioned review of Kuczkowski and Gillick are reported several examples of reactive antioxidants designed for the attachment to synthetic and natural rubbers by the reaction with the polymeric double bonds, during the vulcanization process.<sup>72</sup> Examples of such reactive antioxidants are nitroso, *N,N'*-disubstituted quinone, carbene, azidoformyl, sulfonylazide, nitrone, tetrazole or epoxide derivatives of both aromatic amines and hindered phenols, and in most cases they were successfully incorporated into rubbers during vulcanisation so as to obtain network-bound antioxidants. In Scheme 10 is reported an example of the functionalization of polyisoprene with a nitroso derivative of an aromatic amine.<sup>77</sup>

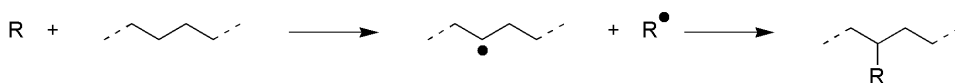


**Scheme 10**

The presence of the reactive antioxidant generally interferes with the vulcanization process, limiting the generality of this approach.<sup>78</sup> More versatile is the use of grafting for the preparation of self-stabilized polymers because it allows the direct linking of the reactive stabilizers on the polymer backbone during customary operations like mastication and extrusion for rubbers and polyolefins, respectively. Grafting is a radical



reaction that requires the generation of free radicals on both the polymer chain and another compound (additives, polymers, *etc*) allowing the direct formation of a chemical bond between the two components (Scheme 11).



### Scheme 11

Most of the early works on the preparation of self-stabilized polymers through grafting reactions are on dienic polymers *i.e.* rubbers because, thanks to the presence of labile double bonds on their backbone, the formation of free radicals can occur spontaneously during mechanochemical procedures like mastication.<sup>79-82</sup> Obviously the stabilizer has to contain a chemical group which gives rise to a free radical. Examples of groups that are suitable for grafting are thiols, monoacrylate, maleate and maleimide.<sup>60,71,78,83,84</sup> The use of antioxidant derivatives bearing mercaptans for the grafting of natural and synthetic rubbers is copiously reported in literature and a list of patents and papers concerning this topic can be found in the review by Kuczkowski and Gillick.<sup>72</sup> The generation of free radicals on rubbers can easily occur without the need of chemical initiators because, due to the reactivity of rubbers double bonds, free radicals are generated by the high shear stress produced during mechanochemical processes like mastication.<sup>85</sup> However, the free radicals induction can be boosted with the addition of chemical initiators like peroxides, azo compounds, and redox systems.<sup>71</sup> Generation of free radicals can also be achieved by initiation with ultraviolet light, preferably in the presence of photoactivators. It is possible to find in literature many examples of diene based polymers functionalized with phenolic and amine antioxidants bearing graftable groups after a chemical or photo free radicals induction.<sup>71,75,86-91</sup> For the grafting of saturated polyolefins with stabilizers the same basic concepts stated for rubbers are true except that the shear stress alone is not sufficient for the generation of free radicals then the addition of radical initiators is mandatory.<sup>60</sup> Noteworthy is the work of Scott and Al-Malaika about the grafting of antioxidants and anti-UV derivatives on polyolefins through a process called reactive processing, because it is done using conventional extruder or mixer technologies in the presence of various radical initiators. In several works, they reported the successful grafting on polyethylene or polypropylene with hindered phenols and HALS derivatives bearing non-polymerizable groups like maleate and maleimide.<sup>71,84</sup> Generally polymers with a 0.05-3.0% content of grafted additive are prepared. As a conclusion of this introduction on the stabilization of commercial polymers, in the family of macromolecular additives is also included the use of nanoparticles for the immobilization of low molecular weight antioxidants.<sup>92,93</sup>

### 3.2 Non-releasing antioxidants for polyolefins stabilization

The shortcomings of polar low molecular weight antioxidants like **BHT** and **BHA** when used as additives for the stabilization of polyolefins has already been examined in depth in section 3.1, highlighting that their aptitude to physical loss from the polymer matrix is not only a problem of accelerated degradation but also of environmental concern when the additive migrates into the environment and of toxicological hazard in the case of polymers used in human contact applications like medical implants or food and drug packaging. The problem of migration from plastics into food is not typical of antioxidants but concerns also other additives like plasticizers, thermal stabilizers, slip compounds, and residual monomers when they are able to interact with food components during processing and storage.<sup>94</sup> For each potential migrant contained in a polymeric packaging material a Specific Migration Limit (SML) is set, defined as the maximum permitted amount of a given substance released from a material or article into food or food simulants. These SMLs are based on toxicological studies and are expressed in mg of substance per kg of food (mg/kg).<sup>95</sup> They represent the migration limits beyond which the food quality and safety may be jeopardized. Migration is a process where substances (the additives) diffuse from a zone of higher concentration (the food-contact polymer) to one of a lower concentration (the food surface) to reach thermodynamic equilibrium. The extent to which migration takes place depends on various factors:<sup>96</sup>

- The physico-chemical properties of the migrant, of the packaging polymer, and of the food
- Temperature
- Storage time
- The relative volumes between the packaging material and the foodstuff

The additives migration is mainly a diffusion-controlled process<sup>97</sup> divided into 4 major steps:<sup>98</sup>

1. Diffusion of chemical compounds through the polymers
2. Desorption of the diffused molecules from the polymer surface
3. Sorption of the compounds at the plastic-food interface
4. Desorption of the compounds into the food

The diffusion process occurs through the amorphous portion of the polymer matrix and in the last step the diffused additive is partitioned between the polymeric material and the food until the chemical equilibrium is reached. The mathematical treatment of the mass diffusion process is well known and in most cases, as for polymeric materials like polyethylene or polypropylene, it can be assumed that the migration of additives from their matrixes obeys Fick's laws.<sup>99</sup> The migration at the polymer-foodstuff boundary depends first of all by the partition coefficient ( $K_p$ ), defined as the ratio of additive

equilibrium concentration in the polymeric material ( $C_p$ ) to its equilibrium concentration in the food phase ( $C_s$ ).

$$K_p = \frac{C_p}{C_s}$$

A value of  $K_p < 1$  means that there is a high predisposition to additive migration into food. Generally, the migration of an additive is enhanced in the presence of fatty foods due to the higher compatibility with the latter. Temperature is an additional important parameter that influences the process of diffusion because high temperatures increase the likelihood of additives migration. Indeed, both the values of  $K_p$  and of the diffusion coefficient of the migrant in the polymer ( $D$ ) are related to the temperature by Arrhenius type equations:

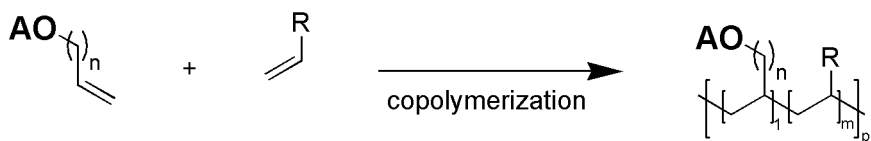
$$\ln K_p = \frac{1}{T} \left( \frac{-\Delta H}{R} \right) \quad D = D_0 \exp\left(\frac{-E}{RT}\right)$$

Where  $T$  is the absolute temperature of the system,  $-\Delta H$  is the enthalpy of the partition process,  $R$  is the perfect gas constant,  $D_0$  is the pre-exponential factor, and  $E$  is the activation energy for diffusives molecules. The diffusion process is also influenced by the polymer morphology and generally the diffusion in glassy polymers is much slower than in rubbery ones. Migration of additives from polymeric material is then dependent upon several factors like processing and storage conditions, chemical and physical properties of both the polymer and the additive, type of food, surface area of contact, and duration of contact. To quantify the extent of additive migration food simulants are generally used because are less chemically complex than real foods. These formulations are test mediums use for imitate real food and, depending on the type of food (aqueous, acidic, alcoholic, and fatty), 4 different simulants are recommended by regulatory authorities. The migration of polar and low molecular weight antioxidants like **BHT** or **BHA** is particularly relevant because of their low compatibility with the polymer matrix, even though depending on the type of food and surrounding conditions also less polar and bigger antioxidant molecules like Irganox1076 and Irganox1010 can be released from the polymeric material.<sup>6,100-112</sup> For these reasons, the development of additives that are able of being firmly integrated in the polymer matrix, so that their migration from the plastic to the contents is completely avoided, would allow to circumvent any toxicological risk.

### 3.2.1 Non-releasing polymeric antioxidants

In section 3.1 the different ways for obtaining nonpolar high molecular weight antioxidant additives with high compatibility and then minimal physical loss from the polymer have been described. Polymeric antioxidants are among the additive types that are appropriate for this goal because allow the immobilization of a traditional antioxidant moiety, characterized by a low molecular weight and a high polarity, on a polymeric support that provides a better compatibility with the virgin polymer. Our research group examined in depth the preparation of such systems by a copolymerization reaction between a reactive antioxidant and a monomer like ethylene

or propylene in order to obtain polyethylene- or polypropylene-like chains containing a certain percentage, possibly controlled, of antioxidant comonomer (Scheme 12).



**Scheme 12:** AO=Antioxidant moiety.

The input for the feasibility of these systems were the already cited works of Wilén, that in several papers described the copolymerization of ethylene or propylene with hindered phenols bearing a polymerizable double bond catalysed by metallocene-based catalysts.<sup>47–49</sup> This was a breakthrough in the field of polymeric additives preparation because unlike Ziegler-Natta heterogeneous catalysts, metallocene/methylaluminoxane (MAO) systems are able to incorporate bulky polar comonomers without being poisoned by the presence of heteroatoms like oxygen or nitrogen in the inserted comonomer.<sup>113,114</sup> Moreover, even if using appropriate precautions it is possible to maintain, at least in part, the catalyst activity of Ziegler-Natta systems, the antioxidant copolymers prepared with the latter are characterized by a not-uniform distribution of the stabilizer moiety.<sup>43</sup> On the other hand, metallocene/MAO catalyst systems produce macromolecular chains with a more homogeneous distribution of comonomers and with a high degree of comonomer incorporation. The industrial synthesis of polyolefins is still mainly done using Ziegler-Natta type catalysts, then it is not conceivable the use of metallocene/MAO systems for the direct preparation of a self-stabilized polymer. On the other hand, the preparation of polymeric antioxidants suitable for the melt-blending with the virgin polymer as common masterbatches is a viable option that fulfils industry requirements. The synthesis of these systems requires the use of a reactive antioxidant, *i.e.* a molecule bearing both a traditional antioxidant group and a reactive function able to take part to a copolymerization process. For this purpose, our research group synthesized four different derivatives of **BHA** characterized by an alkyl chain of different length between the antioxidant moiety and the polymerizable function, a terminal double bond (Figure 21).<sup>53,54</sup> Previous literature reported only the use of antioxidant comonomers derived from **BHT** then it was attractive to explore the copolymerization of ethylene with comonomers derived from **BHA** because of its well known better radical scavenger activity and hence a theoretically superior ability in the stabilization of polyolefins against oxidation.

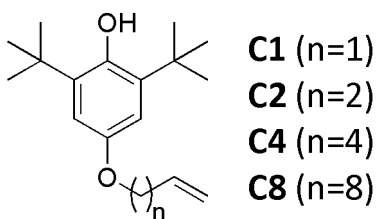
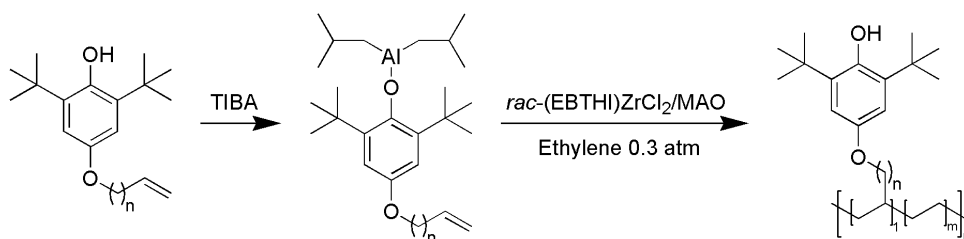


**Figure 21**

Indeed, considering the ability of the two antioxidants in the inhibition of peroxy radicals through the donation of the hydroxyl hydrogen atom, **BHA** has a clear better performance with a rate constant ( $k_{inh}$ ) of  $3 \times 10^5 \text{ mol}^{-1}\text{s}^{-1}$  compared with  $1 \times 10^4$  of **BHT**.<sup>115,116</sup> In order to understand if the presence, in the reaction medium, of a species bearing both a hydroxyl and an alkoxy group like **C1-C8** can deactivate the catalytic system, the simple polymerization of ethylene was tried in the presence of **BHA**. Three different stereorigid metallocene catalysts were used in the presence of MAO as cocatalyst, and the phenol was pretreated with triisobutylaluminum (TIBA) to prevent the catalyst deactivation. This aluminium species is indeed able to coordinate the oxygen atoms thus preventing their interaction with the catalyst.<sup>117</sup> Depending on the metallocene catalyst used, there was a different impact of the ether oxygen on its activity then it was chosen the one that was less affected by the presence of **BHA** and that yielded a polymer with the lower molecular weight. Indeed, a high molecular weight makes difficult the dispersion of the polymeric additive in the virgin polymer. Once demonstrated that the presence of **BHA** did not sensibly affect the catalyst activity, the same procedure was done using the four different polymerizable antioxidants in order to understand their ability to be inserted with respect to ethylene (Scheme 13).



**Scheme 13:** n=1 (**C1**), 2 (**C2**), 4 (**C4**), 8 (**C8**)

The efficiency of the procedures was evaluated in terms of bound comonomer (mol% and wt%), activity and yield of the resulting copolymer in grams (Table 1).

**Table 1:** Copolymers obtained by the copolymerization of ethylene with comonomers **C1-C8**.

Comonomer	Bound Comonomer (mol%)	Bound Comonomer (wt%)	Yield	Activity [(g <sub>pol</sub> /mmol <sub>cat</sub> h)/P]	M <sub>n</sub>	M <sub>w</sub> /M <sub>n</sub>
<b>C1</b>	1.0	8.6	0.305	407	21000	2.8
<b>C2</b>	0.2	2.2	0.093	124	15200	2.5
<b>C4</b>	0.5	5.7	0.278	371	26000	2.8
<b>C8</b>	3.0	28.5	0.315	413	13500	4.4

Polymerization conditions: solvent used is toluene (V=50 mL), Al/Zr = 1500 (mol/mol), t<sub>pol</sub> = 30 min, T = 35 °C, P<sub>ethylene</sub> = 0.3 atm, [comonomer] = 1 mmol, [catalyst] = 5 μmol, [ethylene]/[comonomer] = 1.75.

Best results were obtained with comonomers **C1** and **C8**, with one and eight methylene spacers respectively, even though despite a similar yield and activity the bound comonomer achieved in the case of **C1** was considerably lower. A possible explanation of the low incorporation of **C1** is the short distance between the double bond and the hindered phenol. Indeed, the proximity of a bulky group could encumber the double bond thus reducing its incorporation ability. In the case of **C4** a comparable yield and activity respect to **C1** and **C8** were obtained but with a clear decrease in terms of bound comonomer, while **C2** gave the worst results. The hypothesis for the behaviour of **C2** is that, after the comonomer insertion, there is the formation of an intramolecular species where the ether oxygen interacts with the zirconium saturating its coordinative vacancies (Figure 22).

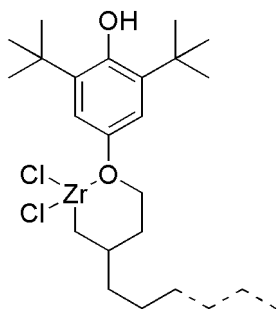


**Figure 22**

A series of copolymers were prepared using different [ethylene]/[C1-C8] ratios. These copolymers, containing 0.55-1 mol% of **C1**, **C4** or **C8** (**C2** was not used due to the low copolymerization yield), were melt-blended with additive-free polyethylene in order to obtain a polymeric material with an antioxidant moiety content of 500 ppm. Thermal and thermo-oxidative stability of resulting blends were evaluated and compared with polyethylene stabilized with commercial **BHA** in the same concentration.<sup>55</sup> All of the polyethylene samples mixed with the polymeric antioxidants showed a better stabilizing performance respect to those containing **BHA**, confirming the validity in the use of such stabilizing systems. Among the different polymeric antioxidants, best performance was obtained with **C4** as comonomer. This behaviour was explained by the influence of the spacer length on the antioxidant activity: indeed, the increase of the spacer length allows a better mobility of the antioxidant moiety but, at the same time, does not exert an efficient steric protection on the tertiary carbon of the polymer chain, that is a weak point for the formation of radicals (Figure 23).

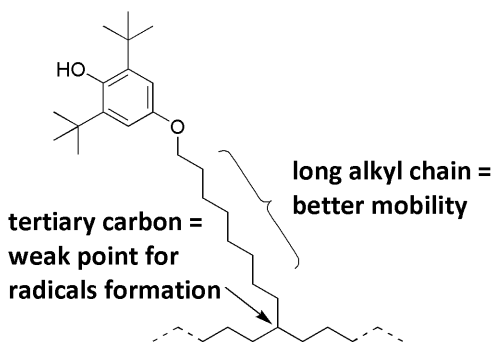
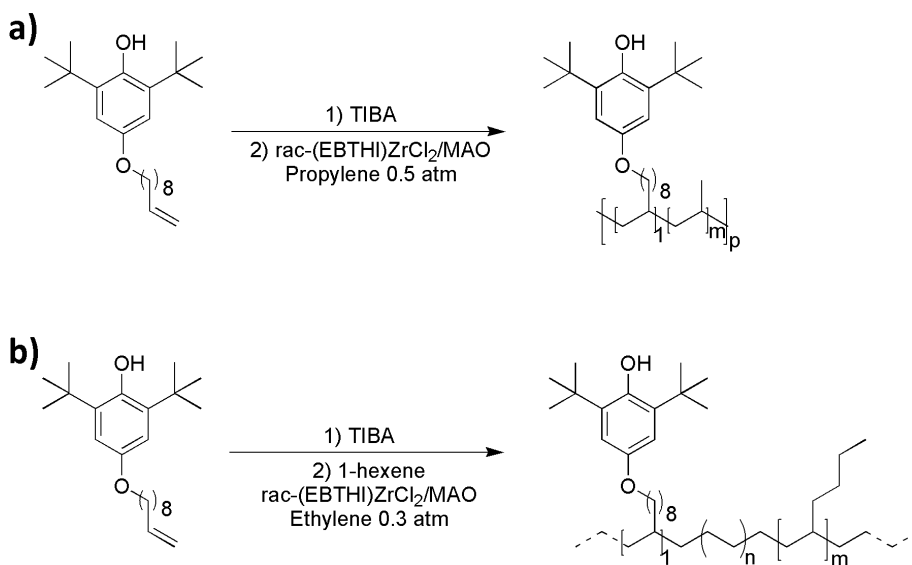


**Figure 23**

As a consequence, the mid-length spacer of **C4** was the better compromise between mobility of the antioxidant moiety and steric protection of the main chain. These polymer antioxidants also proved a better performance compared to **BHA** both in the long-term stabilization and specific migration tests with food-simulating liquids, confirming the total absence of additive release. These positive results suggested the preparation of other polymeric stabilizers using **C8** as comonomer because it was the most easily incorporated into the polymer chain in controlled and tunable amount. Solubility of the additive in the virgin polymer matrix is a crucial point for the stabilizing efficacy, then tailor-made polymeric antioxidants designed for specific materials were prepared. This goal was obtained by using different monomers depending on the structure of the polymers that had to be stabilized.<sup>56</sup> Propylene was then used for the preparation of copolymers with **C8** planned for the antioxidant stabilization of polypropylene (Scheme 14, a). Low-density polyethylene used for the packaging of food is generally a copolymer of ethylene with a small amount (2-4 mol%) of an  $\alpha$ -olefin like 1-hexene, then terpolymers of ethylene, **C8** and a low percentage of 1-hexene (1-3 mol%) were prepared (Scheme 14, b).



**Scheme 14**

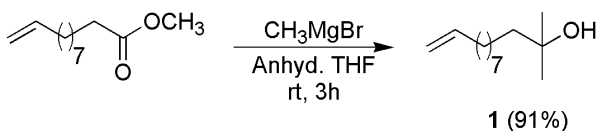
The **C8** content was planned to be up to about 1 mol% because we observed that higher concentrations led to poor miscibility of the copolymer with the polyolefinic matrix. Both the polypropylene- and polyethylene-based copolymers were used as masterbatches and melt-blended with the corresponding unstabilized commercial polymers, providing a better stabilizing performance than traditional antioxidant **BHA**. Very interesting was the behaviour of ethylene/1-hexene/**C8** terpolymeric additives. Indeed, between the two samples used for the stabilizing tests, a better performance was achieved with that containing a lower amount of **C8** and a higher content of 1-hexene. Such chemical composition theoretically favours a better dispersion suggesting that the efficacy of the polymeric additive is more related to its compatibility with the host polyolefin than to the quantitative content of antioxidant comonomer. Such successful results confirmed that effective stabilizing additives can be achieved by the immobilization of traditional antioxidant moieties on polymeric chains through a process of copolymerization between an olefinic monomer (e.g. ethylene) and an antioxidant comonomer bearing a polymerizable function. A massive antioxidant efficacy requires the preparation of a polymeric additive whose molecular structure resembles as well as possible that of the virgin polymer that has to be stabilized. Using **C8** or the others BHA-like comonomers some shortcomings were however evident because of the ether oxygen atom, whose influence on the catalytic system prevents an actual control of the insertion of the antioxidant comonomer in controlled and tunable amount in the growing polymer chain.



### 3.3 Results and Discussion

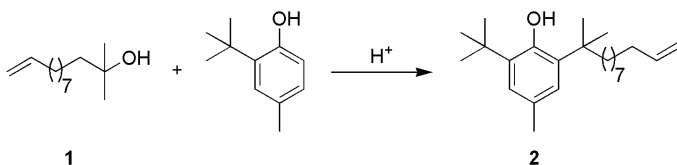
#### 3.3.1 Synthesis of BHT-like comonomers for the copolymerization with polyolefins

During my PhD we focused our efforts on the preparation of BHT-like comonomers in order to use them for the preparation of polymeric additives characterized by an actual control of the antioxidant moiety insertion. For this purpose, we took advantage of the wide availability of commercially available hindered phenols like 2-*tert*-butyl-4-methylphenol. These derivatives were modified in order to introduce on their aromatic ring a long alkyl chain with a terminal double bond. As seen in section 3.2.1, a spacer of at least 8 methylene units between the antioxidant moiety and the terminal olefin ensures an efficient copolymerization process. It was then necessary the preparation of a long alkyl chain ending at one side with a double bond and at the other with a bulky group also suitable for the bonding in *ortho* to the hydroxyl group of 2-*tert*-butyl-4-methylphenol. Starting from commercial methyl 10-undecenoate, the corresponding tertiary alcohol **1** was prepared after the reaction with an excess of methylmagnesium bromide ( $\text{CH}_3\text{MgBr}$ ) in anhydrous THF (Scheme 15).<sup>118</sup>



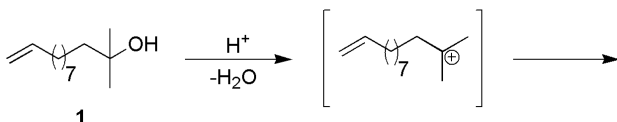
**Scheme 15**

Derivative **1** was then used for a Friedel-Crafts alkylation on 2-*tert*-butyl-4-methylphenol in order to obtain **2**, a suitable candidate as antioxidant comonomer (Scheme 16).



**Scheme 16**

The tertiary alcohol is a precursor of the actual reagent, a tertiary carbocation, that takes part to the  $\text{S}_{\text{E}}\text{Ar}$  on the aromatic ring (Scheme 17).



**Scheme 17**

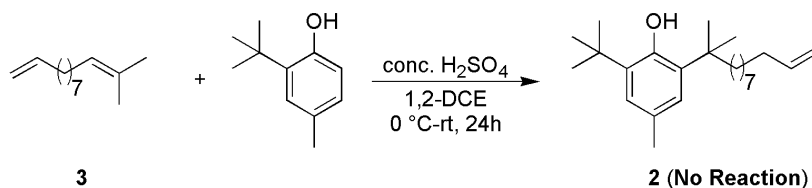
The generation of the carbocation from the tertiary alcohol requires the presence of a dehydrating agent, generally a strong acid. Several attempts were done using different acids and reaction conditions (Table 2).

**Table 2:** Friedel-Crafts alkylation of 2-*tert*-butyl-4-methylphenol with **1**.

Entry	Acid (equiv)	Phenol (equiv)	Solvent	T (°C)	Time (h)	Yield % (2)
<b>1</b>	CF <sub>3</sub> SO <sub>3</sub> H (0.33)	0.33	1,2-DCE	r.t.	24	0
<b>2</b>	CF <sub>3</sub> SO <sub>3</sub> H (0.33)	0.33	1,2-DCE	50-reflux	24	0
<b>3</b>	ZnCl <sub>2</sub> (1)	1	Hexane/DCM 5/1	r.t.-60	18	0
<b>4</b>	SnCl <sub>4</sub> (1)	1	DCM	r.t.	24	0
<b>5</b>	BF <sub>3</sub> .OEt <sub>2</sub> (1.3)	2	Petroleum ether	Reflux	0.5	0
<b>6</b>	CH <sub>3</sub> SO <sub>3</sub> H (3.57)	1	1,2-DCE	0-r.t.	24	23
<b>7</b>	CH <sub>3</sub> SO <sub>3</sub> H (3.57)	1	Neat	0-r.t.	24	0
<b>8</b>	CH <sub>3</sub> SO <sub>3</sub> H (3.57)	3	1,2-DCE	0-r.t.	15	0
<b>9</b>	CH <sub>3</sub> SO <sub>3</sub> H (12)	1	1,2-DCE	0-r.t.	1	0
<b>10</b>	CH <sub>3</sub> SO <sub>3</sub> H (1.19)	0.33	1,2-DCE	0-r.t.	24	29
<b>11</b>	CH <sub>3</sub> SO <sub>3</sub> H (1.19)	0.33	1,2-DCE	0-r.t.	168	17

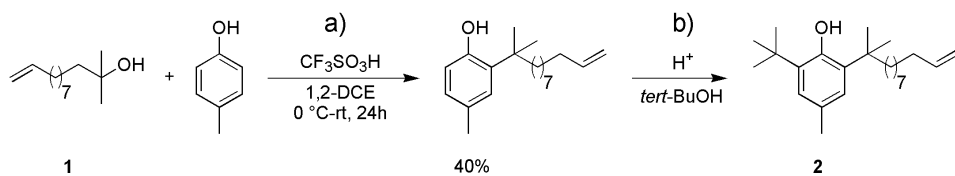
With triflic acid (CF<sub>3</sub>SO<sub>3</sub>H) as catalyst in 1,2-DCE at room temperature (entry 1) the starting 2-*tert*-butyl-4-methylphenol was absolutely inert while **1** was completely recovered as its corresponding dehydration product (Scheme 18, **3**). Using the same combination of acid and solvent at reflux (entry 2) the starting phenol was still inert while **1** was decomposed to give a complex crude with a <sup>1</sup>H-NMR spectrum showing the absence of any terminal double bonds. Both the starting reagents resulted absolutely

inert using  $\text{ZnCl}_2$  (entry 3),  $\text{SnCl}_4$  (entry 4)<sup>119</sup> or  $\text{BF}_3 \cdot \text{OEt}_2$  (entry 5)<sup>120</sup> as acid catalysts. A successful outcome was achieved using  $\text{CH}_3\text{SO}_3\text{H}$ , even if after a careful optimization of the reaction conditions. Indeed, from the procedure found in literature (entry 6),<sup>121</sup> only a 23% yield was obtained using a large excess of acid at room temperature. Moreover, a significative amount of the dehydration product of **1** (Scheme 18, **3**) was recovered. Repeating the same conditions but without the solvent (entry 7) the desired product **2** was isolated in low yield and mixed with an impurity that was identified as the corresponding product of water addition to the olefinic double bond. We tried to use an excess of 2-*tert*-butyl-4-methylphenol (entry 8) or a large excess of the acid (entry 9) but in both cases no reaction occurred. Finally, we were able to increase the yield to 29% by using the phenol in substoichiometric amount and a slight excess of  $\text{CH}_3\text{SO}_3\text{H}$  (entry 10). From this reaction 58% of the starting phenol was recovered, thus suggesting its low reactivity under the conditions used, and the main reaction product was **3** (Scheme 18), an indication of the predisposition of **1** to dehydration at the expense of the Friedel-Crafts alkylation. Increasing the reaction time (entry 11) gave worse results and again the main isolated product was **3** (34%). However, also 1,1-dimethyl alkenes can be precursors of a tertiary carbocation, then the dehydration product of **1** (**3**) was directly used for the reaction with 2-*tert*-butyl-4-methylphenol in the presence of conc.  $\text{H}_2\text{SO}_4$ <sup>47</sup> but these conditions proved to be detrimental for the olefinic function (Scheme 18).



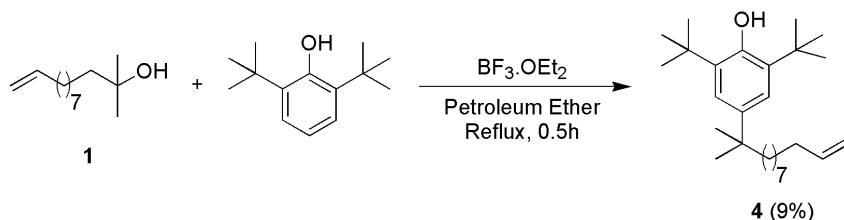
**Scheme 18**

Due to the low yields achieved we changed our synthetic strategy by trying to introduce both the bulky groups adjacent to the phenolic hydroxyl in two different steps. Indeed, the Friedel-Crafts alkylation of *tert*-butyl groups is a reversible process and in acid conditions molecules bearing a *tert*-butyl substituent can undergo a retro-alkylation reaction that, in turn, leads to the formation of different regioisomers. In order to avoid this undesired reaction, it was reasonable to try first to alkylate the phenolic ring with **1** and then to run the *tert*-butylation. For the first reaction (Scheme 19, a) the best yield (40%) was obtained using triflic acid as catalyst and *para*-cresol as phenol. Unfortunately, the subsequent *tert*-butylation (Scheme 19, b) failed under both the conditions used: 1) an excess of conc.  $\text{H}_2\text{SO}_4$  and *tert*-butyl alcohol in 1,2-DCE;<sup>122</sup> 2) using 75%  $\text{H}_2\text{SO}_4$  and *tert*-butyl alcohol in the presence of urea.<sup>123,124</sup>



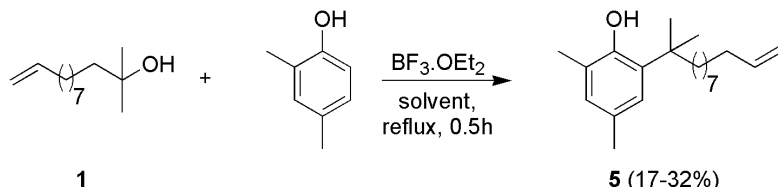
**Scheme 19**

Due to the serious synthetic problems found with 2-*tert*-butyl-4-methylphenol another hindered phenol was used as starting material for the alkylation reaction. 2,6-di-*tert*-butylphenol was used for the reaction with **1** in order to obtain a candidate as antioxidant comonomer like **4** characterized by the olefinic alkyl chain in *para* to the phenolic hydroxyl group. The reaction was done using  $\text{BF}_3 \cdot \text{OEt}_2$  in the same conditions seen for entry 5 (Table 2) but allowed to isolate the desired product **4** in a very low yield after a difficult purification and also 2,4,6-tri-*tert*-butylphenol and **3** were recovered as side products (Scheme 20).



**Scheme 20**

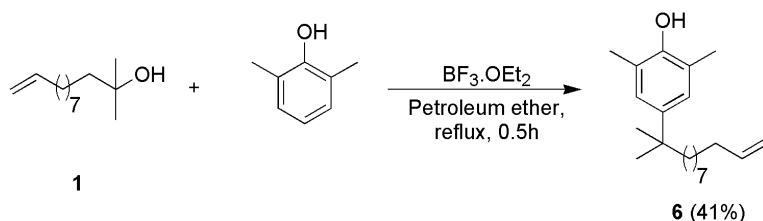
The problem of retro-*tert*-butylation prompted us to use methyl substituted phenols instead of *tert*-butyl ones in order to avoid this undesired reaction. Indeed, even if with methyl substituents adjacent to the hydroxyl group there is less steric hindrance and then a worse stabilization of the corresponding phenoxyl radical,  $k_{inh}$  values are essentially the same<sup>125</sup> and the BDE(O-H) is only slightly lower<sup>126,127</sup>. In order to have at least one bulky groups adjacent the phenolic OH, first we tried the alkylation of 2,4-dimethylphenol on **1** using the same conditions seen in Scheme 20:  $\text{BF}_3 \cdot \text{OEt}_2$  as catalyst and an excess of the phenolic derivative (Scheme 21).



**Scheme 21**

The reaction was carried out at reflux with petroleum ether as solvent achieving the desired product **5** in 32% yield while, using anhydrous hexane, the yield decreased to 17%. A hypothesis of this difference is the anhydricity of the distilled hexane that would facilitate the loss of water from **1**, whose dehydrated product **3** was indeed recovered

in higher amount respect to the reaction carried out with petroleum ether. We tried the alkylation with **1** using an excess of both  $\text{BF}_3 \cdot \text{OEt}_2$  and the phenol, and the desired product **6** was isolated in 41% yield (Scheme 22).



**Scheme 22**

After the copious attempts of direct alkylation of different phenols (Table 3) we were able to make a few comments.

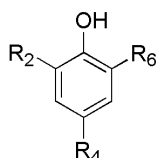
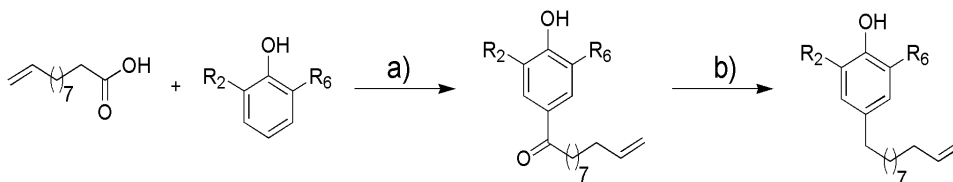


**Table 3:** Outcomes of the Friedel-Crafts alkylation of **1** with different hindered phenols.

Entry	R <sub>2</sub>	R <sub>4</sub>	R <sub>6</sub>	Product	Yield (%)
<b>1</b>	<i>tert</i> -Bu	Me	H	<b>2</b>	0
<b>2</b>	<i>tert</i> -Bu	H	<i>tert</i> -Bu	<b>4</b>	9
<b>3</b>	Me	Me	H	<b>5</b>	32
<b>4</b>	Me	H	Me	<b>6</b>	41

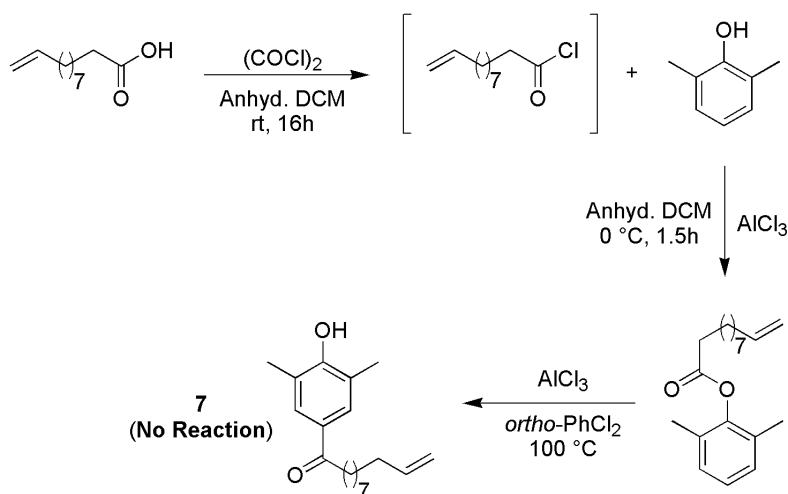
Depending on the type and position of substituents there are different outcomes. With the same substituent on R<sub>2</sub> (*tert*-butyl or methyl), the alkylation occurred in better yields in *para* respect to the OH group than in its *ortho* position. Indeed, when R<sub>2</sub> = *tert*-butyl the alkylation took place only in *para* (entries 1 vs 2) even if in low yield, while when R<sub>2</sub> = Me both the possible products were obtained with *para* substituted in higher amount (entries 3 vs 4). This was probably due to the steric hindrance between the hydroxyl group of the phenol and the bulky tertiary carbocation of **1** when the latter approaches the OH *ortho* position. Between the two products alkylated in *para* to the OH, **4** and **6**, a best yield was obtained with that bearing the less bulky methyl groups adjacent to the hydroxyl substituent (**6**). This was probably due not only to the less steric hindrance of methyl substituents but also to the aptitude for retro-alkylation of *tert*-butyl ones. However, the best yield obtained with **6** were too low for our aim and, because of the ever-present formation of **3**, the purification by column

chromatography was not too simple. In order to overcome these problems, we again changed our synthetic strategy to a multi-step one characterized by a Friedel-Crafts acylation on the *para* position of the phenolic OH (Scheme 23, a) followed by the reduction of the resulting aryl-alkyl ketone (Scheme 23, b).



**Scheme 23**

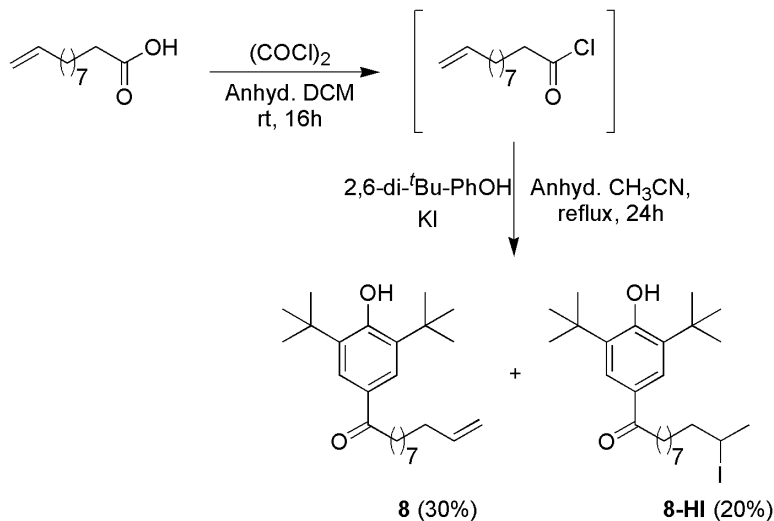
The *in situ* formation of the acyl chloride derived from 10-undecenoic acid was used for the esterification on the hydroxyl group of 2,6-dimethylphenol in order to obtain the desired derivative **7** after a Fries rearrangement. For this purpose,  $\text{AlCl}_3$  was used as acid catalyst in *ortho*-dichlorobenzene at  $100\text{ }^\circ\text{C}$ <sup>128</sup> after the esterification of the acyl chloride with 2,6-dimethylphenol (Scheme 24).  $^1\text{H-NMR}$  and FTIR spectra of the crude showed the actual acylation in *para* on the phenol derivative but also the absence of the olefinic signals, suggesting that the conditions used were too harsh.



**Scheme 24**

Due to the unsatisfying results obtained with 2,6-dimethylphenol we decided to repeat the Friedel-Crafts acylation synthetic strategy using 2,6-di-*tert*-butylphenol because the steric hindrance of the two adjacent bulky groups prevents the esterification on the hydroxyl group and then it is not necessary the subsequent Fries rearrangement. The procedure was carried out on a one-pot stepwise manner. The first reaction was the transformation of 10-undecenoic acid in the corresponding acyl chloride using oxalyl chloride. The following Friedel-Crafts acylation on 2,6-di-*tert*-butylphenol was

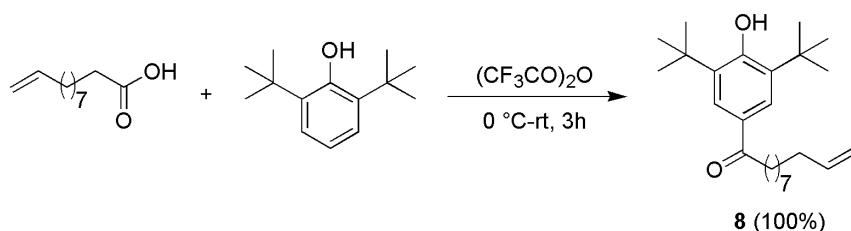
accomplished following a procedure found in literature<sup>129</sup> that required the use of KI in acetonitrile at reflux, but the desired product **8** was obtained only in 30% yield together with the corresponding derivative (**8-HI**) as the result of HI addition to the double bond (Scheme 25).



**Scheme 25**

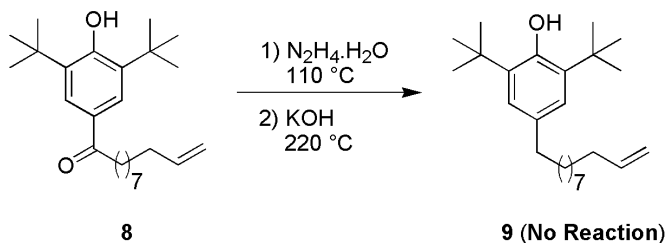
In order to avoid the latter side reaction, the acylation was repeated using  $\text{AlCl}_3$  in equimolar amount to the phenol in DCM at  $0^\circ\text{C}$  for 2h but in these conditions the retro-alkylation of *tert*-butyl substituents took place.

After an in-depth literature search, we found a procedure that apparently allowed an efficient acylation on 2,6-di-*tert*-butylphenol. This procedure<sup>130</sup> required the use of trifluoroacetic anhydride that, after the reaction with the carboxylic acid, leads to the *in situ* formation of a highly reactive mixed anhydride which in turn takes part to the Friedel-Crafts acylation. Indeed, the reaction of 2,6-di-*tert*-butylphenol with an excess of 10-undecenoic acid and of trifluoroacetic anhydride at room temperature allowed the quantitative isolation of the desired product **9** without any further purification (Scheme 26).



**Scheme 26**

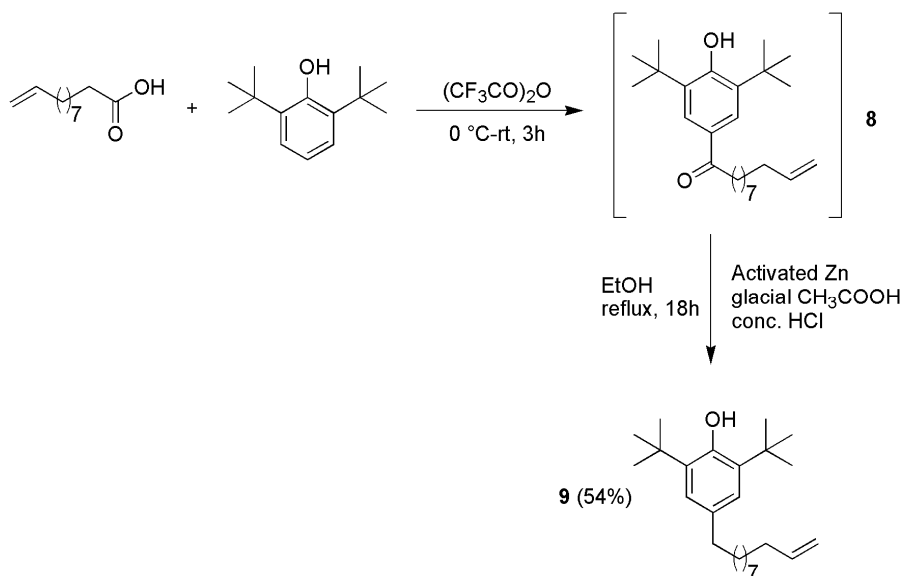
The direct reduction of ketones to alkanes can be done using two traditional reactions, the so-called Wolff-Kishner and Clemmensen reduction respectively. Because double bonds are theoretically labile to the strong acid conditions of the Clemmensen reduction, first attempts were done using the Wolff-Kishner reaction. The latter required the use of hydrazine for the condensation with the carbonyl compound to form an intermediate hydrazone that, thanks to the presence of a strong base like KOH, collapses leading to the reduction of the carbonyl and the loss of N<sub>2</sub>. The reaction is generally accomplished using high-boiling solvents like diethylene glycol in order to reach temperatures above 200 °C. Unfortunately, the reaction of **8** with hydrazine monohydrate and KOH in diethylene glycol at 100-220 °C<sup>131,132</sup> (Scheme 27) did not give the desired product **9** due to the degradation of the olefinic function.



**Scheme 27**

It was then decided to try the reduction of **8** using the Clemmensen reaction because, despite the necessary use of a strong acid like HCl that can add to the olefinic double bond, not extreme temperatures are required. Clemmensen reduction is generally carried out using HCl as acid in the presence of a zinc amalgam, however we were able to find a procedure<sup>133</sup> that allows the use of pure zinc and then avoids the undesired mercury. The reaction of **8** with zinc dust (15.3 equiv), conc. HCl (1.2 equiv) and acetic acid in ethanol at reflux gave promising results because, despite the starting ketone (**8**) was the main product, also the desired phenol **9** was obtained in low amount and the olefinic double bond was preserved. We were able to clearly increase the conversion from **8** to **9** by activating the zinc dust after an appropriate washing with aqueous HCl 2%,<sup>134</sup> even though a small amount of **8** was still present. Finally, we achieved the total conversion by using higher amounts of both the activated zinc (20 equiv) and conc. HCl (10 equiv). Because the purification of **8** (Scheme 26) does not require any difficult work-up procedure and the product is isolated in quantitative yield without any byproduct, a one-pot procedure starting from the 2,6-di-*tert*-butylphenol acylation and followed by the successive Clemmensen reduction was realized. For this purpose, the best conditions found for each of the two reactions were used and combined together (Scheme 28).





**Scheme 28**

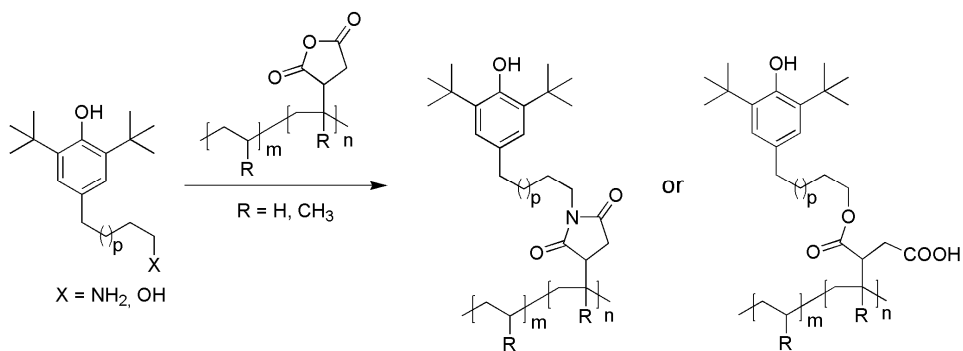
For the reaction were used 1 equiv of 2,6-di-*tert*-butylphenol, 1.33 equiv of 10-undecenoic acid, 1.55 equiv of trifluoroacetic anhydride, 20 equiv of activated zinc, acetic acid and 10 equiv of conc. HCl. This synthetic procedure proved to be intriguing because allowed the insertion of a long alkyl chain with a terminal double bond on the C4 of 2,6-di-*tert*-butylphenol in a one-pot manner and after a single and easy purification. The desired product **9** was isolated in 54% yield. In this way we were able to obtain a hindered phenol where, between the antioxidant moiety and the polymerizable function, there is a spacer with no heteroatoms, *i.e.* an antioxidant molecule that theoretically is able to efficiently take part to copolymerization reactions.

### 3.3.2 Synthesis of BHT-like comonomers for the reactive blending

In section 3.3.1. it was described our work on the synthesis of BHT-like molecules developed for the preparation of antioxidant polymers through a copolymerization process. We also worked on analogous molecules suitable for the reactive blending. As already explained in section 3.1 one of the possible ways for obtaining polymeric antioxidants is the direct functionalization of an existing polymer. Except for the radical grafting, that is described in **Chapter 4**, the functionalization of an existing polymer requires the presence on the latter of suitable reactive groups that can be used for the linking of the antioxidant molecule. The use of these systems is limited by some technological problems. Indeed, it is generally necessary a post-synthesis modification of conventional polymers in order to introduce suitable reactive groups and the reaction between the polymer and the antioxidant is often accomplished through uncustomary techniques. This means that the functionalization of existing polymers requires additional and high cost-performance steps that do not meet the needs of industry. To overcome these shortcomings a possible solution is the so-called reactive

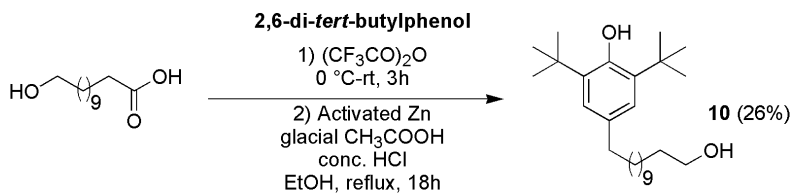
blending (RB). RB is defined as a “mixing process that is accompanied by the chemical reaction(s) of components of a polymer mixture”<sup>135</sup>. Most commonly this technique is used to enhance the compatibility between the components of polymer blends by the *in situ* formation of block or graft copolymers, also called compatibilizers, whose segments are individually miscible with one of the two polymers in the blend.<sup>136</sup> The resulting interaction reduces the interfacial tension and stabilizes the interface thus facilitating the formation of an actual miscible blend. The preparation of copolymeric compatibilizers by RB requires the presence, on each of their parent components, of suitable groups able to readily react in excellent yield each other with the typical conditions of blending. For example, a graft copolymer of polypropylene and polyamide 6 is obtained by reactive blending between commercially available polypropylene grafted with maleic anhydride (PP-g-MAH) and polyamide 6 (PA6).<sup>137</sup> The reactive blending between a polymer grafted with maleic anhydride and another with amine functionalities is frequently reported due to its high efficiency under the used conditions.<sup>138–146</sup> It is also reported the reaction between polymeric derivatives of maleic anhydride and primary alcohols.<sup>147,148</sup>

The commercial availability of polyolefins like polyethylene and polypropylene grafted with maleic anhydride suggested us their use for the preparation of polymeric stabilizing additives through a reactive blending process. We focused then on the preparation of BHT-like derivatives bearing, at the end of a long alkyl chain, amine or alcohol functionalities in order to allow their reaction with the maleic anhydride moieties of the polymers (Scheme 29).



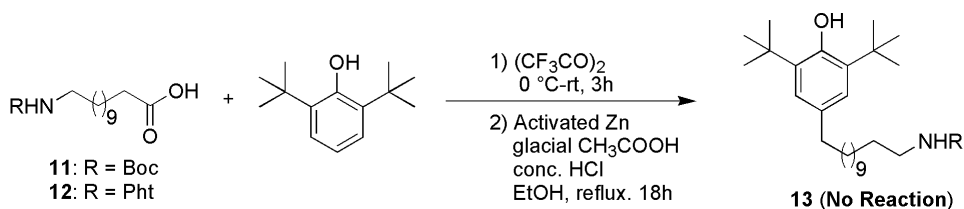
**Scheme 29**

We took advantage of the same synthetic pattern used for the synthesis of **9**. The reaction of 12-hydroxydodecanoic acid with 2,6-di-*tert*-butylphenol actually furnished the desired derivative **10** in 26% yield after the known pattern of the Friedel-Crafts acylation followed by the Clemmensen reduction of the intermediate alkylaryl ketone (Scheme 30).



**Scheme 30**

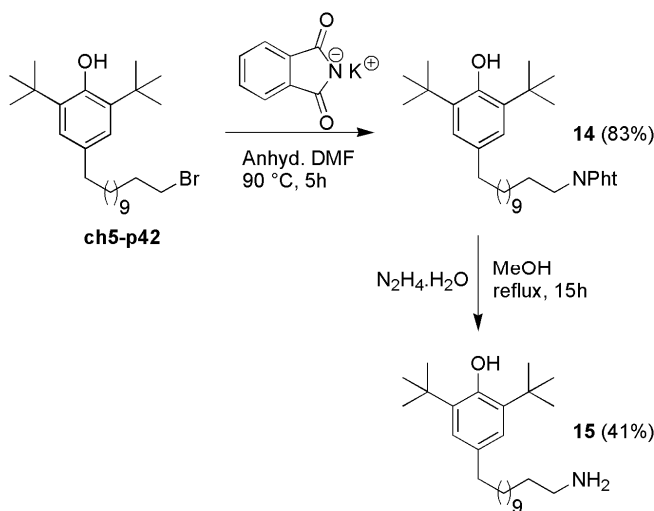
The same procedure using the protected amine derivatives **11**<sup>149</sup> and **12**<sup>150</sup> for the preparation of a BHT like product (**13**) with an amine group at the end of the alkyl chain was tried, but unsuccessfully (Scheme 31).



**Scheme 31:** Pht = phthaloyl

With the Boc-protected amine **11** the total absence of reactivity was observed because the starting phenol was completely recovered. Instead, when Pht-protected (Pht = phthaloyl) amine **12** was used the Friedel-Crafts acylation actually occurred but the following reduction resulted impossible.

After the poor results obtained for the synthesis of the BHT-like derivative bearing an amine group through the one-pot procedure of acylation and Clemmensen reduction, we decided to use a complete different synthetic way. The alkyl halide **ch5-c42**, originally prepared for the coupling with Cobalt nanoparticles *Turbobeads Amine*<sup>®</sup>, was converted to the corresponding amine using Gabriel synthesis. Potassium phthalimide was N-alkylated with **ch5-c42** in anhydrous DMF at 90 °C,<sup>151</sup> furnishing the derivative **14** that was reacted with hydrazine monohydrate to give amine **15** (Scheme 32).



**Scheme 32**

BHT-like amine **15** was obtained with an overall 34% yield and is now studied, like **10**, for the grafting process through reactive blending with commercially available polyethylene- or polypropylene-*graft*-maleic anhydride.

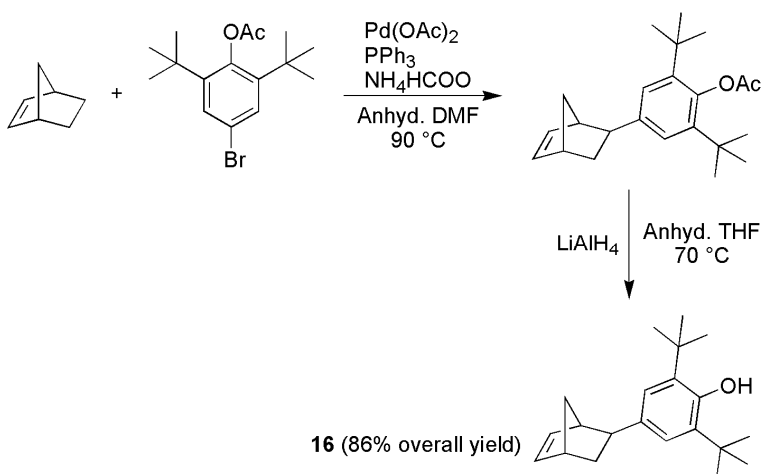
### 3.4 Terpolymeric antioxidant additives

#### 3.4.1 Introduction

Among the reactive antioxidants prepared in our research group, a BHT like derivative bearing a norbornene group resulted particularly interesting for its properties:

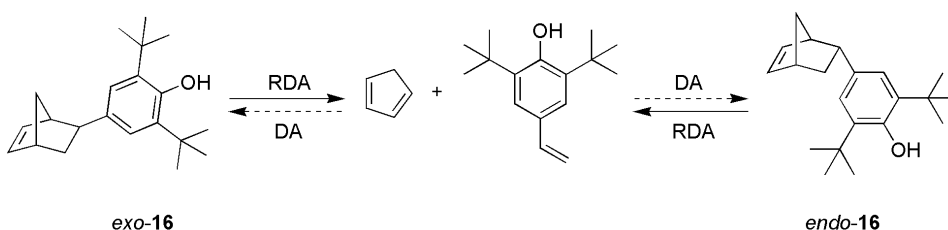
- The presence of an easily polymerizable double bond on its structure
- The absence of additional heteroatoms besides the phenolic oxygen
- A simple and efficient synthetic route

Indeed norbornene (**N**) is well-known for its effectiveness as monomer in polymerization with metallocene-type catalysts<sup>152,153</sup> and the ability of functionalized norbornene derivatives in the copolymerization with ethylene is copiously reported in literature.<sup>154–159</sup> Reactive antioxidant **16** was prepared through a reductive Heck coupling between 4-bromo-2,6-di-*tert*-butyl-phenyl acetate and norbornadiene in the presence of triphenylphosphine, palladium acetate and ammonium formate in anhydrous DMF at 90 °C followed by the lithium aluminium hydride reduction of the acetyl group (Scheme 33).<sup>57</sup>



**Scheme 33**

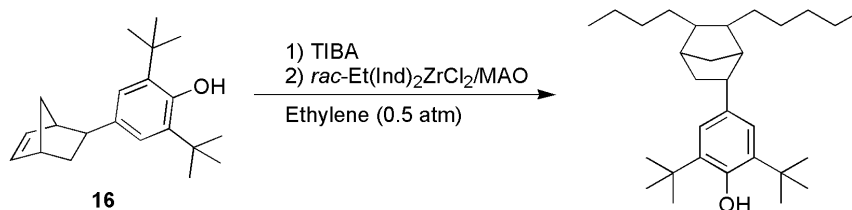
This synthetic route was followed because, unlike the direct Diels-Alder reaction between cyclopentadiene and the proper styrene, it allowed the prevailing formation of the *exo* isomer<sup>160,161</sup> that, as reported, is more reactive than the *endo* one in the polymerization reactions.<sup>162-164</sup> However, it resulted necessary the use of 4-bromo-2,6-di-*tert*-butylphenyl acetate instead of the corresponding free phenol because the coupling with the latter led to the formation in relevant amount (20%) of a byproduct, 2,6-di-*tert*-butylphenol, as the result of a Pd-mediated debromination. Beside the significant yield of this byproducts, its separation from *exo*-**16** was very difficult. Unfortunately, *exo*-**16** is not stereostable on standing either in solution or as pure compound because variable amounts of *endo*-**16** isomer are formed in the course of time. This behaviour was explained by a retro Diels-Alder (RDA) reaction that leads to the formation of cyclopentadiene and 2,6-di-*tert*-butyl-4-vinylphenol that, in turn, take part to a Diels-Alder process that yields both the possible isomers (Scheme 34).



**Scheme 34**

For this reason, an isomeric mixture *exo/endo* 6/1 of **16** was used for the following works and it was demonstrated that, once the double bond of the *exo* isomer has participated to the polymerization, the norbornene moiety is stereochemically stable and the RDA process is avoided.

The copolymerization procedure was done in the same way seen for comonomers **C1-C8** (see section 3.2.1), *i.e.* **16** was pre-treated with an excess of TIBA and copolymerized with ethylene (**E**) using MAO-activated *rac*-Et(Ind)<sub>2</sub>ZrCl<sub>2</sub> as catalyst (Scheme 35).



**Scheme 35**

By varying the **E/16** molar ratio it was possible to tune the comonomer content, at least to a certain extent, within the desired composition range (0.1-2 mol%). The amount of bound phenolic comonomer was determined by <sup>13</sup>C-NMR analysis. The copolymers with a **16** content of 0.35, 0.78 and 1.60 mol% respectively were melt blended with additive-free low-density polyethylene (LDPE) in order to obtain polymeric blends containing 500 ppm of antioxidant functionalities.<sup>58</sup> Blends obtained from the copolymer with a **16** content of 1.60 mol% consisted of two macroscopically distinct phases, confirming that a high amount of the antioxidant comonomer is detrimental for the compatibility between the two components of the blend. After thermal, thermo-oxidative, thermo-ageing and photo-ageing tests these systems proved a better stabilizing performance compared to the same polymers with added the molecular antioxidant **BHT** in the same amount. The higher efficiency was obtained with the copolymeric additive containing the lower comonomer concentration (0.35 mol%), that we hypothesized being related to a better dispersion in the LDPE matrix. Migration tests on the LDPE films containing the polymeric antioxidants confirmed the non-releasing character of these additives.

Data obtained from both the research on reactive antioxidants **C1-C8** (Figure 21) and **16** (Scheme 33) allowed to state that the efficacy of polymeric additives is more related to their compatibility with the host polyolefin than to the quantitative content of antioxidant comonomer. It is then necessary, for the development of highly effective polymeric additives, the fulfilment of two fundamental structural requirements:

- 1) A relatively low content of antioxidant comonomer
- 2) A microstructure that resembles as much as possible that one of the virgin polymer that has to be stabilized

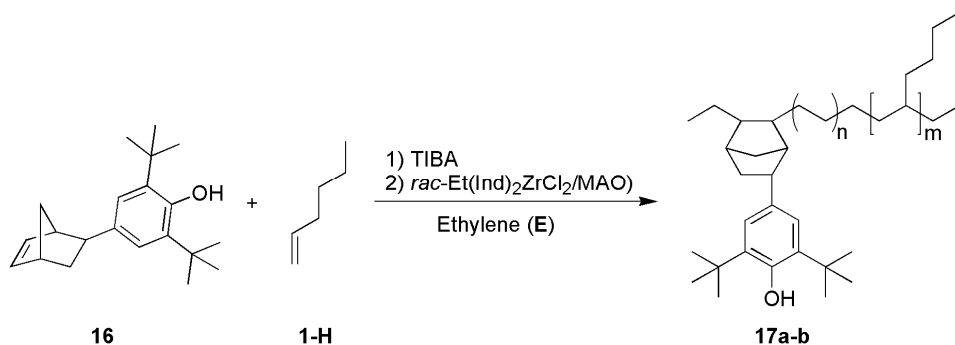
Indeed, considering the terpolymeric additives of ethylene/**C8**/1-hexene (Scheme 14, b) best results were obtained with that having a lower percentage of the antioxidant comonomer and a higher content of the third one (1-hexene). An explanation of this behaviour is the microstructure of the virgin polymer, that contains 2-4 mol% of 1-hexene, then an insertion of the same comonomer in a similar percentage inside the copolymeric additive increases the compatibility between the two components after their mixing through melt-blending. In my PhD work we focused our efforts in the

preparation and characterization of tailor-made polymeric antioxidants specifically designed for commercial polyolefins used in food and drug packaging. This project was carried out in collaboration: with the research group of Dr. S. Sosio and I. Tritto of the CNR ISMAC institute of Milan for the homo- and copolymers preparation; with the research group of Dr. P. Stagnaro of the CNR ISMAC institute of Genova for the blends and films production. For this purpose, **16** was used as antioxidant comonomer due to its efficient synthetic route and the demonstrated ability of the norbornene moiety to take part to copolymerization reactions.

### 3.4.2 Ethylene/1-hexene/16 terpolymers

#### 3.4.2.1 Synthesis and characterization

The first commercial polymer chosen was the aforementioned low-density polyethylene (LDPE) containing about 1.5 mol% of 1-hexene, generally used in different applications: food packaging film, agriculture film, bags and pouches, hygiene film, liner film, and shrink film. The terpolymerization of ethylene (**E**) with 1-hexene (**1-H**) and the antioxidant comonomer **16** (*exo/endo* 6/1) was accomplished after a careful optimization of the reaction conditions (Scheme 36).



**Scheme 36**

MAO-activated *rac*-Et(Ind)<sub>2</sub>ZrCl<sub>2</sub> was chosen because previous works proved its ability for the incorporation of bulky comonomers like norbornene in ethylene-based copolymers.<sup>57-59</sup> Derivative **16** was pre-treated with a slight excess of triisobutylaluminium (TIBA, 1.2 equiv) in order to protect its hydroxyl group and then to avoid the catalyst deactivation. A relatively low pressure of ethylene gas (0.5 atm) was used to promote the insertion of **16** with respect to ethylene and polymerization times (30') were fixed to obtain a sufficiently low comonomer conversion thus preventing the formation of polyethylene chains and ensuring a uniform comonomer distribution. **E/16** and **E/1-H** molar ratios in the mixture were varied in order to tune the **16** and **1-H** final contents to 1.0 and 1-3 mol% respectively. These conditions proved to be a satisfactory compromise between the desired good yield in terms of grams of terpolymer obtained and the insertion of both the comonomers in sufficient amounts for our purposes (Table 4). In this way, two terpolymeric additives were prepared, one with a **16** and **1-H**

content of 0.31 and 1.39 mol% respectively (**17a**), and the other with a **16** and **1-H** content of 0.68 and 2.49 mol% respectively (**17b**). In the same conditions were prepared as references a polymer of only ethylene (**PE**, Table 5) and a copolymer of ethylene with 2.25 mol% of **1-H** without the antioxidant comonomer (**18**). Also, a copolymer of ethylene with **16** (0.78 mol%) without **1-H** was used as reference (**19**).

**Table 4:** Chemical composition and yield of **E/1-H/16** terpolymers.

Run <sup>a</sup>	[E]/[16]	[E]/[1-H]	Yield (g)	Activity <sup>b</sup>	16 mol% <sup>c</sup>	16 conv.	1-H mol%	1-H conv.
<b>18<sup>d</sup></b>	-	4.31	1.8	7396	-	-	2.25	88.3
<b>19<sup>e</sup></b>	13.34	-	0.4	1560	0.78	20.1	-	-
<b>17a</b>	13.34	4.31	2.5	1987	0.31	51.8	1.39	97.2
<b>17b</b>	6.67	2.16	1.3	1055	0.68	25.8	2.49	43.8

<sup>a</sup> Polymerization conditions: solvent used is toluene (V=100 mL), Al/Zr = 1500 (mol/mol),  $t_{\text{pol}} = 30$  min, T = 35 °C,  $P_{\text{ethylene}} = 0.5$  atm, [catalyst] = 5  $\mu\text{mol}$ ; <sup>b</sup> Activity =  $[(g_{\text{pol}} \text{ mmol}_{\text{cat}}^{-1} \text{ h}^{-1}) \text{ P}^{-1}]$ ; <sup>c</sup> Determined by <sup>13</sup>C-NMR; <sup>d</sup> [catalyst] = 2  $\mu\text{mol}$ ,  $t_{\text{pol}} = 15$  min; <sup>e</sup> Ref.<sup>57,58</sup>.

The comonomer contents were determined by <sup>13</sup>C-NMR analysis using as comparisons the corresponding copolymers **E/1-H** and **E/16** for the assignments. Noteworthy these systems proved a relative good solubility in common organic solvents and were then easily purified and characterized, on the contrary of common polymeric additives. The thermal behaviour of the terpolymers was investigated by DSC analysis and, as clearly visible in Table 5, their crystallization and melting temperatures as well as the corresponding enthalpies are similar to those of the **E/16** copolymer (**19**) and in line to what expected for random co- and terpolymers of ethylene containing small amounts of higher  $\alpha$ -olefin co-units.

**Table 5:** Physical properties of **E/1-H/16** terpolymers.

Sample	16 (mol%)	1-H (mol%)	$T_c$ (°C)	$\Delta H_c$ (J/g)	$T_m$ (°C)	$\Delta H_m$ (J/g)
<b>PE<sup>a</sup></b>	-	-	112	-219	141	222
<b>19<sup>b</sup></b>	0.78	-	109	-130	121	136
<b>17a</b>	0.31	1.39	109	-122	124	122
<b>17b</b>	0.68	2.49	115	-126	126	128

<sup>a</sup> reference PE prepared in the same conditions used for **E/1-H/16** terpolymers; <sup>b</sup> Ref.<sup>57,58</sup>.



### 3.4.2.2 Blends with the LDPE matrix

The synthesized terpolymers were then used as masterbatches, *i.e.* a solid product containing the antioxidant function in relatively high concentration and is dispersed inside a commercial polymer using customary operations like molding. In our case, the terpolymeric additives were melt blended with the additive-free LDPE using a simple internal batch mixer at the appropriate temperature (130 °C). Concerning the relative amount of additive-free LDPE and terpolymers mixed, the specific monomers composition of the latter was considered in order to have 500 ppm of dispersed antioxidant into the LDPE. As references, neat LDPE and its mixtures with 500 and 2000 ppm of **BHT** (**LDPE + 500 BHT** and **LDPE + 2000 BHT** respectively) were processed under the same conditions used for the blends with the terpolymeric additives.

### 3.4.2.3 Thermal and thermo-oxidative stability tests

Thermal and thermo-oxidative stability of the prepared blends were evaluated by TGA analysis, both in isothermal and dynamic mode, after the preparation of thin films of 350  $\mu\text{m}$  thickness. Dynamic TGA under  $\text{N}_2$  atmosphere showed, as expected, that the onset of degradation temperature was substantially the same ( $T_D$  onset values of 475-480 °C) for all of the LDPE blends and then they have a similar thermal stability. Different results were obtained by dynamic and isothermal TGA experiments under  $\text{O}_2$  atmosphere (Figure 24).

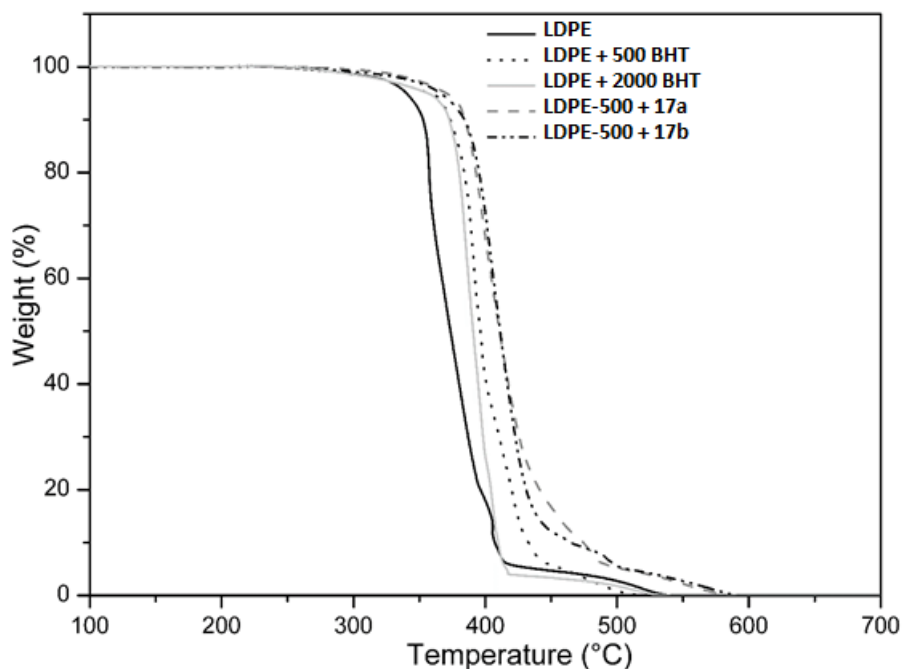


**Figure 24:** Dynamic TGA curves under  $\text{O}_2$  of LDPE-based blends.

In dynamic mode, for the blends containing the terpolymeric antioxidants (**LDPE-500 + 17a** and **LDPE-500 + 17b**) the degradation started at a temperature about 15 °C higher than that measured for the LDPE samples containing 500 or 2000 ppm of **BHT** respectively. Analogous isothermal experiments were used to measure the Oxidative Induction Time (OIT), that is defined as the time to the onset of oxidation of a test specimen exposed to an oxidizing atmosphere at an elevated isothermal temperature.<sup>165</sup> The chosen temperature for OIT measurements was 180 °C so as to do the experiment in conditions similar to those typical in industrial processing of LDPE. Measured OITs are reported in Table 6 and clearly show the excellent performance of the terpolymeric stabilizers compared to both the additive-free LDPE and LDPE stabilized with **BHT**.

**Table 6:** Oxidative Induction time at 180 °C under O<sub>2</sub> for neat LDPE, its blends with **BHT** and with **E/1-H/16** terpolymeric antioxidants.

Sample	1-H mol%	16 mol%	OIT 180 °C (min)
<b>LDPE</b>	-	-	2.7
<b>LDPE + 500 BHT</b>	-	-	2.7
<b>LDPE + 2000 BHT</b>	-	-	6.5
<b>LDPE-500 + 19<sup>a</sup></b>	-	0.78	7.4
<b>LDPE-500 + 17a</b>	1.39	0.31	3.8
<b>LDPE-500 + 17b</b>	2.49	0.68	7.7

<sup>a</sup> Ref.<sup>58</sup>.

It is noteworthy that both the samples containing the terpolymeric additives have OIT values higher than that containing 500 ppm of **BHT** which, in turn, has a stabilizing performance identical to non-stabilized LDPE. Actually, the blends containing the higher amount of both **16** and **1-H** (**LDPE-500 + 17b**) showed OIT values even superior to the LDPE sample stabilized with 2000 ppm of **BHT** despite an antioxidant moieties content four-fold lower. The trend of isothermal TGA curves obtained at 180 °C under O<sub>2</sub> clearly explains the difference between LDPE samples containing terpolymeric antioxidants and those stabilized with **BHT** (Figure 25).

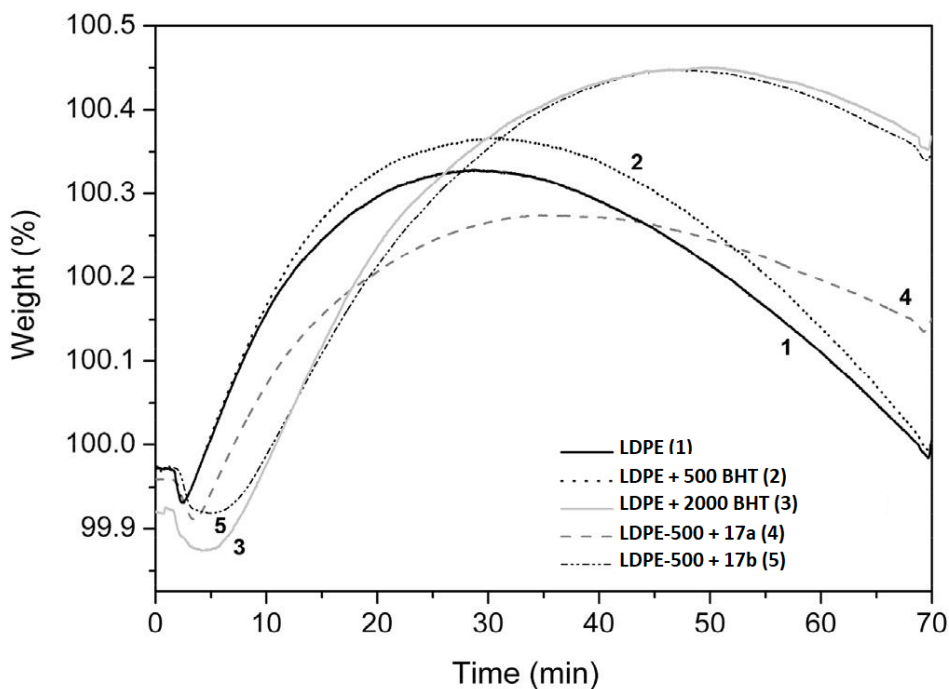


**Figure 25:** Isothermal TGA curves at 180 °C under O<sub>2</sub> of LDPE blends containing E/1-H/16 terpolymer antioxidants. Curves of the additive-free LDPE and its blends containing 500 and 2000 ppm **BHT** antioxidant are reported for comparison.

First of all, the samples of LDPE with no additive and containing 500 ppm of **BHT** exhibited a very similar degradation behavior, probably due to the physical loss that **BHT** undergoes either during film specimen preparation by compression moulding and during TGA heating run up to the chosen temperature of 180 °C. This was expected due to the volatility of low-molecular weight antioxidants, and indeed a significant loss of different stabilizers during the exposure at elevated temperatures is reported in literature.<sup>166–168</sup> To avoid this problem it is generally necessary to overload the plastic with the additive to take account of its loss during compounding or transformation processes, as explained by the sample with a **BHT** loading of 2000 ppm that has a better stabilizing performance. Instead, our terpolymeric additives guarantee a stabilizing performance comparable or even superior to that obtained for the LDPE added with 2000 ppm **BHT** despite the concentration of the antioxidant moieties is four times lower.

### 3.4.2.4 Thermo-ageing tests

Beside the thermal and thermo-oxidative stability studies seen in the previous section, also ageing tests are useful in order to evaluate the stabilizing performance of the additives in conditions of storage and end use. For this purpose, the samples are generally exposed to conditions milder than those used for the TGA analysis. Each film

was exposed in air in an oven maintained at 70 °C and controlled by ATR-FTIR every 7 days. The oxidative degradation of the samples was evaluated in terms of carbonyl index progression during the thermo-ageing, calculated by the following formula:

$$\text{Carbonyl Index} = \frac{A_{\text{C=O}}}{A_{1465}} - \text{CI}_0$$

where  $A_{\text{C=O}}$  is the area of the stretching of carbonyl band centered at 1740  $\text{cm}^{-1}$ ,  $A_{1465}$  is that of the band typical of polyethylene used as internal reference to minimize errors from sample thickness,  $\text{CI}_0$  is the CI value before the ageing experiment. In Table 7 is reported the CI progression during the thermo-ageing for the samples containing the terpolymeric antioxidants compared to those containing molecular antioxidant **BHT** or copolymeric antioxidant **E/16**.

**Table 7:** Carbonyl Index evolution during thermo-ageing in air at 70 °C of films of blends of neat LDPE with 500 ppm **BHT**, or proper amounts of copolymer **19** or terpolymers **17a** and **17b**.

Time (days)	LDPE + 500 BHT	LDPE-500 + 19 <sup>a</sup> (0.78 mol% 16)	LDPE-500 + 17a (0.31 mol% 16)	LDPE-500 + 17b (0.68 mol% 16)
0	0	0	0	0
7	0.8	0.4	0.1	0.3
14	2.3	0.5	0.1	0.3
28	4.2	1.2	0.1	0.3
42	7.8	1.3	0.4	0.7
77	8.8	1.3	0.6	1.2

<sup>a</sup> Ref<sup>58</sup>.

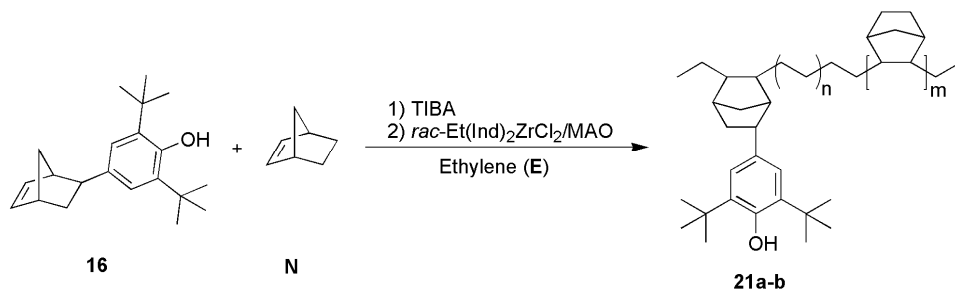
It is evident that with commercial **BHT** (**LDPE + 500 BHT**) the degradative oxidation occurred from the first stage of the ageing test, leading to the complete failure of the sample in few days. Instead, both the samples containing a terpolymeric additive (**LDPE-500 + 17a** and **LDPE-500 + 17b**) showed a clear better stability performance not only compared to **LDPE + 500 BHT** but also to the blend of LDPE with the **E/16** copolymer as additive (**LDPE-500 + 19**).

### 3.4.3 Ethylene/Norbornene/16 terpolymers

#### 3.4.3.1 Synthesis and characterization

Our work on the preparation of non-releasing antioxidant additives designed for the stabilization of polyolefins used in human contact applications continued with the Cyclic Olefins Copolymers (COCs). COCs are copolymers of ethylene (**E**) with a content

of norbornene (**N**) >30% and are used in different pharmaceutical, medical and food packaging applications.<sup>169</sup> We planned the preparation of **E/N/16** terpolymers in order to obtain an antioxidant function content below 1 mol% and that of norbornene (25-35 mol%) similar to the commercial unstabilized COC. For this purpose, the polymerization conditions used were analogous to those seen in section 3.4.2.1 for the preparation of **E/1-H/16** terpolymers, *i.e.* MAO-activated *rac*-Et(Ind)<sub>2</sub>ZrCl<sub>2</sub> as catalyst, low pressure of ethylene (0.5 atm) and an excess of TIBA to avoid catalyst deactivation (Scheme 37).



**Scheme 37**

In order to find the best conditions for obtaining the desired **N** insertion of 25-35 mol%, first attempts of copolymerization were carried out between ethylene and unsubstituted **N** (Sample **20**, Table 8). Two terpolymers containing about 25 mol% of **N** and 0.17 (**21a**) or 0.38 (**21b**) mol% of **16** were prepared by varying the ratio between ethylene and the functionalized comonomer, 13.34 or 6.67 respectively (Table 8).

**Table 8:** Chemical composition and yield of **E/N/16** terpolymers.

Run <sup>a</sup>	<b>16</b> (mmol)	[E]/[ <b>16</b> ]	[E]/[ <b>N</b> ]	Yield (mg)	Activity <sup>b</sup>	<b>16</b> mol% <sup>c</sup>	<b>16</b> conv.	<b>N</b> mol%	<b>N</b> conv
<b>20</b>	-	-	0.83	450	720	-	-	29.49	34.9
<b>21a</b>	0.5	13.34	0.83	1292	1033	0.17	4.3	25.37	82.6
<b>21b</b>	1	6.67	0.83	1140	912	0.38	4.4	24.03	7602

<sup>a</sup> Polymerization conditions: solvent used is toluene (V=100 mL), Al/Zr = 1500 (mol/mol),  $t_{\text{pol}} = 30$  min,  $T = 35$  °C,  $P_{\text{ethylene}} = 0.5$  atm, [catalyst] = 5  $\mu\text{mol}$ ; <sup>b</sup> Activity =  $[(g_{\text{pol}} \text{ mmol}_{\text{cat}}^{-1} \text{ h}^{-1}) \text{ P}^{-1}]$ ; <sup>c</sup> Determined by <sup>13</sup>C-NMR.

The <sup>13</sup>C-NMR assignment of the terpolymers was performed by comparison with the spectra of the corresponding **E/N**<sup>152,170,171</sup> and **E/16**<sup>57</sup> copolymers. The thermal behaviour of the prepared terpolymers was investigated by DSC analysis and, as expected, only the glass transition temperature was detected due to the amorphous nature of polymers with a high content of norbornene (Table 9).

**Table 9:** Physical properties of E/N/16 terpolymers.

Sample	16 mol% <sup>a</sup>	N mol% <sup>a</sup>	T <sub>g</sub> (°C)
20	-	29.49	88.3
21a	0.17	25.37	97.2
21b	0.38	24.03-	-

### 3.4.3.2 Blends with the COC matrix

Samples **21a** and **21b** were added by melt blending at 200 °C to a commercially available additive-free COC matrix. The procedure used allow the preparation of blends containing 500 ppm (**COC-500 + 21a** and **COC-500 + 21b**) of the antioxidant moiety dispersed in the matrix for both the terpolymers and also blends containing 250 and 100 ppm of **21a** were prepared (**COC-250 + 21a** and **COC-100 + 21a**).

### 3.4.3.3 Thermal and thermo-oxidative stability tests

Resulting samples were submitted to TGA analysis in order to compare their thermal and thermo-oxidative stability with that of the additive-free COC and with those of the same matrix containing 500 (and 2000) ppm of the commercial antioxidant **BHT**. Data obtained from TGA analysis in dynamic mode under O<sub>2</sub> atmosphere showed that all of the blends containing a terpolymeric antioxidant have a T<sub>onset</sub> and a T<sub>D25</sub> higher than those containing **BHT** at 500 or 2000 ppm (Table 10). These results were particularly interesting for the samples containing less than 500 ppm of **21a** (**COC-250 + 21a** and **COC-100 + 21a**) because despite the lower concentration of antioxidant they were able to ensure an effective stabilization.

**Table 10:** Degradation temperature under O<sub>2</sub> of neat COC, its blends with **BHT**, and with E/N/16 terpolymeric additives.

Sample	N (mol%) <sup>a</sup>	16 (mol%) <sup>a</sup>	T <sub>onset</sub> (°C)	T <sub>D25</sub> (°C)
COC	-	-	472.2	474.3
COC + 500 BHT	-	-	471.2	473.1
COC + 2000 BHT	-	-	479.9	480.2
COC-500 + 21a	25.37	0.17	491.4	492.3
COC-250 + 21a	25.37	0.17	489.2	489.1
COC-100 + 21a	25.37	0.17	492.4	489.4

<b>COC-500 + 21b</b>	24.03	0.38	488.2	489.1
----------------------	-------	------	-------	-------

<sup>a</sup> Determined by <sup>13</sup>C-NMR.

OIT measurements by isothermal TGA analysis in O<sub>2</sub> atmosphere were carried out at 180 °C and, additionally, at 220 °C because the processing temperature of commercial COCs usually falls between 200 and 230 °C (Table 11).

**Table 11:** Oxidative Induction Time at 180 °C and 220 °C under O<sub>2</sub> for neat COC, its blends with **BHT** and with **E/N/16** terpolymeric antioxidants.

Sample	N (mol%) <sup>a</sup>	16 (mol%) <sup>a</sup>	T <sub>OIT</sub> (°C)	OIT (min)
<b>COC</b>	-	-	180	5.4
<b>COC + 500 BHT</b>	-	-	180	15.4
<b>COC + 2000 BHT</b>	-	-	180	24.5
<b>COC-500 + 21b</b>	24.03	0.38	180	>30
<b>COC-500 + 21a</b>	25.37	0.17	180	>30
<b>COC</b>	-	-	220	2.5
<b>COC + 500 BHT</b>	-	-	220	2.6
<b>COC + 2000 BHT</b>	-	-	220	2.6
<b>COC-500 + 21b</b>	24.03	0.38	220	4.0
<b>COC-500 + 21a</b>	25.37	0.17	220	10.5
<b>COC-250 + 21a</b>	25.37	0.17	220	8.2
<b>COC-100 + 21a</b>	25.37	0.17	220	2.6

<sup>a</sup> Determined by <sup>13</sup>C-NMR.

At 180 °C both the samples containing **BHT** (500 and 2000 ppm) showed a better stability than additive-free COC but were overcome by the better performance of the blends stabilized with the terpolymers (**COC-500 + 21b** and **COC-500 + 21a**). Moreover the performance of **COC-500 + 21a** and **COC-500 + 21b** is even better (>30 min) to that obtained with the previously studied **E/16** copolymeric additives where the functionalized comonomer content was even higher.<sup>58</sup> The enhanced stability achieved with the terpolymeric antioxidant additives can be accounted for their better dispersion in the COC matrix as a consequence of their higher microstructural similarity. At 220 °C no difference in the OIT values were measured between the additive-free COC and its two blends stabilized with **BHT**, suggesting that most of the added **BHT** is lost in the TGA furnace during the heating ramp to reach 220 °C. Instead, with terpolymeric additives a better stabilizing performance was achieved. In particular, the sample **COC-**

**500 + 21a** that contains 500 ppm of antioxidant moiety showed an OIT value about three times higher than that of the blend containing 2000 ppm of **BHT**. The blends containing a lower amount of terpolymeric additive showed additional interesting results. Indeed, the blend containing 250 ppm of antioxidant moieties (**COC-250 + 21a**) had an OIT value only slightly lower than **COC-500 + 21a**, suggesting the possibility of reducing the amount of additive without clearly affecting the stabilizing efficacy. The further reduction of the antioxidant moiety (**COC-100 + 21a**) was anyway able to guarantee a stabilizing performance analogous to that offered by 500 or 2000 ppm of the molecular antioxidant **BHT**. This interesting behavior of the blends containing different amounts of **21a** is clearly visible by the curves plotted from the isothermal TGA experiments performed under  $O_2$  (Figure 26), where **COC-500 + 21a** and **COC-250 + 21a** have a similar trend, as well as **COC-100 + 21a** and **COC + 500 BHT**.

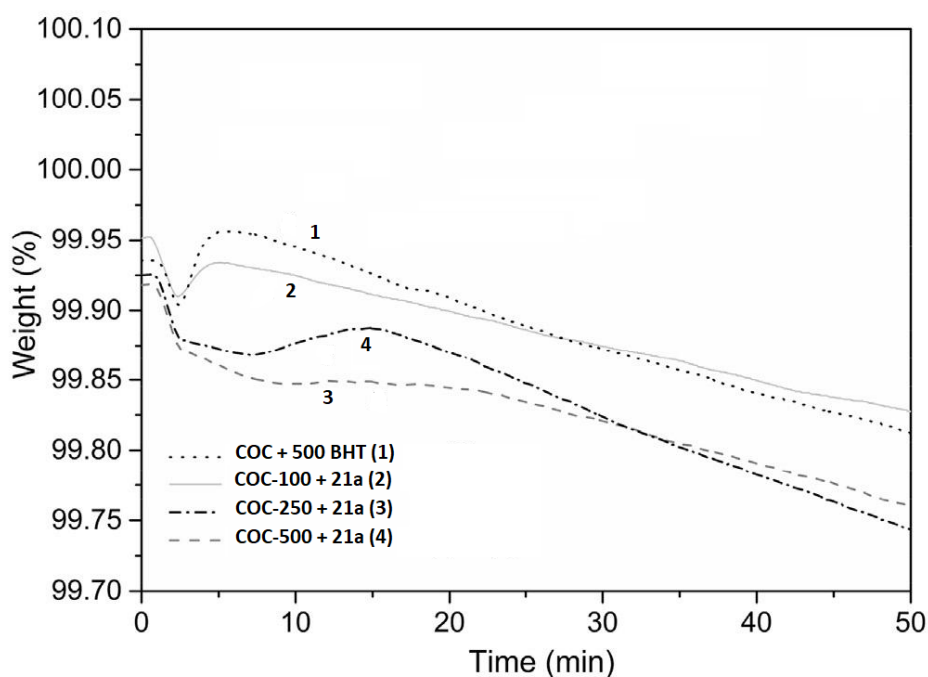


**Figure 26:** Isothermal TGA curves at 220 °C under  $O_2$  of COC blends containing 500, 250 and 100 ppm of antioxidant functionalities of the **E/N/16** terpolymer of run **21a**. COC containing 500 ppm of **BHT** is reported as comparison.

OIT measurements provided a strong evidence of the efficacy of the **E/N/16** terpolymers as antioxidant additives for COC systems: indeed at 180 °C 500 ppm of antioxidant functionalities bounded to the terpolymeric additive are more effective than 2000 ppm of molecular **BHT**, and at 220 °C even 100 ppm of antioxidant functionalities are sufficient to guarantee a protection analogous to that offered by 2000 ppm **BHT**.



### 3.4.3.4 Thermo-ageing tests

The thermo-ageing of COC based samples was carried out in the same way seen in section 3.4.2.4 for LDPE based samples, even though the recorded ATR-FTIR spectra are more complex in terms of number of bands and overlapping, as expected due to the chemical structure of the COC polymer chain.<sup>172,173</sup> The results are reported in Table 12 and show that the presence of a terpolymeric antioxidant as additive (**COC-500 21a** and **COC-500 21b**) provided a satisfactory stabilizing performance thus confirming the results obtained by TGA analysis.

**Table 12:** Carbonyl Index evolution during thermo-ageing in air at 70 °C of films of blends of neat LDPE with 500 ppm **BHT**, or proper amounts of terpolymers **21a** and **21b**.

Time (days)	COC + 500 BHT	COC-500 + 21a (0.17 mol% 16)	COC-500 + 21b (0.38 mol% 16)
0	0.07	0.04	0.04
7	0.06	0.05	0.06
14	0.17	0.08	0.11
42	0.10	0.07	0.25
77	0.12	0.09	0.16

### Conclusions

Macromolecular antioxidants represent an efficient option when searching for polymer stabilizers with high efficacy and non-releasing properties. In our work, the preparation and characterization of polymeric antioxidants was investigated continuing our previous researches. These systems are copolymers of  $\alpha$ -olefins (e.g. ethylene) and a comonomer bearing an antioxidant moiety linked to an easily polymerizable group (norbornene). Additionally, the presence of a third comonomer allows to increase the resemblance of the additive terpolymeric structure with that of the virgin polymer where it is added. The stabilizing performance of these terpolymeric antioxidants was evaluated and proved to be better than both the molecular antioxidant **BHT** and the analogous antioxidant copolymers (i.e. lacking of the third comonomer in their structure). These data confirm that the effectiveness of polymeric additives is mostly related to their ability of being easily dispersed in the polymer matrix and, for this purpose, two structural properties are fundamentals:

- 1) A low percentage (0.2-0.7 mol%) of antioxidant comonomer
- 2) A microstructure that resembles as well as possible that one of the polymer that requires the stabilization

Two types of terpolymeric antioxidants were prepared using **16** as antioxidant comonomer. The first are terpolymers of ethylene/1-hexene/**16** (**17a-b**) developed for the stabilization of LDPE used for food packaging. The second are terpolymers of ethylene/norbornene/**16** (**21a-b**) and were used as additives for the family of polymers called COCs. An attractive characteristic of the COCs is that, like out terpolymeric additives, their industrial synthesis is done with metallocene-based catalysts. The development of ethylene/norbornene/**16** terpolymers was then attractive not only for the goal of an enhanced stabilization and substantivity of the additive, but also because the similar production procedure is attractive for industry requirements. Indeed, the direct preparation in the plant polymerization reactor of a COC material containing **16** as stabilizer would avoid any post-polymerization addition of the antioxidant additives.

Simultaneously with the work on terpolymers, we synthesized further molecular antioxidant characterized by a BHT like structure and destined for the preparation of new copolymeric antioxidants with  $\alpha$ -olefins. The absence of further heteroatoms (except the oxygen of the phenolic OH) and the presence of a long alkyl chain between the antioxidant moiety and the polymerizable double bond should allow their effective insertion in tunable amount along the growing polymeric chain. Moreover, similar BHT like molecules were prepared with the purpose of being anchored to polyolefins-*graft*-maleic anhydride through reactive blending. The preparation of polymeric antioxidants with these molecular antioxidants is in development.

## 3.5 Experimental section

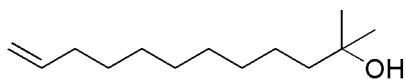
### 3.5.1 Materials

$^1\text{H}$  and  $^{13}\text{C}$  NMR spectra were recorded with Varian Gemini 200 or Varian Mercury Plus 400, using as solvent:  $\text{CDCl}_3$  using the reference at 7.26 ppm of the residue of chloroform in  $^1\text{H}$ -NMR spectrum and at 77.0 ppm in the  $^{13}\text{C}$ -NMR. FT-IR spectra were recorded with FT Infrared Spectrometer 1600 Perkin-Elmer in  $\text{CDCl}_3$  solutions of KBr pellets. GC-MS spectra were recorded with a QMD 100 Carlo Erba. ESI-MS spectra were recorded with a JEOL MStation JMS700. Melting points were measured with Melting Point Buchi 510 or Stuart SMP50 and are uncorrected. All the reactions were monitored by TLC on commercially available precoated plates (silica gel 60 F 254) and the products were visualized with acidic vanillin or  $\text{KMnO}_4$  solution. Silica gel 60 (230–400 mesh) was used for column chromatography. Commercial available reagents and catalysts were used as obtained from freshly open container without further purifications. Dry tetrahydrofuran, dichloromethane, dimethylformamide, and methanol were obtained by Pure Solv Micro. Hexane was freshly distilled over metallic sodium.  $\text{Et}_3\text{N}$  was distilled over KOH, dried on anhydrous  $\text{CaCl}_2$ . Hexane was distilled over metallic sodium. Commercial zinc dust ( $\text{Ø} < 10 \mu\text{m}$ ) was activated by stirring for 3-4' with 2% HCl. The zinc was immediately filtered in vacuo, washed to neutrality with water, and then washed with ethanol, acetone, and  $\text{Et}_2\text{O}$ . The resulting powder was dried at 90 °C under vacuum for 10' and immediately used. Manipulations of air and/or moisture-sensitive materials were carried out under an inert atmosphere using a glove-box apparatus or a dual vacuum/nitrogen line and standard Schlenk-line techniques. Toluene (Fluka, >99.5% pure) was dried and distilled from sodium under nitrogen atmosphere.

Methylaluminoxane (MAO) (10 wt% in toluene solution, Aldrich) was used after removing all volatiles and drying the resulting powder at 50 °C for 3 h in vacuum (0.1 mmHg). Triisobutylaluminoxane (TIBA) (Witco, in toluene solution) was used as received. *rac*-Et(Ind)<sub>2</sub>ZrCl<sub>2</sub> was purchased from Witco. Nitrogen and ethylene gases were dried and deoxygenated by passage over columns of CaCl<sub>2</sub>, molecular sieves, and BTS catalysts. Deuterated solvent for NMR measurements (C<sub>2</sub>D<sub>2</sub>Cl<sub>4</sub>) (Cambridge Isotope Laboratories, Inc.) was used as received. A commercial low-density polyethylene, LDPE, (Lupolen LP 2420F) kindly provided by Lyondelbasell Italia S.r.l. was used as the LDPE matrix. Lupolen LP 2420F is an additive-free LDPE grade [d 0.923 g cm<sup>-3</sup>; MFR (190 °C, 2.16 kg) 0.75 g (10 min)<sup>-1</sup>; melting temperature 111 °C] containing about 1.5 mol% of 1-hexene comonomer and rare long branches (as determined by <sup>13</sup>C NMR). A commercial ethylene/norbornene copolymer, COC, (Topas® 8007F-04) kindly supplied by Topas Advanced Polymers GmbH (Germany) was used as the COC matrix. Topas® 8007F-04 [d 1.02 g cm<sup>-3</sup>; glass temperature 79.7 °C] is an additive-free ethylene/norbornene copolymer, that contains 35.5 mol% of norbornene. The low molecular weight antioxidant 2,6-di-*tert*-butyl-4-methylphenol (BHT) was purchased from Sigma Aldrich (Italy).

### 3.5.2 Synthesis

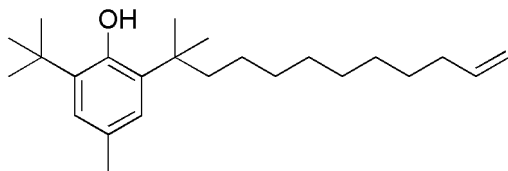
#### 2-Methyl-dodec-11-en-2-ol (**1**)



In a Schlenk tube, to a solution of Methyl 10-undecenoate (341 mg, 1.72 mmol) in anhydrous THF (3.6 mL), Methylmagnesium Bromide (3.0 M in Et<sub>2</sub>O, 2 mL, 6 mmol) was added dropwise at -78 °C. The mixture was left under magnetic stirring and N<sub>2</sub> atmosphere allowing warming to room temperature, then after 3.5h it was quenched with ice and acidified to pH 4 with aq. HCl 3N. The so-obtained suspension was extracted with AcOEt, then collected organic phases were washed with water, dried over anhydrous Na<sub>2</sub>SO<sub>4</sub> and evaporated *in vacuo*, furnishing **1** as a colourless oil of 311 mg that did not require any further purification (91% yield).

<sup>1</sup>H NMR (200 MHz, CDCl<sub>3</sub>) δ 1.21 (s, 6H), 1.29-1.48 (m, 15H), 2.00-2.05 (m, 2H); 4.90-5.05 (m, 2H), 5.71-5.92 (m, 1H).

#### 2-*tert*-Butyl-6-(1,1-dimethyl-undec-10-enyl)-4-methyl-phenol (**2**)



A solution of **1** (66 mg, 0.33 mmol) and 2-*tert*-butyl-4-methylphenol (19 mg, 0.12 mmol) in 1,2-DCE (1.5 mL) was added dropwise at 0 °C to a suspension of CH<sub>3</sub>SO<sub>3</sub>H (38 mg, 0.40 mmol) in 1,2-DCE (1 mL). The resulting red solution was left under magnetic

stirring at room temperature, monitored by TLC (eluent: petroleum ether/Et<sub>2</sub>O 4/1 and petroleum ether). After 24h the reaction was quenched with saturated aq. NaHCO<sub>3</sub>, then the resulting mixture was diluted with DCM (30 mL) and washed with saturated aq. NaHCO<sub>3</sub> (3x10 mL) and water (3x10 mL). The organic phase was dried over anhydrous Na<sub>2</sub>SO<sub>4</sub> and evaporated *in vacuo* furnishing a yellow oil of 0.07 g that was purified by silica gel column chromatography (eluent: petroleum ether), giving the desired product **2** as a colourless oil of 12 mg (29% yield).

**<sup>1</sup>H NMR** (400 MHz, CDCl<sub>3</sub>) δ 1.22-1.38 (m, 12H), 1.40 (s, 6H), 1.43 (s, 9H), 1.76-1.80 (m, 2H), 1.99-2.05 (m, 2H), 2.28 (s, 3H), 4.91-5.01 (m, 3H), 5.76-5.86 (m, 1H), 6.90 (d, *J* = 2.0 Hz, 1H), 6.98 (d, *J* = 2.0 Hz, 1H).

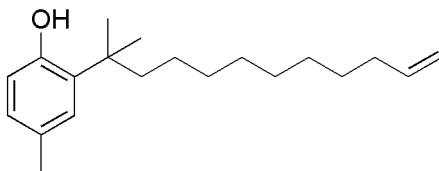
**<sup>13</sup>C NMR** (100 MHz, CDCl<sub>3</sub>) δ 21.2 (1C), 25.1 (1C), 28.9 (1C), 29.1 (1C), 29.2 (1C), 29.3 (1C), 29.4 (1C), 30.18 (2C), 30.24 (3C), 33.8 (1C), 34.2 (1C), 37.7 (1C), 41.8 (1C), 114.1 (1C), 125.4 (1C), 126.6 (1C), 128.0 (1C), 134.1 (1C), 135.6 (1C), 139.3 (1C), 151.5 (1C).

**IR** (CDCl<sub>3</sub>, cm<sup>-1</sup>) ν 3639, 3078, 2929, 2857, 1639, 1434.

**MS (ESI)**: *m/z* 343.58 [M-H]<sup>-</sup>, 687.25 [2M-H]<sup>-</sup>.

Anal. Calcd for C<sub>24</sub>H<sub>40</sub>O: C, 83.66%; H, 11.70%. Found: C, 83.51%; H, 11.91%.

2-(1,1-Dimethyl-undec-10-enyl)-4-methyl-phenol



CF<sub>3</sub>SO<sub>3</sub>H (50 μL, 0.57 mmol) was added dropwise at 0 °C to a solution of *para*-cresol (56 mg, 0.52 mmol) and **1** (311 mg, 1.57 mmol) in 1,2-DCE (9 mL). The resulting red solution was left under magnetic stirring at room temperature, monitored by TLC (eluent: petroleum ether/Et<sub>2</sub>O 4/1). After 24h the reaction was quenched with saturated aq. NaHCO<sub>3</sub>, then the resulting mixture was diluted with DCM (50 mL) and washed with saturated aq. NaHCO<sub>3</sub> (3x20 mL) and water (3x20 mL). The organic phase was dried over anhydrous Na<sub>2</sub>SO<sub>4</sub> and evaporated *in vacuo* furnishing a yellow oil of 0.29 g that was purified by silica gel column chromatography (eluent: petroleum ether/Et<sub>2</sub>O 11/1 → 2/1), giving the desired product as a colourless oil of 60 mg (40% yield).

**<sup>1</sup>H NMR** (400 MHz, CDCl<sub>3</sub>) δ 1.22 (bs, 12H), 1.36 (s, 6H), 1.78-1.82 (m, 2H), 2.00-2.05 (m, 2H), 2.28 (s, 3H), 4.57 (bs, 1H), 4.91-5.02 (m, 2H), 5.76-5.86 (m, 1H), 6.54 (d, *J* = 8.0 Hz, 1H), 6.87 (dd, *J* = 8.0 Hz, *J* = 1.6 Hz, 1H), 6.99 (d, *J* = 1.6 Hz, 1H).

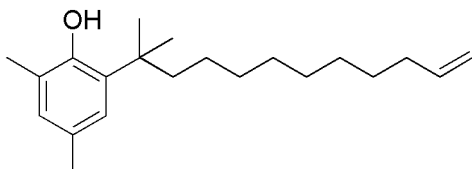
**<sup>13</sup>C NMR** (100 MHz, CDCl<sub>3</sub>) δ 20.8 (1C), 25.2 (1C), 28.2 (1C), 28.9 (1C), 29.1 (1C), 29.5 (2C), 30.4 (1C), 33.8 (1C), 37.7 (1C), 41.0 (1C), 114.0 (1C), 116.2 (1C), 127.1 (1C), 128.9 (1C), 129.4 (1C), 134.4 (1C), 139.3 (1C), 151.8 (1C) [18 of 19 C chemically equivalent].

**IR** (CDCl<sub>3</sub>, cm<sup>-1</sup>) ν 3600, 2928, 2857, 1639, 1506, 1179.

**MS (ESI)**  $m/z$  287.50 [M<sup>-</sup>-H], 575.00 [2M<sup>-</sup>-H].

Anal. Calcd. for C<sub>20</sub>H<sub>32</sub>O: C, 83.27%; H, 11.18%. Found: C, 83.09%; H, 11.27%.

2-(1,1-Dimethyl-undec-10-enyl)-4,6-dimethyl-phenol (**5**)



A solution of **1** (100 mg, 0.50 mmol) and 2,4-dimethylphenol (136 mg, 1.11 mmol) in petroleum ether (10 mL, bp 40-60 °C) was heated to 65 °C in inert atmosphere, then BF<sub>3</sub>.OEt<sub>2</sub> (100 μL, 0.80 mmol) was added dropwise. The resulting solution was left under magnetic stirring at 65 °C, monitored by TLC (eluent: petroleum ether/Et<sub>2</sub>O 4/1). After 3h the reaction was quenched at 0 °C with water (20 mL) and the mixture was stirred for 30'. The organic phase was washed with water (5x30 mL), dried over anhydrous Na<sub>2</sub>SO<sub>4</sub> and evaporated in vacuo furnishing a yellow oil that was purified by silica gel column chromatography (eluent: petroleum ether→petroleum ether/AcOEt 5/1). **5** was isolated as a yellow oil of 48 mg (32% yield).

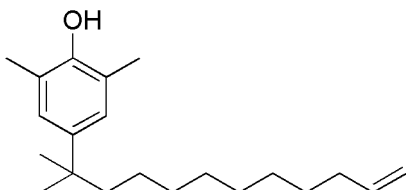
**<sup>1</sup>H NMR** (CDCl<sub>3</sub>, 400 MHz) δ 1.22-1.37 (m, 18H), 1.79-1.83 (m, 2H), 2.00-2.03 (m, 2H), 2.22 (s, 3H), 2.25 (s, 3H), 4.57 (s, 1H), 4.92-5.02 (m, 2H), 5.77-5.87 (m, 1H), 6.82 (s, 1H), 6.88 (s, 1H).

**<sup>13</sup>C NMR** (CDCl<sub>3</sub>, 100 MHz) δ 16.0, 20.8, 25.2, 28.4, 28.9, 29.1, 29.50, 29.52, 30.4, 33.8, 37.7, 41.1, 114.1, 122.6, 126.7, 128.6, 129.0, 134.0, 139.2, 150.3.

**IR** (CDCl<sub>3</sub>, cm<sup>-1</sup>) ν 3610, 2928, 2857, 1717, 1639, 1478, 1436.

**MS (ESI)**  $m/z$  366.00 [M + Na]<sup>+</sup>.

4-(1,1-Dimethyl-undec-10-enyl)-2,6-dimethyl-phenol (**6**)



A solution of **1** (98 mg, 0.49 mmol) and 2,6-dimethylphenol (126 mg, 1.03 mmol) in petroleum ether (10 mL, bp 40-60 °C) was heated to 65 °C in inert atmosphere, then BF<sub>3</sub>.OEt<sub>2</sub> (80 μL, 0.65 mmol) was added dropwise. The resulting solution was left under magnetic stirring at 65 °C, monitored by TLC (eluent: petroleum ether/Et<sub>2</sub>O 4/1). After 3h the reaction was quenched at 0 °C with water (20 mL) and the mixture was stirred for 30'. The organic phase was washed with water (5x30 mL), dried over anhydrous Na<sub>2</sub>SO<sub>4</sub> and evaporated in vacuo furnishing a yellow oil that was purified by silica gel

column chromatography (eluent: petroleum ether→petroleum ether/Et<sub>2</sub>O 4/1). **6** was isolated as a colourless oil of 61 mg (41% yield).

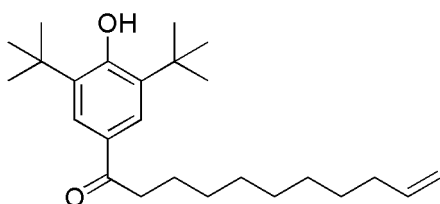
<sup>1</sup>H NMR (CDCl<sub>3</sub>, 400 MHz) δ 1.05-1.38 (m, 18H), 1.52-1.56 (m, 2H), 2.01-2.07 (m, 2H), 2.26 (s, 6H), 4.49 (s, 1H), 4.92-5.03 (m, 2H), 5.77-5.87 (m, 1H), 6.93 (s, 2H).

<sup>13</sup>C NMR (CDCl<sub>3</sub>, 100 MHz) δ: 16.2, 24.7, 28.9, 29.2, 29.5, 30.4, 33.8, 36.8, 44.7, 114.1, 122.2, 126.0, 139.3, 141.5, 149.7.

IR (CDCl<sub>3</sub>, cm<sup>-1</sup>) ν 3612, 2959, 2928, 2873, 1463.

MS (ESI) m/z 301.42 [M-H]<sup>-</sup>.

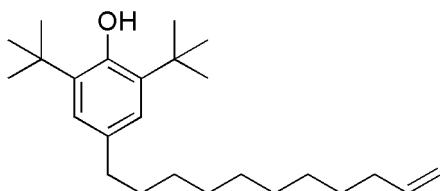
1-(3,5-Di-*tert*-butyl-4-hydroxy-phenyl)-undec-10-en-1-one (**8**)



10-undecenoic acid (245 mg, 1.33 mmol) was dissolved in 220 μL of trifluoroacetic anhydride, then after 10' 2,6-di-*tert*-butylphenol (206 mg, 1.00 mmol) was added at 0 °C. The so formed brown solution was stirred at 0 °C for 30' and then at room temperature until the disappearance of the starting phenol after 3h (eluent for TLC control: Ep/Et<sub>2</sub>O 10/1). The reaction was quenched with ice and saturated ac- NaHCO<sub>3</sub>, then the resulting mixture was diluted with DCM (50 mL) and washed with saturated aq. NaHCO<sub>3</sub> (3x10 mL) and water (3x10 mL). The organic phase was dried over anhydrous Na<sub>2</sub>SO<sub>4</sub> and evaporated *in vacuo* furnishing **8** as a brown oil of 416 mg that did not require any further purification.

<sup>1</sup>H NMR (200 MHz, CDCl<sub>3</sub>) δ 1.32 (bs, 12H), 1.43 (s, 18H), 2.00-2.05 (m, 2H), 2.90 (t, J= 8.0 Hz, 2H) 4.90-5.05 (m, 2H), 5.70 (bs, 1H), 5.75-5.92 (m, 1H), 7.80 (s, 2H).

2,6-Di-*tert*-butyl-4-undec-10-enyl-phenol (**9**)



10-undecenoic acid (245 mg, 1.33 mmol) was dissolved in 220 μL of trifluoroacetic anhydride, then after 10' 2,6-Di-*tert*-butylphenol (206 mg, 1.00 mmol) was added at 0 °C. The so formed brown solution was stirred at 0 °C for 30' and then at room temperature until the disappearance of the starting phenol after 3h (eluent for TLC control: Ep/Et<sub>2</sub>O 10/1). To the resulting dark solution absolute EtOH (5 mL), glacial

acetic acid (2.5 mL) and 37% HCl (0.82 mL) were added, then the mixture was heated to reflux and activated Zn dust (<10 $\mu$ , 1360 mg, 20.80 mmol) was added in small portions. The resulting colourless suspension was vigorously stirred under reflux for 18h, then after TLC control (eluent: Ep/Et<sub>2</sub>O 15/1) the absence of the intermediate ketone was demonstrated and the reaction was quenched with saturated aq. NaHCO<sub>3</sub>. The residual Zinc was filtered off and the filtrate was extracted with petroleum ether (3x15 mL), then the organic phase was washed with saturated aq. NaHCO<sub>3</sub> (3x20 mL) and water (3x20 mL). The organic phase was dried over anhydrous Na<sub>2</sub>SO<sub>4</sub> and evaporated *in vacuo* furnishing a yellow oil of 280 mg that was purified by silica filtration (eluent: petroleum ether/DCM 50/1), giving the product **9** as a colourless oil of 190 mg (54% yield).

**<sup>1</sup>H NMR** (400 MHz, CDCl<sub>3</sub>)  $\delta$  1.31 (bs, 12H), 1.46 (s, 18H), 1.56-1.62 (m, 2H), 2.04-2.09 (m, 2H), 2.53 (t, *J* = 8.0 Hz, 2H), 4.94-5.05 (m, 2H), 5.05 (bs, 1H), 5.79-5.89 (m, 1H), 7.00 (s, 2H).

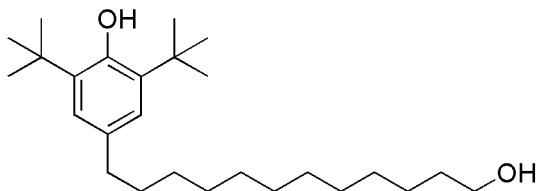
**<sup>13</sup>C NMR** (100 MHz, CDCl<sub>3</sub>)  $\delta$  28.9 (1C), 29.1 (1C), 29.49 (1C), 29.52 (1C), 29.57 (1C), 29.63 (1C), 30.3 (6C), 32.0 (1C), 33.8 (1C), 34.3 (2C), 36.0 (1C), 114.1 (1C), 124.8 (1C), 133.5 (2C), 135.5 (2C), 139.3 (1C), 151.6 (1C).

**IR** (CDCl<sub>3</sub>, cm<sup>-1</sup>)  $\nu$  3643, 2929, 2856, 1639, 1436, 1234, 1159.

**MS (ESI)** *m/z* 357.67 [M-H]<sup>-</sup>; 715.33 [2M-H]<sup>-</sup>.

Anal. Calcd. C<sub>25</sub>H<sub>42</sub>O: C, 83.73%; H, 11.81%. Found: C, 83.91%; H, 11.74%.

2,6-Di-*tert*-butyl-4-(12-hydroxy-dodecyl)-phenol (**10**)



12-hydroxydodecanoic acid (412 mg, 1.91 mmol) was dissolved in 1 mL of trifluoroacetic anhydride, then after 10' 2,6-Di-*tert*-butylphenol (296 mg, 1.43 mmol) was added at 0 °C. The so formed brown solution was stirred at 0 °C for 30' and then at room temperature until the disappearance of the starting phenol after 3h (eluent for TLC control: Ep/Et<sub>2</sub>O 5/1). To the resulting dark solution absolute EtOH (5 mL), glacial acetic acid (2.5 mL) and 37% HCl (2 mL) were added, then the mixture was heated to reflux and activated Zn dust (<10 $\mu$ , 2000 mg, 30.67 mmol) was added in small portions. The resulting colourless suspension was vigorously stirred under reflux for 18h, then after TLC control (eluent: Ep/Et<sub>2</sub>O 15/1) the absence of the intermediate ketone was demonstrated and the reaction was quenched with saturated aq. NaHCO<sub>3</sub>. The residual Zinc was filtered off and the filtrate was extracted with petroleum ether (3x15 mL), then the organic phase was washed with saturated aq. NaHCO<sub>3</sub> (3x20 mL) and water (3x20 mL). The organic phase was dried over anhydrous Na<sub>2</sub>SO<sub>4</sub> and evaporated *in*

*vacuum* furnishing a yellow oil of 280 mg that was purified by silica column chromatography (eluent: petroleum ether/Et<sub>2</sub>O 4/1), giving the product **10** as a yellow oil of 145 mg (26% yield).

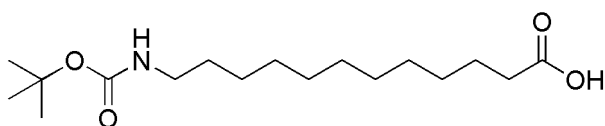
**<sup>1</sup>H NMR** (CDCl<sub>3</sub>, 400 MHz) δ 1.29-1.59 (m, 38H), 2.52 (t, *J* = 8.0 Hz, 2H), 3.65 (t, *J* = 6.6 Hz, 2H), 5.02 (s, 1H), 6.98 (s, 2H).

**<sup>13</sup>C NMR** (CDCl<sub>3</sub>, 100 MHz) δ 25.7, 29.4, 29.5, 29.59, 29.61, 29.63, 29.7, 30.4, 32.0, 32.8, 34.3, 36.0, 83.1, 124.8, 135.6.

**IR** (CDCl<sub>3</sub>, cm<sup>-1</sup>) *v*: 3642, 2929, 2856, 1466, 1436.

**MS (ESI)** *m/z* 389.67 [M-H]<sup>-</sup>.

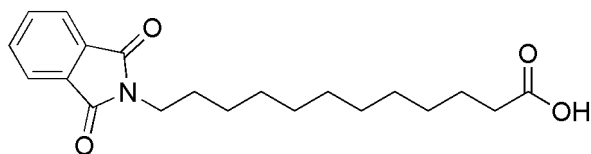
12-*tert*-Butoxycarbonylamino-dodecanoic acid (**11**)



To a suspension of 12-aminododecanoic acid (433 mg, 2.01 mmol) and TEA (400 μL, 2.88 mmol) in anhydrous MeOH (20 mL), a solution of Boc<sub>2</sub>O (880 mg, 4.04 mmol) in anhyd. MeOH (10 mL) was added dropwise at room temperature. The mixture was stirred for 1h at 60 °C, then it was diluted with CHCl<sub>3</sub> and the organic phase was washed with saturated aq. NH<sub>4</sub>Cl (5x30 mL). The organic phase was dried over Na<sub>2</sub>SO<sub>4</sub>, filtered and concentrated *in vacuum*, giving **11** as a white solid of 618 mg that did not require any further purification (97% yield).

**<sup>1</sup>H NMR** (CDCl<sub>3</sub>, 200 MHz) δ 1.26-1.65 (m, 27H), 2.33 (t, *J* = 7.4 Hz, 2H), 3.04-3.13 (m, 2H), 4.55 (bs, 1H).

12-(1,3-Dioxo-1,3-dihydro-isoindol-2-yl)-dodecanoic acid (**12**)



A solution of 12-aminododecanoic acid (860 mg, 4.00 mmol) and phthalic anhydride (592 mg, 4.00 mmol) in anhyd. DMF (10 mL) was stirred at reflux for 3h, then it was diluted with AcOEt (60 mL) and washed with water (8x20 mL). The organic phase was dried over Na<sub>2</sub>SO<sub>4</sub>, filtered and concentrated *in vacuum*, giving **12** as a white solid of 1130 mg that did not require any further purification (82% yield).

**Mp.** 87-91 °C.

**<sup>1</sup>H NMR** (CDCl<sub>3</sub>, 400 MHz) δ 1.25-1.31 (m, 14H), 1.58-1.67 (m, 4H), 2.33 (t, *J* = 7.6 Hz, 2H), 3.66 (t, *J* = 7.2 Hz, 2H), 7.69-7.71 (m, 2H), 7.82-7.85 (m, 2H).

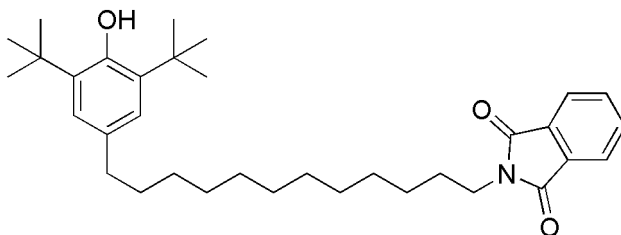


$^{13}\text{C}$  NMR ( $\text{CDCl}_3$ , 100 MHz)  $\delta$  24.6, 26.8, 28.5, 29.0, 29.10, 29.13, 29.3, 29.36, 29.39, 34.0, 38.0, 123.1, 132.1, 133.8, 168.5, 179.6.

IR ( $\text{CDCl}_3$ ,  $\text{cm}^{-1}$ )  $\nu$  3448, 3332, 2927, 2849, 1770, 1710, 1627, 1467, 1437.

MS (ESI)  $m/z$  344.50  $[\text{M}-\text{H}]^-$ .

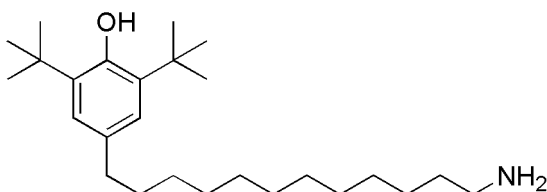
2-[12-(3,5-Di-*tert*-butyl-4-hydroxy-phenyl)-dodecyl]-isoindole-1,3-dione (**14**)



Potassium phthalimide (50 mg, 0.27 mmol) was added to a solution of the derivative **ch5-c42** (107 mg, 0.24 mmol) in anhyd. DMF (2.5 mL) at room temperature. The reaction mixture was left under magnetic stirring at 90 °C and monitored by TLC (eluent: Ep/Et<sub>2</sub>O 5/1). After 5h the reaction was quenched with water and extracted with DCM (3x30 mL). The organic phase was washed with water (10x30 mL), dried over Na<sub>2</sub>SO<sub>4</sub>, filtered and concentrated *in vacuo*, giving **14** as a brown oil of 109 mg that did not require any further purification (83% yield).

MS (ESI)  $m/z$  518.75  $[\text{M}-\text{H}]^-$ .

4-(12-Amino-dodecyl)-2,6-di-*tert*-butyl-phenol (**15**)



A solution of **14** (86 mg, 0.17 mmol) and hydrazine monohydrate (35 mg, 0.70 mmol) in MeOH (2 mL) was stirred under reflux for 16h, then aq. KOH (10%, 1 mL) was added and the mixture was extracted with Et<sub>2</sub>O (3x30 mL). The organic phase was washed with water (3x30 mL), dried over anhydrous Na<sub>2</sub>SO<sub>4</sub> and evaporated *in vacuo* furnishing a brown oil that was purified by silica column chromatography (eluent: DCM/MeOH 10:1→7/1), giving the product **15** as a yellow oil of 27 mg (41% yield).

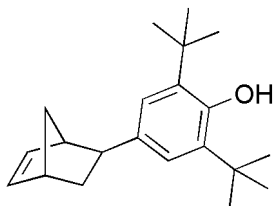
$^1\text{H}$  NMR ( $\text{CDCl}_3$ , 400 MHz)  $\delta$  1.23-1.59 (m, H), 2.51 (t,  $J = 8.0$  Hz, 2H), 2.75 (bs, 2H), 6.97 (s, 2H).

$^{13}\text{C}$  NMR ( $\text{CDCl}_3$ , 100 MHz)  $\delta$  26.8, 29.4, 29.5, 29.59, 29.62, 30.3, 30.5, 32.0, 34.2, 36.0, 124.8, 133.5, 135.6, 151.6.

IR (CDCl<sub>3</sub>, cm<sup>-1</sup>)  $\nu$  3642, 2928, 2855, 1436, 1363, 1315, 1234, 1158, 1121.

MS (ESI) m/z 390.50 [M+H]<sup>+</sup>.

4-Bicyclo[2.2.1]hept-5-en-2-yl-2,6-di-*tert*-butyl-phenol (**16**)



A Schlenk tube was charged with 4-bromo-2,6-di-*tert*-butylphenyl acetate (1.50 g, 4.58 mmol) and triphenylphosphine (118 mg, 0.45 mmol) then was evacuated and refilled with nitrogen three times, anhydr. DMF (7 mL) and bicycle[2.2.1]-hepta-2,5-diene (norbornadiene) (2.5 mL, 23.00 mmol) were added through the rubber stopper via a syringe and stirred to dissolve the solid. Palladium acetate (49 mg, 0.22 mmol) and ammonium formate (1.13 g, 17.88 mmol) were added in sequence and the reaction mixture stirred at 90 °C overnight. Then, it was cooled to room temperature, diluted with DCM (200 mL), washed with 0.1M hydrochloric acid (150 mL) and water (3x150 mL), the organic layer was dried over Na<sub>2</sub>SO<sub>4</sub> filtered and concentrate in vacuo. The crude product was purified by flash chromatography on silica gel using 2:1 petroleum ether:DCM as eluent to give the O-acetylated analogue of **16**. A solution of the latter (1.634 g, 4.79 mmol) in anhydr. THF (50 mL) was added to a suspension of lithium aluminium hydride (0.557 g, 14.66 mmol) in anhydr. THF under a nitrogen atmosphere at 0 °C and refluxed for 16h. A solution 0.1M of hydrochloric acid (200 mL) was added to the reaction mixture under ice cooling and extracted with DCM (3x150 mL), the combined organic layers were dried over Na<sub>2</sub>SO<sub>4</sub>, filtered and concentrated in vacuum to afford **16** as a colourless oil in 86% of yield.

<sup>1</sup>H NMR (400 MHz, CDCl<sub>3</sub>)  $\delta$  1.40–1.44 (m, 1H), 1.46 (s, 18H), 1.57–1.63 (m, 2H), 1.71–1.76 (m, 1H), 2.64 (dd, *J* = 8.2, 5.0 Hz, 1H), 2.84 (bs, 1H), 2.96 (bs, 1H), 5.04 (s, 1H), 6.15 (dd, *J* = 5.6, 2.8 Hz, 1H), 6.26 (dd, *J* = 5.6, 2.8 Hz, 1H), 7.09 (s, 2H).

<sup>13</sup>C NMR (100 MHz CDCl<sub>3</sub>)  $\delta$  30.4 (6C), 33.6, 34.4 (2C), 42.2, 43.7, 45.8, 48.7, 124.1 (2C), 135.5 (2C), 136.4, 137.1, 137.5, 151.6.

IR (KBr, cm<sup>-1</sup>)  $\nu$  3639, 3156, 2957, 1659, 1460.35.

MS (EI) m/z (%): 298 [M<sup>+</sup>, 2], 232 [100], 217 [78], 57 [41].

Anal. calcd for C<sub>21</sub>H<sub>30</sub>O: C 84.51, H 10.13; found: C 84.44, H 10.50.

### 3.5.3 Polymerization experiments

The polymerizations were performed in a round-bottom Schlenk flask containing a stirring bar, at 25 °C and 0.5 atm of ethylene gas pressure. The comonomer **16** (exo/endo 6/1), was pre-treated with TIBA (ratio between TIBA and comonomer = 1.2)

and the solution was stirred for 2 h under N<sub>2</sub> pressure. The proper amounts of toluene (total volume = 100 mL) and comonomer, 1-hexene (ratio between ethylene and 1-hexene = 4.31 or 2.16) or norbornene (ratio between ethylene and norbornene = 0.83) were introduced into the evacuated and N<sub>2</sub> purged flask, then the solution of **16** and TIBA was added. Afterward the flask was filled with 6 mmol of MAO solution, 2 mmol of the *rac*-Et(Ind)<sub>2</sub>ZrCl<sub>2</sub>/MAO based catalyst (ratio between Al and Zr = 3000), and ethylene at 0.5 atm pressure (ratio between ethylene and the comonomer = 6.67 or 13.34), maintained with the correct proportion of N<sub>2</sub> and ethylene gas in the flask. The polymerization was quenched, after 30 min, with ethanol containing a small amount of hydrochloric acid. The precipitated polymers were collected by filtration, repeatedly washed with fresh ethanol and dried in vacuum to constant weight.

### 3.5.4 Polymer characterization

#### <sup>13</sup>C NMR analysis

For <sup>13</sup>C NMR, about 100 mg of polymers were dissolved in C<sub>2</sub>D<sub>2</sub>Cl<sub>4</sub> in a 10 mm tube. HMDS (hexamethyldisiloxane) was used as internal chemical shift reference. The spectra were recorded on a Bruker NMR AVANCE 400 spectrometer operating at 100.58 MHz (<sup>13</sup>C) in the PFT mode working at 103 °C. The applied conditions were the following: 10 mm probe, 90° pulse angle, 64 K data points, acquisition time 5.56 s, relaxation delay 20 s, 3-4 K transient. Proton broad-band decoupling was achieved with a 1D sequence using bi\_waltz16\_32 power-gated decoupling.

**Table 13:** <sup>13</sup>C NMR assignment of ethylene/1-H/**16** terpolymers.

Carbon	Comonomer	Chemical Shift (ppm)		
		E/1-H/16	E/16	E/1-H
C <sub>dx</sub>	<b>16</b>	149.45	149.45	
C <sub>ax</sub>	<b>16</b>	136.18	136.18	
C <sub>cx</sub>	<b>16</b>	133.95	133.95	
C <sub>bx</sub>	<b>16</b>	121.46	121.46	
C <sub>4x</sub>	<b>16</b>	46.67	46.67	
C <sub>5x</sub>	<b>16</b>	46.27	46.27	
C <sub>2x</sub>	<b>16</b>	45.75	45.75	
C <sub>3x</sub>	<b>16</b>	44.37	44.37	
C <sub>1x</sub>	<b>16</b>	40.07	40.07	
C <sub>7x</sub>	<b>16</b>	37.73	37.73	

$T_{\alpha\beta}$	1-H	35.81		35.81
$C_{ex}$	<b>16</b>	32.46	32.46	
$S_{\alpha\delta}$	1-H	32.23		32.23
4B4	1-H	31.85		31.85
$C_{6x}$	<b>16</b>	28.80	28.80	
$C_{fx}$	<b>16</b>	28.73	28.73	
$S_{\gamma\delta}$	1-H	28.25		28.25
$S_{\alpha\delta} + S_{\gamma\delta}$	<b>16</b>	28.12	28.12	
$S_{\beta\delta}$	<b>16</b>	27.93	27.93	
$S_{\delta\delta}$		27.73	27.73	27.73
3B4	1-H	27.26		27.26
$S_{\beta\delta}$	1-H	25.00		25.00
2B4	1-H	21.18		21.18
1B4	1-H	12.08		12.08

**Table 14:**  $^{13}\text{C}$  NMR assignment of ethylene/N/16 terpolymers.

Carbon	Comonomer	Chemical shift (ppm)		
		<b>E/N/16</b>	<b>E/16</b>	<b>E/N</b>
$C_{dx}$	<b>16</b>	149.45	149.45	
$C_{ax}$	<b>16</b>	136.18	136.18	
$C_{cx}$	<b>16</b>	133.95	133.95	
$C_{bx}$	<b>16</b>	121.46	121.46	
$C_{4x}$	<b>16</b>	46.67	46.67	
$C_{5x}$	<b>16</b>	46.27	46.27	
$C_{2x}$	<b>16</b>	45.75	45.75	
$C_{2/3}$	N			44.60-47.20

C <sub>3x</sub>	<b>16</b>	44.37	44.37	
C <sub>1x</sub>	<b>16</b>	40.07	40.07	
C <sub>1/4</sub>	<b>N</b>			38.60-40.40
C <sub>7x</sub>	<b>16</b>	37.73	37.73	
C <sub>ex</sub>	<b>16</b>	32.46	32.46	-
C <sub>7</sub>	<b>N</b>			30.40-31.60
C <sub>6x</sub>	<b>16</b>	28.80	28.80	
C <sub>f</sub>	<b>16</b>	28.73	28.73	-
C <sub>5/6</sub>	<b>N</b>			26.21-29.66
S <sub>αδ</sub>	<b>E</b>	28.20		28.20
S <sub>αδ<sup>+</sup></sub> -S <sub>γδ</sub>	<b>E</b>	28.12	28.12	28.07-28.12
S <sub>βδ<sup>+</sup></sub>	<b>E</b>	27.93	27.93	27.95
S <sub>δδ<sup>+</sup></sub>	<b>E</b>	27.80		27.80
S <sub>δ<sup>+</sup>δ<sup>+</sup></sub>	<b>E</b>	27.73	27.73	27.73

On the basis of the proposed assignments, the **16** contents in the produced polymers was calculated by the following equations:

$$\text{mol\%I}_{16} = \frac{I_{16}}{I_{16} + I_{N} + I_{E}} \times 100$$

$$IN_{16} = IN_{16} / (IN_{16} + IN + IE)$$

Where

$$\bar{I}_{16} = I_{7x}$$

in which only the *exo* signal of enchainned **16** carbons not (partially) overlapped with **N** signals is considered, and

$$IN = \frac{1}{2}(I_7 + \frac{1}{2}I_{1/4} + \frac{1}{2}I_{2/3}) \quad (4S)$$

where I<sub>7</sub>, I<sub>1/4</sub>, I<sub>2/3</sub> are the total area of peaks from 30.40 to 31.60 ppm, from 38.60 to 40.40 ppm, and from 44.60 to 47.20 ppm, respectively, and

$$IE = \frac{1}{2}(IE' - 2IN - 7IN_{16})$$

where IE' is the total area of peaks from 29.40 to 27.40 ppm.

#### *DSC analysis*

Melting and crystallization behaviour of the synthesized terpolymers was analysed by differential scanning calorimetry (DSC) using a Mettler DSC 821<sup>e</sup> instrument (scanning rate 10 °C min<sup>-1</sup>, under nitrogen). All samples were treated as follows: a first heating run was conducted up to 180 °C, the specimens were then cooled down to -100 °C, and a second heating up to 180 °C was imposed.

#### *TGA analysis*

Thermal stabilities of the prepared terpolymers were investigated under N<sub>2</sub> atmosphere (flow rate 40 mL min<sup>-1</sup>) with a Perkin-Elmer TGA7 analyser in dynamic mode (heating rate 20 °C min<sup>-1</sup>) from 50 up to 700 °C.

### **3.5.5 Blends and films**

#### *Preparation of blends*

Blends made of the additive-free LDPE and the synthesized **E/1-H/16** terpolymers were prepared by melt blending using an internal batch mixer (Brabender W50 EHT Plasti-CorderVR) operating at 130 °C with a rotor speed of 50 rpm for 15 min under N<sub>2</sub>. Blends based on the commercial additive-free COC matrix and containing the **E/N/16** terpolymers were analogously prepared using the following mixing conditions: 200 °C, 50 rpm, 10 min under N<sub>2</sub>. In order to have 500 ppm of dispersed antioxidant into the LDPE or the COC matrix, a typical amount of antioxidant added to stabilize polyolefinic materials, a proper amount of terpolymer was used for each prepared blend, taking into account the specific terpolymer composition. Blends of the COC matrix and **E/N/16** terpolymers containing 250 and 100 ppm of antioxidants moieties were prepared as well. For reference purposes, neat LDPE and COC matrixes and their mixtures with 500 and 2000 ppm of BHT were processed under the conditions used for the blends with macromolecular additives.

#### *Preparation of films*

To ensure correct sampling, thus optimizing reproducibility and reliability of the successive TGA analysis, films with thickness of about 350 μm were obtained from the abovementioned blends by compression moulding with a P 200E semiautomatic laboratory press (Collin GmbH). The compression moulding step was conducted at 150 bar and 160 °C, for the polyethylene-based samples, or 220 °C, for those based on the COC matrix.

#### *TGA analysis*

Thermal and thermo-oxidative stabilities on blends and/or films were tested by thermogravimetric analysis (TGA) performed, respectively, under N<sub>2</sub> or O<sub>2</sub> atmosphere, using a Perkin-Elmer TGA7 analyser. TGA measurements were carried out both in dynamic and isothermal conditions. In the dynamic mode (heating rate 20 °C min<sup>-1</sup>), the

explored temperature range was 50-700 °C. Isothermal experiments were carried out to determine the oxygen induction time (OIT) at 180 °C for LDPE-based samples, and at 180 °C and 220 °C for COC-based counterparts. Operative details are as follows: the furnace temperature was rapidly increased to reach the chosen temperature under N<sub>2</sub> atmosphere; after 10 min the purge gas was switched to oxygen to start the OIT measurement (considering t<sub>0</sub> the instant in which oxygen enters the instrument furnace). To guarantee optimal comparison and reproducibility of the OIT experimental results, the isothermal measurements were carried out on film specimens with the same weight and surface area exposed to the oxygen atmosphere.

### *Thermo-ageing tests*

Thermo-ageing tests in air were carried out by maintaining film specimens (2 x 4 cm) into a thermostated oven at 70 ± 1 °C for 77 days. During samples storage the evolution of carbonyl groups was monitored by means of Fourier transform infrared spectroscopy in attenuated total reflectance mode (ATR-FTIR) operating with a Perkin-Elmer Spectrum 200 spectrometer and recording spectra in absorbance mode in the wave number range 4000-e400 cm<sup>-1</sup> (16 scans, resolution 1 cm<sup>-1</sup>). Before determining the carbonyl index, the baseline was corrected by an adaptive fit software, the absorbance normalized between 0 and 1, and the curves superimposed at 2010 cm<sup>-1</sup>.<sup>172,173</sup>

## **3.6 References**

- (1) PlasticsEurope. *Plastic - the Facts 2016*; 2016.
- (2) Billingham, N. C. *Mater. Sci. Technol.* **2013**, 469–507.
- (3) Folarin, O. M.; Sadiku, E. R. *Int. J. Phys. Sci.* **2011**, 6, 4323–4330.
- (4) Al-Malaika, S. *Compr. Polym. Sci. Suppl.* **1989**, 6, 539–578.
- (5) Vulic, I.; Vitarelli, G.; Zenner, J. M. *Polym. Degrad. Stab.* **2002**, 78 (1), 27–34.
- (6) Dopico-García, M. S.; López-Vilariño, J. M.; González-Rodríguez, M. V. *J. Agric. Food Chem.* **2007**, 55, 3225–3231.
- (7) *Oxidative Stabilization of Polymers*; Shlyapnikov, Y. A., Kiryuskin, S. G., Mar'in, A. P., Eds.; Bristol, PA, 1996.
- (8) Li, C.; Wang, J.; Ning, M.; Zhang, H. *J. Appl. Polym. Sci.* **2012**, 124, 4127–4135.
- (9) Wang, X.; Wang, B.; Song, L.; Wen, P.; Tang, G.; Hu, Y. *Polym. Degrad. Stab.* **2013**, 98 (9), 1945–1951.
- (10) Gray, R. L.; Lee, R. E. *J. Vinyl Addit. Technol.* **1998**, 4 (3), 189–196.
- (11) Haider, N.; Karlsson, S. *Polym. Degrad. Stab.* **1999**, 64, 321–328.
- (12) Pospisil, J. *Die Angew. Mackromolekulare Chemie* **1988**, 158/159, 221–231.

- (13) Dubin, P. L.; Leonard, W. J. *Plast. Eng.* **1977**, 33 (10), 29.
- (14) Starnes, W. H. J.; Patton, T. L. Allyl phenols. U.S. Patent 3,526,668, September 1, 1970.
- (15) Starnes, W. H. J. Polyolefins stabilized with alkenyl phenols. U.S. Patent 3,635,885, January 18, 1972.
- (16) Starnes, W. H. J. Synthesis of hindered alkenyl phenols. U.S. Patent 3,644,539, February 22, 1972.
- (17) Starnes, W. H. J. Hindered alkenyl phenols form quinone methide. U.S. Patent 3,660,505, May 2, 1972.
- (18) Parker, D. K. Process for production of 2,6-di-tert-alkenyl phenols. U.S. Patent 4,366,331, December 28, 1982.
- (19) Malshe, V. C.; Elango, S.; Rane, S. *J. Appl. Polym. Sci.* **2006**, 100 (4), 2649–2651.
- (20) Sabaa, M. W.; Madkour, T. M.; Yassin, A. A. *Polym. Degrad. Stab.* **1988**, 22, 195–203.
- (21) Sabaa, M. W.; Madkour, T. M.; Yassin, A. A. *Polym. Degrad. Stab.* **1988**, 22, 205–222.
- (22) Oh, D. R.; Kim, H.; Lee, N.; Chae, K. H.; Kaang, S.; Lee, M. S.; Kim, T. H. *Bull. Korean Chem. Soc.* **2001**, 22 (6), 629–632.
- (23) Xue, B.; Ogata, K.; Toyota, A. *Polym. Degrad. Stab.* **2008**, 93 (2), 347–352.
- (24) Xue, B.; Ogata, K.; Toyota, A. *Des. Monomers Polym.* **2009**, 12, 69–81.
- (25) Fertig, J.; Goldberg, A. I.; Skoultchi, M. *J. Appl. Polym. Sci.* **1966**, 10, 663–672.
- (26) Patton, T. L.; Horeczy, J. T. Alkenyl hindered phenol and a copolymer of an alkenyl phenol and a monoolefin. U.S. Patent 3,477,991, November 11, 1969.
- (27) Mullins, M. J.; Soto, J.; Nickias, P. N. Incorporation of functionalized comonomers in polyolefins. U.S. Patent 6,166,161, December 26, 2000.
- (28) Iwata, T.; Sasaki, J. Stabilized polyolefin and process for the preparation thereof. CA Patent 876796, July 27, 1971.
- (29) Braun, D.; Meier, B. *Die Makromol. Chemie* **1974**, 791–810.
- (30) Layer, R. W. Norbornene polymers containing bound antioxidant. EP Patent 0048439, March 31, 1982.
- (31) Kline, R. H. Antioxidants and age resistant polymeric compositions. U.S. Patent 3,714,122, January 30, 1973.
- (32) Kline, R. H. 2,6-di-tert-alkyl-4-vinylphenols as polymerizable antioxidants. U.S.



- Patent 4,097,464, June 27, 1978.
- (33) Kline, R. H. Age resistors and age resistant polymeric compositions. U.S. Patent 4,152,319, May 1, 1979.
- (34) Grosso, P.; Vogl, O. *J. Macromol. Sci. Part A Chem.* **1986**, 23 (9), 1041–1056.
- (35) Grosso, P.; Vogl, O. *J. Macromol. Sci. Part A - Chem.* **1986**, 23 (11), 1299–1313.
- (36) Grosso, P.; Vogl, O. *Polym. Bull.* **1985**, 14, 245–250.
- (37) Dickstein, W.; Vogl, O. *J. Macromol. Sci. Part A - Chem.* **1985**, 22 (4), 387–402.
- (38) Costanzi, S.; Gussoni, D.; Pallini, L. Process of co(polymerization) of alpha-olefins in the presence of stabilizers. EP Patent 0255181, February 3, 1988.
- (39) Bartus, J.; Simonsick, W. J.; Vogl, O. *J. Macromol. Sci. Part A* **1999**, 36 (3), 355–371.
- (40) Stoeber, L.; Sustic, A.; Simonsick, W. J.; Vogl, O. *J. Macromol. Sci. Part A* **2000**, 37 (9), 943–970.
- (41) Vogl, O.; Albertsson, A. C.; Janovic, Z. *Polymer (Guildf)*. **1985**, 26, 1288–1296.
- (42) Chmela, S.; Hrdlovic, P.; Manasek, Z. *Polym. Degrad. Stab.* **1985**, 11, 233–241.
- (43) Wilén, C. In *Antioxidant Polymers: Synthesis, Properties and Applications*; Cirillo, G., Iemma, F., Eds.; John Wiley & Sons, Inc.: Hoboken, NJ, USA, 2012; pp 355–383.
- (44) Wilén, C.; Auer, M.; Näsman, J. H. *Polymer (Guildf)*. **1992**, 33 (23), 5049–5055.
- (45) Iwata, T.; Sasaki, J. Massen auf Basis von stabilisierten alpha-Monoolefinpolymeren und Verfahren zu deren Herstellung. Patent DE 1947590, September 23, 1970.
- (46) Wilén, C.; Auer, M.; Näsman, J. H. *J. Polym. Sci. Part A Polym. Chem.* **1992**, 30 (6), 1163–1170.
- (47) Wilén, C.-E.; Näsman, J. H. *Macromolecules* **1994**, 27, 4051–4057.
- (48) Wilén, C.-E.; Luttkhedde, H.; Hjertberg, T.; Näsman, J. H. *Macromolecules* **1996**, 29 (27), 8569–8575.
- (49) Auer, M.; Nicolas, R.; Rosling, A.; Wilén, C. *Macromolecules* **2003**, 36 (22), 8346–8352.
- (50) Wilén, C.; Auer, M.; Strandén, J.; Näsman, J. H.; Rotzinger, B.; Steinmann, A.; King, R. E.; Zweifel, H.; Drewes, R. *Macromolecules* **2000**, 33 (14), 5011–5026.
- (51) Auer, M.; Nicolas, R.; Vesterinen, A.; Luttkhedde, H.; Wilén, C. *J. Polym. Sci. Part A Polym. Chem.* **2004**, 42, 1350–1355.

- (52) Stehling, U. M.; Malmström, E. E.; Waymouth, R. M.; Hawker, C. J. *Macromolecules* **1998**, *31*, 4396–4398.
- (53) Sacchi, M. C.; Cogliati, C.; Losio, S.; Costa, G.; Stagnaro, P.; Menichetti, S.; Viglianisi, C. *Macromol. Symp.* **2007**, *260*, 21–26.
- (54) Menichetti, S.; Viglianisi, C.; Liguori, F.; Cogliati, C.; Boragno, L.; Stagnaro, P.; Losio, S.; Sacchi, M. C. *J. Polym. Sci. Part A Polym. Chem.* **2008**, *46*, 6393–6406.
- (55) Boragno, L.; Stagnaro, P.; Sosio, S.; Sacchi, M. C.; Menichetti, S.; Viglianisi, C.; Piergiovanni, L.; Limbo, S. *J. Appl. Polym. Sci.* **2012**, *124*, 3912–3920.
- (56) Sacchi, M. C.; Losio, S.; Stagnaro, P.; Mancini, G.; Boragno, L.; Menichetti, S.; Viglianisi, C.; Limbo, S. *Polyolefins J.* **2014**, *1* (1), 1–15.
- (57) Viglianisi, C.; Menichetti, S.; Assanelli, G.; Sacchi, M. C.; Tritto, I.; Losio, S. *J. Polym. Sci. Part A Polym. Chem.* **2012**, *50* (22), 4647–4655.
- (58) Stagnaro, P.; Mancini, G.; Piccinini, A.; Losio, S.; Sacchi, M. C.; Viglianisi, C.; Menichetti, S.; Adobati, A.; Limbo, S. *J. Polym. Sci. Part B Polym. Phys.* **2013**, *51*, 1007–1016.
- (59) Sacchi, M. C.; Losio, S.; Stagnaro, P.; Menichetti, S.; Viglianisi, C. *Macromol. React. Eng.* **2013**, *7*, 84–90.
- (60) Pospisil, J.; Habicher, W. D.; Nešpůrek, S. *Macromol. Symp.* **2001**, *164*, 389–399.
- (61) MacLeay, R. E. Process for producing polymer bound hindered amine light stabilizers. EP 0303281, February 15, 1989.
- (62) MacLeay, R. E. Polymer bound hindered amine light stabilizers. EP 0303987, February 22, 1989.
- (63) MacLeay, R. E.; Myers, T. N. Polymer bound UV stabilizers. U.S. 4,981,914, January 1, 1991.
- (64) Myers, T. N.; MacLeay, R. E. Polymer bound antioxidant stabilizers. EP 0306729, March 15, 1989.
- (65) MacLeay, R. E.; Myers, T. N. Process for preparing polymer bound antioxidant stabilizers. U.S. 4,981,917, January 1, 1991.
- (66) Fu, F. T.; Winter, R. A. E.  $\alpha$ -olefin copolymers containing pendant hindered amine groups. U.S. 4,413,096, November 1, 1983.
- (67) Costanzi, S.; Cassar, L.; Busetto, C.; Neri, C.; Gussoni, D. UV stabilizers for organic polymers. EP 0343717, November 29, 1989.
- (68) Tseng, T.; Tsai, Y.; Lee, J. *Polym. Degrad. Stab.* **1997**, *58* (3), 241–245.
- (69) Zhang, G.; Li, H.; Antensteiner, M.; Chung, T. C. M. *Macromolecules* **2015**, *48*

- (9), 2925–2934.
- (70) Zhang, Y.; Li, H.; Zhang, Y.; Li, Q.; Ma, Z.; Dong, J. Y.; Hu, Y. *Macromol. Chem. Phys.* **2014**, *215* (8), 763–775.
- (71) Rekers, J. W.; Scott, G. Method for preparing polymer bound stabilizers made from non-homopolymerizable stabilizers. U.S. 4,743,657, May 19, 1988.
- (72) Kuczkowski, J. A.; Gillick, J. G. *Rubber Chem. Technol.* **1984**, *57*, 621–651.
- (73) Kline, R. H. Age Resisters and Age Resistant Polymeric Compositions. U.S. Patent 3,767,628, October 23, 1973.
- (74) Meyer, G. E.; Kavchok, R. W.; Naples, F. J. *Rubber Chem. Technol.* **1973**, *46*, 106–114.
- (75) Kanagawa, S.; Miki, T. Elastomer. U.S. Patent 3,993,714, November 23, 1976.
- (76) Stachelek, S. J.; Alferiev, I.; Choi, H.; Chan, C. W.; Zubiate, B.; Sacks, M.; Composto, R.; Chen, I.-W.; Levy, R. J. *J. Biomed. Mater. Res. Part A* **2006**, *78*, 653–661.
- (77) Cain, M. E.; Knight, G. T.; Lewis, P. M.; Saville, B. J. *Rubb. Res. Inst. Malaya* **1969**, *22*, 289–299.
- (78) Al-Malaika, S. *Polym. Degrad. Stab.* **1991**, *34*, 1–36.
- (79) Pike, M.; Watson, W. F. *J. Polym. Sci.* **1952**, *9* (3), 229–251.
- (80) Ayrey, G.; Moore, C. G.; Watson, W. F. *J. Polym. Sci.* **1956**, *19*, 1–15.
- (81) El-Wakil, A. E.-A.; Bakarati, M. A. *J. Appl. Polym. Sci.* **2011**, *119*, 2461–2467.
- (82) El-Wakil, A. A. *Polym. Plast. Technol. Eng.* **2007**, *46*, 661–666.
- (83) Munteanu, D. *Polym. Degrad. Stab.* **1991**, *34*, 295–307.
- (84) Al-Malaika, S. *Adv. Polym. Sci.* **2004**, *169*, 121–150.
- (85) Scott, G.; Chakraborty, K. B.; Tavakoli, S. M. In *Advances in Elastomers and Rubber Elasticity*; Lal, J., Mark, J. E., Eds.; Springer: Boston, MA, USA, 1986; pp 189–196.
- (86) Sirimevan Kularatne, K. W.; Scott, G. *Eur. Polym. J.* **1978**, *14* (2), 835–843.
- (87) Scott, G. Process for preparing oxidatively-stable polymers by reaction with antioxidant in the presence of free radical. U.S. 4,213,892, July 22, 1980.
- (88) Scott, G. Process for preparing oxidatively-stable polymers. U.S. 4,354,007, October 12, 1982.
- (89) Al-Malaika, S.; Honggokusumo, S.; Scott, G. *Polym. Degrad. Stab.* **1986**, *16*, 25–

34.

- (90) Al-Ghonamy, A. I.; Barakat, M. A. *Int. J. Polym. Sci.* **2010**, 7 pages.
- (91) Samantarai, S.; Mahata, D.; Nag, A.; Nando, G. B.; Das, N. C. *Rubber Chem. Technol.* **2017**, <https://doi.org/10.5254/rct.17.83728>.
- (92) Gao, X.; Hu, G.; Qian, Z.; Ding, Y.; Zhang, S.; Wang, D.; Yang, M. *Polymer (Guildf)*. **2007**, *48* (25), 7309–7315.
- (93) Lei, H.; Huang, G.; Weng, G. *J. Macromol. Sci. Part B Phys.* **2013**, *52*, 84–94.
- (94) Bhunia, K.; Sablani, S. S.; Tang, J.; Rasco, B. *Compr. Rev. Food Sci. Food Saf.* **2013**, *12*, 523–545.
- (95) Garcia, R. S.; Silva, A. S.; Cooper, I.; Franz, R.; Paseiro Losada, P. *Trends Food Sci. Technol.* **2006**, *17*, 354–366.
- (96) Arvanitoyannis, I. S.; Bosnea, L. *Crit. Rev. Food Sci. Nutr.* **2004**, *44*, 63–76.
- (97) Jackson, R. A.; Oldland, S. R. D.; Pajaczkowski, A. *J. Appl. Polym. Sci.* **1968**, *12*, 1297–1309.
- (98) Ferrara, G.; Bertoldo, M.; Scoponi, M.; Ciardelli, F. *Polym. Degrad. Stab.* **2001**, *73*, 411–416.
- (99) Brandsch, J.; Mercea, P.; Piringer, O. In *Plastic Packaging Materials for Food: Barrier Function, Mass Transport, Quality Assurance, and Legislation*; Piringer, O. G., Baner, A. L., Eds.; Weinheim, Germany, 2000.
- (100) Goydan, R.; Schwoppe, A. D.; Reid, R. C.; Cramer, G. *Food Addit. Contam.* **1990**, *7*, 323–337.
- (101) Jickells, S. M.; Gramshaw, J. W.; Castle, L.; Gilbert, J. *Food Addit. Contam.* **1992**, *9*, 19–27.
- (102) Beldi, G.; Pastorelli, S.; Franchini, F.; Simoneau, C. *Food Addit. Contam. Part A* **2012**, *29*, 836–845.
- (103) Garde, J. A.; CatalÁ, R.; Gavara, R.; Hernandez, R. J. *Food Addit. Contam.* **2001**, *18*, 750–762.
- (104) Reinas, I.; Oliveira, J.; Pereira, J.; Machado, F.; Poças, M. F. *Food Control* **2012**, *28*, 333–337.
- (105) Alin, J.; Hakkarainen, M. *J. Agric. Food Chem.* **2011**, *59*, 5418–5427.
- (106) Alin, J.; Hakkarainen, M. *J. Appl. Polym. Sci.* **2010**, *118*, 1084–1093.
- (107) Dopico-Garcia, M. S.; López-Vilarino, J. M.; González-Rodríguez, M. V. *J. Chromatogr. A* **2003**, *1018*, 53–62.

- (108) Jeon, D. H.; Park, G. Y.; Kwak, I. S.; Lee, K. H.; Park, H. J. *LWT* **2007**, *40*, 151–156.
- (109) Linssen, J. P. H.; Reitsma, J. C. E.; Cozijnsen, J. L. *Packag. Technol. Sci.* **1998**, *11*, 241–245.
- (110) Lundback, M.; Hedenqvist, M. S.; Mattozzi, A.; Gedde, U. W. *Polym. Degrad. Stab.* **2006**, *91*, 1571–1580.
- (111) Alin, J.; Hakkarainen, M. *Polym. Degrad. Stab.* **2012**, *97*, 1387–1395.
- (112) Bertoldo, M.; Ciardelli, F. *Polymer (Guildf)*. **2004**, *45*, 8751–8759.
- (113) Aaltonen, P.; Fink, G.; Löfgren, B.; Seppälä, J. *Macromolecules* **1996**, *29*, 5255–5260.
- (114) Atiqullah, M.; Tinkl, M.; Pfaendner, R.; Akhtar, M. N.; Hussain, I. *Polym. Rev.* **2010**, *50*, 178–230.
- (115) Burton, G. W.; Doba, T.; Gabe, E. J.; Hughes, L.; Lee, F. L.; Prasad, L.; Ingoldo, K. U. *J. Am. Chem. Soc.* **1985**, *107*, 7053–7065.
- (116) Enes, R. F.; Tomé, A. C.; Cavaleiro, J. A. S.; Amorati, R.; Fumo, M. G.; Pedulli, G. F.; Valgimigli, L. *Chem. - A Eur. J.* **2006**, *12*, 4646–4653.
- (117) Hagihara, H.; Tsuchihara, K.; Takeuchi, K.; Murata, M.; Ozaki, H.; Shiono, T. *J. Polym. Sci. Part A Polym. Chem.* **2004**, *42*, 52–58.
- (118) Richardson, M. B.; Williams, S. J. *Beilstein J. Org. Chem.* **2013**, *9*, 1807–1812.
- (119) Attanasi, O. A.; Filippone, P.; Balducci, S. *Gazz. Chim. Ital.* **1991**, *121*, 487–489.
- (120) Ruß, A. S.; Vinken, R.; Schuphan, I.; Schmidt, B. *Chemosphere* **2005**, *60*, 1624–1635.
- (121) Huffman, J. W.; Miller, J. R. A.; Liddle, J.; Yu, S.; Thomas, B. F.; Wiley, J. L.; Martin, B. R. *Bioorganic Med. Chem.* **2003**, *11*, 1397–1410.
- (122) Vol'eva, V. B.; Prokof'eva, T. I.; Belostotskaya, I. S.; Komissarova, N. L.; Gorbunov, D. B.; Kurkovskaya, L. N. *Russ. J. Org. Chem.* **2011**, *47*, 1310–1312.
- (123) Huang, Z.; Cui, Q.; Xiong, L.; Wang, Z.; Wang, K.; Zhao, Q.; Bi, F.; Wang, Q. *J. Agric. Food Chem.* **2009**, *57*, 2447–2456.
- (124) Nevrekar, N. B.; Sawardekar, S. R.; Pandit, T. S.; Kudav, N. . *Chem. Ind.* **1983**, *7*, 206–207.
- (125) Ohkatsu, Y.; Nishiyama, T. *Sekiyu Gakkaishi* **1998**, *41*, 251–257.
- (126) Bordwell, F. G.; Cheng, J.-P. *J. Am. Chem. Soc.* **1991**, *113*, 1736–1743.
- (127) Lucarini, M.; Pedrielli, P.; Pedulli, G. F.; Cabiddu, S.; Fattuoni, C. *J. Org. Chem.* **1996**, *61*, 9259–9263.

- (128) Wang, X.; Zhao, T.; Yang, B.; Li, Z.; Cui, J.; Dai, Y.; Qiu, Q.; Qiang, H.; Huang, W.; Qian, H. *Bioorg. Med. Chem.* **2015**, *23*, 132–140.
- (129) Wakeham, R. J.; Taylor, J. E.; Bull, S. D.; Morris, J. A.; Williams, J. M. *J. Org. Lett.* **2013**, *15*, 702–705.
- (130) Nishinaga, A.; Shimizu, T.; Toyoda, Y.; Matsuura, T.; Hirotsu, K. *J. Org. Chem.* **1982**, *47*, 2278–2285.
- (131) Huang-Minlon, B. *J. Am. Chem. Soc.* **1946**, *68*, 2487–2488.
- (132) Huang-Minlon, B. *J. Am. Chem. Soc.* **1949**, *71*, 3301–3303.
- (133) Kappe, T.; Aigner, R.; Roschger, P.; Schnell, B.; Stadlbauer, W. *Tetrahedron* **1995**, *51*, 12923–12928.
- (134) Vedejs, E. *Org. React.* **1975**, *22*, 401–422.
- (135) Horie, K.; Báron, M.; Fox, R. B.; He, J.; Hess, M.; Kahovec, J.; Kitayama, T.; Kubisa, P.; Maréchal, E.; Mormann, W.; Stepto, R. F. T.; Tabak, D.; Vohlídal, J.; Wilks, E. S.; Work, W. J. *Pure Appl. Chem.* **2004**, *76*, 889–906.
- (136) Koning, C.; Van Duin, M.; Pagnouille, C.; Jerome, R. *Prog. Polym. Sci.* **1998**, *23*, 707–757.
- (137) Teng, J.; Otaigbe, J. U.; Taylor, E. P. *Polym. Eng. Sci.* **2004**, *44*, 648–659.
- (138) Orr, C. A.; Adediji, A.; Hirao, A.; Bates, F. S.; Macosko, C. W. *Macromolecules* **1997**, *30*, 1243–1246.
- (139) Lyu, S.-P.; Cernohous, J. J.; Bates, F. S.; Macosko, C. W. *Macromolecules* **1999**, *32*, 106–110.
- (140) Oyama, H. T.; Ougizawa, T.; Inoue, T.; Weber, M.; Tamaru, K. *Macromolecules* **2001**, *34*, 7017–7024.
- (141) Yin, Z.; Koulic, C.; Pagnouille, C.; Jérôme, R. *Macromolecules* **2001**, *34*, 5132–5139.
- (142) Ibuki, J.; Piyada, C.; Chiba, T.; Ougizawa, T.; Inoue, T.; Weber, M.; Koch, E. *Polymer (Guildf)*. **1999**, *40*, 647–653.
- (143) Charoensirisomboon, P.; Chiba, T.; Solomko, S. I.; Inoue, T.; Weber, M. *Polymer (Guildf)*. **1999**, *40*, 6803–6810.
- (144) Charoensirisomboon, P.; Inoue, T.; Weber, M. *Polymer (Guildf)*. **2000**, *41*, 4483–4490.
- (145) Pernot, H.; Baumert, M.; Court, F.; Leibler, L. *Nat. Mater.* **2002**, *1*, 54–58.
- (146) Jones, T. D.; Macosko, C. W.; Moon, B.; Hoye, T. R. *Polymer (Guildf)*. **2004**, *45*,

- 4189–4201.
- (147) Villalpando-Olmos, J.; Sánchez-Valdes, S.; Yáñez-Flores, I. G. *Polym. Eng. Sci.* **1999**, *39*, 1597–1603.
- (148) Evenson, S. A.; Fail, C. A.; Badyal, J. P. S. *J. Phys. Chem. B* **2000**, *104*, 10608–10611.
- (149) Dorn, I. T.; Neumaier, K. R.; Tampé, R. *J. Am. Chem. Soc.* **1998**, *120*, 2753–2763.
- (150) Vidal, T.; Petit, A.; Loupy, A.; Gedye, R. N. *Tetrahedron* **2000**, *56*, 5473–5478.
- (151) Jeong, I.-Y.; Lee, W. S.; Goto, S.; Sano, S.; Shiro, M.; Nagao, Y. *Tetrahedron* **1998**, *54*, 14437–14454.
- (152) Tritto, I.; Boggioni, L.; Ferro, D. R. *Coord. Chem. Rev.* **2006**, *250*, 212–241.
- (153) Li, X.; Hou, Z. *Coord. Chem. Rev.* **2008**, *252*, 1842–1869.
- (154) Radhakrishnan, K.; Sivaram, S. *Macromol. Rapid. Commun.* **1998**, *19*, 581–584.
- (155) Goretzki, R.; Fink, G. *Macromol. Rapid Commun.* **1998**, *19*, 511–515.
- (156) Goretzki, R.; Fink, G. *Macromol. Chem. Phys.* **1999**, *200*, 881–886.
- (157) Wendt, R. A.; Fink, G. *Macromol. Chem. Phys.* **2000**, *201*, 1365–1373.
- (158) Wendt, R. A.; Fink, G. *Macromol. Chem. Phys.* **2002**, *203*, 1071–1080.
- (159) Wendt, R. A.; Angermund, K.; Jensen, V.; Thiel, W.; Fink, G. *Macromol. Chem. Phys.* **2004**, *205*, 308–318.
- (160) Arcadi, A.; Marinelli, F.; Bernocchi, E.; Cacchi, S.; Ortari, G. *J. Organomet. Chem.* **1989**, *368*, 249–256.
- (161) Roberts, R. S. *J. Comb. Chem.* **2005**, *7*, 21–32.
- (162) Kaminsky, W.; Bark, A.; Arndt, M. *Makromol. Chemie. Macromol. Symp.* **1991**, *47*, 83–93.
- (163) Bergstrom, C. H.; Starck, P. G.; Seppa, J. V. *J. Appl. Polym. Sci.* **1998**, *67*, 385–393.
- (164) Bergstrom, C. H.; Ruotoistenmaki, J.; Aitola, E. T.; Seppa, J. V. *J. Appl. Polym. Sci.* **2000**, *77*, 1108–1117.
- (165) Blaine, R. L.; Lundgren, C. J.; Harris, M. B. *Oxidative Behavior of Materials by Thermal Analytical Techniques*; Riga, A. T., Patterson, G. H., Eds.; American Society for Testing and Materials: West Conshohocken (USA), 1997.
- (166) Chang, T. C.; Yu, P. Y.; Hong, Y. S.; Wu, T. R.; Chiu, Y. S. *Polym. Degrad. Stab.* **2002**, *77*, 29–34.

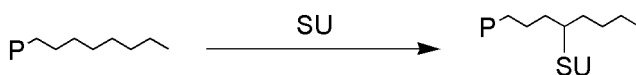
- (167) Tocháček, J. *Polym. Degrad. Stab.* **2004**, *86*, 385–389.
- (168) Boersma, A. *Polym. Degrad. Stab.* **2006**, *91*, 472–478.
- (169) TOPAS - Cyclic Olefin Copolymers  
[http://www.topas.com/sites/default/files/files/TOPAS\\_Brochure\\_E\\_2014\\_06\(1\).pdf](http://www.topas.com/sites/default/files/files/TOPAS_Brochure_E_2014_06(1).pdf).
- (170) Tritto, I.; Marestin, C.; Boggioni, L.; Zetta, L.; Provasoli, A.; Ferro, D. R. *Macromolecules* **2000**, *33*, 8931–8944.
- (171) Tritto, I.; Boggioni, L.; Jansen, J. C.; Thorshaug, K.; Sacchi, M. C.; Ferro, D. R. *Macromolecules* **2002**, *35*, 616–623.
- (172) Nakade, K.; Nagai, Y.; Ohishi, F. *Polym. Degrad. Stab.* **2010**, *95*, 2654–2658.
- (173) Nagle, D. J.; George, G. A.; Rintoul, L.; Fredericks, P. M. *Vib. Spectrosc.* **2010**, *53*, 24–27.



## 4. Free Radical grafting of reactive antioxidants on polyethylene

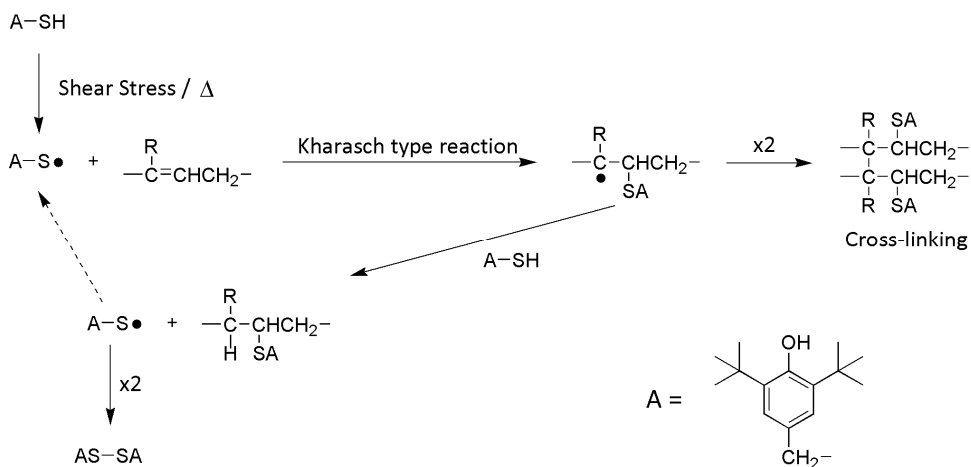
### 4.1 Introduction

As already mentioned in section 3.1 one of the possible ways for the stabilization of plastics against thermo-oxidative stress is the direct linking of traditional antioxidant (AO) moieties on the polymer chain through grafting reactions. Indeed, this method allows for chemical bonding of the AO on the virgin polymer that has to be stabilized (Scheme 1).



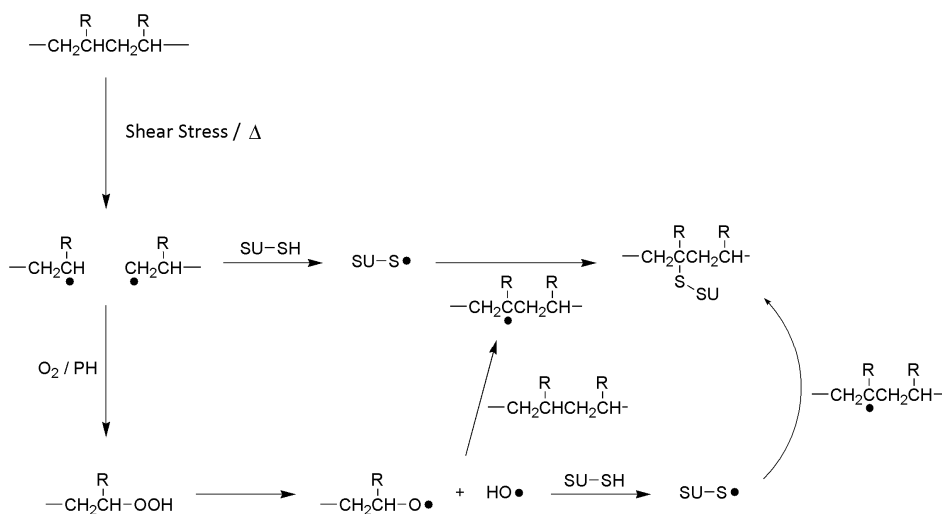
**Scheme 1:** P=polymer; SU=Stabilizing Unit.

Using this method, the stabilizing moiety is chemically linked to the polymer backbone and then it cannot migrate out of the polymer under aggressive extractive environments. This goal of non-migratory antioxidants can therefore be achieved using customary and low-cost processes like extrusion or melt blending, and this process is generally labelled as reactive processing. In-situ melt grafting of reactive (or functional) additives and particularly antioxidants using reactive processing is one of the main research topics of the Polymer Processing and Performance Group of professor S. Al-Malaika at the Aston University in Birmingham (UK), where I have spent about seven months during the third year of my PhD. Their long experience on the use of reactive processing dates back to the early 1970s and proved not only the efficacy of this method in terms of stabilization performance but also allowed a better knowledge of the process from a mechanistic point of view and of all the factors that influence the grafting yields.<sup>1,2</sup> Grafting is a free radical reaction where, after the formation of free radicals on the polymer chain, a reactive modifier is chemically bound directly on the main polymer backbone. For the stabilization of polymers against oxidative degradation it is possible to use, as reactive modifiers, low molecular weight compounds bearing both one or more AO function(s) and one or more reactive function(s) able to link with the polymer chain. These molecules are generally labelled as reactive antioxidants (rAOs). The antioxidant function is generally based on traditional antioxidants like hindered phenols or amines while reactive functions are those able to take part in a radical reaction like thiols or maleimides. Early works of in-situ melt grafting of AOs on polymers were done on rubbers due to their ability of giving rise to free radicals during the mastication,<sup>3,4</sup> a shearing process where mechano-scission of polymer chains takes place. Scott and co-workers at Aston University reported the functionalization of rubbers<sup>5</sup> and rubber modified plastics (ABS)<sup>6</sup> with rAOs bearing thiols as reactive functions due to their ability to take part in Kharasch-type radical reactions with double bonds (Scheme 2).



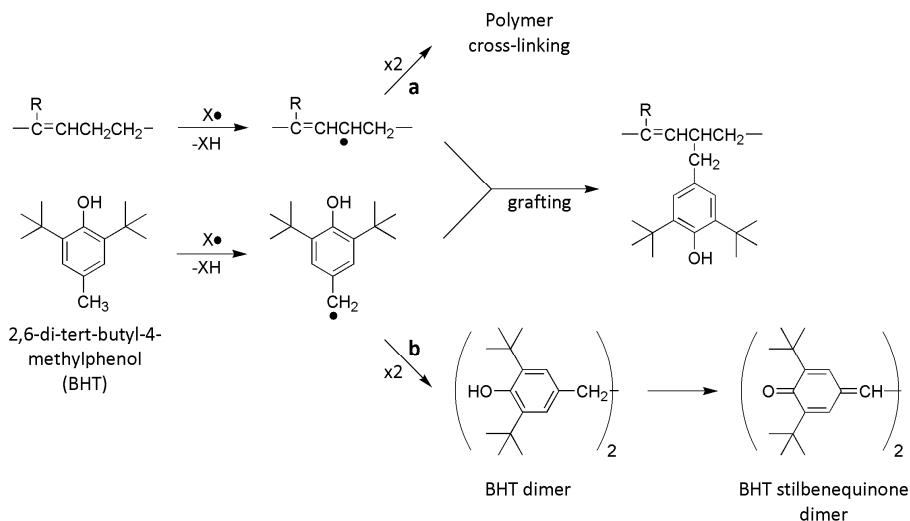
**Scheme 2:** Grafting of rAOs on rubbers through mechanochemical formation of free radicals.<sup>6</sup>

This reaction is possible because the shear stress resulting from mastication is responsible for the formation of thiyl radicals of the reactive antioxidant which are able to react with the double bonds of the polymer. The so-formed macroalkyl radicals can react with each other or generate a new thiyl radical which, in turn, can take part to a new Kharasch-type reaction or dimerizes to the corresponding disulfide. Similar reactions in saturated polymers like polyethylene (PE) and polypropylene (PP) are not feasible due to the lack of unsaturation in their macromolecular structure. However, the grafting of thiol derivatives on polyolefins during mastication is possible through a different mechanism. Indeed, while the binding with rubbers is a one-stage process, in the case of saturated polymers binding can be achieved in two stages (Scheme 3).



**Scheme 3:** PH=saturated polymer; SU=stabilizing unit.<sup>7</sup>

At the beginning, the high level of applied shear leads to the mechanical scission of the polymer chains with the subsequent formation of macroalkyl radicals that, in turn, abstract hydrogen from the thiol antioxidant. The resulting thiyl radical reacts with another macroalkyl radical to form a polymer-bound antioxidant. In the second stage, the residual macroalkyl radicals react with the trace of oxygen present in the chamber to form hydroperoxides which, in turn, decompose to hydroxyl and alkoxy radicals that are subsequently responsible for the formation of new macroalkyl and thiyl radicals and giving rise to more bound antioxidants. However, grafting reactions in saturated polyolefins using mechanochemical processes (for the generation of free radicals) is possible only for antioxidant derivatives bearing highly reactive groups like thiols. In most cases, however, it is necessary to use radical initiators to affect the melt grafting of reactive antioxidants in PE and PP. The most commonly used radical initiators are the peroxides, hydroperoxides, azo compounds and redox systems; UV irradiation can be used also for the generation of free radicals. Kularatne and Scott reported the vinyl grafting of 2,6-di-*tert*-butyl-4-methylphenol (BHT) on natural rubber latex using different radical initiators like benzoyl peroxide, 4,4'-azobis(4-cyanovaleric acid), potassium ferricyanide and the redox couple *tert*-butyl-hydroperoxide/tetraethylenepentamine.<sup>8</sup> Their work proved that the grafting yield depends on several variables: temperature, type of initiator, initiator/reactive antioxidant molar ratio (MR), and the percentage by weight of reactive antioxidant added to the polymer. Best results were obtained with low amounts of antioxidant added (1%) because at higher levels, significant undesirable side reactions took place, involving both the rubber (cross-linking, Scheme 4, a) and the formation of phenolic antioxidant (BHT dimer and stilbenequinone, Scheme 4, b), resulting in a low level of bound AO.



**Scheme 4:** Vinyl grafting of 2,6-di-*tert*-butyl-4-methylphenol (BHT) with natural rubber.<sup>8</sup>

Despite the low levels of bound AO achieved, the grafted polymers showed<sup>8</sup> better performance compared to analogous ones stabilized with conventionally added antioxidants under aggressive conditions of air oven ageing and solvent or detergent extraction. Studies<sup>9</sup> from model compounds demonstrated that the reaction between the rAO and the rubber is not a simple addition of the BHT-derived benzyl radical to the rubber double bonds but results by the radical pairing of a polymer allylic radical with the aforementioned BHT-derived benzyl radical (Scheme 4). The formation of the latter as intermediate is proved by the recovery as major by-products of the dimerized derivative and of the derived stilbenequinone. The cross-linking formation instead is a prove of the allylic radical involvement because the same radical is necessary in order that this process takes place. This paper highlighted that it is possible to graft benzylic antioxidants on rubber and to achieve a better stabilizing performance thanks to the substantivity of the additive despite the low level of grafting. However, the use of a benzyl as reactive group showed several drawbacks like the low efficiency of grafting and the formation of side products, while thiol-based antioxidants generally give high level of adducts, do not cause cross-linking nor do they lead to the formation of coloured by-products. Indeed, the same research group reported the grafting of rAOs bearing thiol groups on different polymers, both unsaturated and saturated: natural rubber,<sup>9,10</sup> acrylonitrile-butadiene-styrene terpolymer,<sup>6</sup> styrene-butadiene,<sup>11,12</sup> nitrile rubber,<sup>13</sup> ethylene-propylene-diene terpolymer,<sup>14</sup> polypropylene,<sup>15,16</sup> polyethylene<sup>17</sup>. However, thiol-based antioxidants too are compromised by side reactions depending on their structure, and some type of radical initiators can lead also to undesired effects like rubber coagulation. Some of the reactive groups suitable for grafting are reported in Figure 1.

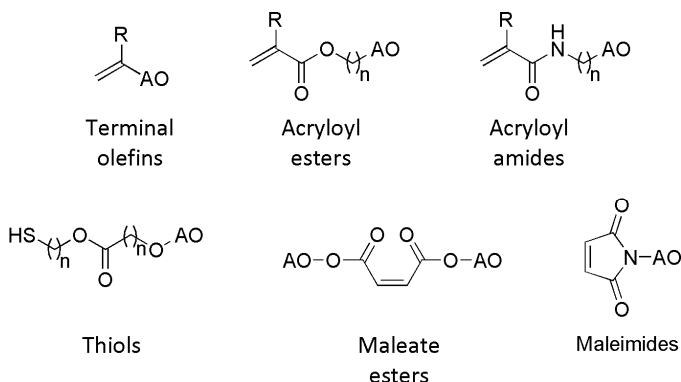
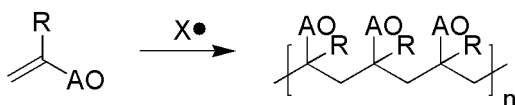


**Figure 1:** Reactive groups for grafting reactions (AO=antioxidant moiety).

It seems reasonable that the grafting mechanism of reactive antioxidants bearing groups like those shown in Figure 1 is similar to the one outlined in Scheme 4, *i.e.* during processing free radicals are generated in the melt both by the shearing forces applied (which cause cleavage of the polymer chains) and as a result of decomposition of free radical generators. Such free radicals can in turn strip hydrogen atoms off the polymer molecule to form the corresponding free radicals on the polymer chain, allowing the reaction with the polymerizable groups of the reactive antioxidant and the

formation of side chains bearing the active moiety.<sup>2</sup> Usually, reactive antioxidants bearing terminal olefins as reactive function are able to graft on saturated polyolefins in the presence of radical initiators but the bound antioxidant yield is generally below 50%.<sup>18,19</sup> Such low level of grafting is a consequence of the predisposition of -CR=CH<sub>2</sub> moiety toward homo-polymerization (Scheme 5) which is one of the main challenges in their grafting reactions .



**Scheme 5:** Homopolymerization of reactive antioxidants (AO) bearing terminal olefins as reactive groups (X•=radical initiator).

As an alternative, Al-Malaika, Scott and coworkers synthesised rAOs bearing non-polymerizable reactive functions, like maleate esters and maleimides (Figure 1), to achieve higher levels of grafting, up to 90 and 75%, respectively.<sup>20,21</sup> Similar results were obtained maintaining a polymerizable group as reactive function but using antioxidants with two (instead of only one) of the just mentioned group. In this way hindered amine light stabilizers (HALS) bearing a double acrylic group (**bis-HALS**) as reactive function achieved a grafting yield close to 100% to polypropylene while the correspondent *mono*-acrylated (**mono-HALS**) remained below 40% of bound antioxidant due to the competitive homo-polymerization process (Figure 2).

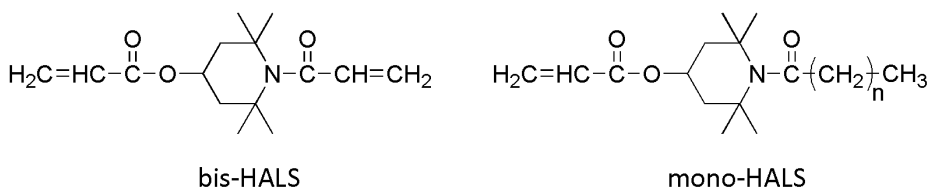
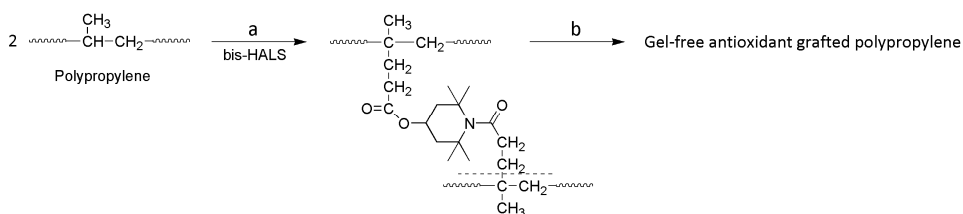


**Figure 2:** *bis*- and *mono*-HALS structures.

The reason for the high binding degree of *bis*-acryloyl HALS has been suggested to occur through the formation, during the initial processing stage, of a cross-linked structure due to the presence of two reactive groups on each of the antioxidant molecules (Scheme 6, a).<sup>21</sup> Further, it was shown that the processing led to a rearrangement, during which the cross-linked structure becomes broken-up, giving rise to a gel-free antioxidant-grafted polymer (Scheme 6, b). The proposed mechanism is explained from two main observations:<sup>21</sup>

- 1) In the first minutes of processing of *bis*-acryloyl HALS there is a sharp increase in the viscosity as demonstrated by the presence of a peak in the measured mixing torque followed by a reduction to torque levels analogous to *mono*-acryloyl HALS. This observation is in accordance with the formation at the beginning of a cross-linked structure that is destroyed with further processing.

- 2) Gel content measurements at different processing times confirmed the initial formation of a cross-linked structure with a high content in antioxidant followed by its decrease.



**Scheme 6:** Grafting on polyolefins with bis-functional reactive antioxidants.

However, it is important to mention that the corresponding HALS derivative functionalized with two methacryloyl groups as reactive functions were found to bind to polypropylene to a much smaller extent (under the same conditions) due to a higher predisposition to homopolymerization of the methacrylates and the lower reactivity of the corresponding radicals toward the polymer.<sup>21</sup> All of these results showed that the grafting process proceeds in competition with other undesirable processes which can be minimised through optimisation by e.g., the correct choice of chemicals, process variables (temperature, screw speed, time), amount of antioxidant, type of initiator, radical initiator/antioxidant molar ratio so as to increase the levels of grafting without altering significantly the properties of the starting polymer, e.g. gel content, morphology and physical properties. Al-Malaika and co-workers have studied thoroughly additional methods for increasing the low grafting efficiency of reactive groups like acryloyl esters and found that the use of specific reactive compounds labelled as coagents allowed a huge enhancement in the grafting yields.<sup>1</sup> These reactive coagents (Figure 3) are polyfunctional compounds (without antioxidant activity) that usually take part to cross-linking reactions in the polymer and this reactivity can be used to facilitate the binding of the reactive antioxidant on the polymer chain through a co-grafting process.

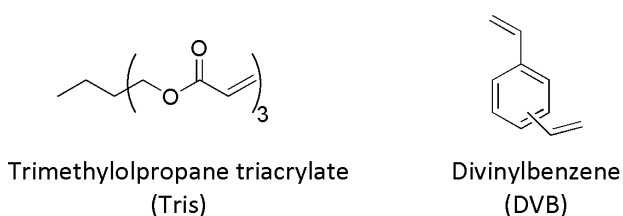


**Figure 3:** Structure of Tris and DVB coagents.

In this way the grafting efficiency on polypropylene of an antioxidant bearing an acryloyl ester as reactive group like 3,5-di-*tert*-butyl-4-hydroxybenzyl acrylate (DBBA, Figure 4) had risen from only 40% to about 90% when trimethylolpropane triacrylate (Tris) was used as coagent in the presence of the radical initiator Trigonox101 (T101).<sup>22</sup>

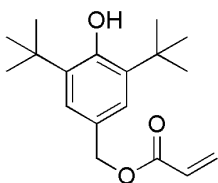
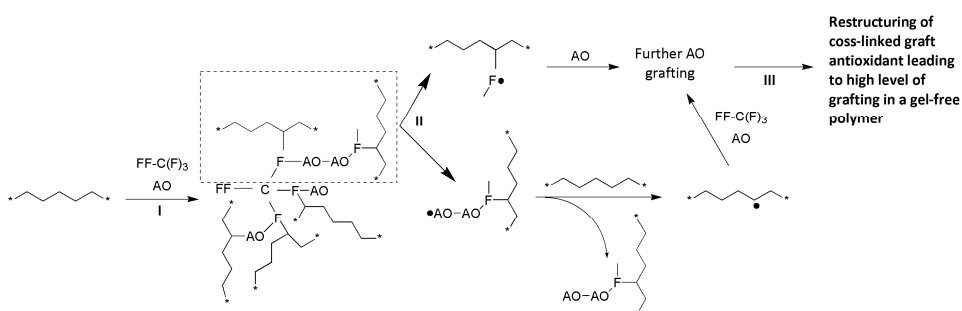


**Figure 4:** 3,5-di-*tert*-butyl-4-hydroxybenzyl acrylate (DBBA).

An in-depth characterization study<sup>22</sup> had shown that in the sample processed without the coagent, the portion of non-bound antioxidant (60%) was fully recovered as the product of antioxidant homopolymerization (Poly-DBBA), highlighting the predominance of this undesired side reaction. Indeed, when Tris was used as a coagent, only 9% of poly-DBBA was recovered. Further,<sup>22</sup> the use of decalin (as a hydrocarbon model for polypropylene) showed that Tris grafts together with the DBBA on the polymer chain, as well as the possible formation of the homopolymer (as side products) derived from Tris and of the copolymer Tris-DBBA. This means that Tris or similar coagents are very effective in the enhancement of grafting efficiency; it is critical however to optimise the processing conditions in order to avoid or minimize undesired side reactions. In addition to optimising the different process variables, e.g. temperature, screw speed, processing time, type of initiator, antioxidant concentration, and initiator/antioxidant molar ratio, it is necessary to use an appropriate coagent for the process at the correct level relative to the AO and the initiator. A mechanism of the grafting process in the presence of coagents was proposed<sup>22</sup> based on the type of side products, studies on the hydrocarbon model and the evolution of the measured torque by the extruder over time. As already seen for the reactive processing without coagents there is a sharp rise in the torque at the beginning followed by a progressive decrease to values similar to those observed in samples processed with only DBBA and T101, and is typical for process showing an initial formation of a transient cross-linked structure followed by its break-up. The overall mechanism comprises three main steps (Scheme 7):



**Scheme 7:** Schematic representation of the grafting mechanism of DBBA (AO) on polyolefins in the presence of Tris ( $FF-C(F)_3$ ).<sup>22</sup>

- I. Polypropylene undergoes a cross-linking process with the formation of a cross-linked structure based on the Tris moiety bearing the DBBA antioxidant; a graft antioxidant copolymer is formed.
- II. Further processing leads to the scission of some of the graft copolymer chains and the consequent rearrangement of the cross-linked structure. In this way new free radicals are then generated on the copolymer allowing further antioxidant grafting. In the example shown (see scheme 7), chain scission processes taking place within the Tris and the DBBA moieties lead to the formation of the corresponding free radicals. The radical derived from Tris is able to directly take part in new grafting reactions with the rAO, while the one derived from DBBA leads, indirectly, to the same result through the formation of new free radicals on the polymer chain.
- III. The continuation of this process allows the full rearrangement of the cross-linked structure yielding a gel-free polymer with a high content of grafted antioxidant.

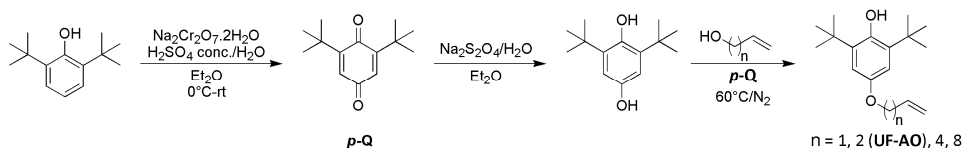
Other reactive additives having different properties were grafted on polymers through reactive processing in order to modify the polymer properties. For example, glycidyl methacrylate (GMA) was grafted on ethylene-propylene diene terpolymer (EPDM) in order to obtain a polymeric compatibilizer for poly(ethylene terephthalate)/EPDM blends.<sup>23</sup> The reactive processing in the presence of the radical initiator alone resulted in a low grafting efficiency (<2%) and its moderate increase consequent to the enhancement of initiator concentration was accompanied by a drastic increase of cross-linking (35%). The latter is the main side reaction that takes place at the expense of the expected additive homopolymerization because of the high reactivity of unsaturated polymers towards cross-linking. The incorporation of Tris as a reactive comonomer allowed a remarkable improvement of GMA grafting yield to about 25% and the cross-linking side reaction was minimized to only 6%. Similarly, the use of coagents like Tris or divinylbenzene (DVB, Figure 3) for the grafting of GMA onto polypropylene confirmed the actual effectiveness of these molecules not only in the increase of grafting efficiency but also in the reduction of undesired side reactions.<sup>24</sup> Indeed, in the presence of these reactive comonomers the grafting takes place using only small amount of radical initiator thus preventing undesired reactions like homopolymerization and polymer chain scission that are common when a high concentration of radical initiator is used.

From this brief introduction it is easy to understand the feasibility and importance in the use of grafting through reactive processing for the immobilization of stabilizers on polyolefins because it allows the direct binding of the additive on the polymer backbone using customary operations like extrusion and a simple treatment of the polymer that has only to be mixed with the reactive antioxidant, the radical initiator and eventually the coagent before processing. Moreover, AO-grafted polymers showed<sup>21</sup> better stabilization performance compared to analogous systems stabilized



with conventionally-added AOs thanks to the substantivity of the polymer-bound stabilizers.

In Florence we have developed polymer-bound antioxidants (see section 3.2) using a completely different methodology, *i.e.* the copolymerization between an antioxidant comonomer and a monomer like ethylene or propylene. This methodology allowed the preparation of polyethylene or polypropylene/antioxidant copolymers suitable as polymeric masterbatches for the stabilization of the correspondent virgin polymers.<sup>25,26</sup> Even if completely different, the two strategies both require the use of a reactive antioxidant bearing both a traditional antioxidant moiety and a reactive function able to take part in polymerization or grafting reactions, respectively. The first rAOs prepared were the alkoxy derivatives of butylated hydroxyanisole (BHA) bearing a terminal alkenyl chain with different length. These compounds were prepared starting from the oxidation of 2,6-di-*tert*-butylphenol to the corresponding *para*-quinone (**p-Q**) and their reduction to 2,6-di-*tert*-butylhydroquinone. The latter was then alkylated (at the less hindered hydroxyl group) using the appropriate  $\alpha,\omega$ -alkenols in the presence of a small amount of **p-Q** (Scheme 8).<sup>27</sup>



**Scheme 8:** Synthetic procedure for **UF-AO** and other polymerizable rAOs.

Four derivatives were prepared bearing an alkyl chain with 1, 2, 4 and 8 methylene units between the oxygen and the terminal double bond, respectively. Each compound showed a different polymerization reactivity and comonomer incorporation; **UF-AO**, n=2, gave the worst results and was therefore not evaluated for its stabilisation performance as a polymeric additive. Terminal olefins are groups able not only to take part in polymerization reactions but also in radical reactions, therefore **UF-AO** is a potentially suitable rAO to use for the immobilization on polymers through both copolymerization and grafting reactions. Indeed, as seen in section 4.1 (Figure 1), several groups are active in grafting reactions, including terminal double bonds which generally show only modest yields of polymer-bound antioxidant.<sup>28,29</sup> Considering that an alkyl chain of 3-4 carbon atoms length between the aromatic ring and the terminal double bond is considered ideal for the grafting process, we decided to examine the suitability of **UF-AO** (n=2) as a graftable AO in polyethylene.

## 4.2 Results and Discussion

### 4.2.1 Characterization of **UF-AO** and grafting on polyethylene (PE)

A crude product of **UF-AO** (n=2), received from University of Florence, was purified by flash column chromatography. Both its synthesis and characterisation has been reported in the literature.<sup>27</sup> The purified **UF-AO**, a yellowish oil, was fully characterized to ascertain its purity and to identify a methodology for detecting and quantifying its

level of grafting on PE. The main fraction of the antioxidant that was used for all of the grafting studies was not completely pure as seen by HPLC-MS analysis where, in addition to the main peak related to **UF-AO** (Exact Mass 276.21), other tiny signals were visible (Figure 5).

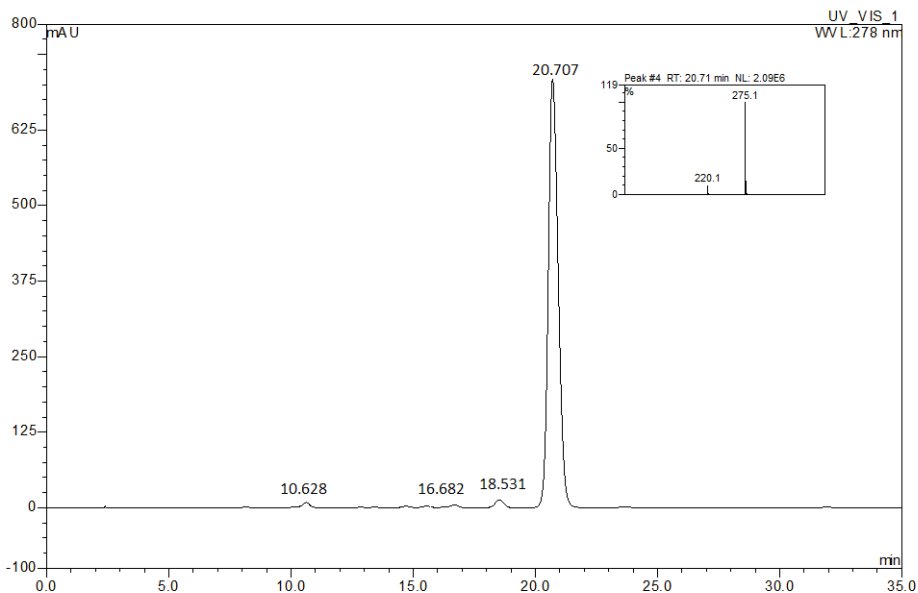


**Figure 5:** HPLC-MS spectrum of **UF-AO**.

The ATR-FTIR spectrum of the flash 'purified' **UF-AO** confirmed the presence of an impurity with an unknown signal at  $1704\text{ cm}^{-1}$  adjacent to that of the olefinic C=C stretching ( $1643\text{ cm}^{-1}$ ) (Figure 6).

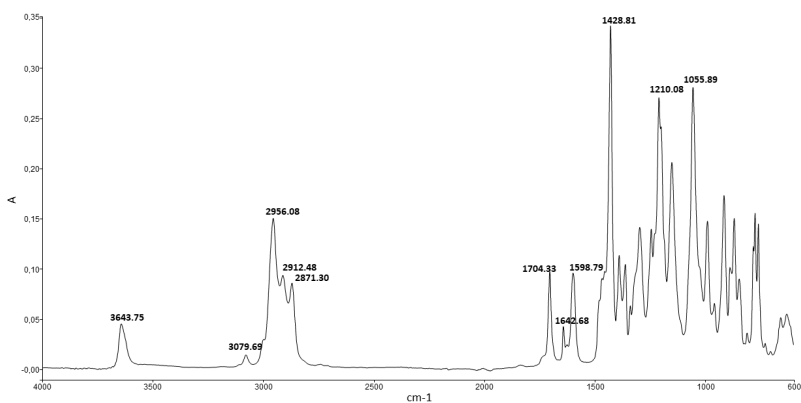


**Figure 6:** ATR-FTIR spectrum of **UF-AO**.

Probably the impurity is a quinonoid-type by-product because the UV spectrum of **UF-AO** in n-hexane solution showed an absorption in the region 400-450 nm (Figure 7), typical of *ortho*-quinones,<sup>30,31</sup> even though the ATR-FTIR absorption peak of the C=O stretching vibration should be below 1700 cm<sup>-1</sup>.<sup>32,33</sup>

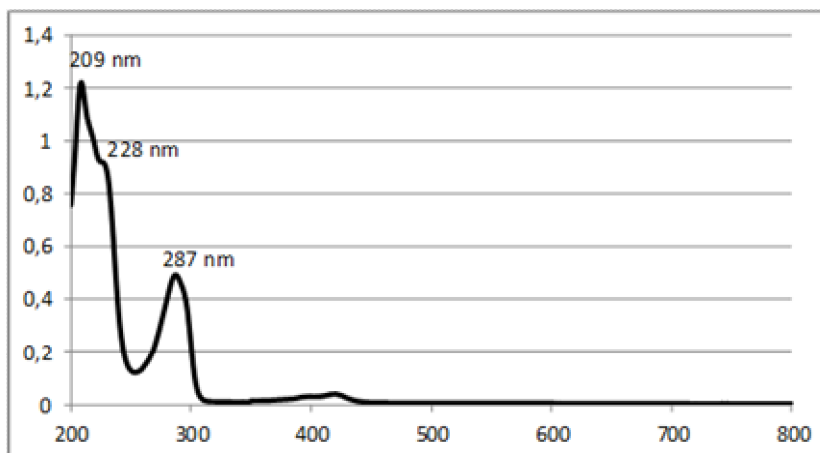


**Figure 7:** UV-Vis spectrum of **UF-AO**.

A small amount of 'totally' pure **UF-AO** was finally prepared where all the 'impurity signals' mentioned above were absent.

#### 4.2.2. Reactive processing of UF-AO in High Density Polyethylene (HDPE)

A counter-rotating conical twin-screw Mini-Haake extruder was used for producing polymer samples containing the antioxidant for subsequent characterisation and testing of performance. About 5 g of HDPE (.7 cm<sup>3</sup>) was used for each processing; the precise sample weight was determined using the following formula,

$$m = V (\text{cm}^3) \times \rho_M (\text{g/cm}^3) \times K$$

where, m=mass of the test material; V=mixer volume;  $\rho_M$ =density of the sample material at ambient temperature; K=non-dimensional coefficient which considers the optimum filling level for different dynamic loads (usually <1).

Combining the mass calculated for the HDPE used (Lupolen 5261Z, **L5261**) with a process of trial and error it was found that the optimal amount of polymer loading was 3.0 g. First attempts of processing were done on the virgin (unstabilized) polymer in order to find the best conditions of temperature, screw speed and processing time that did not cause polymer degradation. Indeed the shear stress has to be sufficient to blend the components of the reaction melt but not too high as to cause significant degradation of the virgin polymer; a process called polymer melt fracture which was clearly evident in the unstabilized polymers from the appearance of the "sharkskin" on the strands of extruded sample (Figure 8).<sup>34</sup>



**Figure 8:** Picture of an extruded virgin unstabilized polymer (**L5261**) showing 'sharkskin' due to melt fracture.

The processing time depends upon the polymer properties and the reactivity of both the rAOs and the radical initiator, and the type of equipment used for the extrusion (efficiency in heating, mixing and applying shear to the melt). In general, processing time is between 2 and 15 minutes depending on the production machinery used; long processing times often cause significant degradation of the polymer. Typical reaction conditions include the exclusion of free molecular oxygen and a processing temperature higher than both the polymer melting point and the decomposition temperature of the free radical generator. Earlier experiments in the Mini-Haake extruder had indicated that best processing conditions for producing sharkskin-free polymer strands are:  $T = 190\text{--}220\text{ }^{\circ}\text{C}$ , screw speed = 40 rpm, overall process time = 8 min. Moreover, the two pressure transducers (at the entrance and exit of the backflow channel), see screws of the Mini-Haake and the backflow channels below Fig. 9, enable the calculation of changes in the relative viscosity during process and give an indication of the relative stability of the different polymer formulation for a quick evaluation.



**Figure 9**

In general, an increase in relative viscosity is an indication of a polymer cross-linking process whereas a drop in this value points to a predominance of chain scission reactions.

Having determined the basic conditions for the polymer extrusion, the next step was to decide on the choice of the radical initiator, the concentration of the AO and the radical initiator/antioxidant molar ratio to be used in the polymer formulation. The choice of a free radical generator depends on both its decomposition temperature ( $T_d$ ) and its half-life ( $t_{1/2}$ ) at that temperature. For grafting reactions, the initiator of choice has its  $T_d$  higher than the melting point ( $T_m$ ) of the polymer. When a polymer with a high melting point is used it is necessary therefore to select a radical initiator which is able to decompose substantially at the processing temperature. The rate of decomposition for radical initiators is generally defined by their half-life ( $t_{1/2}$ ), *i.e.* the time required to reduce the original initiator content at a given temperature by 50%. In general, therefore, an initiator with  $t_{1/2}$  less than that of the total processing time (but not too short in order to allow the reaction to take place) is selected. For the HDPE used in these experiments (Lupolen 5261z, **L5261**) the processing temperature had to be equal to or higher than 180 °C and that the processing time was about 8 minutes, the free radical generator selected was 2,5-dimethyl-2,5-di(*tert*-butylperoxy)hexane (generally labelled as Trigonox®101, **T101**).

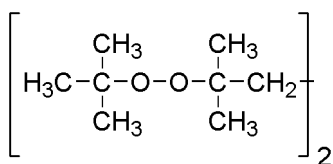


**Figure 10:** Molecular structure of **T101**;  $t_{1/2} = 14\text{s}$  at 190 °C.

As mentioned earlier (Section 4.1) the range of **UF-AO** concentration chosen depends on the purpose of the experiment: for a single grafting/stabilisation process, a typical antioxidant concentration of 0.05-3.0% is used to attach the AO/stabiliser to the polymer chains; for producing a master-batch with further melt blending (letting down/dilution) with the virgin polymer, higher concentrations, typically 4-10% is used. Because the aim of this work was the direct stabilization of the commercial polymer, first attempts were done using a low concentration of 0.05% (w/w) of the **UF-AO** in **L5261** and a low **T101/UF-AO** molar ratio (MR) of 0.03. The composition of the samples of **L5261** processed with **UF-AO** and **T101**, as well as of the reference ones, are presented in Table 1.

**Table 1:** a) **MR** is the molar ratio **T101/UF-AO**; b) Corresponding to the amount of **T101** for a **MR** of **0.03**.

Sample	UF-AO (% w/w)	Irg1076 (% w/w)	T101 (MR) <sup>a</sup>	HDPE (% w/w)
<b>L1</b>	0.05	-	0.03	99.95
<b>L2</b>	0.05	-	-	99.95
<b>L3</b>	-	0.05	0.03	99.95
<b>L4</b>	-	0.05	-	99.95
<b>L5</b>	-	-	1.63x10 <sup>-4</sup> mmol <sup>b</sup>	99.99
<b>NoAdd</b>	-	-	-	100.00

After the extrusion at 190 °C, 40 rpm for 8 min, thin film samples (.150-200 µm thick) were prepared by compression moulding in order to optimize the reproducibility and reliability of successive tests. FT-IR and UV-Vis spectra of each film were done with the aim of understanding the grafting reaction, e.g. if the characteristic absorption peak of **UF-AO** was visible and this will then be usable for evaluating the actual grafting after solvent extraction. As expected, in the FT-IR spectrum of **L5261** samples containing **UF-AO** (**L1** and **L2**), there was no diagnostic signals for the antioxidant to use because all of its characteristic peaks were strongly overlapped by the polymer bands. In contrast, in the polymer sample processed with only **Irg1076** (**L3** and **L4**), the C=O stretching vibration of the antioxidant ester group was clearly visible at 1740 cm<sup>-1</sup>. The UV-Vis spectra of **L1** and **L2** showed also a tiny signal around 287 nm suggesting the presence of the antioxidant albeit too weak to use for quantification. Also in the samples containing **Irg1076** (**L3** and **L4**), the typical absorption of the additive at 279-283 cm<sup>-1</sup> was visible but very faint; it was concluded that an antioxidant concentration of 0.05% was probably too low to use for monitoring purposes.

Indeed, after Oxidative Induction Time (OIT, DSC) measurements at 190 °C it was verified that also in those samples containing 0.05% of the antioxidant, the stabilizing performance was very low and is only slightly above that of both the sample processed without additives (**L6**) and the one with only **T101** (**L5**), see Table 2.

**Table 2:** OIT (DSC) measurement at 190°C of L5261 samples processed (190 °C, 40 rpm, 8 min).

Sample	OIT (min)
L1	1.84
L2	1.99
L3	10.64
L4	2.25
L5	0.43
NoAdd	0.53

However, these preliminary results have highlighted already some important points. The OIT value of **L3** was the best (10.64 min) but it clearly decreased when also **T101** was present (2.25 min) because, as expected, **Irg1076** does not bear any reactive group able to graft on the polymer chain during the extrusion and is depleted by its radical scavenger activity towards the peroxy radicals generated by **T101**. Instead the OIT value of the sample containing only **UF-AO** (1.99 min) was lower than the analogous containing **Irg1076**, but when processed together with **T101** the resulting OIT did not change clearly (1.84 min). This meant that under the conditions used, **UF-AO** was not substantially consumed by the radical scavenger activity of its phenoxyl group and then its olefinic double bond can theoretically take part in a grafting reaction. The extrusion was then repeated using the same processing conditions (190 °C, 40 rpm, 8 min) for samples of **L5261** but using higher antioxidant concentration of 0.5% w/w of the **UF-AO** with different **T101/UF-AO** molar ratios. Reference samples of **L5261** containing 0.5% of **UF-AO** or **Irg1076** were also extruded under the same conditions (see Table 3).

**Table 3:** Samples of **L5261** extruded (190°C, 40 rpm, 8min). a) MR is the molar ratio **T101/UF-AO**.

Sample	UF-AO (% w/w)	Irg1076 (% w/w)	T101 (MR) <sup>a</sup>	HDPE (% w/w)
L-Irg1076	-	0.5	-	99.50
L-UF-AO	0.5	-	-	99.50
UF-AO+T101 0.08	0.5	-	0.08	99.46
UF-AO+T101 0.16	0.5	-	0.16	99.42

<b>UF-AO+T101</b> <b>0.24</b>	0.5	-	0.24	99.40
----------------------------------	-----	---	------	-------

Each sample was submitted to Soxhlet extraction using a solvent like dichloromethane (DCM) that is inert towards the polymer and at the same time it easily solubilizes the antioxidant so as to remove all the unbound additive. Indeed, the extent of grafting is generally determined by detecting and quantifying the persistence, after such solvent extraction procedure, of the antioxidant characteristic absorption peaks using FT-IR or UV-Vis spectroscopic methods. In the case of **UF-AO**, no suitable FT-IR absorption peaks were present while its UV-Vis spectrum could be used diagnostically due to the characteristic absorption at 287 nm (Figure 7). Indeed, in all the samples of **L5261** processed with 0.5% of **UF-AO** and **T101**, the absorption at 287 nm was clearly visible but, after the Soxhlet extraction with DCM, this peak completely disappeared (see UV-Vis spectrum in Figure 11); for simplicity, only sample **T101/UF-AO** MR =0.24 is shown.

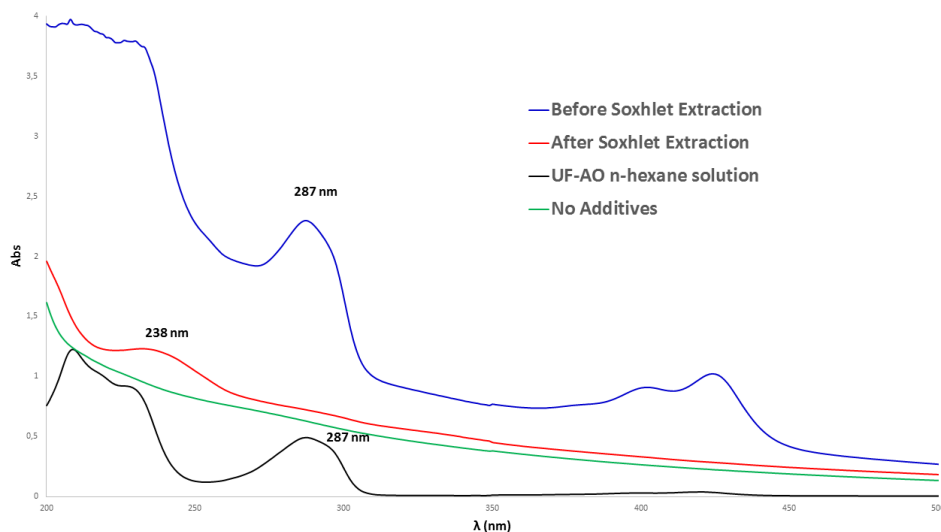


**Figure 11:** UV-Vis spectra of HDPE-UF-AO+T101, M.R.=0.24, film before (blue) and after (red) DCM extraction. For comparison, HDPE (L5261) film without additives (green) and **UF-AO** in hexane (black) are shown.

Apparently, no residual traces of **UF-AO** seemed to be present after the solvent extraction, as well as of the aforementioned impurity due to the disappearance of the absorption between 400 and 450 nm. Indeed, the UV-Vis spectrum of the extracted sample was almost identical to that of the sample of **L5261** processed without any additives (green line), suggesting the failure of the grafting reaction. However, the OIT measurement at 190 °C provided different information (Figure 12). As expected the OITs of **L5261** samples processed with an antioxidant alone (**L-Irg1076** and **L-UF-AO**) decreased after the extraction to values similar to that of the unstabilized polymer



(**NoAdd**) because the added additive is simply blended inside the polymeric matrix and then completely removed by the extraction process. Instead, in the case of **UF-AO+T101** (**MR=0.08, 0.16** and **0.24**) the OIT had only partially decreased passing from the unextracted to the extracted samples, suggesting that at least partially the grafting must have occurred; the presence of a DCM non-extractable AO-bearing 'transformation product' may be inferred from these OIT data and from the UV peak centred at 238 nm (Fig. 11) seen in the film after extraction.

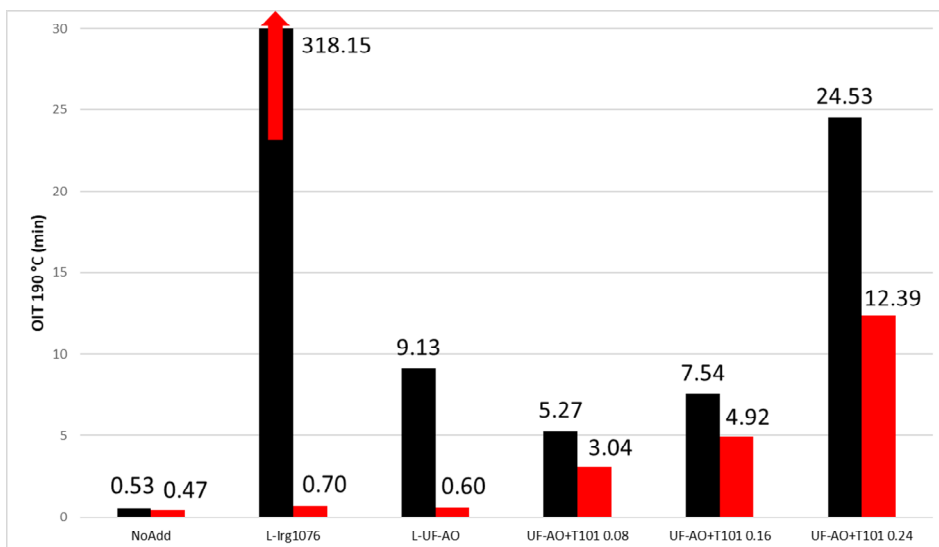


**Figure 12:** OIT values of HDPE (L5261) samples processed at 190 °C; black = unextracted, red = extracted.

Indeed, in the sample **NoAdd** had an OIT of <1 min both before and after extraction; samples with 0.5% Irganox 1076 (**L-Irg1076**) or with UF-AO (**L-UF-AO**; in absence of added peroxide) the values dropped from 318.15 min and 9.13 min to 0.70 min and 0.60 min, respectively, because in both cases all the antioxidants remained unbound and were completely removed from the polymer after Soxhlet extraction. In contrast, samples prepared in the presence of **UF-AO+T101** (**MR=0.08, 0.16** and **0.24**) showed only a partial decrease in their OIT values after the solvent extraction, with OIT values from 5.27, 7.54 and 24.53 min going down to 3.04, 4.92 and 12.39 min, respectively after extraction. The best results were obtained in the sample with a **T101/UF-AO** MR of 0.24 that showed the higher values of OIT (among the **UF-AO/T101** containing samples) both before and after extraction. This is consistent with the previous literature from Al-Malaika and co-workers<sup>23,24,35,36</sup> that had reported a general enhancement in the grafting yields with an increase in the radical initiator/reactive antioxidant MR, albeit at the risk of simultaneously increasing the extent of formation of additive homopolymers and polymer gels due to the ability of radical initiators in facilitating polymer cross-linking. Also, an increase in the processing temperature can enhance the grafting yield because it raises the rate of radical initiators decomposition

and of the subsequent reaction between the generated macroalkyl radical and the reactive antioxidant. However, as for the radical initiator/reactive antioxidant MR, the positive effect of the temperature enhancement on the grafting yields is preserved until a certain point beyond which undesired side reactions like antioxidant homopolymerization prevails (also polymer degradation must be taken into account).

With the aim of increasing the grafting efficiency of **UF-AO** on **L5261**, further extrusion experiments were carried out using sample composition that had given the best results in terms of OIT, *i.e.* a **UF-AO** concentration of 0.5% and a **T101/UF-AO** MR of 0.24, at a higher temperature (220 °C). Also, samples of HDPE (**L5261**) without additives, or containing only **Irg1076** or **UF-AO**, respectively, were extruded at 220 °C and used as references (Table 4).

**Table 4:** Samples of HDPE (**L5261**) extruded (220 °C, 40 rpm, 8 min).

Sample	UF-AO (%w/w)	Irg1076 (%w/w)	T101 (MR)	HDPE (% w/w)
NoAdd-220	-	-	-	100.0
L-Irg1076-220	-	0.5	-	99.50
L-UF-AO-220	0.5	-	-	99.50
UF-AO+T101 0.24-220	0.5	-	0.24	99.40

As for the samples processed at 190 °C, thin films were also prepared and subsequently extracted with DCM in order to remove all the unbounded antioxidant. Again, the UV-Vis spectra of the sample processed with **UF-AO** and **T101** showed the disappearance of the antioxidant characteristic absorption at 287 nm after the extraction, indicating the low levels of grafting achieved. However, OIT-DSC measurements for these samples showed similar results to those found for samples processed at 190 °C (Figure 13).

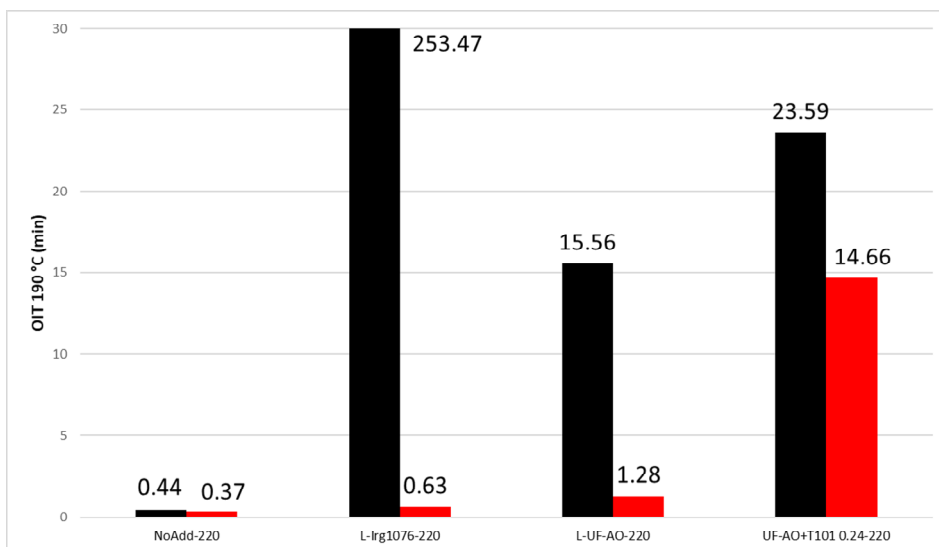


**Figure 13:** OIT values of HDPE (L5261) samples processed at 220°C; unextracted=black, extracted = red.

Indeed, for the samples containing no additives or only **T101**, the OIT was <1 min both before and after Soxhlet extraction, while the high value of OIT of those containing only an antioxidant (**L-Irg1076-220** or **L-UF-AO-220**) without **T101** dropped to about 1 min after the extraction. However, **UF-AO+T101 0.24-220** showed OIT of about 24 min that decreased to ~ 15 min after extraction, suggesting again a partially successful grafting, these results are similar to those shown earlier (Fig. 12) for analogous samples but processed at the lower temperature of 190 °C.

It was also possible to monitor effectively the reaction process during the extrusion of each sample by measuring the torque (of the drive motor) and the pressure in the backflow channel of the instrument so as to calculate the relative viscosity change over time, see Figure 14. In the presence of only the radical initiator **T101** (**L5261+T101** at peroxide concentration of **0.24** and processing temperature of **190 °C**, violet trace) the viscosity increased sharply at the beginning and then decreased to a stable level which is only slightly above all the other samples. This is an expected behaviour because the **T101** decomposition leads to the polymer cross-linking and then to an increase in the melt viscosity; further processing partially destroys the cross-linked structure associated with the decrease observed in the relative melt viscosity.

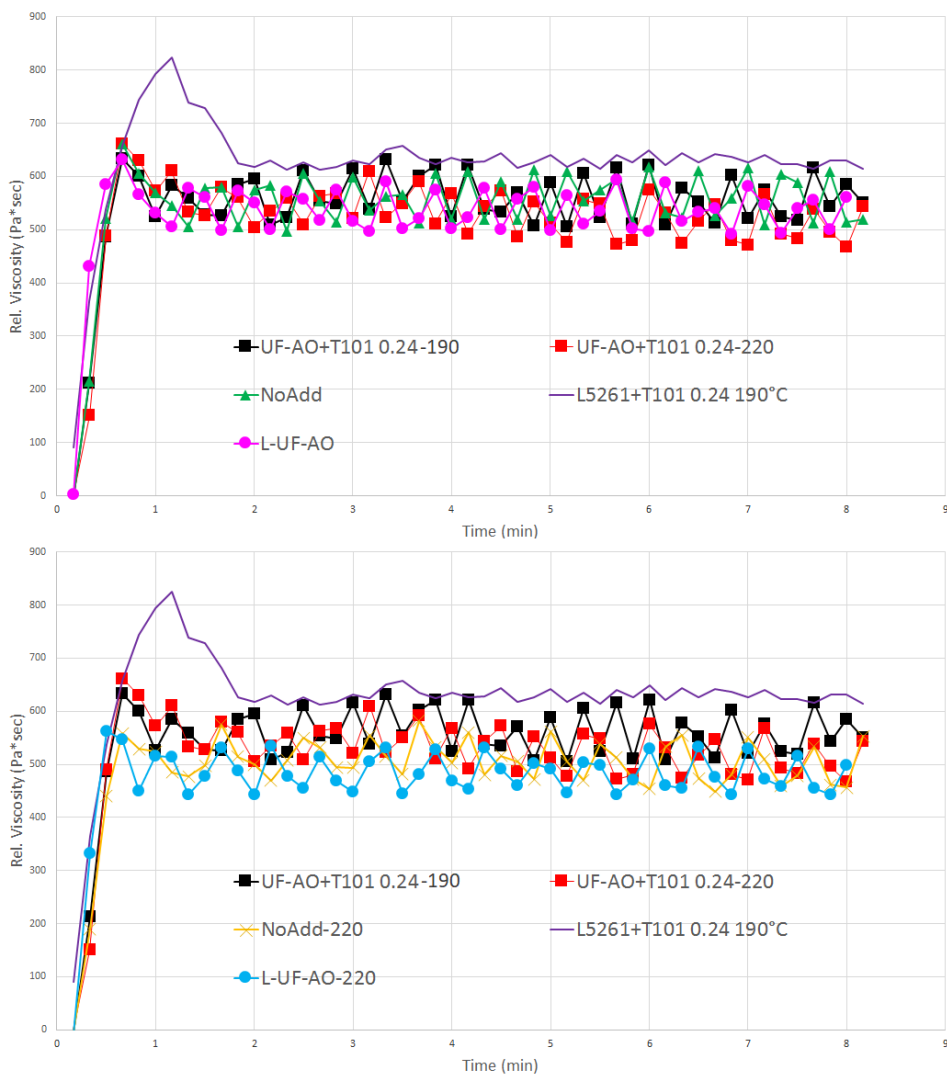


**Figure 14:** Relative viscosity-time curves of HDPE(L5261)+UF-AO 0.5%+T101, MR=0.24, samples compared to reference ones processed at 190 (top) and 220 °C (bottom).

In the case of **UF-AO+T101 0.24-190** (MR=0.24, T= 220 °C) and **UF-AO+T101 0.24-220** (MR=0.24, T=220) there was a moderate increase of the viscosity in the first minute that had later decreased to a level that is lower compared to the sample containing only **T101** but similar to the samples containing no additives (**NoAdd** and **NoAdd-220**) or only the antioxidant (**L-UF-AO** and **L-UF-AO-220**). These data indicate that when both the radical initiator and the antioxidant are present at the correct level, the undesired polymer cross-linking process is minimised in favour of the reaction between the free radicals on the polymer chain and the **UF-AO** vinyl function. This indication was

confirmed by the measurement of the gel content; the amount of gel was not detectable for both **UF-AO+T101** and **UF-AO+T101 (MR=0.24, T=190 and 220)**.

#### 4.2.2 Long-term thermo-oxidative stability studies.

The OIT-DSC measurement was used in a preliminary study for screening the best processing conditions for carrying out reactive processing (for the grafting of the rAOs on HDPE (L5261), *i.e.* 0.5% of **UF-AO, T101/UF-AO**, MR=0.24, T=190 or 220 °C). The samples thus obtained were submitted, both before and after the Soxhlet extraction with DCM, to accelerated thermal ageing at 125°C in individual cell (to prevent cross contamination) air circulating ovens. The composition of all of the processed samples of **L5261** subjected to the accelerated thermal ageing are listed below in Table 5. For discussion purposes, samples are referred to by numbers.

**Table 5:** Sample composition processed at different T101/UF-AO molar ratios.

Sample	UF-AO (%w/w)	Irg1076 (%w/w)	T101 (MR)	HDPE (%w/w)	T (°C)	Number
<b>UF-AO+T101 0.24</b>	0.5	-	0.24	99.40	190	<b>1</b>
<b>UF-AO+T101 0.24-220</b>	0.5	-	0.24	99.40	220	<b>2</b>
<b>NoAdd</b>	-	-	-	100.0	190	<b>3</b>
<b>NoAdd-220</b>	-	-	-	100.0	220	<b>4</b>
<b>L-Irg1076</b>	-	0.5	-	99.50	190	<b>5</b>
<b>L-Irg1076-220</b>	-	0.5	-	99.50	220	<b>6</b>
<b>L-UF-AO</b>	0.5	-	-	99.50	190	<b>7</b>
<b>L-UF-AO 220</b>	0.5	-	-	99.50	220	<b>8</b>

The thermal ageing was monitored by the determination of the Carbonyl Index (**CI**) variation over the time for each sample. Indeed the oxidative degradation of polymers causes the formation of different oxidation products containing carbonyl groups<sup>7,21,37</sup> on the polymer chain that can be used to monitor the progress of degradation. For this purpose, FTIR spectroscopy is a very useful technique because it allows a quantitative determination of carbonyl groups by the measurement of the area of their C=O stretching absorptions. Various carbonyl containing species can be found depending on the polymer structure and degradation conditions: lactones (-1780 cm<sup>-1</sup>), esters (-1735 cm<sup>-1</sup>), ketones (-1720 cm<sup>-1</sup>) and carboxylic acids (-1713 cm<sup>-1</sup>).<sup>38</sup> The **CI** has been calculated as the ratio between the absorbance area of carbonyl groups (1780-1670

$\text{cm}^{-1}$ ) and the absorbance area of a reference band ( $2100\text{-}1980\text{ cm}^{-1}$ ) so as to correct for variations in the thickness of films.<sup>39</sup>

A plot of the carbonyl index values over time for unextracted and extracted samples of **1** and **2** together with some reference ones is shown in Figure 15.

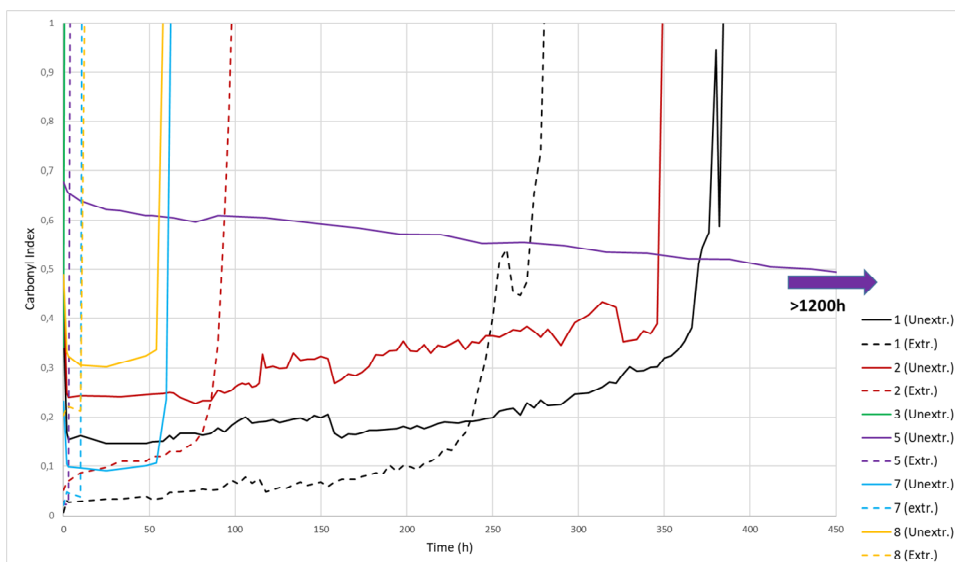


**Figure 15:** Carbonyl index variation over time of unextracted (bold lines) and extracted (dash lines) samples, see Table 6 for the numbers that give the sample identity.

This figure shows clearly that the thermal ageing of samples containing the **UF-AO** reactively processed in the presence of **T101** ( $\text{MR}=0.24$ ) at both temperatures of  $190\text{ }^{\circ}\text{C}$  and  $220\text{ }^{\circ}\text{C}$  (samples **1** and **2**) gave rise to a good level of retention of the polymer stability after solvent extraction confirming that the grafting, even if partially, had almost certainly taken place. Indeed, the unextracted polymer-**UF-AO** sample processed at  $190\text{ }^{\circ}\text{C}$  (sample **1**) gave a **CI** stability of 350h which decreased to 230h after the solvent extraction. This confirms that some of the antioxidant has become bound/grafted onto the polymer and it had therefore continued protecting the polymer from oxidative degradation (for 230 h) after exhaustive extraction of all the unbound AO. The corresponding sample processed at the higher temperature of  $220\text{ }^{\circ}\text{C}$  (sample **2**) was also stable for just under 350h but, after the extraction, its CI stability decreased to a lower extent than in sample 1 down to 90 h. Even though the overall stabilising performance of this sample (sample 2) is lower than when processed at lower temperature (sample 1), overall these results confirm without any doubt that the antioxidant **UF-AO** does become grafted onto HDPE in the melt during a reactive processing procedure

In the absence of an antioxidant grafting reaction, that is when no peroxide is used during the processing of the polymer, then as expected, the commercial hindered phenol antioxidant, Irg 1076 (samples **5** and **6**), which has not been extracted resulted

in the highest polymer long-term thermal oxidative stability as it had not undergone a significant increase in the **CI** for over 1200 h of ageing time, see Fig. 15. However, once these samples containing Irg 1076 were subjected to solvent extraction, the extracted polymer lost all its stability with a dramatic decrease in the **CI** stability from 1200 h down to only few hours. It is important to highlight here that the starting **CI** values of unextracted polymer containing Irg 1076 (samples **5** and **6**) were higher than all the other samples ( $CI=0.6-0.7$ ) because of the antioxidant ester group that absorbs at  $1740\text{ cm}^{-1}$ , this peak did then undergo a gradual decrease with ageing time due to the **Irg1076** slow volatilization/loss.

The unextracted polymer samples containing UF-AO processed at both temperatures ( $T=190$  and  $220\text{ }^{\circ}\text{C}$ ) but in the absence of an added peroxide (i.e. NOT reactively processed, samples **7** and **8**) were stable for only 50-60 h, indicating a low performance of this antioxidant when it is not grafted compared to the performance of unextracted **Irg1076** (both were subjected to simply mixing in the polymer).

As aforementioned, results of polymer samples obtained at  $220\text{ }^{\circ}\text{C}$  showed lower polymer stability than samples processed at  $190\text{ }^{\circ}\text{C}$ . This could be due to an increase of the antioxidant homopolymerization as well as to its partial thermal degradation. A full FTIR characterization of the grafted polymers, before and during the thermal ageing, was done in order to have a better understanding of their degradation process. As can be seen from Figure 14 the starting **CI** values of extracted **1** and **2** are lower than those of the analogous unextracted samples. This is due to the presence of carbonyl region of some unknown signals, probably related to the impurities contained in **UF-AO**, which may have been removed by extraction. Indeed, the FTIR spectrum of unextracted sample **1**, showed signals at  $1740$  and  $1708\text{ cm}^{-1}$  that had disappeared after extraction; these signals are responsible for the initial high values of the **CI** observed (see Figure 16). A similar finding was observed for sample 2 (spectra not shown).

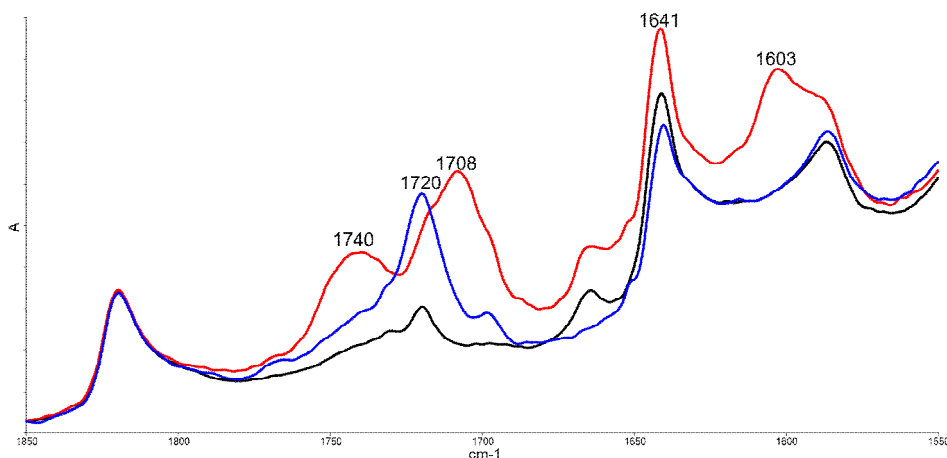


**Figure 16:** FTIR carbonyl region of unextracted (—) and extracted (—) film sample of **1** and of unextracted **3** (—).

Other signals that disappeared after the extraction are present outside the carbonyl region like those at 1603 (Figure 16), 1212 and 1154  $\text{cm}^{-1}$  (Figure 17). Moreover, in the unextracted samples **1** and **2** all of these additional signals, except that at 1740  $\text{cm}^{-1}$ , vanished after few hours of thermal aging suggesting that they are probably related to some unknown volatile impurities of the synthesised antioxidant.

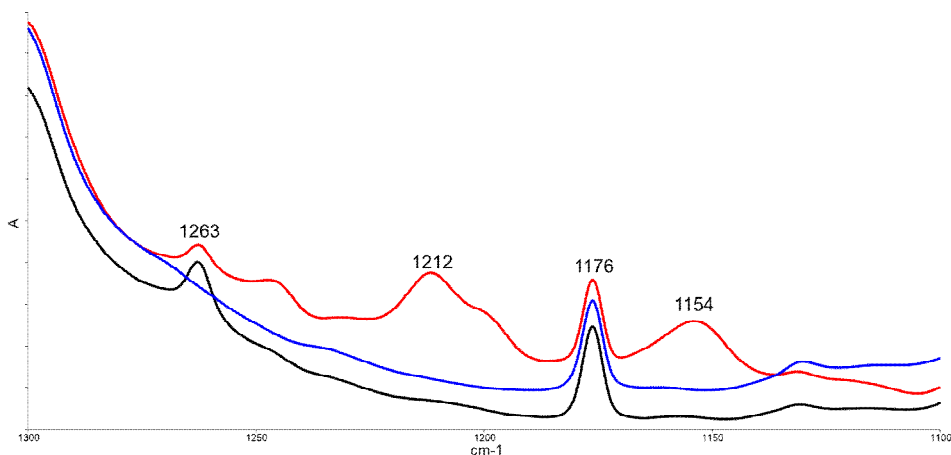


**Figure 17:** FTIR 1300-110 region of unextracted (—) and extracted (—) **1** and of unextracted **3** (—).

FTIR spectroscopy also revealed information about the type of oxidation products that are formed during the thermal ageing. As can be seen in Figure 18 for sample **1** (the same results were obtained with sample **2**) the main absorption maximum in the carbonyl region during the thermal ageing was observed at 1719  $\text{cm}^{-1}$ , which is characteristic of ketones. Indeed, ketones are generally the main products formed by thermal oxidation of polyethylene polymers because after their formation they do not decompose through Norrish type I or II cleavages that are instead typical of photooxidation processes.<sup>38</sup>



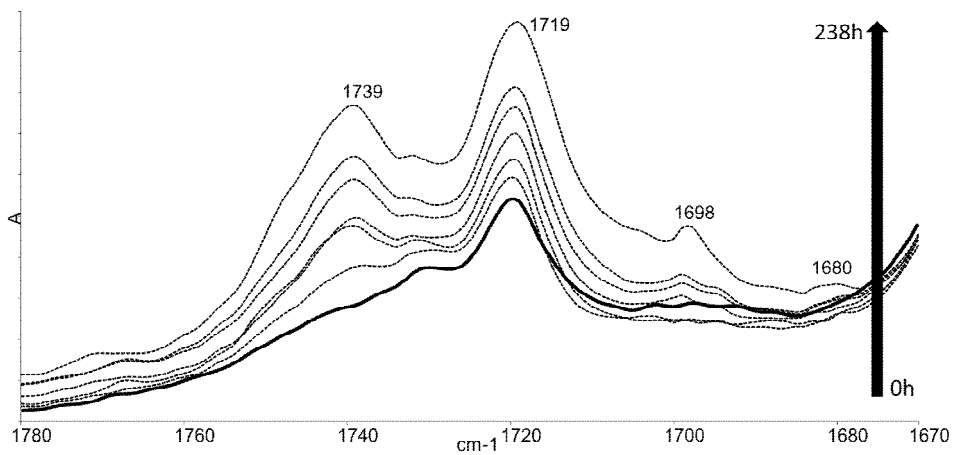
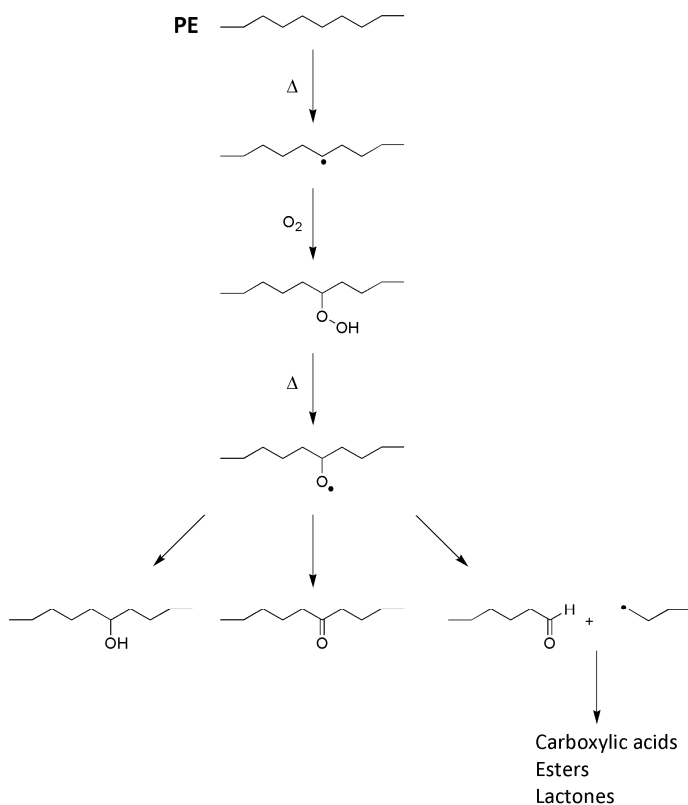


**Figure 18:** Carbonyl groups absorptions developed during the thermal ageing of sample 1.

The simplified mechanism for the oxidation of polyethylene during thermal oxidation is sketched out in Scheme 9 below.<sup>38</sup>



**Scheme 9:** Thermal oxidation of polyethylene

The presence of thermo-labile defects on the polymer chain allows the formation of a macro-alkyl radical that readily reacts with the atmospheric oxygen leading to the formation of a macro-alkyl peroxide. The latter decomposes giving a macro-alkoxy and a hydroxyl radical  $\text{HO}^\bullet$ . The mechanism of chain ketones formation has not been well clarified yet; a cage reaction between the peroxy and the hydroxyl radicals has been proposed.<sup>39</sup> Macro-peroxy radicals also undergoes a  $\beta$ -scission of the main chain that leads to the formation of an aldehyde and a new macro-alkyl radical that are responsible for the development of other carbonyl functions like carboxylic acids, esters and lactones. Another degradation pathway is the hydrogen abstraction on the macro-peroxy radical without cleavage of the chain to form hydroxyls.

The polymer oxidation is also associated with some modifications in the absorption infrared region of carbon-carbon unsaturations. The three most important unsaturated groups of polyethylene are: vinyl ( $\text{CH}_2=\text{CHR}$ ,  $909\text{ cm}^{-1}$ ), *t*-vinylene ( $\text{CH}=\text{CH}$ ,  $965\text{ cm}^{-1}$ ), and vinylidene ( $\text{CH}_2=\text{CR}_2$ ,  $888\text{ cm}^{-1}$ ); each of these behaves differently from each other depending on the type of oxidation (photo- or thermo-). In the case of samples **1** and **2**, the variation in the concentration of these unsaturated groups during thermal oxidation was consistent with literature data, *i.e.* an increase of *t*-vinylene and a decrease of both vinyl and vinylidene (Figure 19).<sup>38,40</sup>

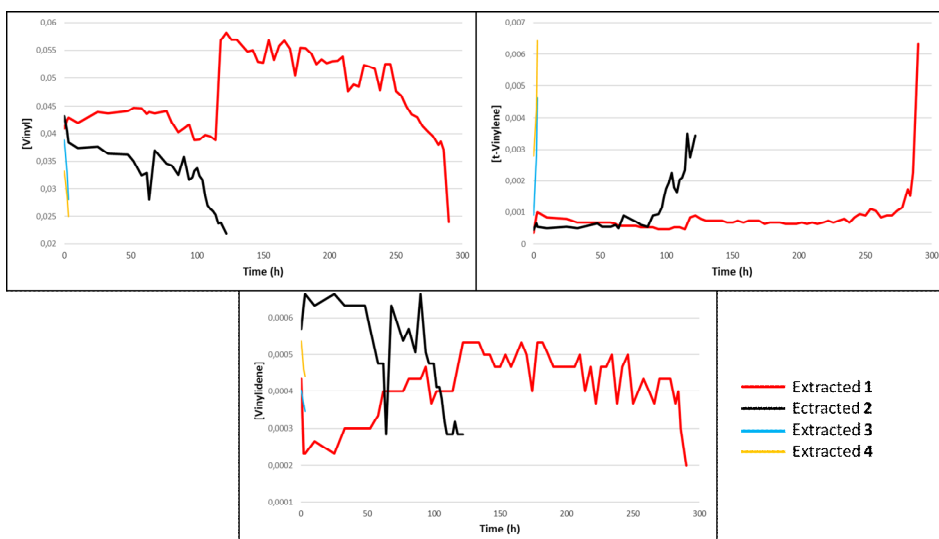


**Figure 19:** Vinyl, *t*-vinylene and vinylidene concentrations during thermal ageing of grafted **1** and **2** (data for **3** and **4** are shown for reference).

#### 4.2.3 Grafting in the presence of a reactive coagent.

After the characterization of the oxidation process of samples **1** and **2** preliminary attempts were made to increasing the grafting yield through the use of reactive coagents. As seen in section 4.1, these compounds are species able to build a transient cross-linked structure between the polymer chains thus facilitating the reactive antioxidant binding through a co-grafting process. Their use requires a careful study on the choice and of the relative quantity of the coagent compared to both the antioxidant and the radical initiator. Indeed the use of a coagent means that a second species containing reactive groups besides the antioxidant (**UF-AO**) is present in the melt and then it is necessary to achieve a delicate balance between each component of the chemical system together with the optimization of processing conditions (temperature, screw speed, *etc.*) in order to promote the grafting ahead of all the other competing side reactions like polymer cross-linking.<sup>21</sup> Due to the short time available only few attempts were done using divinylbenzene (**DVB**, Figure 3 section 4.1) as the coagent. Two samples of HDPE were prepared (see Table 6).

**Table 6:** Samples of HDPE (**L5261**) extruded in the presence of DVB (220°C, 40 rpm, 8 min) at two different molar ratios (M.R.) of **T101**/(**UF-AO**+**DVB**)

Sample	UF-AO (%w/w)	UF-AO/DVB (w/w)	T101 (MR)	HDPE (% w/w)
<b>9</b>	0.5	6/4	0.10	99.05
<b>10</b>	0.5	6/4	0.20	98.93

The MR. values referred to here, represent the molar ratio of the peroxide to the sum of the moles of both the reactive antioxidant and the coagent; important to point out here that the calculated MR value of 0.10 used for sample **9** corresponds to a MR of **T101/UF-AO** of 0.24 used in samples **1** and **2**. The preparation of a sample containing a higher amount of **T101** (sample **10**) was done considering that the radical initiator is consumed by both the reactive antioxidant and the coagent and then it is probably necessary to enhance the extent of the reaction initiation in order to generate an adequate amount of free radicals. The reactive processing was performed in the presence of DVB on a batch mixer (Brabender) with a high torque motor. Indeed, the first extrusions done on the Mini Haake previously used failed due to the high torque reached in the first minutes of processing which is attributed to the cross-linking activity of **DVB**. As can be seen from the diagram in Figure 20 the relative viscosity of sample **9** processed at 190 and 220 °C is clearly higher than that of sample **1** processed at the same temperatures. Especially in the processing of sample **9** processed at 220 °C (red trace) there is a behaviour consistent with a successful grafting in the presence of a coagent, *i.e.* a neat rise of the viscosity at the beginning followed by its gradual decrease until levels comparable to that observed for sample **1**. Indeed, the initial formation of a higher viscosity peak is almost certainly due to the formation of a cross-linked structure based on the **DVB** moiety (with possibly bound AO species) that with further processing would undergoes a rearrangement which is associated with the gradual decrease observed in the viscosity of the melt. Figure 20 shows the relative viscosity curves for sample **9** at 190 °C and 220 °C but analogous results were obtained also with sample **10**.

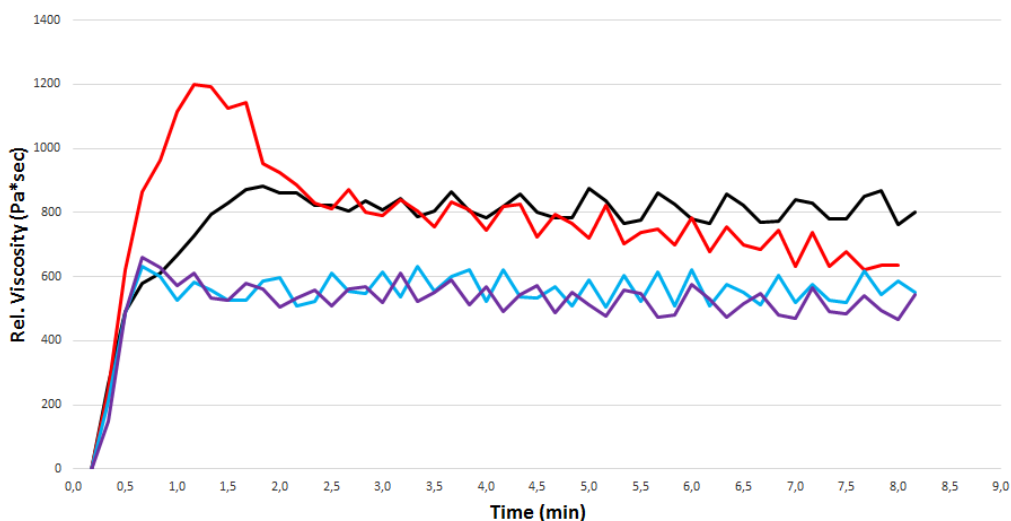


**Figure 20:** Relative viscosity-time curves of sample **9** processed in a Brabender Torquerheometer at 190 (—) and 220 °C (—) and of sample **1** processed at 190 (—) and 220 °C (—).

Because this curve trend, characterized by the formation of a peak at the beginning followed by a gradual decrease in the viscosity, was seen only in the samples **9** and **10** processed at 220 °C, they were the only ones used for further stability tests. Thin films were prepared from samples **9** and **10** which were submitted to Soxhlet extraction with DCM in order to remove all the unbound antioxidant. As was the observed case for samples **1** and **2**, the OIT measurement suggested a partial success of the grafting of UF-AO using **DVB** as coagent. Indeed, for sample **9** the OIT value decreased from 22.18 min to 14.70 min after the extraction while for sample **10** it decreased from 19.73 min to 12.04 min. These results were similar to those shown earlier for the analogous samples but processed without DVB (Figures 12 and 13, section 4.2.1) confirming that, at least, part of the antioxidant was able to chemically bind/graft to the polymer chain. However, it is clear from these very preliminary experiments, that the conditions used in terms of the relative concentration of each reagent was not optimal for increasing the grafting yield. In spite of this, samples **9** and **10** were submitted further to accelerated thermal ageing at 125°C but the results were not as good as those achieved previously with samples **1** and **2**. The thermal aging curves for samples **9** and **10** are shown in Figure 21 alongside those of extracted samples **1** and **2**, and this clearly shows that the extracted sample **10** preserved its stability for a time analogous to extracted sample **2** (~100h) while the extracted sample **9** had a little bit better performance (~120h).

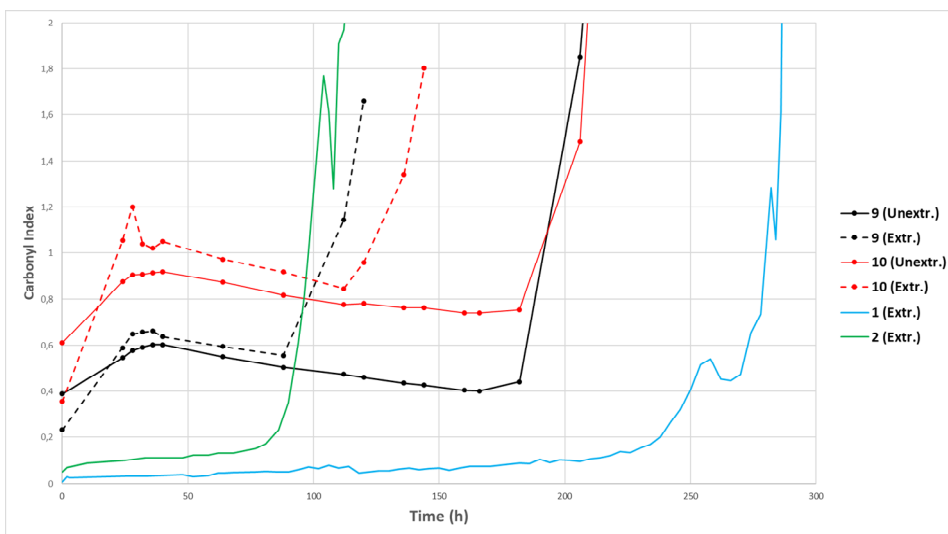


**Figure 21:** Carbonyl index variation over time of unextracted (bold lines) and extracted (dash lines) samples **9** and **10**; samples **1** and **2** are shown for comparison.

However, both unextracted and extracted samples **9** and **10** showed lower stabilization performance than extracted sample **1** which gave the best results. Moreover, the curves of samples **9** and **10** showed an odd trend with an initial rise of the CI value followed by a gradual decrease and then a new stable increase that led to the final degradation.

The starting CI values of unextracted samples **9** and **10** were higher than the extracted ones but all of them were however greater than the starting CI values of unextracted samples **1** and **2**. This is explained by the presence in the carbonyl region of samples **9** and **10** of the already observed peak at  $1708\text{ cm}^{-1}$  along with an additional one at  $1731\text{ cm}^{-1}$  (Figure 22).

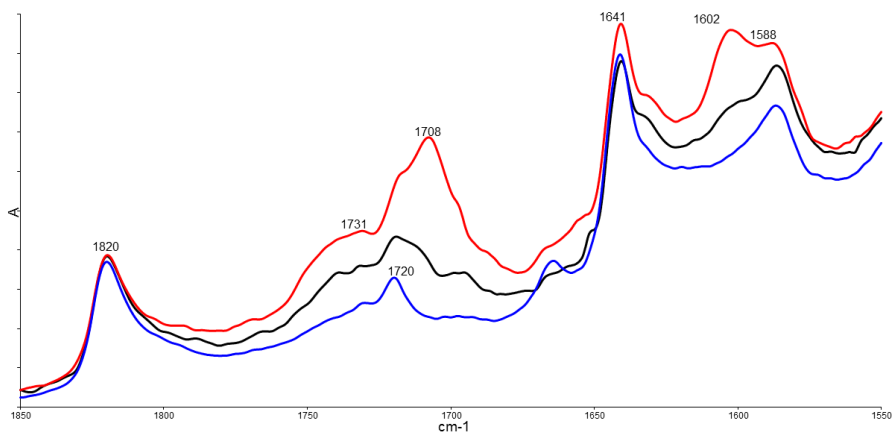


**Figure 22:** FTIR carbonyl region of unextracted (—) and extracted (—) **9** and of extracted **1** (—).

However, while the peak at  $1708\text{ cm}^{-1}$  decreased after few hours of thermal ageing due to the volatilization of the aforementioned impurity, the one at  $1731\text{ cm}^{-1}$  increased and was responsible of the initial rise of the **CI** in the first 32h (Figure 23, a). The successive drop in the **CI** is related to the decrease of the peak at  $1731\text{ cm}^{-1}$  (Figure 23, b) followed by the formation of the characteristic oxidation peak of ketones at  $1719\text{ cm}^{-1}$ .

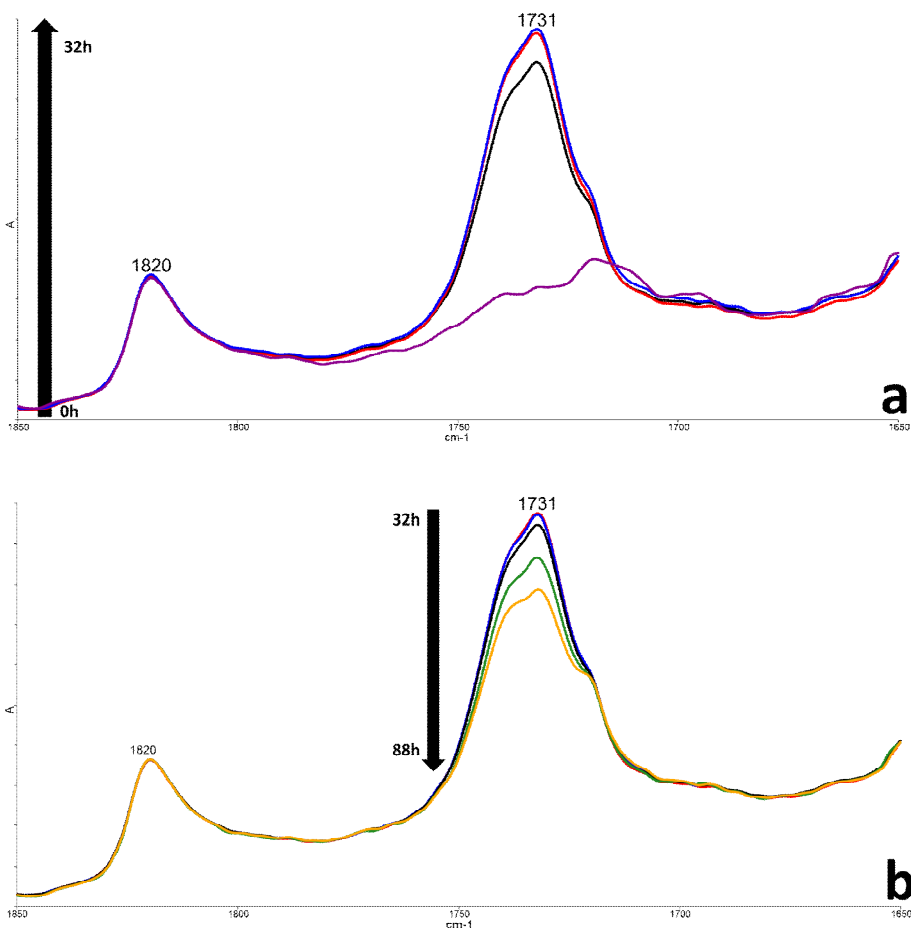


**Figure 23:** FTIR carbonyl region of extracted **9** during thermal aging.

Apparently, the use of DVB as coagent decreased the grafting efficiency, however it is important to highlight that due to the short time that was available, only few attempts were done and was not possible to try other **T101/(UF-AO+DVB)** molar ratios or different coagents.

In conclusion, the feasibility of the use of a reactive antioxidant like **UF-AO** bearing a terminal vinyl group for the grafting on high density polyethylene was clearly demonstrated in this work despite the well-known predisposition of terminal double bonds being less useful due to undesired side reactions like homopolymerization. Moreover, the immobilization of the antioxidant on the polymer chain ensured a better stabilizing performance compared to the same system conventionally stabilized by a simple mixing with the additive.

### 4.3 Experimental section

Unstabilized high-density polyethylene (HDPE) used was a powder supplied by Lyondell Basell with the trade name Lupolen 5261Z having MFR (190 °C/21.6 Kg) of 2 g/10 min and density of 0.954 g/cm<sup>3</sup>. Commercially available reagents (Trigonox 101, divinylbenzene) and reference Irganox 1076 were used as received by Ciba Specialty Chemicals (now BASF). HPLC grade solvents were generally used. NMR experiments were done on a Bruker-Advance 300 spectrometer at ambient temperature using tetramethylsilane (TMS) as internal standard. The NMR samples were prepared by dissolving 15 mg of the material in CDCl<sub>3</sub>. FTIR measurements were performed on a Perkin Elmer Spectrum 100 FT-IR spectrometer over the range of 4000-400 cm<sup>-1</sup>; spectral collections were taken over 16 scans with resolution of 4 cm<sup>-1</sup>. ATR measurements were performed on a Perkin Elmer Frontier fitted with a zinc-selenide (ZnSe) Horizontal Attenuated Total Reflectance (HATR) attachment (Specac). Electronic absorption spectra were recorded at room temperature on a Cary 5000i (Agilent) UV-Vis spectrophotometer at a scanning rate of 600 nm/min. The HPLC analysis was performed on a Thermo Scientific UltiMate 3000 HPLC system equipped with vacuum degasser, quaternary pump, an autosampler and a UV/Vis diode array detector. A Zorbax C-18 (Agilent) 4.6x250 mm, 5 μm was used as column. HPLC experiments were performed using MeOH/H<sub>2</sub>O 77.5/22.5 as eluent, flow rate 1.0 mL/min, T = 50 °C, t = 35 min, λ<sub>detector</sub>=278 nm.

#### 4.3.2 Polymer processing

Melt processing of HDPE samples were carried out on a lab-scale conical twin-screw extruder (Haake MiniLab II) or, in the case of samples processed in the presence of DVB, on a Brabender Plasti-Corder PLE651. The extrudates/melt were cooled in a water bath, dried and stored in the dark at room temperature until required for further analysis. Thin film specimens (150-200 μm) were prepared by compression moulding at 160°C under full pressure (20 Ton) and submitted to exhaustive Soxhlet extraction in DCM under nitrogen atmosphere.

#### 4.3.3 Determination of the Oxidative Induction time (OIT)

Oxidative Induction Time (OIT) of the processed samples was measured in an open pan under a stream of oxygen (flow rate 40 ml/min) at 190 °C using a Mettler Toledo DSC 823<sup>e</sup>. Each sample was first heated at 25 °C/minute to 190 °C under a nitrogen flow, then after 5 min the gas was switched to oxygen to start the OIT measurement.

#### 4.3.4 Determination of long-term thermo-oxidative stability

Long-term thermo-oxidative stability of polymer film samples was determined following extended periods of thermo-oxidative ageing at 125 °C in a multi-cell single cell air-circulating ageing oven (Wallace O7E) with a 0.068 m<sup>3</sup>/min air flow. The evolution of carbonyl groups was monitored by means of FTIR.

#### 4.3.5 Determination of the gel content of polymer samples



The gel content of the processed samples was determined according to ASTM 2765-01 method using xylene extraction. Polymer films were cut into small pieces and weighed ( $w_0$ ), placed in weighed stainless mesh thimbles of weight  $W_t$ , and Soxhlet extracted in 150 mL xylene for 48h under nitrogen. After extraction, the thimbles were dried to constant weight ( $w_x$ ) in a vacuum oven (80°C). The percent gel content was calculated using the following formula:

$$\text{Gel Content \%} = \frac{w_x - W_t}{w_0} \times 100$$

#### 4.4 References

- (1) Al-Malaika, S. In *Chemistry and Technology of Polymer Additives*; Al-Malaika, S., Golovoy, A., Wilkie, C. A., Eds.; Blackwell Science: London, 1999; pp 1–20.
- (2) Scott, G.; Al-Malaika, S. *Modified Polymers*. U.S. 5,382,633, January 17, 1995.
- (3) Pike, M.; Watson, W. F. *J. Polym. Sci.* **1952**, *9* (3), 229–251.
- (4) Ayrey, G.; Moore, C. G.; Watson, W. F. *J. Polym. Sci.* **1956**, *19*, 1–15.
- (5) Al-Malaika, S.; Honggokusumo, S.; Scott, G. *Polym. Degrad. Stab.* **1986**, *16*, 25–34.
- (6) Ghaemy, M.; Scott, G. *Polym. Degrad. Stab.* **1981**, *3*, 405–422.
- (7) Al-Malaika, S. *Compr. Polym. Sci. Suppl.* **1989**, *6*, 539–578.
- (8) Sirimevan Kularatne, K. W.; Scott, G. *Eur. Polym. J.* **1978**, *14* (2), 835–843.
- (9) Kularatne, K. W. S.; Scott, G. *Eur. Polym. J.* **1979**, *15*, 827–832.
- (10) Ajiboye, O.; Scott, G. *Polym. Degrad. Stab.* **1982**, *4*, 397–413.
- (11) Scott, G.; Tavakoli, S. M. *Polym. Plast. Technol. Eng.* **1982**, *4*, 343–351.
- (12) Scott, G.; Suharto, R. *Eur. Polym. J.* **1985**, *9*, 765–768.
- (13) Ajiboye, O.; Scott, G. *Polym. Degrad. Stab.* **1982**, *4*, 415–425.
- (14) Scott, G.; Setoudeh, E. *Polym. Degrad. Stab.* **1983**, *5*, 81–88.
- (15) Scott, G.; Yusoff, M. F. *Polym. Degrad. Stab.* **1981**, *3*, 53–59.
- (16) Scott, G.; Yusoff, M. F. *Polym. Degrad. Stab.* **1981**, *3*, 13–23.
- (17) Scott, G.; Setoudeh, E. *Polym. Degrad. Stab.* **1983**, *5*, 11–22.
- (18) Monteanu, D. In *Developments in Polymer Stabilization*; Scott, G., Ed.; Applied Science Publishers: London, 1987.
- (19) Sharma, Y. N.; Naqvi, M. K.; Gawande, P. S.; Bhardwaj, I. S. *J. Appl. Polym. Sci.*

- 1982**, 27, 2605–2613.
- (20) Al-Malaika, S.; Ibrahim, A. Q.; Scott, G. *Polym. Degrad. Stab.* **1988**, 22, 233–239.
- (21) Al-Malaika, S. *Adv. Polym. Sci.* **2004**, 169, 121–150.
- (22) Al-Malaika, S.; Suharty, N. *Polym. Degrad. Stab.* **1995**, 49, 77–89.
- (23) Al-Malaika, S.; Kong, W. *Polym. Degrad. Stab.* **2005**, 90, 197–210.
- (24) Al-Malaika, S.; Eddiyanto, E. *Polym. Degrad. Stab.* **2010**, 95, 353–362.
- (25) Boragno, L.; Stagnaro, P.; Sosio, S.; Sacchi, M. C.; Menichetti, S.; Viglianisi, C.; Piergiovanni, L.; Limbo, S. *J. Appl. Polym. Sci.* **2012**, 124, 3912–3920.
- (26) Sacchi, M. C.; Losio, S.; Stagnaro, P.; Mancini, G.; Boragno, L.; Menichetti, S.; Viglianisi, C.; Limbo, S. *Polyolefins J.* **2014**, 1 (1), 1–15.
- (27) Menichetti, S.; Viglianisi, C.; Liguori, F.; Cogliati, C.; Boragno, L.; Stagnaro, P.; Losio, S.; Sacchi, M. C. *J. Polym. Sci. Part A Polym. Chem.* **2008**, 46, 6393–6406.
- (28) Al-Malaika, S. *Polym. Degrad. Stab.* **1991**, 34, 1–36.
- (29) Munteanu, D. *Polym. Degrad. Stab.* **1991**, 34, 295–307.
- (30) Hamann, J. N.; Tuczek, F. *Chem. Commun.* **2014**, 50 (18), 2298–2300.
- (31) Hahn, V.; Mikolasch, A.; Kuhlisch, C.; Schauer, F. *J. Mol. Catal. B Enzym.* **2015**, 122, 56–63.
- (32) Ishii, Y.; Tashiro, K.; Hosoe, K.; Al-zubaidi, A.; Kawasaki, S. *Phys. Chem. Chem. Phys.* **2016**, 18, 10411–10418.
- (33) Yilmaz, M.; Aydin, B.; Dogan, O.; Dereli, O. *J. Mol. Struct.* **2017**, 1128, 345–354.
- (34) Bagley, E. B. *J. Appl. Polym. Sci.* **1963**, 7, S7–S9.
- (35) Al-Malaika, S.; Scott, G.; Wirjosentono, B. *Polym. Degrad. Stab.* **1993**, 40, 233–238.
- (36) Al-Malaika, S.; Riasat, S.; Lewucha, C. *Polym. Degrad. Stab.* **2017**, <http://dx.doi.org/10.1016/j.polymdegradstab.2017.0>.
- (37) Billingham, N. C. *Mater. Sci. Technol.* **2013**, 469–507.
- (38) Gardette, M.; Perthue, A.; Gardette, J.-L.; Janecska, T.; Földes, E.; Pukánszky, B.; Therias, S. *Polym. Degrad. Stab.* **2013**, 98, 2383–2390.
- (39) Ginjac, J.-M.; Gardette, J.-L.; Arnaud, R.; Lemaire, J. *Die Makromol. Chemie* **1981**, 182, 1017–1025.
- (40) Arnaud, R.; Moisan, J.-Y.; Lemaire, J. *Macromolecules* **1984**, 17, 332–336.

## 5. Nanostructured antioxidants

### 5.1 Introduction

Nanomaterials (NMs) are small objects, typically with dimensions under 100 nm, that behave as a whole unit and with unique physicochemical properties that differ substantially from those bulk materials of the same composition.<sup>1</sup> Among the numerous properties that distinguish NMs from bulk materials, probably the most important is their high surface to volume ratio because a greater portion of the atoms are found at the surface compared to those inside.<sup>2</sup> This characteristic leads to a higher chemical reactivity that, in turn, is related to the other NMs unique properties like optical and mechanical ones that make them very attractive for both industrial and biomedical applications.

NMs can exist in different forms (nanoparticles, nanowires, nanofibers, and nanotubes) and with different material composition.<sup>3</sup> Inorganic non-metallic NMs include synthetic amorphous silica, aluminium oxide and titanium dioxide and are widely used in lots of applications as additives to chemical polishing products, food, sunscreens and cosmetics.<sup>4</sup> Organic, carbon based and metal nanoparticles on the other side have not already found actual large-scale deployments but are at the centre of deep researches for different applications.

Besides their possible use in different areas like catalysis, electronic, magnetic, opto-electronic, energy, micro-wiring and materials applications, metallic nanoparticles (MNPs) are deeply studied for biology and medicine applications.<sup>5</sup> Large surface area compared with small size is a very important property of MNPs and is responsible of their high biological activity: indeed MNPs show high cellular uptake and strong ability for interaction with different macromolecules, and their behaviour can be modulated with appropriate modifications of surface properties (chemical composition, charge, coating, functionalization, size, shape, *etc.*) so as to change MNPs biological activity.<sup>6</sup> Over the last few years MNPs are increasingly being studied for lots of biomedical applications:

- Hyperthermia
- Drug delivery
- Bioimaging
- Photo-ablation therapy
- Biosensing

The wide range of biomedical applications is related to the possibility to use different MNPs systems in terms of the chemical nature of the core, its size, shape, charge and coating, and the eventual functionalization. **Hyperthermia**<sup>7</sup> is surely the area of MNPs

applications that is in a more advantage stage, with some products that are in clinical trials. Their use depends on the ability of superparamagnetic NPs like  $\text{Fe}_3\text{O}_4$  ones to dissipate as heat the electromagnetic energy they absorb when are exposed to an alternating magnetic field. The heating of the particles allows the raise of the local surrounding temperature in order to destroy cancerous cells and tissues (“thermoablation”) without damaging health ones. The magnetic field can also be used to address the MNPs towards the tumorous tissues and, additionally, their surface can be covered with a targeting ligand so as to allow a specific binding with the cancer cells. MNPs are also studied as **drug delivery systems**,<sup>8</sup> *i.e.* for the targeting of anticancer drugs on their specific location. For this aim the drug molecules are loaded on the MNPs by conjugation on their surface or by encapsulation inside them. The specific delivery on the tumorous tissues is achieved in three different ways: 1) By the Enhanced Permeability and Retention (EPR) effect, a passive mechanism typical of colloidal size objects like MNPs that allows their preferential accumulation on tumour tissues; 2) The functionalization of the MNPs surface with a targeting ligand like a tumour-specific antibody; 3) The application of an external magnetic field to guide the MNP-drug complex to the specific tumour site (possible only when superparamagnetic MNPs are used). Iron oxide, gold, silver, iron-platinum, titanium dioxide and zinc oxide are among the MNPs most studied as nanocarriers in targeted drug delivery. Superparamagnetic MNPs are also under investigation as contrast agents for **bioimaging**<sup>9</sup> techniques like Magnetic Resonance Imaging (MRI) and computed tomography. Other possible applications of MNPs are in the **photo-ablation** therapy of tumours<sup>10</sup> and as **biosensors**<sup>11</sup> for a variety of biomolecules.

The increased use of MNPs for industrial and biomedical applications has risen concerns about their potential adverse health effects. Indeed, very little is known about the behaviour of nanoscale entities in biological systems because corresponding bulk materials, due to the different properties, are unreliable for toxicological comparisons. For this reason, a specific branch of toxicology labelled as **nanotoxicology** has been developed in order to have a better understand of the possible toxicity of these systems that, reasonably, could be widely used in the near future.<sup>12,13</sup> First data for the comprehension and assessment of MNPs potential hazards derives from toxicological studies of the ambient particulate matter that relates the exposure to ultrafine particles of air pollution with adverse biological effects. It is copiously reported in literature that the inhalation of ambient ultrafine particles derived from different sources (volcanoes, fires, automobiles, diesel powered vehicles, coal combustion industry, incinerators, *etc.*) are responsible of pulmonary inflammation, oxidative injury, fibrosis, cytotoxicity, and distal organ involvement.<sup>14</sup> Among the several mechanisms that have been reported to explain these adverse health effects, ROS generation and oxidative stress induction are commonly accepted having a central role. Indeed, it has been demonstrated that the toxicity related to the exposure to nanomaterials derived from combustion processes (*e.g.* of diesel and coal), soot, tires debris, welding fumes, silica and asbestos is mainly due to ROS production and the generation of oxidative stress.<sup>15</sup> The toxicology of engineered nanomaterials like MNPs used for biomedical applications can not strictly associated with that of particulate

pollutants because there are important differences in terms of physical and chemical characteristics. Indeed, even if both ambient ultrafine particles and engineered MNPs have size below 100 nm and a large surface area, the first are heterogenous in size, shape and chemical composition while the second are homogenous. Moreover, ambient ultrafine particles are generally inhaled and then perform most of their action in the respiratory tract while MNPs have different exposure routes like parenteral administration and skin contact.

The reasons that make MNPs attractive tools for different applications, *i.e.* the high surface reactivity and the ability to easily pass through cell membranes and other biological barriers due to their tiny dimensions, are responsible for their potential toxicity.<sup>13,16-18</sup> *In vitro* and *in vivo* data obtained up to now on the MNPs toxicity are contradictory and unreliable, however the ROS formation and oxidative stress induction is the best-developed paradigm to explain their toxicity.<sup>19</sup> The level of ROS and the type of oxidative damage induced by MNPs depends on their properties like the chemical composition of the core, size, shape and the possible presence of an organic coating.<sup>20-22</sup> It is important to highlight that each different MNP system shows different mechanisms of oxidative stress damage and that not always *in vitro* and *in vivo* data are in accordance, however the ROS generation and the increase of the oxidation level are a common pathway.<sup>23-25</sup> Actually not all of the MNPs induce oxidative stress: cerium oxide,<sup>26-31</sup> platinum<sup>32</sup> and gold/platinum diamond<sup>33</sup> NPs exhibit a relevant radical scavenger activity and have been proposed as therapeutic agents for the treatment of stress related pathologies.

Some of the proposed mechanism of ROS formation by MNPs are the following:<sup>14,16</sup>

- UV catalysed formation of electron hole pairs on the metallic surface which, in turn, lead to the formation of superoxide anion or hydroxyl radicals.
- Electron jumping from semiconductor MNPs that allows the reduction of O<sub>2</sub> to O<sub>2</sub><sup>•-</sup>.
- Dissolution of the external layer of the MNPs with the subsequent release of metal ions that catalyse ROS formation.
- Transition metal catalysed generation of HO<sup>•</sup> through the Fenton reaction.

*In vitro* oxidative stress toxicity has been found for almost all type of MNPs like gold,<sup>34,35</sup> silver,<sup>36</sup> iron oxide,<sup>37</sup> titanium dioxide,<sup>38</sup> cadmium-chalcogen quantum dots<sup>39,40</sup> and the same for non-metallic nanomaterials like carbon nanotubes<sup>41</sup> and silica nanoparticles<sup>42</sup>. Oxidative stress induction was also observed in *in vivo* experiments in different animal models.<sup>20,35,43-47</sup> ROS generation has a high toxicity potential because it leads to lipid peroxidation, DNA damage, unregulated cell signalling, changes in cell motility, cytotoxicity, apoptosis, and cancer initiation and propagation.<sup>48</sup> Also accelerated ageing and various pathologies are related to the action of oxidative stress.<sup>49-51</sup>

The central role of oxidative stress in the biological activity of MNPs is confirmed by the fact that the simultaneous administration of these nanomaterials with common molecular antioxidants like ascorbic acid or quercetin is able to suppress the ROS generation.<sup>52-57</sup> Also the surface modification is a promising way for decreasing nanotoxicity. A relevant suppression of ROS production was achieved by the coating of different types of MNPs (copper and iron oxide) with polysaccharides such as chitosan or with polyethylene glycol.<sup>58-60</sup> These polymer/metal nanoparticles composites showed indeed a decrease in cellular damage and a moderate production of ROS. The prevention of oxidative stress induction by MNPs was achieved by the encapsulation of ascorbic acid together with silver nanoparticles (AgNPs) and the polymer poly(lactide-co-glycolide) (PLGA) and the resulting PLGA/AgNPs/ascorbic acid particles were able not only to prevent the ROS formation but also proved a radical scavenger activity against intracellular ROS.<sup>61</sup>

It is also possible to directly link antioxidants molecules on the surface of MNPs. To the best of our knowledge only few works are present in literature concerning the preparation of MNPs decorated with antioxidant molecules through a direct chemical bond. In three distinct papers Liu and coworkers reported the preparation, characterization and antioxidant evaluation of gold nanoparticles (AuNPs) functionalized with ligands derived from two different antioxidants, respectively: Trolox (a water-soluble analogue of vitamin E)<sup>62</sup> and Salvianic acid<sup>63,64</sup>. The results proved that the functionalization with antioxidants allowed to prevent the oxidative stress and the cytotoxicity induced by bare nanoparticles, and the nanostructured antioxidants showed a better antioxidant activity compared to the molecular analogous. Similar outcomes were collected by our research group with the successful functionalization of *Turbobeads* cobalt nanoparticles (CoNPs) with a ligand bearing the Trolox moiety.<sup>65</sup> Indeed, the CoNPs decorated with the antioxidant showed a higher radical scavenger activity than the reference  $\alpha$ -tocopherol ( $\alpha$ -TOH), as well as a lower *in vitro* cytotoxicity and oxidative stress induction than the bare nanoparticles. Beside the suppression of the oxidative stress related toxicity, the most remarkable information obtained from these works is that the assembly of antioxidant moieties around the nanoparticles surface through a direct linking is responsible of an exponential increase of the radical scavenger activity. The enhancement is a pure kinetic effect that increases the rate constant of the reaction between nanoantioxidants and ROS. The explanation of this outcome was not well elucidated but some hypothesis was suggested:

- 1) An effect of preconcentration of the radicals near the reactive OH of the phenolic moieties that facilitates the reaction between the two components.
- 2) The  $\pi$ - $\pi$  stacking between the phenolic aromatic rings that favours the ArOH hydrogen atom donation to the radicals.
- 3) In the case of antioxidant functionalized CoNPs was also considered a catalytic effect of the triazole groups that link the nanoparticles with the ligands, or by the presence of a graphite layer around the CoNPs that would act as a

“sponge” of free radicals which would be suppressed by the nearby pendant antioxidant.

The conclusion of these works is that MNPs functionalized with antioxidants could be used to minimize their potential toxicity. An additional conclusion can be done: the immobilization of traditional antioxidant moieties on the MNPs surface is able to soundly enhance their radical scavenger activity. The latter ability suggests a further application of these systems, *i.e.* as innovative pharmacological agents for the treatment of oxidative stress related pathologies.<sup>26</sup>

Oxidative stress is involved in several ophthalmological, cardiovascular, neurodegenerative, and oncological pathologies.<sup>66</sup> The use of antioxidants for the prevention and/or the treatment of these disorders has been suggested but, up to now, poor and contradictory results have been obtained.<sup>49</sup> The ineffectiveness of antioxidant therapies was ascribed to several reasons, included the low bioavailability of molecular antioxidants that are poorly absorbed and rapidly metabolized within the body.<sup>67-69</sup> The direct modification of their structure is a followed strategy that allowed the enhancement of the antioxidant activity,<sup>70</sup> but in some cases the concomitant increase of toxicity was achieved<sup>71</sup>.

Instead of modifying their structure, traditional molecular antioxidants like  $\alpha$ -TOH and quercetin can be linked to supramolecular systems in order to increase their radical scavenger activity. This is the case of the cited works of gold and cobalt nanoparticles functionalized with Trolox<sup>62,65</sup> and Salvianic acid<sup>63,64</sup> derivatives. It is also reported the covalent linking of curcumin on the surface of AuNPs.<sup>72</sup> The encapsulation of molecular antioxidants<sup>73,74</sup> inside oil-in-water emulsions (**nanocapsules**) allows to increase their bioavailability, half-life and *in vivo* antioxidant activity. These outcomes are not related to kinetic effects but to the improved of the molecular antioxidants water-solubility.<sup>75</sup> Encapsulated antioxidants were also successfully tested for the treatment of stress related pathologies in animal models, included Alzheimer's and other neurodegenerative diseases<sup>76,77</sup> because of their ability to cross the blood-brain barrier. Analogous results were obtained from different encapsulated antioxidants like ellagic acid,<sup>78</sup> resveratrol,<sup>79</sup> apigenin,<sup>80</sup> tannic acid,<sup>81</sup> catechins,<sup>82,83</sup> retinol,<sup>84</sup> Trolox<sup>85</sup> and gallic acid<sup>86</sup>. Also the use of **liposomes**, *i.e.* artificially prepared spherical vesicles composed of one or more phospholipid bilayers,<sup>87</sup> has been proposed as system for the encapsulation and biological delivery of antioxidants. The amphiphilic nature of liposomes is an advantage because it allows the loading of these nanosystems with both lipophilic and hydrophilic antioxidants. It was indeed reported the encapsulation inside liposomes and the consequent increase of bioavailability and efficacy of antioxidants like curcumin<sup>88,89</sup> and epigallocatechin gallate<sup>90</sup>. **Inorganic nanocarriers** based on silica NPs were used for the encapsulation and delivery of the antioxidant enzyme SOD<sup>91</sup> or the anti-inflammatory and antioxidant drug Meloxicam<sup>92</sup>.

Nanocapsules, liposomes and inorganic carriers are systems able to facilitate the dissolution of the molecular antioxidants in the biological media and their delivery to the desired target, but do not provide any kinetic enhancement of the radical

scavenger activity. Instead the covalent linking of an antioxidant group to the surface of the nanosystem allows to reach this goal. For example, AuNPs functionalized with Trolox showed a radical scavenger activity eight times higher than the molecular Trolox at the same concentration.<sup>62</sup> Silica NPs functionalized with 3,5-di-*tert*-butyl-4-hydroxycinnamic acid proved to be more effective as antioxidants compared to analogous nanocapsules containing the same molecule.<sup>93</sup> The high radical scavenger activity of antioxidants directly linked to the surface of silica NPs has also been reported with gallic acid<sup>94</sup>.

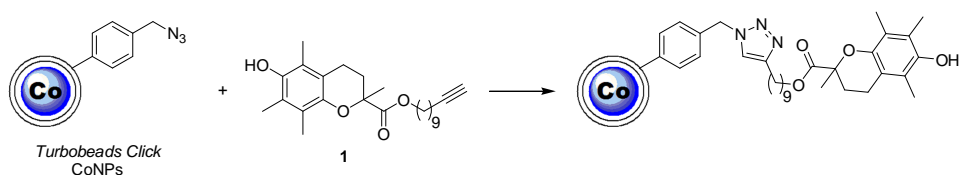
The latter results confirm that the surface modification of MNPs through the covalent bonding with traditional molecular antioxidants is a promising way for obtaining highly effective radical scavenger systems without modifying the original core of the antioxidants.

## 5.2 Results and Discussion

### 5.2.1 Synthesis of antioxidant derivatives for the functionalization of gold nanoparticles (AuNPs)

AuNPs are among the most studied nanosystems for therapeutic and diagnostic applications, especially in cancer therapy as drug delivery systems.<sup>95–97</sup> The reason of the strong interest on these type of MNPs is their ease of synthesis, the chemical stability and excellent optical properties.<sup>98–101</sup> AuNPs are also characterized by an excellent biocompatibility, with several *in vitro* studies that have proved the these systems are not responsible of a strong cytotoxicity.<sup>102</sup> However, like other MNPs, also AuNPs lead to ROS generation and oxidative stress induction in different amount depending on size, shape and surrounding ligands.<sup>34,103–105</sup> It would be then interesting the functionalization of AuNPs with antioxidants molecules in order to suppress their oxidative damage and, ideally, use these systems as pharmacological agents for the treatment of oxidative stress related pathologies.

In the past, our research group developed a derivative of the commercial antioxidant Trolox, a water soluble analogue of  $\alpha$ -TOH, suitable for the functionalization on the surface of *Turbobeads Click* CoNPs.<sup>65</sup> The latter are characterized by a metallic cobalt core surrounded by a graphite layer containing azido functional groups that were used for the linking with the Trolox-like derivative **1** through an azide-alkyne cycloaddition reaction (Scheme 1).



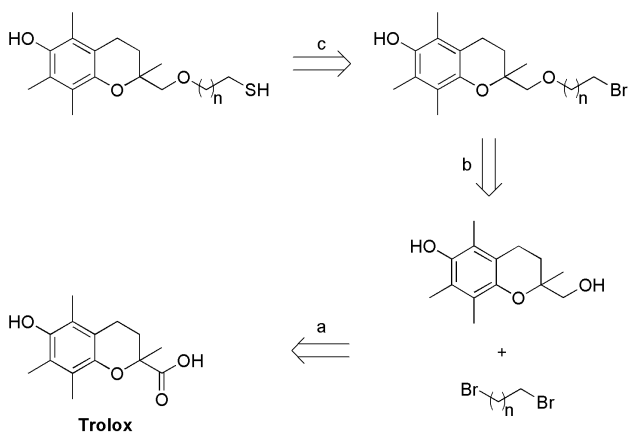
Scheme 1



The resulting CoNPs decorated with **1** showed an outstanding antioxidant activity, then we decided to work on the preparation of an analogous derivative of Trolox suitable for the functionalization with AuNPs. AuNPs are generally stabilized using alkanethiols because, thanks to the soft character of both sulfur and gold, they are able to form a stable covalent bond.<sup>106-109</sup> The insertion of pharmacological active compounds on the AuNPs surface it is indeed generally achieved by using corresponding thiol derivatives.<sup>110</sup> For the preparation of a Trolox-like molecule suitable for the immobilization on AuNPs we had to insert a thiol functionality on its structure taking into account three requirements:

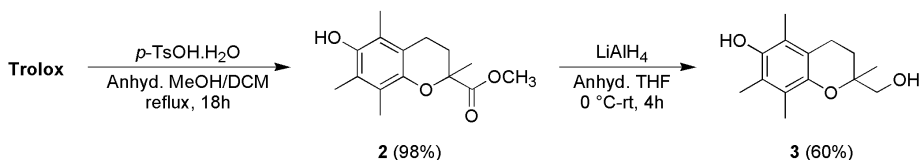
- 1) The active moiety of Trolox, *i.e.* the phenolic chromanol group, could not be modified in order to maintain the antioxidant action.
- 2) The radical scavenger activity of immobilized ligands decreases when they are too close to the anchoring group (the AuNP surface) because their mobility is limited.<sup>111</sup> It was then necessary the insertion of a quite long spacer between the chromanol group of Trolox and the thiol function.
- 3) The esterification on the carboxylic acid group of Trolox is a preferred way for the modification of its structure without worsening its radical scavenger activity, however the *in vivo* lability of esters prompted us to use alternative synthetic routes.

We planned the synthesis of an ether derivative of Trolox bearing a long alkyl chain with a thiol as terminal group (Scheme 2). For this purpose, it was necessary the reduction of the carboxylic group of Trolox to the corresponding alcohol (a) followed by the mono-alkylation with an  $\alpha,\omega$ -di-bromoalkane (b). The final step was the conversion of the terminal bromo-derivative of Trolox to the corresponding thiol (c).



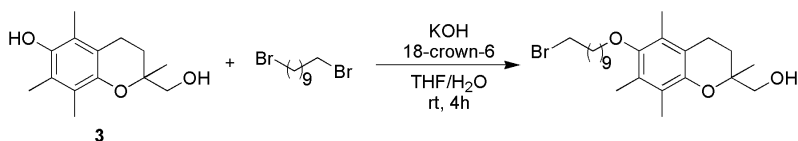
**Scheme 2**

Following two procedures found in literature, the carboxylic acid function of Trolox was reduced to the corresponding alcohol **3** in a two-step way through the reaction of the corresponding methyl ester **2**<sup>112</sup> with LiAlH<sub>4</sub>.<sup>113</sup>



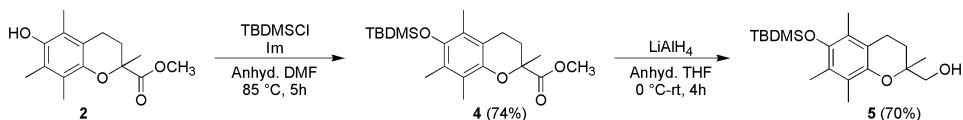
**Scheme 3**

The alkylation of **3** with 1,10-dibromodecane was tried, unsuccessfully, using KOH as base in the presence of the phase-transfer catalyst 18-crown-6.<sup>114</sup> Indeed, despite the steric hindrance around the phenolic OH, the alkylation occurred on this group rather than on the alcoholic one (Scheme 4).



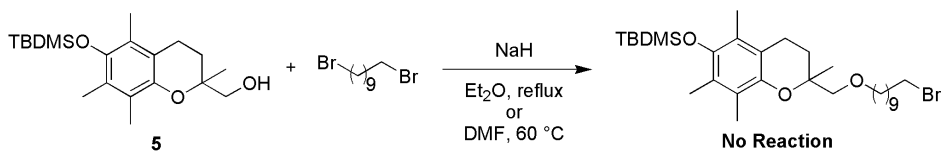
**Scheme 4**

The alkylation was repeated after the protection of the phenolic OH as silyl ether. For this purpose, **2** was reacted with *tert*-butyldimethylsilyl chloride (TBDMSCl) and the resulting silyl ether **4** was converted into the corresponding alcohol **5** using LiAlH<sub>4</sub> (Scheme 5).



**Scheme 5:** Im = imidazole.

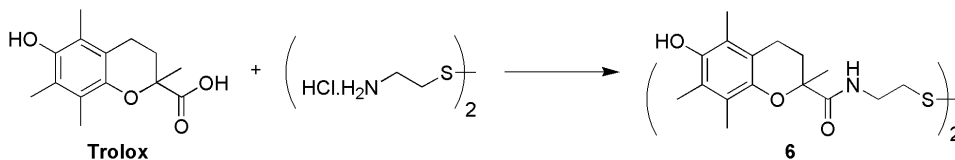
The final step, *i.e.* the alkylation of **5** with 1,10-dibromodecane, was tried using the same procedure depicted for **3** (Scheme 4) but again failed because only starting materials were recovered. The reaction was repeated using sodium hydride as base in diethyl ether at reflux<sup>115</sup> or in dimethylformamide (DMF) at 60 °C<sup>116</sup> but also under these conditions the reaction was unsuccessful (Scheme 6).



**Scheme 6**

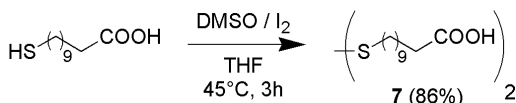
Because of the difficulties encountered in the alkylation of an alcohol derivative of Trolox, we decided to change the synthetic route.

In literature it is reported the synthesis of a Trolox derivative (**6**) by the amidation with cystamine dihydrochloride that was used for the functionalization on AuNPs (Scheme 7).<sup>62</sup>



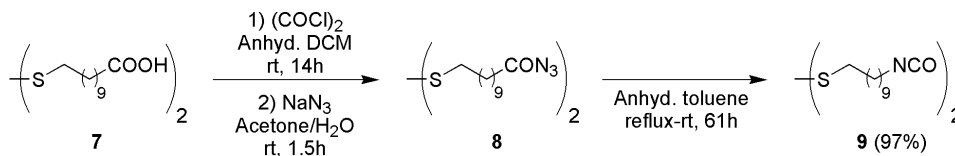
**Scheme 7**

This synthetic way allowed the one-step insertion of a disulfide group directly on the unmodified Trolox skeleton with the contemporary formation of an amide group, typically much more stable *in vivo*. Considering the tendency of thiols to oxidative dimerization the authors synthesized and stored the Trolox derivative as the corresponding disulfide. This was not a problem for the subsequent functionalization on AuNPs because the thiol group can be easily restored before the reaction. Because no commercially available  $\alpha,\omega$ -aminethiols with a long alkyl spacer were available, we synthesized them. For this purpose, 11-mercaptoundecanoic acid was oxidized to the corresponding disulfide **7** as suitable starting material for the preparation of the desired  $\alpha,\omega$ -aminethiol (Scheme 8).<sup>117</sup>



**Scheme 8**

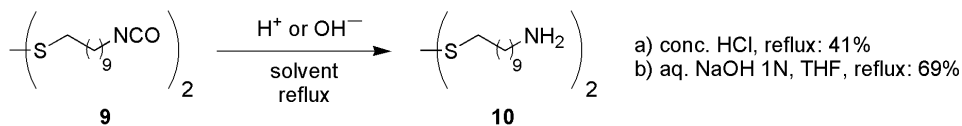
The transformation of the carboxylic groups of **7** to the corresponding amines was accomplished through a synthetic process consisting of three steps. The first was the conversion of the carboxylic group to the acyl azide **8** after the activation of **7** as acyl chloride<sup>118</sup> and the subsequent reaction with sodium azide. The following Curtius rearrangement allowed the formation of the isocyanate **9** in quantitative yield (Scheme 9).



**Scheme 9**

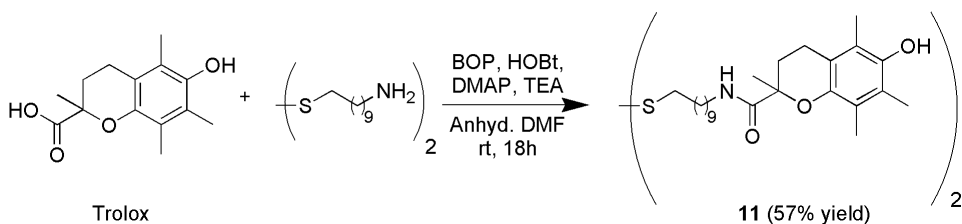
Derivative **9** was subsequently hydrolysed to obtain the desired *bis*-amine **10**. The latter reaction occurred both in acidic and alkaline conditions. The isocyanate hydrolysis in

conc. HCl at reflux<sup>119</sup> gave **10** with a 41% yield, while using aq. NaOH 1N in refluxing THF<sup>120</sup> the yield was increased to 69% (Scheme 10).



### Scheme 10

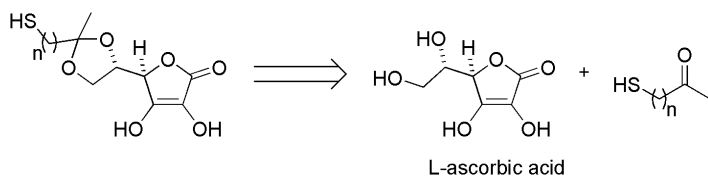
Disulfide **10** was used for the reaction with the carboxylic group of Trolox in the presence of reagents like BOP, HOBT hydrate and DMAP (Scheme 11) that are commonly used for the synthesis of peptides, *i.e.* able to activate the carboxylic group towards the attack of an amine and the subsequent formation of the corresponding amide.



### Scheme 11

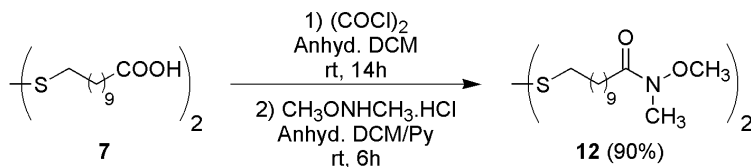
The desired  $\alpha$ -TOH-like derivative **11**, containing a long alkyl chain that ends with a disulfide group, was obtained with a 57% yield and stored as disulfide while waiting for its use for the functionalization of AuNPs.

With the aim to study if and how the nature of the antioxidant influences the radical scavenger activity of the nanostructured system, we focused our efforts on the modification of other common antioxidants in order to allow their functionalization with AuNPs. L-ascorbic acid (vitamin C) is a well-known molecule characterized by an optimal antioxidant activity against different ROS (see **chapter 1**). The 3,4-dihydroxy-5H-furan-2-one moiety is fundamental for the antioxidant activity, thus any modification of its structure had to be done on the dihydroxyethyl substituent. A typical reaction of vicinal diols is the formation of a cyclic acetal after the reaction with a ketone or an aldehyde in mild acid conditions. Cyclic acetals are stable and indeed are commonly used as protecting groups for 1,2-diols because strong acid conditions are necessary for their removal. We planned to modify the structure of L-ascorbic acid by the reaction of its 1,2-dihydroxyethyl group with an appropriate methylketone characterized by a long alkyl chain with a thiol group at the end (Scheme 12).



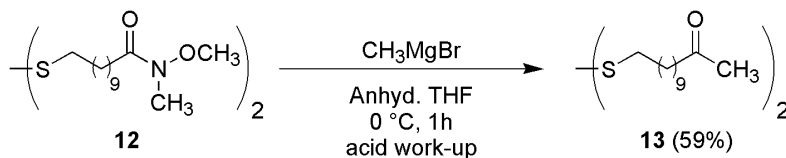
**Scheme 12**

The synthesis of the methylketone started from the disulfide of 11-mercaptoundecanoic acid **7** that was transformed into the corresponding Weinreb amide **12** after the activation of the carboxylic group as acyl chloride and the subsequent reaction with N,O-dimethylhydroxylamine hydrochloride (Scheme 13).<sup>121</sup>



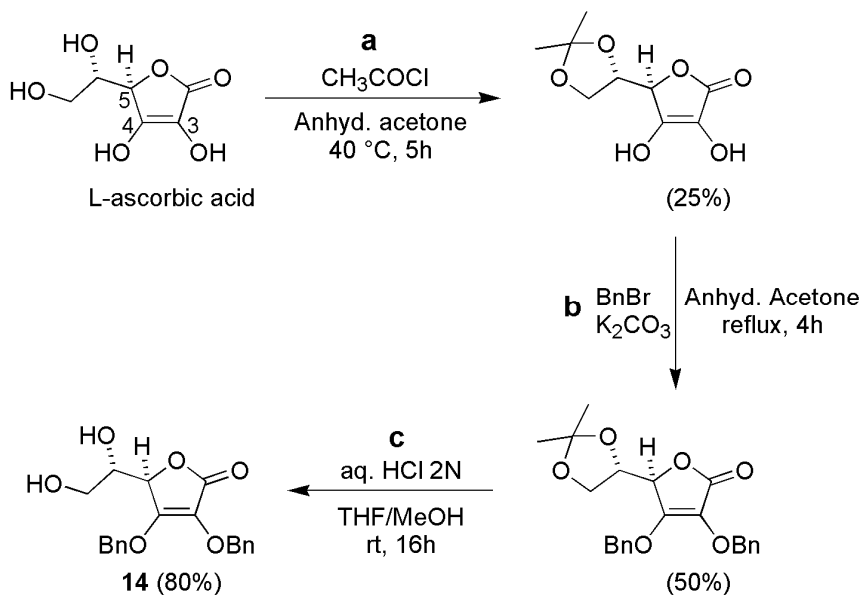
**Scheme 13**

The preparation of a Weinreb amide was done in order to allow, by the reaction with methylmagnesium bromide, the formation of the desired methylketone instead of a tertiary alcohol. The reaction of **12** with methylmagnesium bromide in anhydrous THF allowed the isolation of the methylketone **13** in 59% yield (Scheme 14).<sup>122</sup>



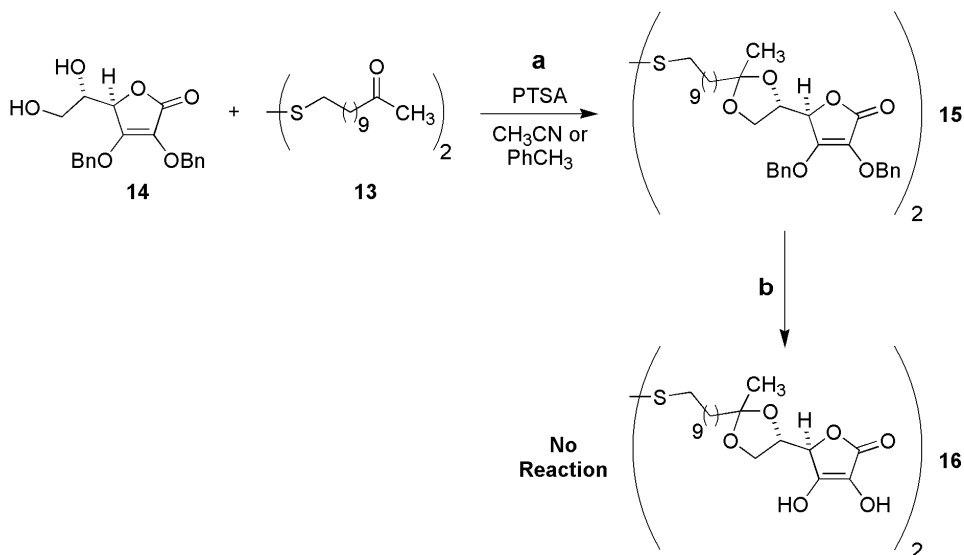
**Scheme 14**

Because of the low solubility of L-ascorbic acid in organic solvents, it was necessary to enhance its liposolubility. For this purpose all the hydroxyl groups of L-ascorbic acid were sequentially protected and deprotected (Scheme 15): first those on C6 and C7 were protected as acetal (a),<sup>123</sup> then those in C3 and C4 as benzyl ethers (b).<sup>124</sup> In the last step the acid hydrolysis of the acetal allowed to obtain the *bis*-benzylated L-ascorbic acid derivative **14** (c) in 80% yield (Scheme 15).<sup>125</sup>



**Scheme 15**

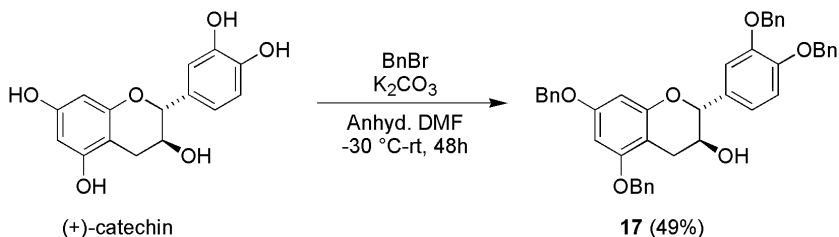
Our plan was to use this molecule, characterized by a good solubility in organic solvents, for the reaction with **13** (a) followed by the cleavage, after the formation of the acetal **15**, of the benzyl ether functions (**b**) in order to restore the hydroxyl groups (**16**) (Scheme 16).



**Scheme 16**

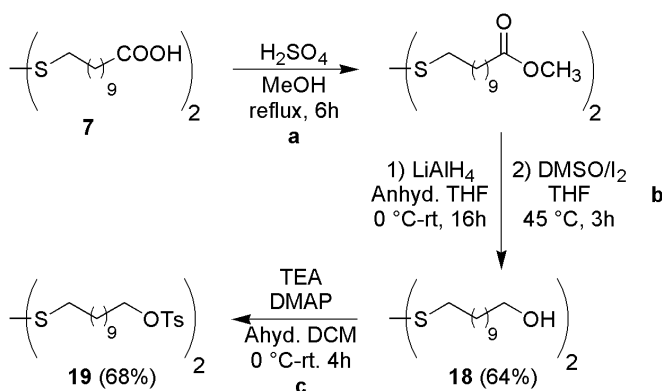
Unfortunately, the reaction of **14** with **13** using *para*-toluenesulfonic acid monohydrate as catalyst did not occur in anhydrous acetonitrile at reflux or in the presence of 4 Å MS in toluene at room temperature.

Due to the poor results obtained with L-ascorbic acid we decided to move to another antioxidant, the flavonoid (+)-catechin. This molecule is characterized by five hydroxyl groups, four of which are phenolic. The catechol ring is necessary for its antioxidant activity and the differentiation among the reactivity of the four phenolic hydroxyls is very difficult. For this reason, the functionalization of (+)-catechin is generally accomplished on the unique alcoholic OH after the protection of the phenolic groups. The reaction of (+)-catechin with an excess of benzyl bromide in the presence of  $K_2CO_3$  allowed the isolation of the tetra-O-benzylated product **17** (Scheme 17).<sup>126</sup>



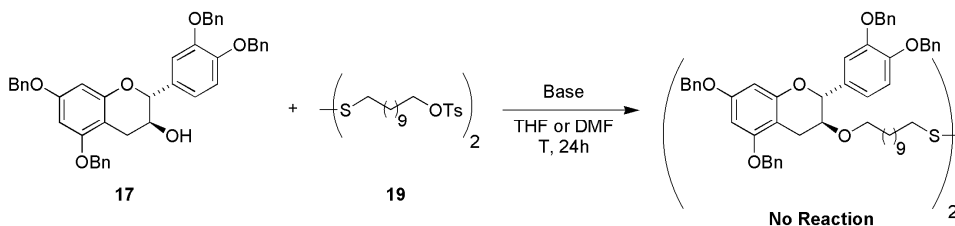
**Scheme 17**

The next step was the modification of the structure of **7** in order to introduce a good leaving group that should have allowed the alkylation with the remaining free OH of **17**. The carboxylic groups of **7** were converted to the corresponding methyl esters<sup>127</sup> (Scheme 18, a) that, in turn, were reduced to the alcohol **18** using  $LiAlH_4$  (Scheme 18, b). Because the conditions used led to the reduction of the disulfide group, the latter was restored by the oxidation with  $DMSO/I_2$ . Finally, the alcohol functions were converted to good leaving groups thanks to the reaction with tosyl chloride ( $TsCl$ , Scheme 18, c).<sup>128</sup> The desired *bis*-tosylated derivative **19** was isolated in 68% yield.



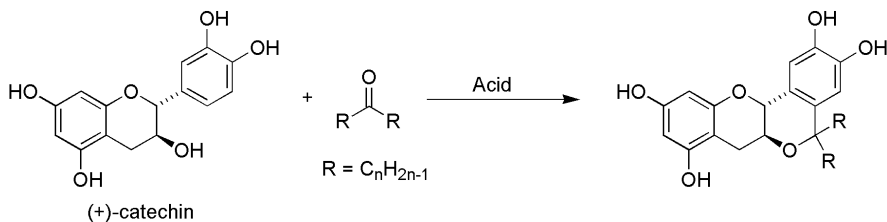
**Scheme 18**

The alkylation of **19** with **17** was tried using NaH, KOH or CsOH as bases and anhydrous DMF or THF as solvents<sup>129-131</sup> both at room temperature and at reflux but in all the cases only starting materials were recovered (Scheme 19).



**Scheme 19**

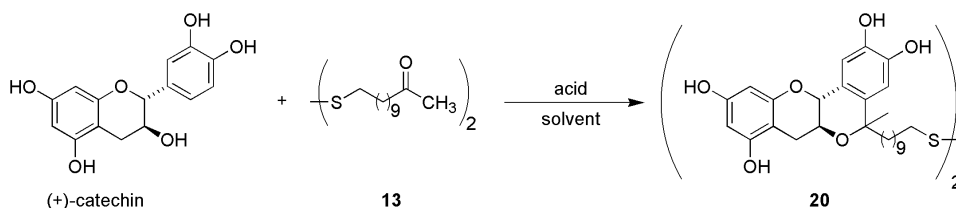
Due to the difficulties met with the nucleophilic substitution for the insertion of a functionalized alkyl chain on the (+)-catechin structure, we decided to change our synthetic strategy. In literature is reported a procedure that allowed the direct modification of the unprotected (+)-catechin without involving the phenolic hydroxyl groups. Indeed the authors reported that it is possible to synthesize an almost planar derivative of (+)-catechin via an oxa-Pictet-Spengler reaction using (+)-catechin and symmetric ketones of different length (Scheme 20).<sup>132,133</sup> The reaction was accomplished using, as acid catalyst,  $\text{BF}_3 \cdot \text{OEt}_2$  in excess when the ketone was acetone, or trimethylsilyl trifluoromethanesulfonate (TMSOTf) in substoichiometric amount when long-alkyl chain ketones were used.



**Scheme 20**

This synthetic way was attractive because it theoretically allowed the insertion of an alkyl chain on the (+)-catechin structure in a single step without the necessity of protecting its phenolic hydroxyls. Moreover, the resulting planar (+)-catechin derivatives showed an enhanced radical antioxidant activity. We decided to use this reaction for the synthesis of a disulfide derivative of (+)-catechin. For this purpose, it was not necessary to prepare a new ketone because an alkylmethyl one was already available, *i.e.* the derivative **13** used in the efforts for the functionalization of L-ascorbic acid. First attempts of the reaction between (+)-catechin and **13** (Scheme 21) in order to obtain **20** failed using both  $\text{BF}_3 \cdot \text{OEt}_2$  and TMSOTf under different conditions (Table 1).





**Scheme 21**

**Table 1:** oxa-Pictet-Spengler reaction between (+)-Catechin and **13**.

Entry <sup>a</sup>	(+)-catechin (equiv)	acid (equiv)	solvent <sup>b</sup>	<b>21</b> (yield %)	<b>20</b> (yield %)
<b>1</b>	1.1	BF <sub>3</sub> .OEt <sub>2</sub> (7.0)	THF	-	-
<b>2</b>	1.1	BF <sub>3</sub> .OEt <sub>2</sub> (7.0)	1,4-dioxane	-	-
<b>3</b>	1.1	BF <sub>3</sub> .OEt <sub>2</sub> (7.0)	Et <sub>2</sub> O	-	-
<b>4<sup>c</sup></b>	1.1	BF <sub>3</sub> .OEt <sub>2</sub> (7.0)	-	-	-
<b>5</b>	1.1	TMSOTf (0.33)	THF	-	-
<b>6</b>	1.1	TMSOTf (0.33)	1,4-dioxane	-	-
<b>7</b>	1.1	TMSOTf (0.33)	Et <sub>2</sub> O	-	-
<b>8<sup>c</sup></b>	1.1	TMSOTf (0.33)	-	Traces	-
<b>9</b>	1.1	<i>p</i> -TsOH (0.1)	MeOH	-	-
<b>10<sup>d</sup></b>	1.1	<i>p</i> -TsOH (0.1)	-	-	-
<b>11<sup>e</sup></b>	1.1	TMSOTf (0.33)	THF	13%	9%
<b>12<sup>e</sup></b>	3.0	TMSOTf (1.0)	THF	-	20%

<sup>a</sup> All the reactions were performed in inert atmosphere at 0 °C during the addition of the acid catalyst and then allowed to heat to r.t.; <sup>b</sup> Anhydrous solvents were used; <sup>c</sup> neat reactions were done under magnetic stirring or sonication; <sup>d</sup> reaction done in a mortar; <sup>e</sup> purified (+)-catechin was used (see experimental section).

Only starting materials were recovered using BF<sub>3</sub>.OEt<sub>2</sub> in THF (entry 1), 1,4-dioxane (entry 2), Et<sub>2</sub>O (entry 3) and without solvents (entry 4). The same results were obtained using TMSOTf (entries 5-7), except when any solvents were used (entry 8) and traces of the derivative **21** (Figure 1) were isolated.

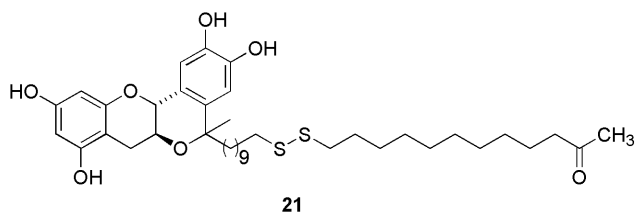


**Figure 1**

Using *p*-TsOH as catalyst resulted in the total absence of reactivity (entries 9-10). Because the presence of residual water in commercial (+)-catechin hydrate could deactivate the catalyst, the antioxidant was purified. In this way, using TMSOTf (0.33 equiv) as catalyst and THF as solvent, we were able to isolate the desired product **20** in 9% yield, even though the major product was **21** (13%, entry 11). Finally, by increasing the amount of both purified (+)-catechin and TMSOTf it was possible to obtain **20** as unique product in 20% yield (entry 12). The final yield was not excellent but alternative methods for the functionalization of (+)-catechin requires the protection and the final deprotection of all of the phenolic hydroxyls of the flavonoid. Instead the oxa-Pictet-Spengler reaction allowed to exploit a specific reactivity of alcoholic hydroxyls thus avoiding the protection and deprotection steps.

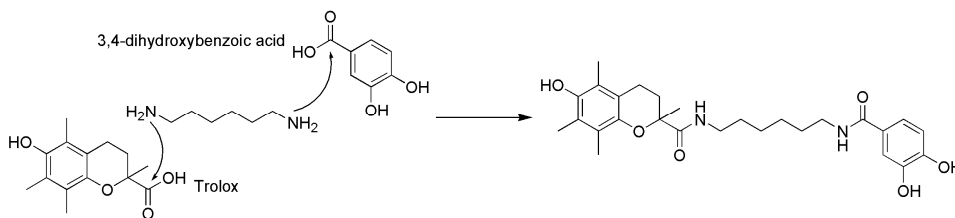
The two antioxidant derivatives prepared for the functionalization of AuNPs, **11** and **20**, have been sent to the research group of professor V. M. Rotello of the University of Massachusetts Amherst (Amherst, USA) for the preparation of the corresponding gold nanostructured antioxidants and the relative characterization of their biological activity in terms of cellular internalization and anticancer activity.

## 5.2.2 Synthesis of antioxidant derivatives for the functionalization of superparamagnetic iron oxide nanoparticles (SPIONs)

Thanks to their outstanding and unique properties, SPIONs are probably the most studied nanostructured system for biomedical applications. Their most important property is the superparamagnetism that allows their detection in MRI.<sup>134</sup> However, the applications of SPIONs are not limited to the bioimaging but also to drug and gene delivery, cell labelling, biosensing and many others.<sup>37</sup> Like other types of nanosystems, also the toxicity of SPIONs is mostly related to the production of ROS and the subsequent arise of oxidative stress. It was then interesting to coat the surface of SPIONs in order to minimize their potential toxicity and, eventually, allows their use as therapeutic agents for stress related pathologies. The surface of SPIONs can be functionalized with ligands bearing different reactive groups at one end. There is a significant literature data about the coating of iron oxide nanoparticles for biomedical applications, in most cases with water-soluble polymers in order to enhance their solubility in the physiological media.<sup>135</sup> It is reported that the functionalization of SPIONs like magnetite (Fe<sub>3</sub>O<sub>4</sub>) and maghemite (γ-Fe<sub>2</sub>O<sub>3</sub>) can be achieved using sulfonates,<sup>136</sup> phosphonates,<sup>137-139</sup> carboxylates,<sup>140</sup> catechols<sup>141-146</sup> and silicates<sup>147-149</sup>. However, most of these groups are able to significantly reduce the magnetization of

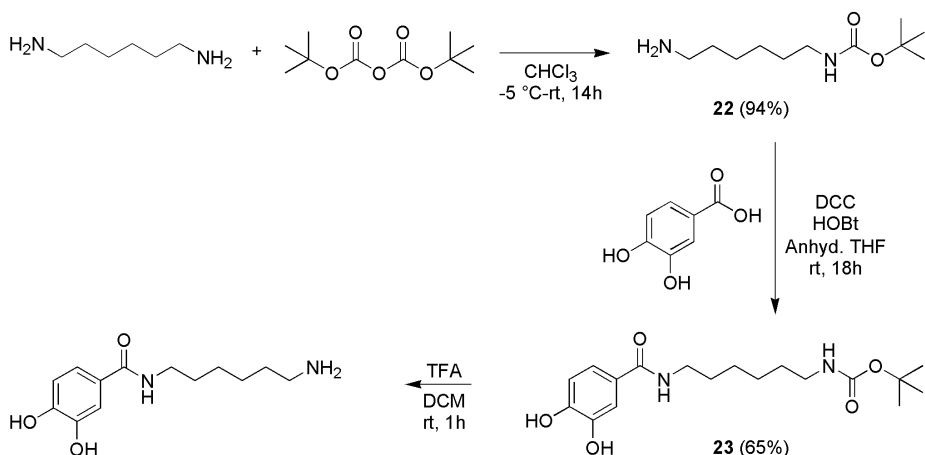
SPIONs,<sup>150</sup> then it is important to use a linking function that forms a strong bond with the nanoparticle surface without negatively affecting its magnetic properties. Catechols are among those groups that comply with these requirements. Indeed, Fe<sup>3+</sup> forms extremely stable complexes with bidentate catechol ligands and the resulting bond is highly covalent.<sup>151</sup> A natural phenomenon that well explains this property of catechol ligands are the adhesive proteins of mussels, that are able to strongly bond with rock surfaces (characterized by a high content of metal oxides) because of the presence of multiple L-DOPA residues in their structure.<sup>152</sup> Moreover iron oxide nanoparticles covered with these bidentate ligands preserve their magnetic properties.<sup>151</sup>

The preparation of nanostructured antioxidants based on SPIONs started from the derivatization of Trolox in order to introduce a long alkyl chain ending with a catechol group. As said in section 5.2.1, the presence of a long alkyl chain between the antioxidant molecule and the anchoring group is necessary for a better mobility of its active moiety when is immobilized on the nanoparticle surface. It is also important to avoid the presence of *in vivo* labile groups like esters. Considering the good results achieved with the preparation of the product **11**, we planned to use a similar synthetic strategy based on amidation reactions. In more detail, we decided to use an  $\alpha,\omega$ -alkyldiamine like 1,6-hexanediamine to link the carboxylic groups of Trolox and of 3,4-dihydroxybenzoic acid at each end, respectively (Scheme 22).



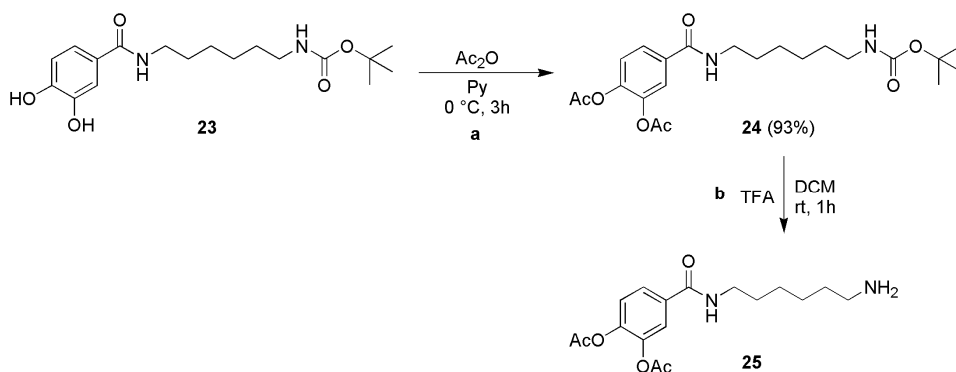
**Scheme 22**

Being very difficult the control of simultaneous amidation of two different carboxylic acid derivatives on an  $\alpha,\omega$ -alkyldiamine, one of the two amine groups of 1,6-hexanediamine was protected with di-*tert*-butyl dicarbonate (Scheme 23, a)<sup>153</sup> and the resulting *mono*-Boc derivative **22** was used for the amidation with 3,4-dihydroxybenzoic acid in the presence of DCC and HOBt (Scheme 23, b). The amide **23** was isolated in 65% yield.<sup>154</sup>



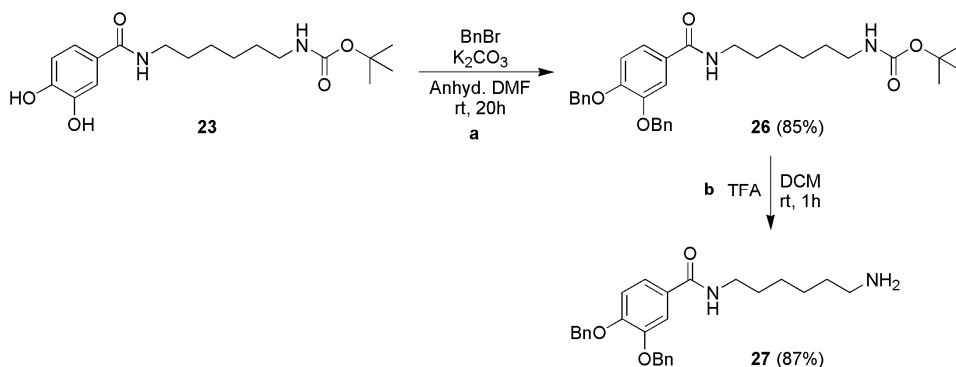
### Scheme 23

The following deprotection of the Boc-protected amine of derivative **23** was tried using an excess of TFA in dichloromethane (Scheme 23, c)<sup>155</sup> but, despite with these conditions the removal of the protecting group occurred, the isolation of the resulting product proved to be difficult. Probably, the simultaneous presence of highly polar groups with opposite acid-base properties like a catechol and an amine makes very difficult to find the exact pH conditions for the extraction of this molecule from water to the organic phase during the work-up. The hydroxyl groups of **23** were then protected as acetyl esters (Scheme 24, a)<sup>156</sup> but, also with the obtained derivative **24**, we came across to the same problems of isolation of the free amine **25** after the deprotection with TFA (Scheme 24, b).



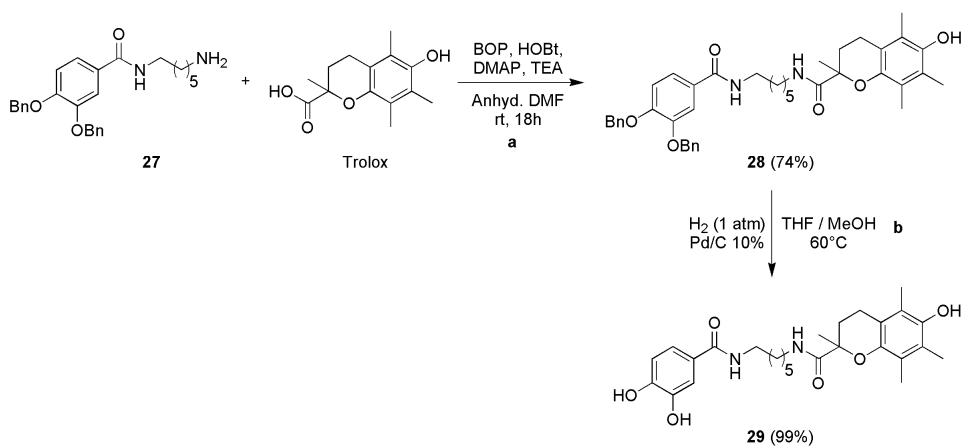
### Scheme 24

A more lipophilic protecting group instead of an acetyl ester was chosen in order to facilitate the solubilization of the free amine in organic solvents. Indeed, after the protection of **23** with benzyl bromide (Scheme 25, a)<sup>157</sup> the resulting product **26**, obtained in 85% yield, was easily deprotected from the Boc group using TFA in DCM. The amine **27** was isolated in 87% yield (Scheme 25, b).



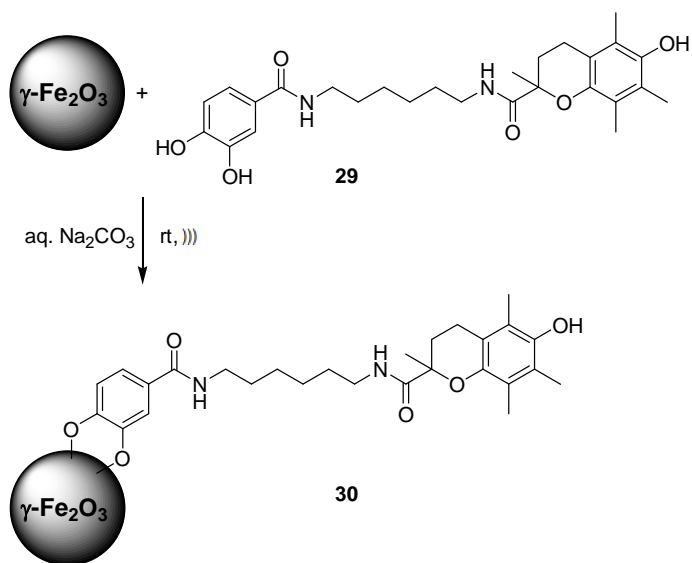
### Scheme 25

The amidation between the carboxylic group of Trolox and the amine group of **27** was done in the same conditions used for the synthesis of **11** (Scheme 11), *i.e.* in the presence of reagents that are commonly used for the synthesis of peptides like BOP, HOBT hydrate and DMAP. In this way we were able to isolate the *bis*-amide derivative **28** in 74% yield (Scheme 26, a). Finally the protecting groups were removed by catalytic hydrogenation, leading to the formation of **29** in quantitative yield (Scheme 26, b).<sup>155</sup>



### Scheme 26

Commercially available  $\text{Fe}_2\text{O}_3$  nanoparticles of 8-10 nm were functionalized with the ligand **29** in a 0.1 M water solution of  $\text{Na}_2\text{CO}_3$  (Scheme 27).<sup>158</sup>



**Scheme 27**

Due to the paramagnetism of these systems, their magnetic agitation with a metallic bar had to be avoided because the nanoparticles are magnetically attracted by the bar. With the sonication, symbolized with the icon ))) in Scheme 27, we were able to obtain a homogenous agitation of the reaction mixture. To check the actual functionalization of the nanoparticles (**30**), being impossible to use NMR spectroscopy due to their paramagnetic nature, FT-IR spectroscopy and TGA analysis were used.

It is reported in literature<sup>159</sup> that when the binding of the catechol to the metal oxide surface takes place the two distinct C-O stretching absorptions of catechol in the region  $1250\text{-}1279\text{ cm}^{-1}$  develop into one band. Indeed, in the FT-IR of the product **29** two signals are present at  $1292$  and  $1259\text{ cm}^{-1}$  (Figure 2 a) and, after the reaction with  $\gamma\text{-Fe}_2\text{O}_3$  nanoparticles, only one absorption peak at  $1281\text{ cm}^{-1}$  is visible in the same area suggesting that the functionalization took place (Figure 2, b).

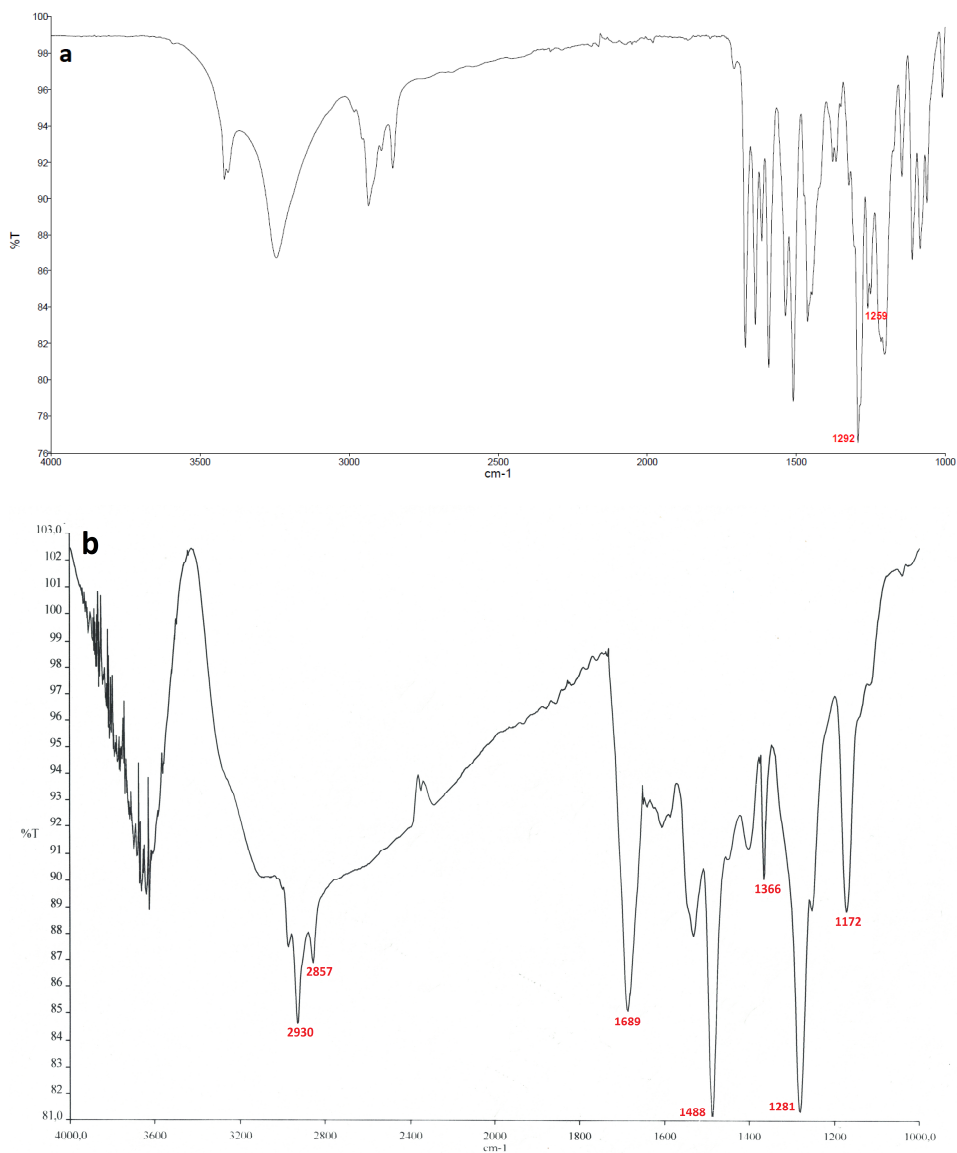


**Figure 2**

TGA analysis gave further interesting results. Indeed in the thermogram of **30** between 35 and 710 °C there is a weight loss of 17.3% (Figure 3, down) while, in the same range, the weight loss of bare  $\gamma$ -Fe<sub>2</sub>O<sub>3</sub> is 5.0% (probably related to the desorption of physically and chemically adsorbed water)<sup>160</sup> (figure 3, top). From the difference between the two values we can assert that the loading of the antioxidant ligand on the nanoparticles is roughly 12%. After the oxygen insertion a weight increase of 4.5% is registered for **30**, a

not well explainable phenomenon that actually occurred, even if negligible, in bare  $\gamma\text{-Fe}_2\text{O}_3$ .

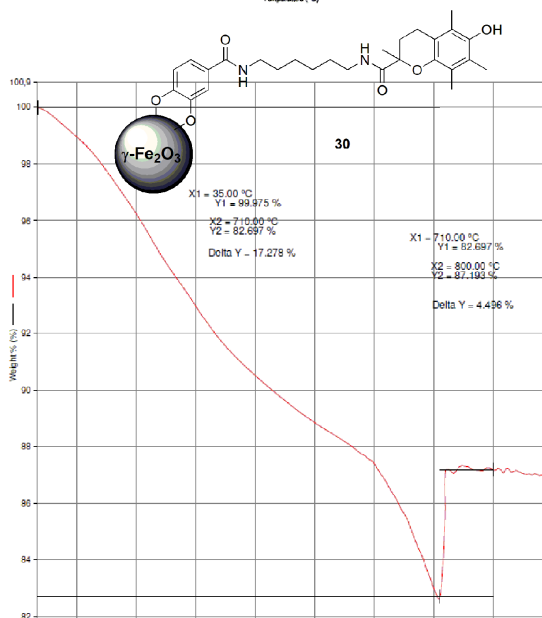
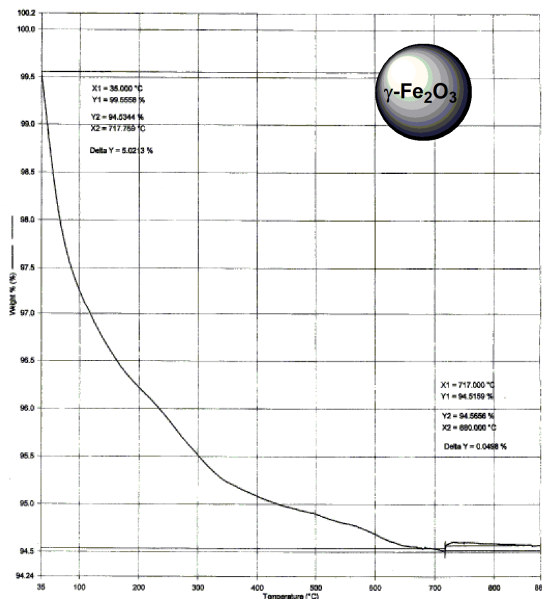


**Figure 3**

Our work with SPIONs allowed the functionalization of their paramagnetic core with an antioxidant analogous of  $\alpha\text{-TOH}$  synthesized with simple reactions and in moderate good overall yield (40%). The complete physico-chemical characterization and the



evaluation of the antioxidant activity of this nanostructured antioxidant is currently underway.

### 5.2.3 Synthesis of antioxidant derivatives for the functionalization of cobalt nanoparticles (CoNPs)

Our work on the preparation of nanostructured antioxidants took into consideration cobalt nanoparticles that, like SPIONS, are superparamagnetic systems. The use of pure metallic nanoparticles is not possible because they are pyrophoric and easily oxidized by the atmospheric oxygen, then they are generally used as metallic alloys or are isolated with an external shell.<sup>161</sup> In the case of CoNPs, the metallic core can be coated with some layers of carbon that makes them air stable without negatively affecting their magnetic properties.<sup>162</sup> Some of these systems are commercially available and are characterized by a metallic core of about 30 nm of diameter coated by approximately three graphene-like carbon layers. The external carbon layer is functionalized with specific reactive groups (azide, amine, carboxylic acid) in order to allow the coating of the nanoparticles with the desired ligands. In this way a superparamagnetic core, a protective shell and appropriate functional groups, all of them highly effective, are joined in a single nanostructured system. Some of the application of these nanoparticles are in biochemistry, magnetic catalysis, heavy metal removal from water, and DNA purification and handling.<sup>163</sup>

The CoNPs used for our work were of two types labelled as *Turbobeads Click* (Co-N<sub>3</sub>) and *Turbobeads Amine* (Co-NH<sub>2</sub>) because functionalized with azido and primary amine groups, respectively (Figure 4).

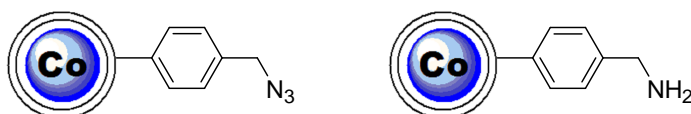


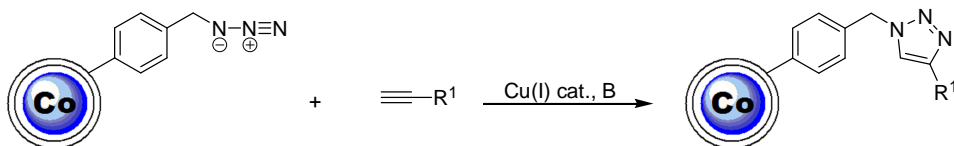
**Figure 4**

For both the products the functional loading is about 0.1 mmol/g. The preparation of nanostructured antioxidants from these systems required, first of all, the synthesis of tailor-made molecular antioxidants specifically designed for exploiting the specific reactivity of the reactive groups anchored on the Co-NPs surface.

#### *Acetylenic derivatives for the functionalization of Turbobeads Click*

The presence of azido groups on the surface of *Turbobeads Click* nanoparticles (Co-N<sub>3</sub>) can be exploited for the functionalization with organic ligands by a Copper (I) catalyzed azide-alkyne cycloaddition (CuAAC).<sup>164</sup> This reaction derives from the Huisgen cycloaddition and is often reported as a typical example of click chemistry, *i.e.* a group of reactions characterized by high yields and control of the stereochemistry, wide in scope, formation of byproducts easily removable without chromatography, and simple to perform. Additionally these reactions are generally performed in "green" or easily removable solvents.<sup>165</sup> In the presence of a Cu(I) catalyst and a base the azido group

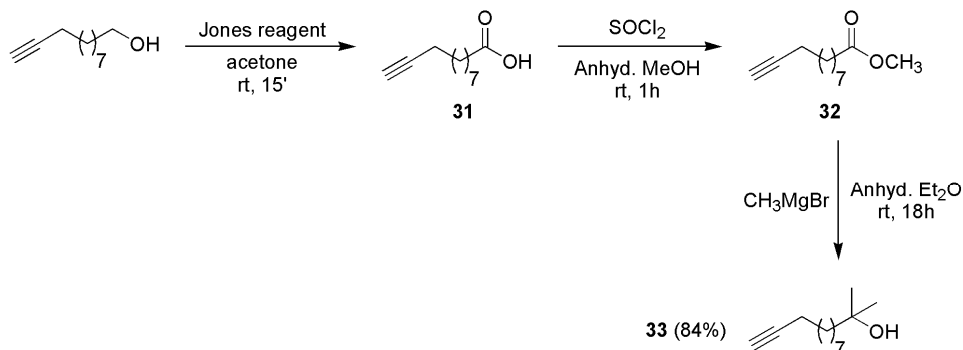
reacts with terminal alkynes leading to the regioselective formation of a 1,4-disubstituted triazole (Scheme 28).



**Scheme 28**

As catalyst can be used a copper(I) salt, like CuI, or a mixture of a copper(II) salt together with a reducing agent like CuSO<sub>4</sub> and sodium ascorbate, respectively. One of the main advantages of this reaction is that the triazole is stable in several conditions and then allows a strong anchoring of the ligand on the nanoparticle surface.

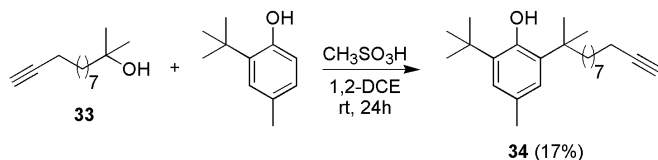
Our scope was the synthesis of a BHT-like molecule bearing a terminal alkyne group suitable for the cycloaddition with the Co-N<sub>3</sub> azido functionalities. Among the several known antioxidants, the choice of BHT as reference compound was related to the massive use of this molecule in numerous applications. **BHT** (see section 3.1) is indeed one of the main antioxidants used to retard the oxidative degradation of different systems like food, polymers, and fuels. Moreover, its simple structure makes possible a series of different chemical modifications that amplify the possible uses. We decided to prepare a derivative analogue to the product **ch3-p2** (see Scheme 16 section 3.3.1) using the same procedure but with a terminal alkyne instead of a double bond. A long alkyl chain bearing at one end a triple C-C bond and at the other a tertiary alcohol was synthesized. 10-undecyn-1-ol was oxidized to the corresponding carboxylic acid **31**<sup>166</sup> which, in turn, was esterified with methanol and SOCl<sub>2</sub><sup>167</sup>. The methyl ester **32** was finally alkylated using methylmagnesium bromide so as to give the desired tertiary alcohol **33** with an 84% overall yield (Scheme 29).



**Scheme 29**

The Friedel-Crafts alkylation of **33** with 2-*tert*-butyl-4-methylphenol was carefully optimized in the same way seen for the preparation of the derivative **ch3-p2** and, also

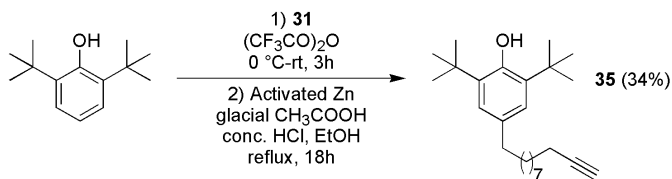
in this case, it was possible to obtain the desired product **34** (17% yield) only when  $\text{CH}_3\text{SO}_3\text{H}$  was used as acid catalyst (Scheme 30).



### Scheme 30

Actually, the conditions used were not identical because, while for the synthesis of **ch3-p2** a slight excess of  $\text{CH}_3\text{SO}_3\text{H}$  and a substoichiometric amount of phenol were used, for the synthesis of **34** the tertiary alcohol and the phenol were equimolar and the acid in large excess (3.57 equiv).

Another BHT-like derivative suitable for the functionalization of  $\text{Co-N}_3$  was prepared taking advantage, again, of the researches done for the synthesis of the olefinic BHT-like comonomers described in chapter 3. Indeed, the one-pot procedure optimized for the synthesis of **ch3-p9** was theoretically suitable also for the preparation of an analogous acetylenic derivative. Actually, using exactly the same procedure, *i.e.* a Friedel-Crafts acylation of **31** with 2,6-di-*tert*-butylphenol catalysed by trifluoroacetic anhydride followed by a Clemmensen reduction in the presence of activated zinc, conc. HCl and acetic acid, it was possible to isolate the desired product **35** in 34% yield (Scheme 31).



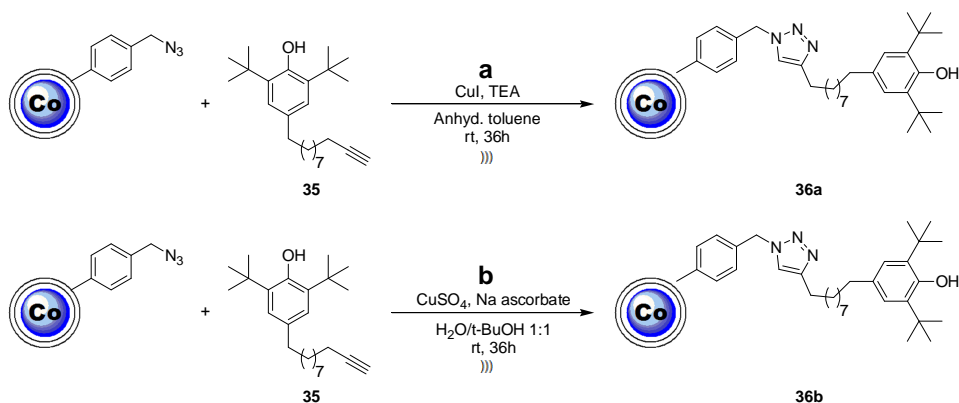
### Scheme 31

#### Functionalization of Turbobeads Click

The two BHT-like derivatives obtained were used for the functionalization of *Turbobeads Click* nanoparticles.

The derivative **35** was reacted with  $\text{Co-N}_3$  using two different procedures (Scheme 32):

- a) A salt of  $\text{Cu}^+$  ( $\text{CuI}$ ) was directly used in the presence of TEA as base and anhyd. toluene as solvent.<sup>65</sup>
- b) The source of copper was  $\text{CuSO}_4$  and the reaction was done in the presence of sodium ascorbate, that is the agent responsible of the reduction of  $\text{Cu}^{2+}$  to  $\text{Cu}^+$ , and water/*tert*-butanol as solvent.<sup>168</sup>



**Scheme 32**

In the procedure **a**, to the suspension of **Co-N<sub>3</sub>**, were added in sequence **35** (10 equiv), CuI (0.5 equiv) and TEA (5 equiv), then the suspension was sonicated at room temperature under nitrogen for 24h and a second addition of the same amount of CuI and TEA were done. The sonication was continued for further 12h. In the procedure **b** the **Co-N<sub>3</sub>** were suspended in water/*tert*-butanol 1/1 before the addition of sodium ascorbate (1.5 equiv) and CuSO<sub>4</sub> (0.05 equiv). The suspension was sonicated at room temperature under nitrogen for 36h.

<sup>1</sup>H-NMR spectrum of the solvents used for work-up showed that the unbounded ligands in excess were recovered unchanged. FT-IR spectroscopy was used to evaluate the occurred functionalization on **Co-N<sub>3</sub>** because the signal relative to the azide cumulated stretching at 2100 cm<sup>-1</sup> disappears when the CuAAC reaction occurs. Actually, the spectrum of the bare **Co-N<sub>3</sub>** showed a signal at 2100 cm<sup>-1</sup> relative to the azide stretching (figure 5) that completely disappeared in the spectrum of **36a** (Figure 6) while in that of **36b** a tiny signal at 2099 cm<sup>-1</sup> was still visible (Figure 7).

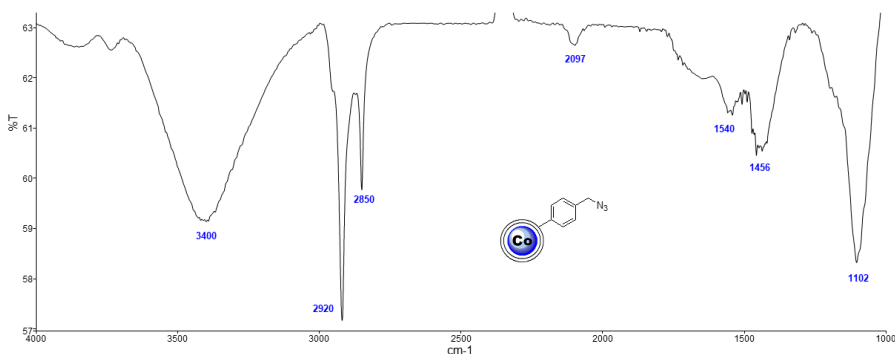


**Figure 5**

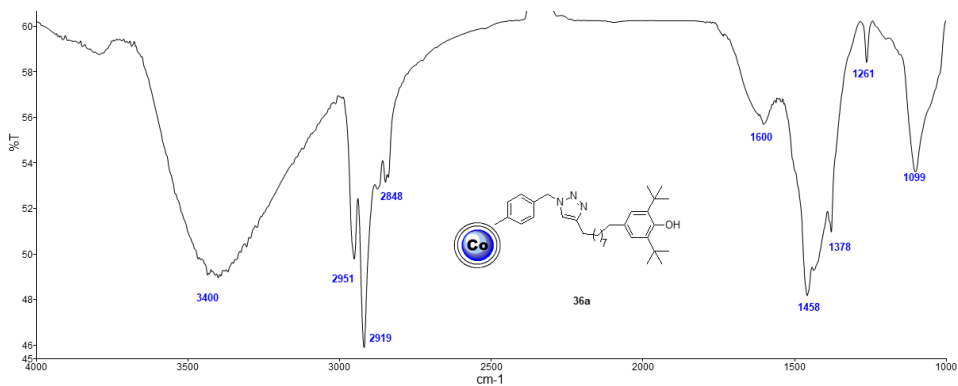


**Figure 6**

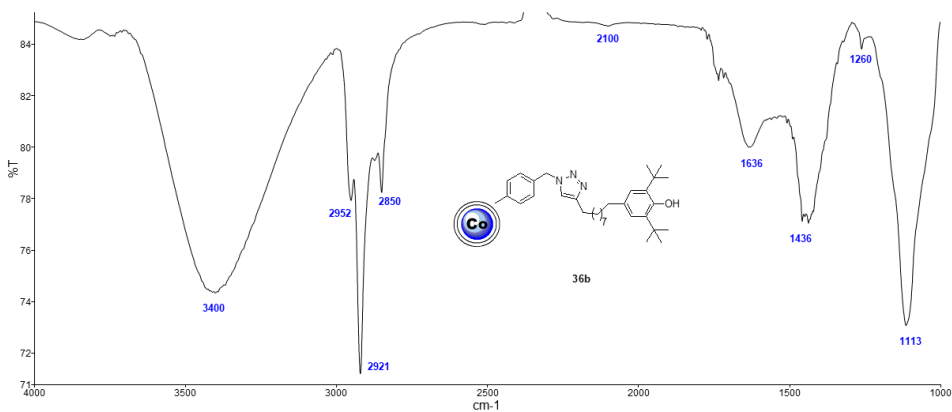
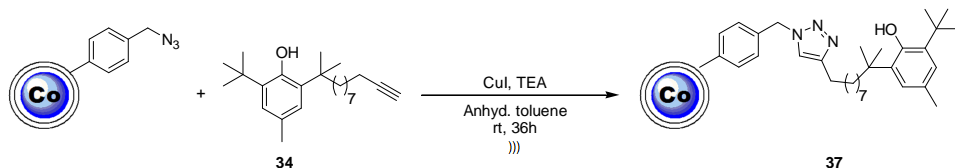


**Figure 7**

These results suggested that with both the procedures the functionalization occurred successfully but a better functionalization was probably achieved with the procedure **a**. For this reason, the functionalization of Co-N<sub>3</sub> with **34** was done using only the procedure **a** (Scheme 33).



**Scheme 33**

The FT-IR spectrum of the product obtained (**37**) showed also in this case the complete disappearance of the azide signal at 2100 cm<sup>-1</sup> thus confirming the actual reaction with the BHT-like derivative **34** (Figure 8).

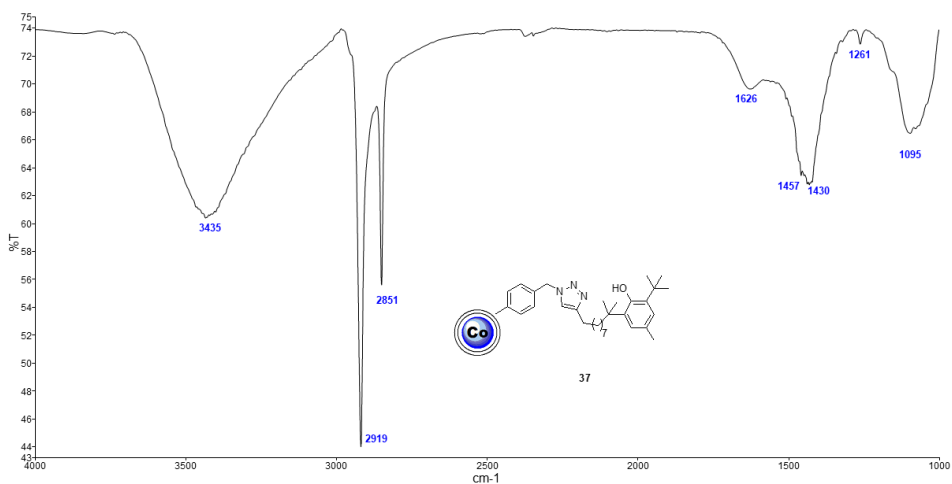


**Figure 8**

Further proofs of the functionalization of Co-N<sub>3</sub> were given by thermogravimetric analysis (TGA) performed by Dr. Stagnaro at ISMAC CNR, Genova. This technique allows to measure the change in weight of a sample when is exposed to heating and is often use to deduce the content of organic ligands on nanoparticles.<sup>169</sup> Indeed, when these systems are heated, some of the measured weight loss is due to the thermal degradation of the molecules bound to their surface. The experiments were done as follows. Between 35 and 700 °C the TGA analysis was performed under N<sub>2</sub> gas, then the weight loss measured in this range is due to non-oxidative processes. After 700 °C the purge gas was switched to oxygen therefore the subsequent weight loss is due to oxidative degradation processes. For all the samples above 700 °C there was a further decrease in weight followed by its rapid increase. The latter phenomenon is probably due to the oxidation of the cobalt core to cobalt oxide that occurs once the graphite-like protective shell is completely degraded. First of all, a thermogram of the bare Co-N<sub>3</sub> was done in order to have a reference (Figure 9).

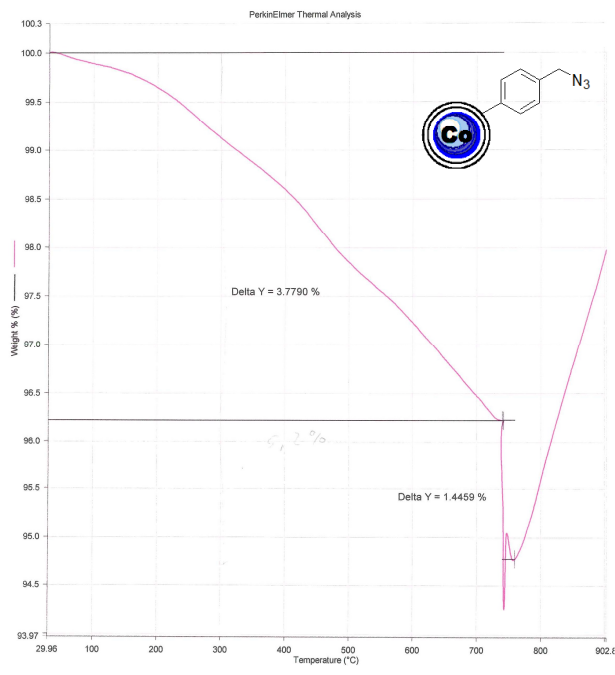


**Figure 9**

In the thermogram of bare Co-N<sub>3</sub> there is a weight loss of 3.8% during the thermal degradation between 35 and 700 °C, then a further decrease of 1.4%. The loading of **36a**, **36b** and **37** was evaluated by the difference in percentage weight loss during the thermal degradation ( $\Delta W\%_{35-700}$ ) respect to the reference Co-N<sub>3</sub> (Table 2).

**Table 2:** weight losses of antioxidant functionalized CoNPs during TGA analysis.

Sample	Weight loss % (35-700 °C)	$\Delta W\%_{35-700}^a$
Co-N <sub>3</sub>	3.8	0
<b>36a</b>	5.1	1.3
<b>36b</b>	4.3	0.5
<b>37</b>	3.9	0.1

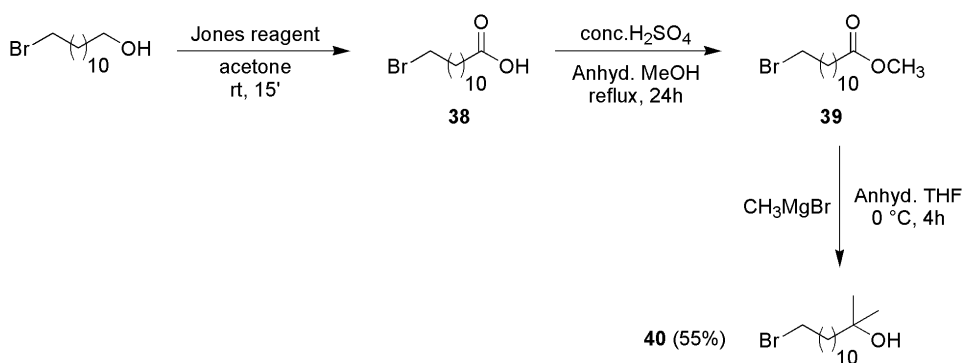
<sup>a</sup>  $\Delta W\%_{35-700} = (\% \text{ weight loss of the sample between 35 and 700 } ^\circ\text{C}) - (\% \text{ weight loss of Co-N}_3 \text{ between 35 and 700 } ^\circ\text{C})$ .

The values of  $\Delta W\%_{35-700}$  showed that the loading of ligand in **36a** is higher (1.3%) than in **36b** (0.5%), thus confirming that the procedure **a** allowed a more efficient functionalization of Co-N<sub>3</sub>. Instead, it seems that in **37** the functionalization occurred but in lower yield.

### Halogenated derivatives for the functionalization of Turbobeeds Amine

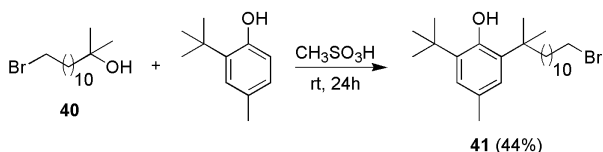
We worked also on the functionalization of another type of cobalt nanoparticles, Turbobeeds Amine (Co-NH<sub>2</sub>), characterized by the presence of primary amine groups on their surface. The choice of these systems was done in order to study if the radical scavenger activity of nanostructured antioxidants is also related to the chemical nature of the anchoring group. Moreover, the presence of primary amines allowed to use a well-known reaction for the functionalization, *i.e.* a nucleophilic substitution. For the functionalization of Co-NH<sub>2</sub> we focused on the preparation of BHT-like molecules bearing a primary organohalide in order to allow a S<sub>N</sub>2 reaction with the CoNPs amine groups. Two derivatives were obtained using the same synthetic strategy used for the preparation of **34** and **35**.

12-bromododecan-1-ol was oxidized to the corresponding carboxylic acid **38** and then converted to the methyl ester **39**<sup>170</sup>. In the last step methylmagnesium bromide was used for the synthesis of the tertiary alcohol **40** (Scheme 34).<sup>171</sup>



### Scheme 34

The Friedel-Crafts acylation of **40** with 2-*tert*-butyl-4-methylphenol was achieved using CH<sub>3</sub>SO<sub>3</sub>H as acid but, differently from the preparation of **34**, using 1,2-DCE as solvent the yield was very low (8%). Instead increasing the excess of acid from 3.57 to 5.0 and performing the reaction in neat the yield of **41** was increased to 44% (Scheme 35).

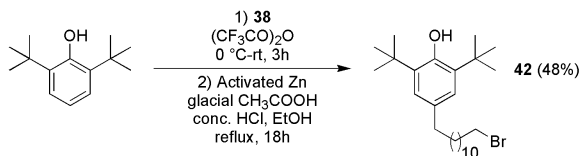


### Scheme 35

The second derivative was obtained through the one-pot procedure used for the preparation of **35** constituted by a Friedel-Crafts acylation and a Clemmensen reduction. The carboxylic acid **38** was reacted with 2,6-di-*tert*-butylphenol in the



presence of trifluoroacetic anhydride, then the transient alkylaryl ketone was reduced using activated zinc, conc. HCl and acetic acid (Scheme 36).

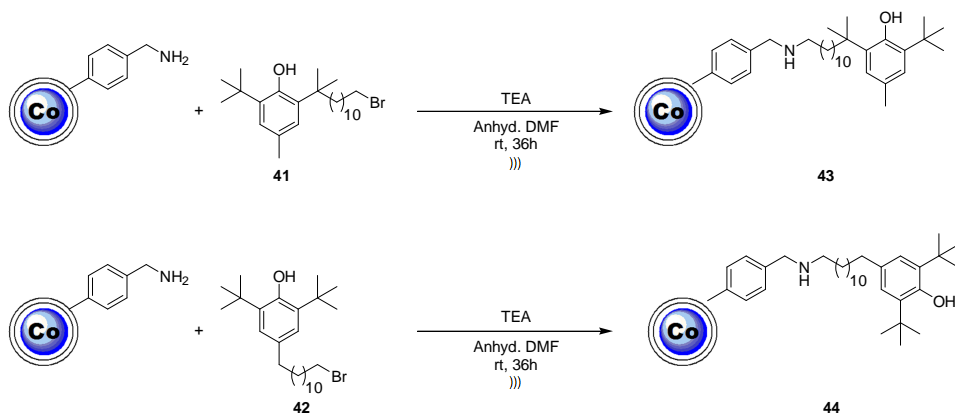


**Scheme 36**

The desired product **42** was obtained in 48% yield.

#### Functionalization of Turbobeads Amine

The two derivatives **41** and **42** were used for the functionalization of Co-NH<sub>2</sub> with a procedure found in literature<sup>172</sup> for S<sub>N</sub>2 reactions that required the use of TEA as base in dry DMF (Scheme 37). The reactions were done using a strong excess of the ligand (10 equiv of **41** or **42**) because first experiments using 1.1 equiv showed that a competing β-elimination reaction occurred.



**Scheme 37**

The FT-IR characterization of **43** and **44** was not as simple as for **36a-b** or **37** because, despite the transformation of a primary to a secondary amine is theoretically detectable by the development of the two N-H stretching to a single signal, in the same IR region there is a strong overlapping band. Indeed, the FT-IR spectra of pure Co-NH<sub>2</sub> (Figure 10, A) and **43** and **44** were very similar (Figure 11, B and C), except below 1700 cm<sup>-1</sup> where different signals were present thus suggesting that some reaction occurred.

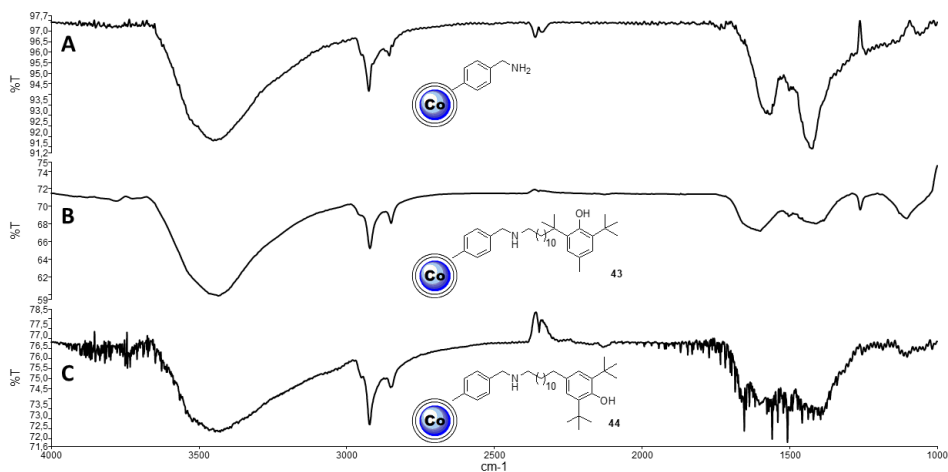


**Figure 10**

The TGA analysis of **43** and **44** reported a weight loss of 8.2 and 9.8% respectively and, despite we are waiting for the thermogram of pure Co-NH<sub>2</sub> as comparison, these values are clearly higher than those obtained with the functionalized Co-N<sub>3</sub> (see table 2, sample **36a-b** and **37**).

### 5.2.3.1 Evaluation of the antioxidant activity of CoNPs-AntiOx

All of our nanostructured products (CoNPs-AntiOx) were evaluated for their potential antioxidant activity through the measurement of the kinetic rate constant of inhibition ( $k_{inh}$ ) of the autooxidation of styrene, an experimental technique that allows to determine the ability of an antioxidant to quench peroxy radicals. The higher the  $k_{inh}$ , the better is the antioxidant activity.

The measures of the inhibition constants have been done by the research group of Dr. R. Amorati of the University of Bologna in the same way described in Chapter 2 but with a slight modification. Indeed, it was impossible to inject the magnetic CoNPs dispersions then they were previously dispersed by sonication for 5'. Moreover, because magnetic Co-NPs are prone to agglomerate around metal objects, a non-metallic stirrer was used in order to allow a good stirring during the experiment. The curves of the sample **36a**, **36b** and **37**, together with those of BHT and Co-NH<sub>2</sub>, are plotted in the diagram of Figure 11, where the pressure of oxygen is reported on the y axis and the time on the x axis. From these curves the values of  $k_{inh}$  and the number of peroxy radicals trapped by each antioxidant molecule ( $n$ ) were obtained (Table 4).

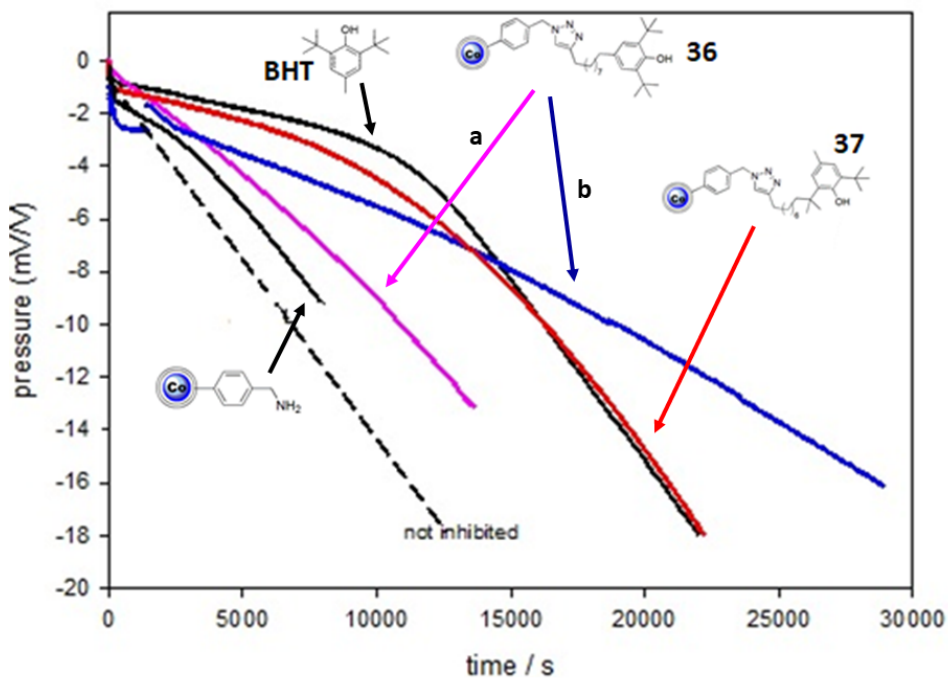


Figure 11

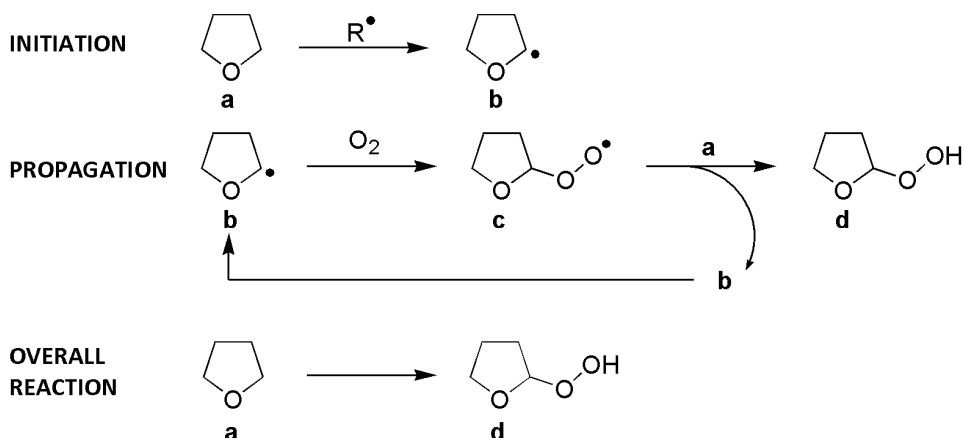
Table 3: Measured  $k_{inh}$  and  $n$  values of antioxidant functionalized CoNPs.

Sample	$k_{inh}$ [ $M^{-1} s^{-1}$ ]	$n$
Co-NH <sub>2</sub>	$< 10^3$	-
BHT	$7.3 \times 10^3$	2
36a	$8.6 \times 10^2$	2
36b	$2.0 \times 10^3$	2
37	$4.0 \times 10^3$	2

The derivative with the better antioxidant activity was **37**, characterized by a value of  $k_{inh}$  slightly lower to that of reference molecular antioxidant **BHT**. However, all of the functionalized product showed a radical scavenger activity higher than that of pure Co-NH<sub>2</sub> and Co-N<sub>3</sub><sup>65</sup>, a further confirm of the actual functionalization. The differences in the values of  $k_{inh}$  could be related to several reasons like a different loading of antioxidant moiety among each product or the heterogeneity of the nanostructured systems that could slow their reaction with peroxy radicals.

## 5.2.4 Conclusions and possible applications

Nanostructured antioxidants are interesting systems because of the numerous applications where they could be used. In our work, we focused on the chemical modification of the skeleton of traditional antioxidants like  $\alpha$ -tocopherol, catechin and BHT in order to allow the functionalization of different metallic nanoparticles (Au, SPIONs, Co). Considering the increasing interest for the use of nanosystems for biomedical applications and the relative toxicological issues, their conjugation with antioxidants could be useful in order to minimize their toxicity. Moreover, the ability of nanoparticles to enhance the biological activity of the ligands linked to their surface makes nanostructured antioxidants also attractive for the treatment of oxidative stress related pathologies (cancer, Alzheimer's disease, premature aging). For this purpose, we synthesized two derivatives of Trolox and (+)-Catechin, respectively, that have been used for the functionalization of AuNPs which, in turn, will be studied as anticancer agents. An  $\alpha$ -tocopherol like derivative was used for the functionalization of SPIONs, and the resulting nanosystems were characterized in order to confirm the presence of the antioxidant ligand on their surface. The study of their antioxidant activity is in development. The Co-NPs functionalized with BHT-like antioxidants that we prepared (CoNPs-AntiOx) were studied in our laboratory for their efficacy as stabilizing additives for ether solvents. Indeed, autooxidation processes are common in numerous solvents used in the daily laboratory activity and lead to the formation of byproducts that can modify their physico-chemical properties. In the case of ether solvents like THF or Et<sub>2</sub>O, the oxidation evolves into the formation of hydroperoxides that are particularly dangerous because they become explosive when their concentration is above 100 ppm. Like several oxidation processes, the autooxidation of THF (Scheme 38, **a**) takes place with a radical mechanism. The hydroperoxides formation is the consequence of the generation of a 2-tetrahydrofuran radical (**b**) from THF that, after the reaction with molecular oxygen, is converted into a peroxy radical (**c**). The latter removes the  $\alpha$  hydrogen from another molecule of THF thus leading to the formation of the hydroperoxide **d** and of a new tetrahydrofuran radical that can restart the entire process.<sup>173</sup> The rate determining step is the removal of the  $\alpha$  hydrogen by the peroxy radical **c**. The autooxidation of THF follows an auto-propagation mechanism that gradually increase the peroxides concentration over time.



**Scheme 38**

The autoxidation of ether solvents is an unavoidable process, then they are generally stabilized using molecular antioxidants like BHT, added in low concentrations (100-300 ppm).<sup>174,175</sup> The presence of these additives in ether solvents requires their removal for applications where they can interfere, for example for some reactions or in HPLC analysis. For this reason, before their use the solvents are generally extracted or distilled in order to remove the additives. In our laboratory we examined the use of CoNPs-AntiOx as stabilizers for THF. This application was justified by a typical property of these systems, *i.e.* the superparamagnetism, that allows the ease removal of the nanostructured additive by the use of a magnet when it is necessary to use the solvent (Figure 12).

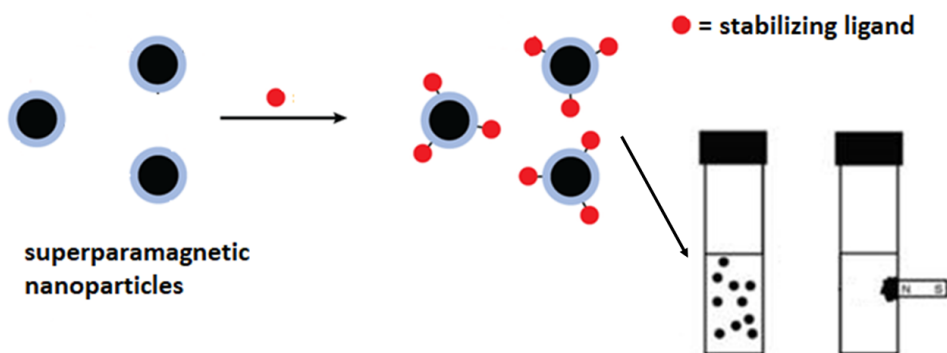


**Figure 12**

The efficacy of the CoNPs-AntiOx **36a**, **36b**, **37**, **43** and **44** (Figure 13) as stabilizers for THF was evaluated by measuring the development of hydroperoxides in the solvent.

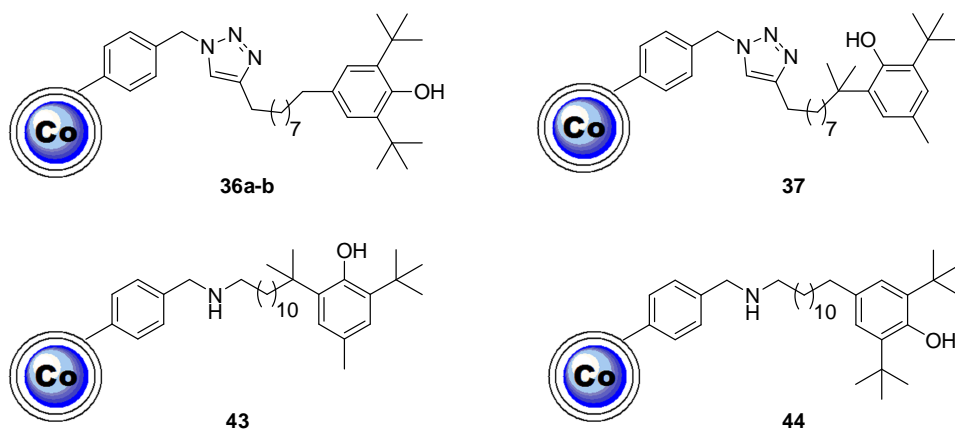


**Figure 13**

The semi-quantitative determination of the hydroperoxides formation in THF was done in a series of THF samples containing each of the CoNPs-AntiOx (**36a**, **36b**, **37**, **43**, **44**) at two different concentrations, 50 and 250 ppm. Not well explainable results were obtained. All of the samples containing CoNPs-AntiOx showed a worse stabilizing performance than those stabilized with molecular antioxidant **BHT** at the same concentrations. Indeed, the latter did not undergo the development of hydroperoxides for all of the period of the stability test (21 days) while in those containing CoNPs-AntiOx traces of hydroperoxides were detected at the first control (7 days). Among the different CoNPs-AntiOx, best results in terms of stabilizing performance were achieved with the derivatives **36b** and **44**. Moreover, a peculiar behaviour was observed in the bottles containing the Co-NH<sub>2</sub> that were prepared as references. Despite the absence of antioxidant moieties on their surface, they proved a better stabilizing performance respect to the samples containing **36a-b**, **37**, **43**, and **44**.

The low performance of CoNPs-AntiOx as antioxidant stabilizers for THF could be associated to a low yield of the functionalization with the molecular antioxidants. Another possible problem could be the heterogeneity of these nanostructured systems that would prevents the reaction of the antioxidant moieties with the peroxy radicals in solution. For these reasons, further works are in development in order to elucidate these contradictory data.

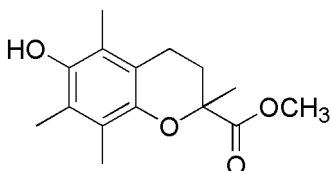
### 5.3 Experimental Section

<sup>1</sup>H and <sup>13</sup>C NMR spectra were recorded with Varian Gemini 200 or Varian Mercury Plus 400. FT-IR spectra were recorded with FT Infrared Spectrometer 1600 Perkin-Elmer in CDCl<sub>3</sub> solutions or KBr disc. GC-MS spectra were recorded with a QMD 100 Carlo Erba. ESI-MS spectra were recorded with a JEOL MStation JMS700. Melting points were measured with Melting Point Buchi 510 or Stuart SMP50 and are uncorrected. All the reactions were monitored by TLC on commercially available precoated plates (silica gel 60 F 254) and the products were visualized with acidic vanillin solution. Silica gel 60 (230–400 mesh) was used for column chromatography. Commercial available reagents

and catalysts were used as obtained from freshly open container without further purifications. Dry solvents were obtained by Pure Solv Micro.  $\text{CHCl}_3$  was washed 10 times with deionized water, dried on anhydrous  $\text{CaCl}_2$ .  $\text{Et}_3\text{N}$  was distilled over  $\text{KOH}$ , dried on anhydrous  $\text{CaCl}_2$ . Iron Oxide ( $\text{Fe}_2\text{O}_3$ ) nanoparticles were purchased from Alfa Aesar, 8-10 nm APS Powder. Cobalt nanoparticles were purchased from Turbobeads Llc; TurboBeads Click (CoNPs- $\text{N}_3$ ) and TurboBeads Amine (CoNPs- $\text{NH}_2$ ) are carbon coated ferromagnetic cobalt nanoparticles (diameter ~ 30 nm) which have a covalent azide or amine functionality (0.1 mmol/g), respectively. Reactions with CoNPs were carried out under sonication with an ultrasonic bath (Sonorex RK 255 H-R, Bandelin). All air and moisture sensitive reactions were carried out in oven-dried glassware under a nitrogen atmosphere using cannulas and septa. Solvents were dried following standard procedures. (+)-Catechin hydrate was purified in a two-step way. First of all, its solution in anhydrous THF was dried with  $\text{CaCl}_2$  twice, then the solvent was evaporated and the resulting solid was further dried *in vacuo* at 50 °C for 8h. Commercial zinc dust ( $\text{Ø} < 10 \mu\text{m}$ ) was activated by stirring for 3-4' with 2%  $\text{HCl}$ . The zinc was immediately filtered *in vacuo*, washed to neutrality with water, and then washed with ethanol, acetone, and  $\text{Et}_2\text{O}$ . The resulting powder was dried at 90 °C under vacuum for 10' and immediately used.

### 5.3.1 Synthesis

6-Hydroxy-2,5,7,8-tetramethyl-chroman-2-carboxylic acid methyl ester (**2**)

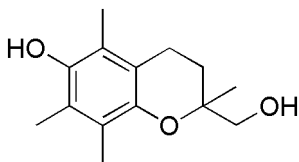


A solution of Trolox (515 mg, 2.00 mmol) was refluxed in anhyd.  $\text{MeOH}/\text{DCM}$  1/1 (50 mL) in the presence of *p*- $\text{TsOH}$  (208 mg, 1.09 mmol) for 18h, then it was cooled to room temperature, diluted with water (50 mL) and extracted with  $\text{DCM}$  (3x30 mL). The organic phase was dried over  $\text{Na}_2\text{SO}_4$  and concentrated *in vacuo*, affording the desired product **2** as a white solid of 520 mg that did not require any further purification (98% yield).

$^1\text{H NMR}$  (200 MHz,  $\text{CDCl}_3$ )  $\delta$  1.60 (s, 3H), 1.79-1.95 (m, 1H), 2.06 (s, 3H), 2.16 (s, 3H), 2.18 (s, 3H), 2.37-2.71 (m, 3H), 3.67 (s, 3H), 4.22 (bs, 1H).

$^{13}\text{C NMR}$  (100 MHz,  $\text{CDCl}_3$ )  $\delta$  11.2, 11.8, 12.1, 21.0, 25.4, 30.7, 52.2, 77.1, 117.0, 118.4, 121.3, 122.7, 145.4, 145.7, 174.4.

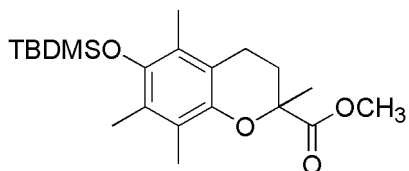
6-Hydroxy-2,5,7,8-tetramethyl-chroman-2-carboxylic acid methyl ester (**3**)



In a Schlenk tube, a solution of **2** (165 mg, 0.62 mmol) in anhyd. THF (6 mL) was added dropwise at 0 °C to a suspension of LiAlH<sub>4</sub> (71 mg, 1.86 mmol) in anhyd. THF (2 mL). The resulting suspension was left under magnetic stirring at 0 °C for 1h and then at room temperature. After 4h the reaction was quenched by the addition of 0.25 N aq. NaOH (4 mL), then it was extracted with AcOEt (3x20 mL) and the organic phase was washed with brine (3x10 mL), dried over Na<sub>2</sub>SO<sub>4</sub> and concentrated in vacuo. The crude was purified through silica gel column chromatography (eluent: hexane/AcOEt 2/1) giving the desired product as a white solid of 88 mg (60% yield).

<sup>1</sup>H NMR (200 MHz, CDCl<sub>3</sub>) δ 1.22 (s, 3H), 1.67-1.79 (m, 1H), 1.91-2.04 (m, 2H) 2.12 (s, 3H), 2.13 (s, 3H), 2.17 (s, 3H), 2.65-2.71 (m, 2H), 3.54-3.70 (m, 2H), 4.29 (bs, 1H).

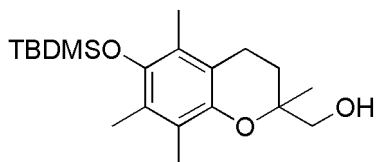
6-(*tert*-Butyl-dimethyl-silyloxy)-2,5,7,8-tetramethyl-chroman-2-carboxylic acid methyl ester (**4**)



A solution of **2** (189 mg, 0.72 mmol), *tert*-butyldimethylsilyl chloride (171 mg, 1.10 mmol) and imidazole (200 mg, 2.90 mmol) in anhyd. DMF (2 mL) was stirred at 85 °C for 5h, then it was cooled to room temperature, diluted with AcOEt (40 mL) and washed in sequence with saturated aq. NH<sub>4</sub>Cl (3x10 mL), water (3x10 mL) and brine (3x10 mL). The organic phase was dried over Na<sub>2</sub>SO<sub>4</sub> and concentrated in vacuo, affording a crude that was purified through silica gel column chromatography (eluent (petroleum ether/DCM 2/1). The product **4** was isolated as a white solid of 202 mg (74% yield).

<sup>1</sup>H NMR (200 MHz, CDCl<sub>3</sub>) δ 0.10 (s, 6H), 1.03 (s, 9H), 1.59 (s, 3H), 1.79-1.94 (m, 1H) 2.01 (s, 3H), 2.10 (s, 3H), 2.14 (s, 3H), 2.35-2.64 (m, 3H), 3.66 (s, 3H).

[6-(*tert*-Butyl-dimethyl-silyloxy)-2,5,7,8-tetramethyl-chroman-2-yl]-methanol (**5**)



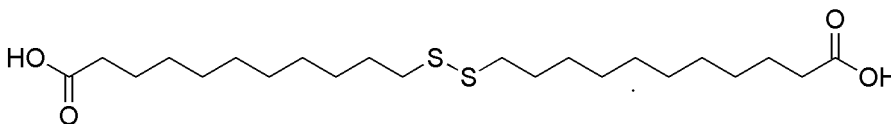
In a Schlenk tube, a solution of **4** (116 mg, 0.31 mmol) in anhyd. THF (4 mL) was added dropwise at 0 °C to a suspension of LiAlH<sub>4</sub> (36 mg, 0.95 mmol) in anhyd. THF (1 mL). The



resulting suspension was left under magnetic stirring at 0 °C for 1h and then at room temperature. After 4h the reaction was quenched by the addition of 0.25 N aq. NaOH (4 mL), then it was extracted with AcOEt (3x20 mL) and the organic phase was washed with brine (3x10 mL), dried over Na<sub>2</sub>SO<sub>4</sub> and concentrated *in vacuo*. The crude was purified through silica gel column chromatography (eluent: SCM/petroleum ether 3/1) giving the desired product as a colourless oil of 76 mg (70% yield).

**<sup>1</sup>H NMR** (200 MHz, CDCl<sub>3</sub>) δ 0.11 (s, 6H), 1.04 (s, 9H), 1.21 (3H) 1.68-1.78 (m, 1H), 1.89-2.04 (m, 2H) 2.06 (s, 3H), 2.07 (s, 3H), 2.10 (s, 3H), 2.58-2.65 (m, 2H), 3.59-3.64 (2, 3H).

11-(10-Carboxy-decylsulfanyl)-undecanoic acid (**7**)



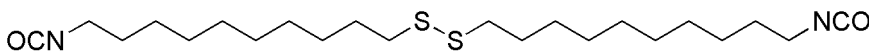
To a solution of 11-mercaptoundecanoic acid (230 mg, 1 mmol) in THF (4 mL) was added a solution of Iodine (10 mg, 0.04 mmol) in DMSO (1 mL). The reaction mixture was stirred at 45 °C until the color changed from pale yellow to red, then it was cooled to room temperature, diluted with AcOEt (50 mL) and washed with Na<sub>2</sub>S<sub>2</sub>O<sub>3</sub> saturated aqueous solution (3x30 mL), water (3x30 mL) and finally with brine (50 mL). The organic phase was dried over anhydrous Na<sub>2</sub>SO<sub>4</sub> and evaporated *in vacuum*, giving **7** as a white solid that did not require any further purification (188 mg, 86% yield).

**<sup>1</sup>H NMR** (400 MHz, DMSO-d<sub>6</sub>) δ 1.25 (bs, 20H), 1.35-1.39 (m, 4H), 1.41-1.52 (m, 4H), 1.53-1.62 (m, 4H), 2.18 (t, *J* = 7.6 Hz, 4H); 2.68 (t, *J* = 7.2 Hz, 4H), 11.90 (bs, 2H).

**<sup>13</sup>C NMR** (100 MHz, DMSO-d<sub>6</sub>) δ 24.9, 28.2, 28.97, 29.0, 29.2, 29.28, 29.30, 34.1, 39.4, 174.9 (10 signals of 11 non-equivalent carbons).

**MS (ESI):** m/z 433.42 [M-H]<sup>-</sup>.

1-Isocyanato-10-(10-isocyanato-decylsulfanyl)-decane (**9**)



To a solution of **7** (218 mg, 0.50 mmol) in 8 mL of anhydrous DCM, oxalyl chloride (300 μL, 3.54 mmol) was added dropwise at 0 °C. The white suspension was stirred at room temperature for 14h, then the solvent was directly evaporated *in vacuum*. The so-formed oil was dissolved in 3 mL of anhydrous acetone, then a saturated solution of NaN<sub>3</sub> in 0.5 mL of degassed deionized water was slowly added at 0 °C. The suspension was stirred at 0 °C for 10', then at room temperature for 60' under N<sub>2</sub> atmosphere. Afterwards, the suspension was diluted with water (50 mL) and extracted with DCM (3x40 mL). The recollected organic phases were dried over anhydrous Na<sub>2</sub>SO<sub>4</sub> and evaporated *in vacuum*, furnishing the corresponding *bis*-acyl azide **8** as a white solid as confirmed by IR spectroscopy. A solution **8** in 7 mL of anhydrous Toluene was heated to reflux for 1h, then it was left under magnetic stirring at room temperature for 60h. The

solvent was evaporated *in vacuo*, furnishing **9** as a brown oil that did not require any further purification (190 mg, 97% yield).

**<sup>1</sup>H NMR** (400 MHz, CDCl<sub>3</sub>) δ 1.28 (bs, 28H), 1.41-1.66 (m, 4H), 2.66 (t, *J* = 7.2 Hz, 4H), 3.27 (t, *J* = 6.6 Hz, 4H).

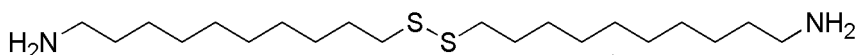
**<sup>13</sup>C NMR** (100 MHz, CDCl<sub>3</sub>) δ 26.5 (2C), 28.5 (2C), 28.9 (2C), 29.1 (2C), 29.2 (2C), 29.3 (2C), 31.3 (2C), 39.3 (2C), 43.0 (2C), 122.1 (2C) (10 signals of 11 non-equivalent carbon atoms).

**IR** (CDCl<sub>3</sub>, cm<sup>-1</sup>) ν 2931, 2857, 2277.

**MS (EI)**: *m/z* (%) 428 (M<sup>+</sup>, 19), 214 (6), 182 (21).

Anal. Calcd. for C<sub>22</sub>H<sub>40</sub>N<sub>2</sub>O<sub>2</sub>S<sub>2</sub>: C, 61.64%; H, 9.40%; N, 6.53%; O, 7.46%; S, 14.96%. Found: C, 61.88%; H, 9.14%; N, 6.30%.

10-(10-Amino-decyldisulfanyl)-decylamine (**10**)



To a stirred solution of **9** (313 mg, 0.73 mmol) in anhydrous THF (1.5 mL), aq. NaOH 1N (1.5 mL) was added dropwise at 0 °C. The mixture was stirred at room temperature for 2h and then heated to reflux (70 °C) for 4h. After cooling to room temperature and dilution with Et<sub>2</sub>O (20 mL), a white precipitate was formed and collected after filtration. The so obtained white solid was dried *in vacuo* and did not require any further purification (190 mg, 69% yield).

**Mp**: 80-85 °C;

**<sup>1</sup>H NMR** (400 MHz, CDCl<sub>3</sub>) δ 1.24-1.33 (m, 28H), 1.62-1.69 (m, 4H), 2.65-2.69 (at, 8H).

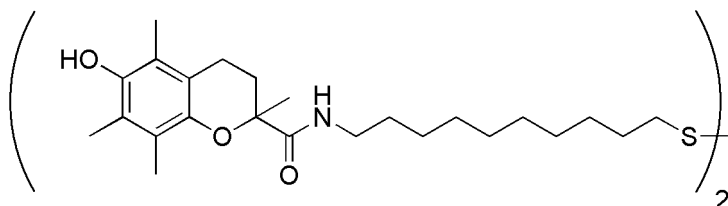
**<sup>13</sup>C NMR** (100 MHz, CDCl<sub>3</sub>) δ 26.9 (2C), 28.5 (2C), 29.2 (2C), 29.42 (2C), 29.43 (2C), 29.5 (2C), 29.7 (2C), 39.2 (2C), 42.1 (2C) (9 signals of 10 non-equivalent carbon atoms).

**IR** (CDCl<sub>3</sub>, cm<sup>-1</sup>): 2929, 2856.

**MS (ESI)** *m/z* 377.33 [M + H]<sup>+</sup>.

Elemental Analysis for C<sub>20</sub>H<sub>44</sub>N<sub>2</sub>S<sub>2</sub>: Calculated: C, 63.77%; H, 11.77%; N, 7.44%; S, 17.02%. Found: C, 64.01%; H, 11.89%; N, 7.23%.

Trolox disulfide derivative (**11**)



In a Schlenk tube Trolox (132 mg, 0.51 mmol), **10** (94 mg, 0.25 mmol), BOP (250 mg, 0.55 mmol), HOBt (77 mg, 0.55 mmol) and DMAP (67 mg, 0.55 mmol) were dissolved in anhydrous DMF (2 mL), then after 10' stirring TEA (230  $\mu$ L, 1.65 mmol) was added dropwise and the so-formed yellow solution was stirred at room temperature for 18h under N<sub>2</sub> atmosphere. The reaction mixture was diluted with AcOEt (100 mL) and washed with aq. H<sub>2</sub>SO<sub>4</sub> 0.5M (3x80 mL), aq. Na<sub>2</sub>CO<sub>3</sub> 1M (3x80 mL) and brine (3x80 mL). The organic phase was dried over anhydrous Na<sub>2</sub>SO<sub>4</sub> and evaporated *in vacuo* furnishing a brown oil of 0.17 g that was purified by silica gel column chromatography (eluent: DCM/MeOH 30/1), giving the desired product **11** as a colorless oil of 124 mg (59% yield).

**<sup>1</sup>H NMR** (400 MHz, CDCl<sub>3</sub>)  $\delta$  1.10-1.42 (m, 28H), 1.50 (s, 6H), 1.62-1.69 (m, 4H), 1.83-1.90 (m, 2H), 2.09 (m, 6H), 2.17 (m, 6H), 2.18 (m, 6H), 2.31-2.37 (m, 2H), 2.50-2.64 (m, 4H), 2.67 (t, *J* = 7.4Hz, 4H), 3.12-3.26 (m, 4H), 4.72 (bs, 2H), 6.45 (bs, 2H).

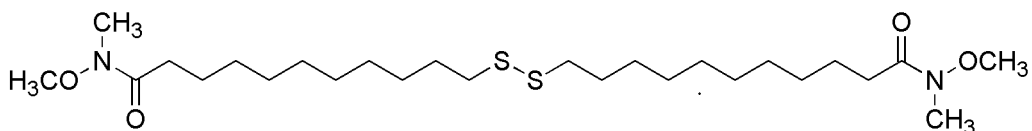
**<sup>13</sup>C NMR** (100 MHz, CDCl<sub>3</sub>)  $\delta$  11.3 (2C), 11.9 (2C), 12.2 (2C), 20.5 (2C), 24.4 (2C), 26.5 (2C), 28.4 (2C), 29.12 (2C), 29.14 (2C), 29.4 (2C), 29.5 (2C), 38.9 (2C), 39.1 (2C), 78.3 (2C), 117.9 (2C), 119.1 (2C), 121.5 (2C), 121.6 (2C), 144.2 (2C), 145.6 (2C), 174.2 (2C) (21 signals of 24 non-equivalent carbon atoms).

**IR** (CDCl<sub>3</sub>, cm<sup>-1</sup>)  $\nu$  3615, 3435, 2930, 2856, 1662, 1261.

**MS (ESI)** *m/z* 839.63 [M-H]<sup>-</sup>.

Elemental Analysis for C<sub>48</sub>H<sub>76</sub>N<sub>2</sub>O<sub>6</sub>S<sub>2</sub>: C, 68.53%; H, 9.11%; N, 3.33%; O, 11.41%; S, 7.62%. Found: C, 68.71%; H, 8.95%; N, 3.56%.

11-[10-(Methoxy-methyl-carbamoyl)-decylidisulfanyl]-undecanoic acid methoxy-methylamide (**12**)



To a solution of **7** (218 mg, 0.50 mmol) in 8 mL of anhydrous DCM, oxalyl chloride (300  $\mu$ L, 3.54 mmol) was added dropwise at 0 °C. The white suspension was stirred at room temperature for 14h, then the solvent was directly evaporated *in vacuo*. To the so-formed oil, N,O-dimethylhydroxylamine hydrochloride (106 mg, 1.06 mmol) was added and they were suspended in anhydrous DCM (1 mL). After that, fresh distilled Pyridine (170  $\mu$ L, 2.10 mmol) was added dropwise at 0 °C. This mixture was left under magnetic stirring at 0 °C for 10 minutes, then at room temperature. After 6h the reaction mixture was diluted with DCM and washed with aq. HCl 0.1N (3x50 mL), saturated aq. NaHCO<sub>3</sub> (3x50 mL), water (2x50 mL) and Brine (100 mL). The organic phase was dried over anhydrous Na<sub>2</sub>SO<sub>4</sub> and evaporated *in vacuo* furnishing **12** as a yellow oil of 234 mg that did not require any further purification (90% yield).

**<sup>1</sup>H NMR** (200 MHz, CDCl<sub>3</sub>) δ 1.29 (bs, 24H), 1.59-1.69 (m, 8H), 2.41 (t, *J* = 7.6 Hz, 4H), 2.68 (t, *J* = 7.2 Hz, 4H), 3.18 (s, 6H), 3.68 (s, 6H).

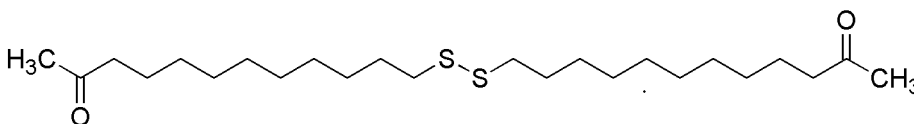
**<sup>13</sup>C NMR** (50 MHz, CDCl<sub>3</sub>) δ 24.6 (2C), 24.8 (2C), 28.5 (2C), 29.1 (2C), 29.2 (2C), 29.4 (2C), 31.9 (2C), 32.3 (2C), 33.6 (2C), 39.3 (2C), 61.1 (2C), 174.7 (2C) [11 of 12C chemically equivalent].

**IR** (CDCl<sub>3</sub>, cm<sup>-1</sup>) ν 2929, 2855, 1647.

**MS (EI):** *m/z* (%) 460 (4).

Elemental Analysis for C<sub>26</sub>H<sub>52</sub>N<sub>2</sub>O<sub>4</sub>S<sub>2</sub> Calculated: C, 59.96%; H, 10.06%; N, 5.38%; O, 12.29%; S, 12.31%. Found: C, 59.77%; H, 9.91%; N, 5.61%.

12-(11-Oxo-dodecyl-disulfanyl)-dodecan-2-one (**13**)



In a Schlenk tube, to a solution of **12** (98 mg, 0.19 mmol) in anhydrous THF (2 mL), Methylmagnesium Bromide (3.0 M in Et<sub>2</sub>O, 250 μL, 0.75 mmol) was added dropwise at 0 °C. The mixture was left under magnetic stirring and N<sub>2</sub> atmosphere at 0 °C for 1h, then it was quenched with ice and acidified to pH 5 with aq. HCl 0.1N. The so-obtained suspension was extracted with DCM, then collected organic phases were washed with water, dried over anhydrous Na<sub>2</sub>SO<sub>4</sub> and evaporated *in vacuum*, furnishing a white solid of 0.09 g that was purified by silica gel column chromatography (eluent: Petroleum ether/AcOEt 8/1). The desired product **13** was isolated as a white solid of 48 mg (59% yield).

**Mp:** 44-46 °C.

**<sup>1</sup>H NMR** (400 MHz, CDCl<sub>3</sub>) δ 1.26-1.37 (m, 24H), 1.53-1.56 (m, 4H), 1.61-1.67 (m, 4H), 2.11 (s, 6H), 2.40 (t, *J* = 7.6 Hz, 4H), 2.66 (t, *J* = 7.4 Hz, 4H).

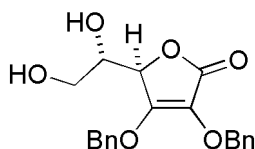
**<sup>13</sup>C NMR** (100 MHz, CDCl<sub>3</sub>) δ 23.8 (2C), 28.5 (2C), 29.1 (2C), 29.2 (2C), 29.3 (3C), 29.4 (2C), 29.8 (2C), 39.1 (3C), 43.8 (2C), 209.2 (2C) [10 of 12 C chemically equivalent].

**IR** (CDCl<sub>3</sub>, cm<sup>-1</sup>) ν 2929, 2856, 1710.

**MS (EI):** *m/z* (%) 430 (7).

Anal. Calcd. for C<sub>24</sub>H<sub>46</sub>O<sub>2</sub>S<sub>2</sub>: C, 66.92%; H, 10.76%; O, 7.43%; S, 14.89%. Found: C, 66.63%; H, 10.91%.

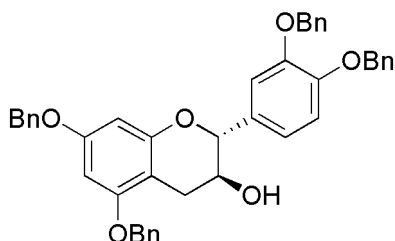
3,4-Bis-benzyloxy-5-(1,2-dihydroxy-ethyl)-5H-furan-2-one (**14**)



L-ascorbic acid (352 mg, 2.00 mmol) was suspended in anhyd. acetone (2 mL), then acetyl chloride (173 mg, 2.20 mmol) was added dropwise at 0 °C and the resulting suspension was stirred at 40 °C 5h. The mixture was cooled to -20 °C and filtered, allowing the isolation of the corresponding cyclic acetal as a white solid of 106 mg (25% yield). 68 mg of the latter (0.31 mmol) and anhydr. K<sub>2</sub>CO<sub>3</sub> (119 mg, 0.86 mmol) were suspended in anhydr. acetone (4 mL), then benzyl bromide (123 mg, 0.72 mmol) was added and the resulting suspension was stirred at reflux for 4h. The so-formed yellow suspension was cooled to room temperature and concentrated *in vacuo*, diluted with water (50 mL) and extracted with Et<sub>2</sub>O (4x20 mL). The organic phase was dried over anhydrous Na<sub>2</sub>SO<sub>4</sub> and evaporated *in vacuo*, furnishing a white solid that was purified by silica gel column chromatography (eluent: Petroluem ether/AcOEt 4/1). The *bis*-benzylated cyclic acetal of L-ascorbic acid was isolated as a white solid of 61 mg (50% yield). In the last step the product (61 mg) was dissolved in a 1/1 mixture of anhyd. THF/anhyd. MeOH (3.0 mL) and aq. 2N HCl (0.2 mL) was added. The mixture was left under magnetic stirring at room temperature for 16h, then it was concentrated *in vacuo*, diluted with AcOEt (50 mL) and washed with water (3x20 mL). The organic phase was dried over anhydrous Na<sub>2</sub>SO<sub>4</sub> and evaporated *in vacuo*, furnishing the product **14** as a brown oil of 43 mg that did not require any further purification (80%).

<sup>1</sup>H NMR (200 MHz, CDCl<sub>3</sub>) δ 3.13 (bs, 2H), 3.75 (t, *J* = 5.2 Hz, 2H), 3.91-3.98 (m, 1H), 4.68 (d, *J* = 2.2 Hz, 1H), 5.06-5.19 (m, 4H), 7.20-7.31 (m, 10H).

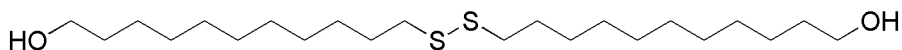
5,7-Bis-benzyloxy-2-(3,4-bis-benzyloxy-phenyl)-chroman-3-ol (**17**)



In a Schlenk tube, to a suspension of (+)-Catechin (402 mg, 1.36 mmol) and anhyd. K<sub>2</sub>CO<sub>3</sub> (1162 mg, 8.41 mmol) in anhyd. DMF (7 mL), benzyl bromide (0.75 mL, 6.31 mmol) was added at -30 °C. The mixture was left under magnetic stirring for 2h at -10 °C and then at room temperature. After 48h the reaction mixture was diluted with AcOEt (50 mL) and washed in sequence with water (3x30 mL) and brine (3x30 mL). The organic phase was dried over anhydrous Na<sub>2</sub>SO<sub>4</sub> and evaporated *in vacuo*, furnishing a brown solid that was purified by silica gel column chromatography (eluent: DCM/Petroleum ether 50/1). The desired product **17** was isolated as a white solid of 449 mg (49% yield).

**<sup>1</sup>H NMR** (200 MHz, CDCl<sub>3</sub>) δ 2.66-2.79 (m, 1H), 3.12-3.23 (m, 1H), 3.99-4.17 (m, 1H), 4.68-4.72 (m, 1H), 5.06 (s, 2H), 5.09 (s, 2H), 5.22 (m, 4H), 6.31-6.32 (m, 1H), 6.36-6.37 (m, 1H), 7.01 (s, 1H), 7.39-7.48 (m, 22H).

11-(11-Hydroxy-undecylsulfanyl)-undecan-1-ol (**18**)



H<sub>2</sub>SO<sub>4</sub> (2 mL) was added to a solution of **7** (435 mg, 1.00 mmol) in anhyd. MeOH (30 mL). The resulting solution was left under magnetic stirring at reflux for 6h, then it was diluted with AcOEt and neutralized to pH 8 with saturated aq. Na<sub>2</sub>CO<sub>3</sub>. The organic phase was washed with saturated aq. NaHCO<sub>3</sub> (3x10 mL), water and brine, dried over anhydrous Na<sub>2</sub>SO<sub>4</sub> and evaporated *in vacuo*, furnishing the *bis*-methyl ester of **7** as a white solid of 369 mg (80%) [**IR** (CDCl<sub>3</sub>, cm<sup>-1</sup>) 2929, 2851, 1720; **MS (EI)** m/z (int. rel. %) 462 (17)] that was reduced to the corresponding alcohol **18** with the following procedure. A solution of the *bis*-methyl ester (369 mg, 0.79 mmol) in anhyd. THF (8 mL) was added dropwise to a suspension of LiAlH<sub>4</sub> (186 mg, 4.90 mmol) in anhyd. THF (2.5 mL) at 0 °C. The suspension was stirred at 0 °C for 1h and then at room temperature for 16h. The reaction mixture was quenched with 0.25N aq. NaOH and extracted with AcOEt (4x20 mL), the organic phase was washed with water (3x10 mL) and brine (3x10 mL), dried over Na<sub>2</sub>SO<sub>4</sub> and concentrated in vacuo. The resulting white solid was dissolved in THF (7 mL), then a solution of I<sub>2</sub> (17 mg, 0.067 mmol) in DMSO (1 mL) was added and the mixture was left under magnetic stirring at 45 °C until its colour changed from yellow to red (1h30'), then it was cooled to room temperature, diluted with AcOEt (50 mL) and washed in sequence with saturated aq. Na<sub>2</sub>S<sub>2</sub>O<sub>3</sub> (3x20 mL) and brine (3x20 mL). The organic phase was dried over Na<sub>2</sub>SO<sub>4</sub> and concentrated in vacuo, affording the desired product **18** as a white solid of 259 mg (80% yield).

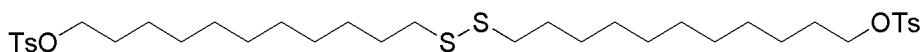
**<sup>1</sup>H NMR** (400 MHz, CDCl<sub>3</sub>) δ 1.28 (bs, 28H), 1.53-1.70 (m, 8H), 2.68 (t, *J* = 7.0 Hz, 4H), 3.64 (t, *J* = 6.2 Hz, 4H).

**<sup>13</sup>C NMR** (100 MHz, CDCl<sub>3</sub>) δ 25.7 (2C), 28.5 (2C), 29.2 (2C), 29.4 (C), 29.46 (2C), 29.48 (2C), 29.6 (2C), 32.8 (2C), 39.2 (2C), 63.0 (2C) [10 of 12 C chemically equivalent].

**IR** (CDCl<sub>3</sub>, cm<sup>-1</sup>) 3622, 2929, 2854.

**MS (ESI)**: m/z 429.55 [M + Na]<sup>+</sup>.

*bis*-Tosylated 11-(11-Hydroxy-undecylsulfanyl)-undecan-1-ol (**19**)



In a Schlenk tube, to a solution of **18** (55 mg, 0.14 mmol), DMAP (3 mg, 0.025 mmol) and TEA 79 mg, 0.78 mmol) in anhyd. DCM (1 mL), a solution of tosyl chloride (117 mg, 0.62 mmol) in anhyd. DCM (3 mL) was added dropwise at 0 °C. The mixture was left under magnetic stirring at room temperature 4h, then the reaction was quenched with water and extracted with AcOEt(3x20 mL). The organic phase was with saturated aq. NH<sub>4</sub>Cl (3x10 mL) and brine (3x10 mL), dried over Na<sub>2</sub>SO<sub>4</sub> and concentrated in vacuo.

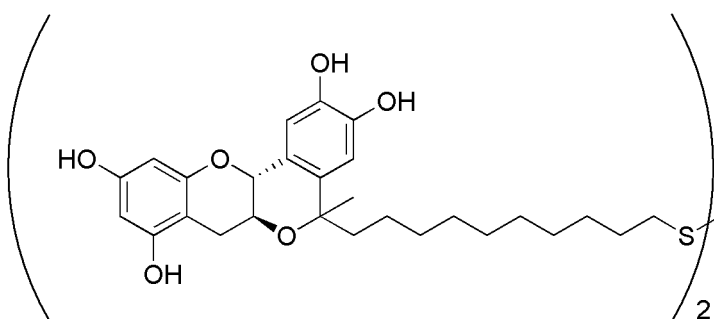
The crude was a white solid that was purified through silica gel column chromatography (eluent Ep/AcOEt 4/1→3/1) and the desired product **19** was isolated as a white solid of 68 mg (68% yield).

**<sup>1</sup>H NMR** (400 MHz, CDCl<sub>3</sub>) δ 1.22 (bs, 28H), 1.53-1.70 (m, 8H), 2.45 (s, 6H), 2.67 (t, *J* = 7.0 Hz, 4H), 4.02 (t, *J* = 6.4 Hz, 4H), 7.32-7.36 (m, 4H), 7.77-7.81 (m, 4H).

**<sup>13</sup>C NMR** (100 MHz, CDCl<sub>3</sub>) δ 21.6 (2C), 25.3 (2C), 28.5 (2C), 28.8 (2C), 28.9 (2C), 29.2 (2C), 29.3 (2C), 29.37 (2C), 29.40 (2C), 39.1 (2C), 70.7 (2C), 127.8 (4C), 129.8 (4C), 133.2 (2C), 144.6 (2C). [15 of 16 C chemically equivalent].

**IR** (CDCl<sub>3</sub>, cm<sup>-1</sup>) 2930, 2930, 2856, 1599, 1358, 1177.

Catechine disulfide derivative (**20**)



In a Schlenk tube, to a solution of purified (+)-Catechin\* (176 mg, 0.60 mmol) and **13** (42 mg, 0.10 mmol) in anhydrous THF (4 mL), TMSOTf (40 μL, 0.22 mmol) was added dropwise at -5 °C. The reaction mixture was left under magnetic stirring at room temperature and N<sub>2</sub> atmosphere for 14h, then it was quenched with ice and extracted with diethyl ether (4x40 mL). Recollected organic phases were subsequently washed with saturated aq. NaHCO<sub>3</sub> (3x50 mL) and Brine (3x50 mL), dried over anhyd. Na<sub>2</sub>SO<sub>4</sub>, filtered and evaporated *in vacuo*. The crude was a brown solid of 0.14g that was purified by silica gel column chromatography (eluent: Petroleum ether/AcOEt 1/3), allowing the isolation of the desired product **20** as a white solid of 19 mg (19% yield).

**Mp:** 190 °C (d).

**<sup>1</sup>H NMR** (400 MHz, (CD<sub>3</sub>)<sub>2</sub>CO) δ 1.18-1.41 (m, 30H), 1.50 (s, 4H), 1.61-1.68 (m, 4H), 1.71-1.85 (m, 4H), 2.42-2.50 (m, 2H), 2.68 (t, *J* = 7.2 Hz, 4H), 2.95-3.01 (m, 2H), 3.77-3.83 (m, 2H), 4.43-4.49 (m, 2H), 5.87-5.99 (m, 2H), 6.06-6.07 (m, 2H), 6.62-6.65 (m, 2H), 7.09-7.01 (m, 2H), 8.02 (bs, 8H).

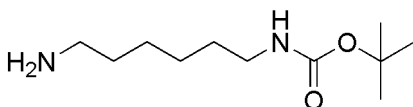
**<sup>13</sup>C NMR** (100 MHz, (CD<sub>3</sub>)<sub>2</sub>CO) δ 24.3, 24.6, 27.9, 28.1, 28.6, 29.9, 30.1, 30.2, 30.29, 30.32, 30.4, 30.8, 39.4, 40.7, 44.8, 67.1, 67.2, 74.1, 74.2, 77.9, 78.6, 95.89, 95.93, 96.6, 100.96, 101.0, 112.3, 112.6, 112.7, 112.8, 125.1, 126.7, 134.0, 136.5, 144.47, 144.5, 145.6, 145.8, 156.75, 156.81, 157.45, 157.47, 157.87, 157.9.

**IR** (KBr disc,  $\text{cm}^{-1}$ ) 3340, 2925, 2852, 1630, 1519, 1466, 1141.

**MS (ESI):**  $m/z$  973.61  $[\text{M}-\text{H}]^-$ .

Anal. Calcd. for  $\text{C}_{54}\text{H}_{70}\text{O}_{12}\text{S}_2$ : C, 66.50%; H, 7.23%; O, 19.69%; S, 6.58%. Found: C, 66.77%; H, 7.02%.

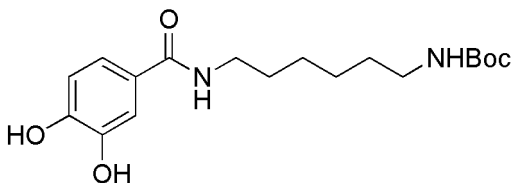
(6-Amino-hexyl)-carbamic acid *tert*-butyl ester (**22**)



To a suspension of 1,6-hexanediamine (876 mg, 7.54 mmol) in anhydrous  $\text{CHCl}_3$  (30 mL), a solution of  $\text{Boc}_2\text{O}$  (327 mg, 1.50 mmol) in anhyd.  $\text{CHCl}_3$  (3 mL) was added dropwise at  $-5^\circ\text{C}$ . The mixture was stirred for 14h at r.t., then it was filtered and the filtrate was concentrated *in vacuo*, dissolved in AcOEt (150 mL) and washed with brine (3x40 mL). The organic phase was dried over  $\text{Na}_2\text{SO}_4$ , filtered and concentrated *in vacuo*, giving **22** as a colourless oil of 304 mg that did not require any further purification (94% yield).

**$^1\text{H NMR}$**  (200 MHz,  $\text{CDCl}_3$ )  $\delta$  1.32-1.56 (m, 17H), 2.65-2.72 (m, 2H), 3.05-3.15 (m, 2H), 4.53 (m, 1H).

[6-(3,4-Dihydroxy-benzoylamino)-hexyl]-carbamic acid *tert*-butyl ester (**23**)



In a Schlenk tube, to a solution of 2,3-dihydroxybenzoic acid (243 mg, 1.58 mmol) and HOBT (212 mg, 1.57 mmol) in anhydrous THF (4 mL), a solution of DCC (395 mg, 1.91 mmol) in anhyd. THF (6 mL) was added dropwise. The solution was stirred for 15' at room temperature, then a solution of **22** (375 mg, 1.73 mmol) in anhyd. THF (2 mL) was added dropwise. The so-formed brown suspension was left under magnetic stirring and  $\text{N}_2$  atmosphere for 18h, then the solvent was evaporated *in vacuo* and the residue was diluted with AcOEt (150 mL) and filtered. After that the filtrate was washed with saturated aq.  $\text{NaHCO}_3$  (3x40 mL), water (3x40 mL) and Brine (100 mL), then the organic layer was dried over  $\text{Na}_2\text{SO}_4$ , filtered and evaporated *in vacuo*. The crude was a brown solid of 0.66 g that was purified by silica gel column chromatography (eluent: DCM/AcOEt 1/3), giving the desired product as a white solid of 359 mg (65% yield).

**Mp:** 75-79  $^\circ\text{C}$ .



**<sup>1</sup>H NMR** (400 MHz, (CD<sub>3</sub>)<sub>2</sub>CO) δ 1.34-1.51 (m, 15H), 1.55-1.62 (m, 2H), 2.95-3.98 (m, 2H), 3.29-3.38 (m, 2H), 5.95 (bs, 1H), 6.84 (d, *J* = 8.0 Hz, 1H), 7.30 (dd, *J* = 8.0 Hz, *J* = 2.0 Hz, 1H), 7.45 (d, *J* = 2.0 Hz, 1H), 7.55 (bs, 1H), 8.33 (bs, 2H).

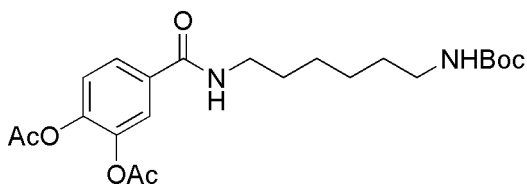
**<sup>13</sup>C NMR** (100 MHz, CDCl<sub>3</sub>) δ 26.0 (1C), 26.2 (1C), 28.4 (3C), 29.3 (1C), 29.8 (1C), 40.0 (1C), 40.3 (1C), 79.5 (1C), 114.6 (1C), 115.0 (1C), 119.7 (1C), 126.0 (1C), 144.4 (1C), 148.3 (1C), 156.5 (1C), 168.4 (1C).

**IR** (KBr, cm<sup>-1</sup>) 3374, 2931, 2852, 1689, 1629, 1590, 1516, 1288, 1171.

**MS (ESI)**: *m/z* 351.25 [M-H]<sup>-</sup>, 703.15 [2M-H]<sup>-</sup>.

Anal. Calcd. for C<sub>18</sub>H<sub>28</sub>N<sub>2</sub>O<sub>5</sub>: C, 61.34%; H, 8.01%; N, 7.95%; O, 22.70%. Found: C, 61.49%; H, 7.87%; N, 8.03%.

Acetic acid 2-acetoxy-4-(6-*tert*-butoxycarbonylamino-hexylcarbamoyl)-phenyl ester (**24**)

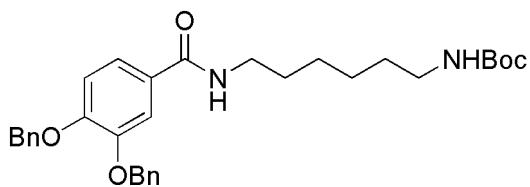


In a Schlenk tube, acetic anhydride (28 mg, 0.27 mmol) was added dropwise at 0 °C to a solution of **23** (45 mg, 0.13 mmol) in anhydrous pyridine (100 μL). The mixture was left under magnetic stirring at 0 °C under nitrogen atmosphere for 3h. After the addition of water, the mixture was diluted with AcOEt (40 mL) and washed with saturated aq. NH<sub>4</sub>Cl (3x20 mL), water (3x20 mL) and brine (3x20 mL). The organic layer was dried over Na<sub>2</sub>SO<sub>4</sub>, filtered and evaporated in vacuo affording the desired product **24** as a white solid of 53 mg without any further purification (93% yield).

**<sup>1</sup>H NMR** (400 MHz, CDCl<sub>3</sub>) δ 1.30-1.49 (m, 15H), 1.54-1.61 (m, 2H), 2.281 (s, 3H), 2.283 (s, 3H), 3.09-3.11 (m, 2H), 3.36-3.41 (m, 2H), 4.60 (bs, 1H), 6.55 (bs, 1H), 7.23 (d, *J* = 8.4 Hz, 1H), 7.65-7.69 (m, 2H).

**<sup>13</sup>C NMR** (100 MHz, CDCl<sub>3</sub>) δ 20.5 (1C), 20.6 (1C), 21.0 (1C), 25.8 (1C), 26.0 (1C), 28.4 (3C), 29.3 (1C), 30.0 (1C), 39.6 (1C), 40.0 (1C), 122.6 (1C), 123.5 (1C), 125.1 (1C), 133.4 (1C), 142.0 (1C), 144.4 (1C), 156.1 (1C), 165.7 (1C), 167.8 (1C), 168.0 (1C).

[6-(3,4-Bis-benzyloxy-benzoylamino)-hexyl]-carbamic acid *tert*-butyl ester (**26**)



In a Schlenk tube, to a suspension of **23** (213 mg, 0.60 mmol) and anhydrous  $K_2CO_3$  (549 mg, 3.97 mmol) in anhyd. DMF (4.5 mL), Benzyl bromide (160  $\mu$ L, 1.35 mmol) was added dropwise at room temperature. The so-obtained white suspension was left under magnetic stirring at room temperature and  $N_2$  atmosphere, then it was quenched with water and diluted with AcOEt (120 mL). The organic phase was washed with water (3x30 mL) and brine (3x30 mL), then the organic layer was dried over  $Na_2SO_4$ , filtered and evaporated *in vacuo*, allowing the isolation of **26** as a white solid of 272 mg that did not require any further purification (85% yield).

**Mp:** 114 °C (d).

**$^1H$  NMR** (400 MHz,  $CDCl_3$ )  $\delta$  1.35-1.49 (m, 14H), 1.56-1.59 (m, 2H), 1.66 (bs, 1H), 3.09-3.14 (m, 2H), 3.37-3.42 (m, 2H), 4.56 (bs, 1H), 5.20 (s, 4H), 6.28 (bs, 1H), 6.90 (d,  $J$  = 8.4 Hz, 1H), 7.28-7.51 (m, 12H).

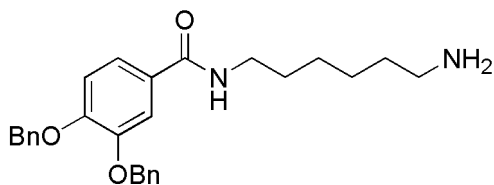
**$^{13}C$  NMR** (100 MHz,  $CDCl_3$ )  $\delta$  25.9 (1C), 26.1 (1C), 28.4 (3C), 29.4 (1C), 30.0 (1C), 39.5 (1C), 40.0 (1C), 70.9 (1C), 71.2 (1C), 113.6 (1C), 113.9 (1C), 119.9 (1C), 127.1 (2C), 127.4 (2C), 127.9 (1C), 128.50 (2C), 128.54 (2C), 136.7 (1C), 136.9 (1C), 148.7 (1C), 151.4 (1C), 156.1 (1C), 166.9 (1C) [23 of 26 C chemically equivalent].

**IR** ( $CDCl_3$ ,  $cm^{-1}$ )  $\nu$  3688, 3456, 2981, 2936, 2862, 1707, 1651, 1502, 1266.

**MS (ESI):**  $m/z$  555.07 [ $M + Na$ ] $^+$ , 1086.65 [ $2M + Na$ ] $^+$ .

Anal. Calcd. for  $C_{32}H_{40}N_2O_5$ : C, 72.15%; H, 7.57%; N, 5.26%; O, 15.02%. Found: C, 72.23%; H, 7.41%; N, 5.33%.

N-(6-Amino-hexyl)-3,4-bis-benzyloxy-benzamide (**27**)



To a solution of **26** (111 mg, 0.21 mmol) in anhydrous DCM (3 mL),  $CF_3COOH$  (0.75 mL) was added dropwise at 0 °C. The solution was left under magnetic stirring at 0 °C for 30' and then at room temperature for 30' more minutes, then the solvent was evaporated *in vacuo* and aq. NaOH 2N was added dropwise until the formation of a white precipitate. The suspension was kept in the fridge for 12h, then it was filtered and the precipitate was dried *in vacuo*. **27** was isolated as a white solid of 78 mg that did not require any further purification (87% yield).

**Mp:** 120-122 °C.

**$^1H$  NMR** (400 MHz,  $(CD_3)_2SO$ )  $\delta$  1.28-1.51 (m, 8H), 2.57 (t,  $J$  = 7.2 Hz, 2H), 3.19-3.24 (m, 2H), 3.51 (bs, 3H), 5.16 (s, 2H), 5.19 (s, 2H), 7.11 (d,  $J$  = 8.8 Hz, 1H), 7.30-7.47 (m, 10H), 7.56 (d,  $J$  = 1.6 Hz, 1H), 8.30-8.32 (at, 1H).

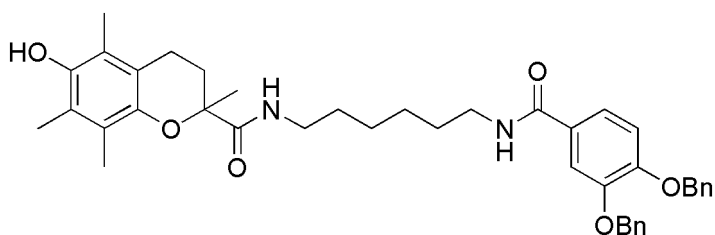
**<sup>13</sup>C NMR** (100 MHz, (CD<sub>3</sub>)<sub>2</sub>SO) δ 26.0 (1C), 26.4 (1C), 29.2 (1C), 31.7 (1C), 40.9 (1C), 69.8 (1C), 70.2 (1C), 113.2 (1C), 113.3 (1C), 120.6 (1C), 127.4 (1C), 127.52 (2C), 127.55 (2C), 127.8 (2C), 128.4 (2C), 137.0 (1C), 137.0 (1C), 147.6 (1C), 150.5 (1C), 165.4 (1C) [20 of 23 C chemically equivalent].

**IR** (KBr, cm<sup>-1</sup>) ν 3429, 3301, 2927, 2855, 1630, 1512, 1276.

**MS (ESI):** m/z 433.21 [M + H]<sup>+</sup>.

Anal. Calcd. for C<sub>27</sub>H<sub>32</sub>N<sub>2</sub>O<sub>3</sub>: C, 74.97%; H, 7.46%; N, 6.48%; O, 11.10%. Found: C, 75.11%; H, 7.33%; N, 6.59%.

6-Hydroxy-2,5,7,8-tetramethyl-chroman-2-carboxylic acid [6-(3,4-bis-benzyloxy-benzoylamino)-hexyl]-amide (**28**)



In a Schlenk tube Trolox (49 mg, 0.20 mmol), **27** (81 mg, 0.19 mmol), BOP (97 mg, 0.222 mmol), HOBt (29 mg, 0.22 mmol) and DMAP (30 mg, 0.25 mmol) were dissolved in anhydrous DMF (1 mL), then after 10' stirring TEA (90 μl, 0.65 mmol) was added dropwise and the so-formed yellow solution was stirred at room temperature for 18h under N<sub>2</sub> atmosphere. The reaction mixture was diluted with AcOEt (70 mL) and washed with aq. H<sub>2</sub>SO<sub>4</sub> 0.5M (3x50 mL), aq. Na<sub>2</sub>CO<sub>3</sub> 1M (3x50 mL) and brine (3x50 mL). The organic phase was dried over anhydrous Na<sub>2</sub>SO<sub>4</sub> and evaporated *in vacuo* furnishing a white solid of 0.13 g that was purified by silica gel column chromatography (eluent: DCM/MeOH 30/1), giving the desired product **28** as a white solid of 93 mg (74% yield).

**Mp:** 62-64 °C.

**<sup>1</sup>H NMR** (400 MHz, CDCl<sub>3</sub>) δ 1.07-1.14 (m, 2H), 1.23-1.39 (m, 5H), 1.54 (s, 3H), 1.72-1.80 (m, 2H), 2.07 (s, 3H), 2.17 (s, 6H), 2.43-2.61 (m, 3H), 2.94-2.99 (m, 1H), 3.22-3.25 (m, 2H), 3.27-3.44 (m, 1H), 5.19 (s, 4H), 5.65 (bs, 1H), 6.33 (bs, 2H), 6.91 (d, *J* = 8.4 Hz, 1H), 7.27-7.38 (m, 7H), 7.42-7.47 (m, 4H), 7.52-7.53 (m, 1H).

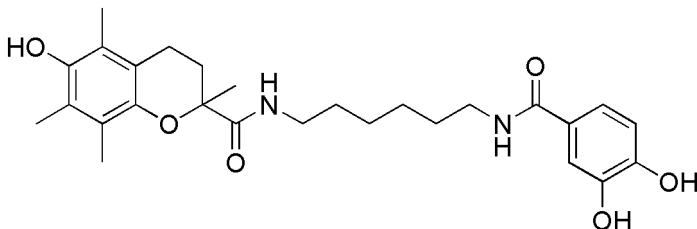
**<sup>13</sup>C NMR** (100 MHz, CDCl<sub>3</sub>) δ 11.5 (1C), 11.9 (1C), 12.4 (1C), 20.7 (1C), 25.4 (1C), 25.7 (1C), 26.4 (1C), 29.5 (1C), 29.57 (1C), 29.64 (1C), 38.5 (1C), 39.9 (1C), 71.0 (1C), 71.3 (1C), 78.5 (1C), 113.7 (1C), 114.0 (1C), 118.1 (1C), 120.1 (1C), 121.4 (1C), 122.5 (1C), 127.2 (2C), 127.4 (2C), 127.7 (1C), 127.9 (1C), 128.50 (1C), 128.54 (1C), 136.7 (1C), 136.9 (1C), 144.40 (1C), 144.43 (1C), 145.9 (1C), 148.8 (1C), 151.6 (1C), 167.1 (1C), 174.3 (1C) [36 of 37 C chemically equivalent].

**IR** (CDCl<sub>3</sub>, cm<sup>-1</sup>) 3624, 3435, 2935, 1702, 1658, 1502, 1266.

**MS (ESI):** m/z 663.49 [M - H]<sup>-</sup>.

Anal. Calcd. for C<sub>41</sub>H<sub>48</sub>N<sub>2</sub>O<sub>6</sub>: C, 74.07%; H, 7.28%; N, 4.21%; O, 14.44%. Found: C, 73.91%; H, 7.11%; N, 4.35%.

6-Hydroxy-2,5,7,8-tetramethyl-chroman-2-carboxylic acid [6-(3,4-dihydroxy-benzoylamino)-hexyl]-amide (**29**)



A solution of **28** (33 mg, 0.050 mmol) in anhydrous THF/MeOH (10/3, 5 mL) was hydrogenated in a mini-H Cube<sup>®</sup> apparatus with Pd/C 10% as catalyst at 60 °C, 1 atm H<sub>2</sub> pressure and 1 mL/min flow. The solvent was evaporated *in vacuo* giving **29** as a white solid of 24 mg that did not require any further purification was obtained (99% yield).

**Mp:** 184-186 °C.

**<sup>1</sup>H NMR** (400 MHz, (CD<sub>3</sub>)<sub>2</sub>CO) δ 1.09-1.17 (m, 2H), 1.25-1.43 (m, 6H), 1.47 (s, 3H), 1.67-1.77 (m, 1H), 2.09 (s, 3H), 2.13 (s, 3H), 2.14 (s, 3H), 2.36-2.42 (m, 1H), 2.45-2.60 (m, 2H), 2.92-3.00 (m, 1H), 3.22-3.27 (m, 2H), 3.28-3.36 (m, 1H), 6.84-6.86 (m, 2H), 7.06 (s, 1H), 7.32 (dd, *J* = 8.0 Hz, *J* = 2.0 Hz, 1H), 7.47 (d, *J* = 2.0 Hz, 1H), 7.70 (bs, 1H), 8.35 (bs, 1H), 8.54 (bs, 1H).

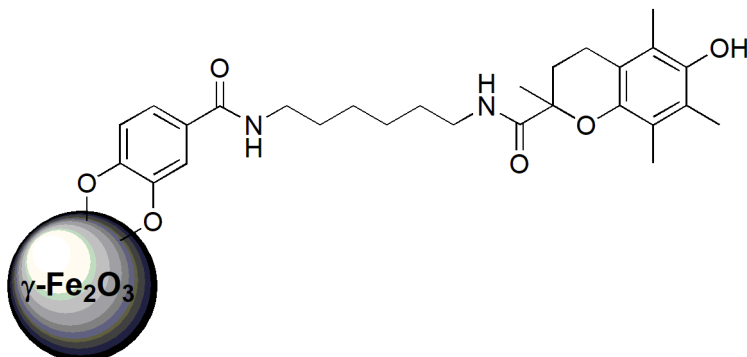
**<sup>13</sup>C NMR** (100 MHz, (CD<sub>3</sub>)<sub>2</sub>CO) δ 12.0, 12.2, 12.9, 21.5, 25.7, 26.7, 27.4, 30.4, 30.6, 39.2, 40.4, 78.9, 115.6, 115.7, 118.7, 120.3, 121.3, 122.2, 123.7, 127.8, 145.3, 145.7, 147.4, 149.1, 167.6, 174.4 [26 of 27 C chemically equivalent].

**IR** (KBr disc, cm<sup>-1</sup>) 3419, 3256, 2934, 2854, 1671, 1637, 1593, 1510, 1461, 1293.

**MS (ESI):** m/z 483.22 [M - H]<sup>-</sup>; 966.54 [2M - H]<sup>-</sup>.

Anal. Calcd. for C<sub>27</sub>H<sub>36</sub>N<sub>2</sub>O<sub>6</sub>: C, 66.92%; H, 7.49%; N, 5.78%; O, 19.81%. Found: C, 67.03%; H, 7.31%; N, 5.89%.

## Fe<sub>2</sub>O<sub>3</sub> conjugate **30**

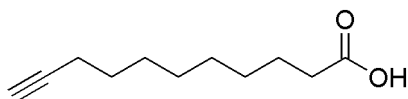


$\gamma$ -Fe<sub>2</sub>O<sub>3</sub> nanoparticles (57 mg) were suspended in a 0.1M Na<sub>2</sub>CO<sub>3</sub> aq. solution (10 mL), then a suspension of **29** (257 mg, 0.53 mmol) in 0.1M Na<sub>2</sub>CO<sub>3</sub> aq. solution (27 mL) was added. The so-obtained mixture was sonicated at room temperature for 2h, then it was acidified to pH 5 and the nanoparticles were washed by magnetic separation using Et<sub>2</sub>O. Residual solvent was eliminated in vacuo, affording a brown solid of 38 mg.

**IR** (KBr disc, cm<sup>-1</sup>) 2930, 2857, 1689, 1488, 1366, 1281, 1172.

**TGA**  $\Delta W$  = -17.278% (35-700 °C, nitrogen atmosphere), +4.496 (700-800 °C, oxygen atmosphere).

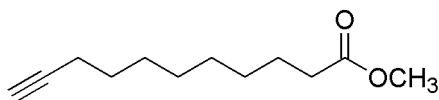
## Undec-10-ynoic acid (**31**)



To a solution 0.05M of 10-undecyn-1-ol (1020 mg, 5.77 mmol) in acetone (160 mL), Na<sub>2</sub>Cr<sub>2</sub>O<sub>7</sub>·2H<sub>2</sub>O (4304 mg, 14.44 mmol) and deionized water (5 mL) were added at 0 °C. Then conc. H<sub>2</sub>SO<sub>4</sub> (1.5 mL) was added dropwise at 0 °C and the reaction mixture was left under magnetic stirring for 15' and filtered. The filtrate was extracted with AcOEt (3x30 mL) and the organic phase washed with water (3x30 mL) and brine (40 mL), dried over Na<sub>2</sub>SO<sub>4</sub> and concentrated in vacuo. The desired product **31** was obtained as a white solid of 1g without any further purification (100% yield).

**<sup>1</sup>H NMR** (CDCl<sub>3</sub>, 200 MHz)  $\delta$  1.26-1.67 (m, 12H), 1.94 (t,  $J$  = 2.6 Hz, 1H), 2.18 (dt,  $J$  = 6.9 Hz,  $J$  = 2.6 Hz, 2H), 2.35 (t,  $J$  = 7.4 Hz, 2H).

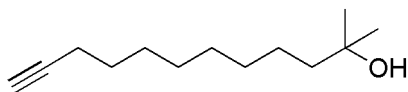
## Undec-10-ynoic acid methyl ester (**32**)



Thionyl chloride (600  $\mu$ L, 8.24 mmol) was added at -15  $^{\circ}$ C to a solution of **31** (750 mg, 4.12 mmol) in anhyd. MeOH (21 mL). The reaction mixture was left under magnetic stirring at room temperature for 1h, then the solvent was evaporated. After the dilution with water, the mixture was extracted with Et<sub>2</sub>O (4x20 mL), washed with water until pH = 7 and finally with brine. The organic phase was dried over Na<sub>2</sub>SO<sub>4</sub> and concentrated in vacuo, affording the desired product **32** as a yellow oil of 701 mg without any further purification (87%).

**<sup>1</sup>H NMR** (CDCl<sub>3</sub>, 200 MHz)  $\delta$  1.31-1.67 (m, 12H), 1.93 (t,  $J$  = 2.6 Hz, 1H), 2.18 (dt,  $J$  = 6.9 Hz,  $J$  = 2.6 Hz, 2H), 2.30 (t,  $J$  = 7.4 Hz, 2H), 3.66 (s, 3H).

#### 2-Methyl-dodec-11-yn-2-ol (**33**)



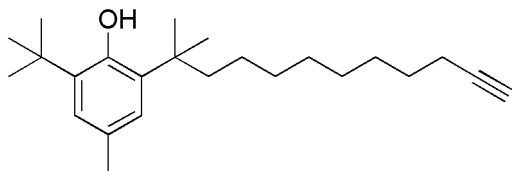
In a Schlenk tube, to a solution of **32** (1009 mg, 5.15 mmol) in anhydrous Et<sub>2</sub>O (20 mL), Methylmagnesium Bromide (3.0 M in Et<sub>2</sub>O, 8 mL, 26.00 mmol) was added dropwise at -78  $^{\circ}$ C. The mixture was left under magnetic stirring and N<sub>2</sub> atmosphere allowing warming to room temperature, then after 15h it was quenched with ice and acidified to pH 4 with aq. HCl 3N. The so-obtained suspension was extracted with AcOEt (3x20 mL), then collected organic phases were washed with water (3x10 mL), dried over anhydrous Na<sub>2</sub>SO<sub>4</sub> and evaporated *in vacuo*, furnishing a crude that was purified through flash column chromatography (eluent Ep/AcOEt 5/1) affording the desired product **33** as a colourless oil of 973 mg (96%).

**<sup>1</sup>H NMR** (CDCl<sub>3</sub>, 400 MHz)  $\delta$  1.20 (s, 6H), 1.29-1.53 (m, 14H), 1.93 (t,  $J$  = 2.6 Hz, 1H), 2.17 (dt,  $J$  = 7.2 Hz,  $J$  = 2.6 Hz, 2H).

**<sup>13</sup>C NMR** (CDCl<sub>3</sub>, 100 MHz)  $\delta$  18.4, 24.3, 28.4, 28.7, 29.0, 29.2, 29.5, 30.1, 44.0, 68.1, 71.0, 84.8.

**IR** (CDCl<sub>3</sub>, cm<sup>-1</sup>)  $\nu$  3607, 3308, 2934, 2858, 2116, 1467.

#### 2-*tert*-Butyl-6-(1,1-dimethyl-undec-10-ynyl)-4-methyl-phenol (**34**)



A solution of **32** (200 mg, 1.02 mmol) and 2-*tert*-butyl-4-methylphenol (170 mg, 1.04 mmol) in 1,2-DCE (6 mL) was added dropwise at 0  $^{\circ}$ C to a suspension of CH<sub>3</sub>SO<sub>3</sub>H (439 mg, 4.57 mmol) in 1,2-DCE (1 mL). The resulting red solution was left under magnetic stirring at room temperature, monitored by TLC (eluent: petroleum ether/Et<sub>2</sub>O 4/1 and petroleum ether). After 24h the reaction was quenched with saturated aq. NaHCO<sub>3</sub>, then the resulting mixture was diluted with DCM (30 mL) and washed with saturated

aq. NaHCO<sub>3</sub> (3x10 mL) and water (3x10 mL). The organic phase was dried over anhydrous Na<sub>2</sub>SO<sub>4</sub> and evaporated in vacuo furnishing a yellow oil that was purified by silica gel column chromatography (eluent: petroleum ether→petroleum ether/DCM 10/1), giving the desired product **34** as a yellow oil of 59 mg (17% yield).

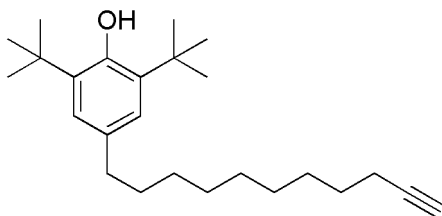
<sup>1</sup>H NMR (CDCl<sub>3</sub>, 400 MHz) δ: 1.04–1.39 (m, 10H), 1.40 (s, 6H), 1.43 (s, 9H), 1.46–1.54 (m, 2H), 1.77–1.81 (m, 2H), 1.94 (t, *J* = 2.6 Hz, 1H), 2.17 (dt, *J* = 7.0 Hz, *J* = 2.6 Hz, 2H), 2.28 (s, 3H), 5.02 (s, 1H), 6.91 (s, 1H), 6.99 (s, 1H).

<sup>13</sup>C NMR (CDCl<sub>3</sub>, 100 MHz) δ 18.40, 18.43, 21.3, 25.1, 28.5, 28.7, 29.0, 29.19, 29.24, 30.2, 30.3, 34.2, 37.7, 41.8, 68.1, 84.8, 125.5, 126.6, 128.0, 134.1, 135.5, 151.5.

IR (CDCl<sub>3</sub>, cm<sup>-1</sup>) ν 3632, 3308, 2931, 2857, 1434, 1386.

MS (ESI) *m/z* 283.50 [M – 58]<sup>-</sup>; 341.58 [M – H]<sup>-</sup>.

#### 2,6-Di-*tert*-butyl-4-undec-10-ynyl-phenol (**35**)



**31** (484 mg, 2.66 mmol) was dissolved in 440 μL of trifluoroacetic anhydride, then after 10' 2,6-Di-*tert*-butylphenol (413 mg, 2.00 mmol) was added at 0 °C. The so formed brown solution was stirred at 0 °C for 30' and then at room temperature until the disappearance of the starting phenol after 3h (eluent for TLC control: Ep/Et<sub>2</sub>O 10/1). To the resulting dark solution absolute EtOH (10 mL), glacial acetic acid (5 mL) and 37% HCl (3.0 mL) were added, then the mixture was heated to reflux and activated Zn dust (<10μ, 3000 mg, 46 mmol) was added in small portions. The resulting colourless suspension was vigorously stirred under reflux for 18h, then after TLC control (eluent: Ep/Et<sub>2</sub>O 15/1) the absence of the intermediate ketone was demonstrated and the reaction was quenched with saturated aq. NaHCO<sub>3</sub>. The residual Zinc was filtered off and the filtrate was extracted with petroleum ether (3x15 mL), then the organic phase was washed with saturated aq. NaHCO<sub>3</sub> (3x20 mL) and water (3x20 mL). The organic phase was dried over anhydrous Na<sub>2</sub>SO<sub>4</sub> and evaporated *in vacuo* furnishing a yellow oil that was purified by silica gel column chromatography (eluent: petroleum ether/DCM 10/1), giving the product **35** as a colourless oil of 237 mg (34% yield).

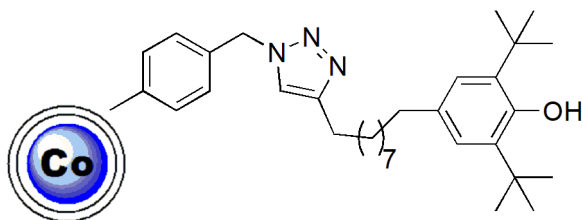
<sup>1</sup>H NMR (CDCl<sub>3</sub>, 400 MHz) δ 1.31-1.60 (m, 32H), 1.95 (t, *J* = 2.6 Hz, 1H), 2.19 (dt, *J* = 7.2 Hz, *J* = 2.6 Hz, 2H), 2.51 (t, *J* = 8.0 Hz, 2H), 5.04 (s, 1H), 6.98 (s, 2H).

$^{13}\text{C}$  NMR ( $\text{CDCl}_3$ , 100 MHz)  $\delta$  18.4, 28.5, 28.7, 29.1, 29.5, 29.6, 30.3, 32.0, 34.2, 36.0, 68.0, 84.8, 124.8, 133.47, 135.50, 151.6.

IR ( $\text{CDCl}_3$ ,  $\text{cm}^{-1}$ ) v: 3643, 3308, 2931, 2857, 2116, 1458, 1435.

MS (ESI)  $m/z$  355.58  $[\text{M} - \text{H}]^-$ .

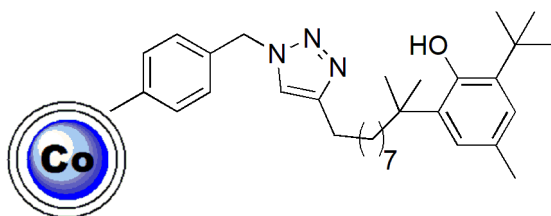
Co- $\text{N}_3$  conjugate **36a**



*Turbobeads Click* (100 mg, 0.1 mmol/g azide-loading, 0.01 mmol) were washed with degassed toluene (3x1 mL) and suspended in the same solvent (4 mL) by sonication (10 min) before **35** (24 mg, 0.07 mmol,) TEA (5 $\mu\text{L}$ , 0.04 mmol) and CuI (1 mg, 0.005 mmol) were added. The resulting slurry was sonicated for 24h at room temperature under a nitrogen atmosphere, then a second crop of CuI (1 mg, 0.005 mmol) was added and the mixture sonicated for additional 12h. The nanoparticles were recovered from the reaction mixture with the aid of a neodymium based magnet and washed with toluene (2x9 mL). Adventitious trace of residual Cu(I) salts were removed by washing with a solution of 33% ammonia/EtOH (2/1, 5 mL) under sonication for 30 min, then the solution was removed and the nanoparticles washed twice with, in sequence, water (2x4 mL), EtOH (2x4 mL) and DCM (2x4 mL) sequentially. Each washing step consisted of suspending the particles in the solvent, sonication (5 min) and retracting the particles from the solvent by the aid of the magnet. After the last washing step, the particles were dried in vacuum overnight and recovered as a black solid of 98 mg.

IR (KBr,  $\text{cm}^{-1}$ ) v: 3400, 2952, 2919, 1601, 1457, 1261, 1099.

Co- $\text{N}_3$  conjugate **37**



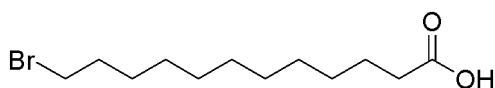
*Turbobeads Click* (120 mg, 0.1 mmol/g azide-loading, 0.01 mmol) were washed with degassed toluene (3x1 mL) and suspended in the same solvent (4 mL) by sonication (10 min) before **34** (50 mg, 0.15 mmol,) TEA (10 $\mu\text{L}$ , 0.08 mmol) and CuI (2 mg, 0.01 mmol) were added. The resulting slurry was sonicated for 24h at room temperature under a nitrogen atmosphere, then a second crop of CuI (2 mg, 0.01 mmol) was added and the



mixture sonicated for additional 12h. The nanoparticles were recovered from the reaction mixture with the aid of a neodymium based magnet and washed with toluene (2x9 mL). Adventitious trace of residual Cu(I) salts were removed by washing with a solution of 33% ammonia/EtOH (2/1, 5 mL) under sonication for 30 min, then the solution was removed and the nanoparticles washed twice with, in sequence, water (2x4 mL), EtOH (2x4 mL) and DCM (2x4 mL) sequentially. Each washing step consisted of suspending the particles in the solvent, sonication (5 min) and retracting the particles from the solvent by the aid of the magnet. After the last washing step, the particles were dried in vacuum overnight and recovered as a black solid of 111 mg.

**IR** (KBr,  $\text{cm}^{-1}$ ) v: 3435, 2919, 2851, 1620, 1430, 1261, 1095.

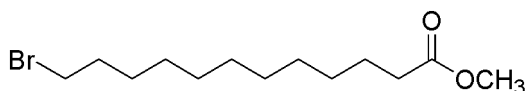
#### 12-Bromo-dodecanoic acid (**38**)



To a solution 0.05M of 12-bromododecan-1-ol (544 mg, 2.05 mmol) in acetone (40 mL),  $\text{Na}_2\text{Cr}_2\text{O}_7 \cdot 2\text{H}_2\text{O}$  (1548 mg, 5.20 mmol) and deionized water (2.5 mL) were added at 0 °C. Then conc.  $\text{H}_2\text{SO}_4$  (0.5 mL) was added dropwise at 0 °C and the reaction mixture was left under magnetic stirring for 15' and filtered. The filtrate was extracted with AcOEt (3x30 mL) and the organic phase washed with water (3x30 mL) and brine (40 mL), dried over  $\text{Na}_2\text{SO}_4$  and concentrated in vacuo. The desired product **38** was obtained as a white solid of 514 mg without any further purification (90% yield).

**$^1\text{H NMR}$**  ( $\text{CDCl}_3$ , 200 MHz)  $\delta$  1.28-1.66 (m, 16H), 1.78-1.91 (m, 2H), 2.34 (t,  $J = 7.5$  Hz, 2H), 3.40 (t,  $J = 6.9$  Hz, 2H).

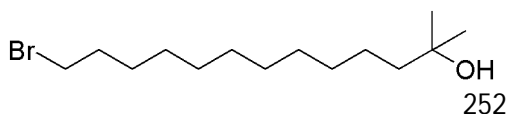
#### 12-Bromo-dodecanoic acid methyl ester (**39**)



Conc.  $\text{H}_2\text{SO}_4$  (0.64 mL) was added dropwise at 0°C to a solution of **38** (509 mg, 1.82 mmol) in anhyd. MeOH (5 mL). The reaction mixture was left under magnetic magnetic stirring at room temperature for 24h, then the solvent was evaporated. After the dilution with petroleum ether the organic phase was washed with saturated aq.  $\text{NaHCO}_3$  (3x30 mL) and brine (2x30 mL), dried over  $\text{Na}_2\text{SO}_4$  and concentrated in vacuo. The desired product **39** was isolated as a yellow oil of 411 mg without any further purification (77%).

**$^1\text{H NMR}$**  ( $\text{CDCl}_3$ , 200 MHz)  $\delta$  1.27-1.64 (m, 16H), 1.78-1.92 (m, 2H), 2.30 (t,  $J = 7.4$  Hz, 2H), 3.41 (t,  $J = 6.8$  Hz, 2H), 3.67 (s, 3H).

#### 13-Bromo-2-methyl-tridecan-2-ol (**40**)



252

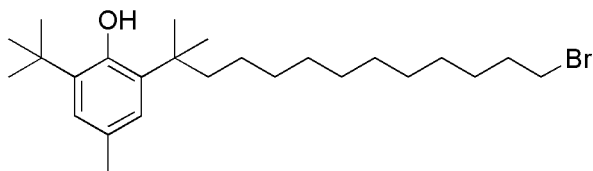
In a Schlenk tube, to a 0.5 M solution of **39** (380 mg, 1.31 mmol) in anhydrous THF (2 mL), Methylmagnesium Bromide (3.0 M in Et<sub>2</sub>O, 2 mL, 6.00 mmol) was added dropwise at -78 °C. The mixture was left under magnetic stirring and N<sub>2</sub> atmosphere at 0 °C, then after 4h it was quenched with ice and saturate aq. NH<sub>4</sub>Cl. The so-obtained suspension was extracted with AcOEt (3x30 mL), then collected organic phases were washed with water (3x20 mL) and brine (3x20 mL), dried over anhydrous Na<sub>2</sub>SO<sub>4</sub> and evaporated *in vacuum*, furnishing the product **40** as a yellow oil of 299 mg that did not require any further purification (79%).

<sup>1</sup>H NMR (CDCl<sub>3</sub>, 400 MHz) δ 1.20 (s, 6H), 1.27-1.45 (m, 18H), 1.81-1.88 (m, 2H), 3.40 (t, *J* = 7.0 Hz, 2H).

<sup>13</sup>C NMR (CDCl<sub>3</sub>, 100 MHz) δ: 24.3, 28.2, 28.8, 29.2, 29.4, 29.5, 29.55, 29.62, 30.2, 32.8, 34.1, 44.0, 71.1.

IR (CDCl<sub>3</sub>, cm<sup>-1</sup>) ν 3608, 2931, 2856.

#### 2-(12-Bromo-1,1-dimethyl-dodecyl)-6-*tert*-butyl-4-methyl-phenol (**41**)



A mixture of **40** (92 mg, 0.32 mmol) and 2-*tert*-butyl-4-methylphenol (53 mg, 0.32 mmol) was heated at 40 °C until the complete dissolution, then CH<sub>3</sub>SO<sub>3</sub>H (154 mg, 1.60 mmol) was added dropwise at 0 °C. The reaction mixture was left under magnetic stirring at 0 °C for 3h and then at room temperature for 15h. After the addition of ice, the mixture was diluted with DCM (40 mL) and washed with saturated aq. NaHCO<sub>3</sub> (3x20 mL) and water (3x20 mL), dried over Na<sub>2</sub>SO<sub>4</sub> and concentrated *in vacuo*. The crude was purified through flash column chromatography (eluent: petroleum ether/DCM 25/1) affording the product **41** as a colourless oil of 60 mg (44%).

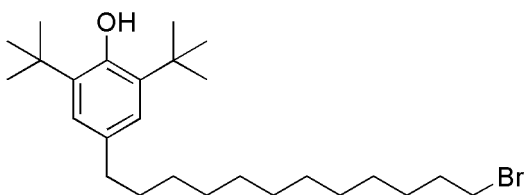
<sup>1</sup>H NMR (CDCl<sub>3</sub>, 400 MHz) δ 1.20-1.28 (m, 16H), 1.38 (s, 6H), 1.42 (s, 9H), 1.75-1.87 (m, 4H), 2.27 (s, 3H), 3.40 (t, *J* = 7.0 Hz, 2H), 5.01 (s, 1H), 6.90 (s, 1H), 6.97 (s, 1H).

<sup>13</sup>C NMR (CDCl<sub>3</sub>, 100 MHz) δ 21.3, 25.1, 28.2, 28.8, 29.2, 29.37, 29.41, 29.49, 29.53, 30.20, 30.23, 32.8, 24.1, 24.2, 27.7, 41.8, 125.4, 26.6, 128.0, 134.1, 135.5, 151.5.

IR (CDCl<sub>3</sub>, cm<sup>-1</sup>) ν 3634, 2927, 2853, 1712, 1456, 1432.

MS (ESI) *m/z* 437.33 [M - H].

#### 4-(12-Bromo-dodecyl)-2,6-di-*tert*-butyl-phenol (**42**)



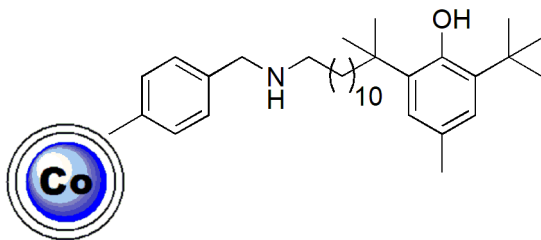
**38** (371 mg, 1.33 mmol) was dissolved in 220  $\mu\text{L}$  of trifluoroacetic anhydride, then after 10' 2,6-di-*tert*-butylphenol (206 mg, 1.00 mmol) was added at 0  $^{\circ}\text{C}$ . The so formed brown solution was stirred at 0  $^{\circ}\text{C}$  for 30' and then at room temperature until the disappearance of the starting phenol after 3h (eluent for TLC control: Ep/Et<sub>2</sub>O 4/1). To the resulting dark solution absolute EtOH (5 mL), glacial acetic acid (2.5 mL) and 37% HCl (2.0 mL) were added, then the mixture was heated to reflux and activated Zn dust (<10 $\mu\text{m}$ , 3000 mg, 46 mmol) was added in small portions. The resulting colourless suspension was vigorously stirred under reflux for 18h, then after TLC control (eluent: Ep/Et<sub>2</sub>O 4/1) the absence of the intermediate ketone was demonstrated and the reaction was quenched with saturated aq. NaHCO<sub>3</sub>. The residual Zinc was filtered off and the filtrate was extracted with petroleum ether (3x15 mL), then the organic phase was washed with saturated aq. NaHCO<sub>3</sub> (3x20 mL) and water (3x20 mL). The organic phase was dried over anhydrous Na<sub>2</sub>SO<sub>4</sub> and evaporated in vacuo furnishing a yellow oil that was purified by silica gel column chromatography (eluent: petroleum ether  $\rightarrow$  petroleum ether/Et<sub>2</sub>O 10/1), giving the product **42** as a yellow oil of 220 mg (48% yield).

<sup>1</sup>H NMR (CDCl<sub>3</sub>, 400 MHz)  $\delta$  1.24-1.40 (m, 18H), 1.44 (s, 18H), 1.82-1.89 (m, 2H), 2.50 (t,  $J = 8.0$  Hz, 2H), 3.41 (t,  $J = 6.8$  Hz, 2H), 5.01 (s, 1H), 6.97 (s, 2H).

<sup>13</sup>C NMR (CDCl<sub>3</sub>, 100 MHz)  $\delta$  28.2, 28.8, 29.4, 29.5, 29.61, 29.63, 30.3, 30.5, 31.5, 32.0, 32.8, 34.0, 34.3, 36.0, 124.8, 133.5, 135.6, 151.6.

IR (CDCl<sub>3</sub>, cm<sup>-1</sup>)  $\nu$  3643, 2918, 2856, 1466, 1436.

Co-NH<sub>2</sub> conjugate **43**

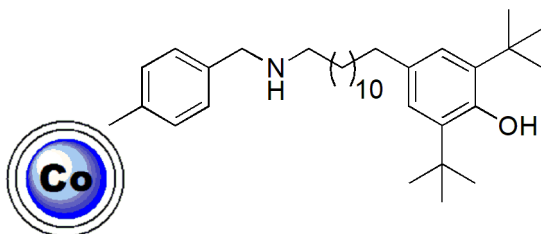


*Turbobeads Amine* (102 mg, 0.1 mmol/g azide-loading, 0.01 mmol) were washed with degassed DMF (3x2 mL) and suspended in the same solvent (6 mL) by sonication (10 min) before **41** (38 mg, 0.09 mmol,) and TEA (5  $\mu\text{L}$ , 0.04 mmol) were added. The resulting slurry was sonicated for 36h at room temperature under a nitrogen atmosphere, then the nanoparticles were recovered from the reaction mixture with the aid of a neodymium based magnet and washed with DMF (2x5 mL), water (2x4 mL),

EtOH (2x4 mL) and Et<sub>2</sub>O (2x4 mL) sequentially. Each washing step consisted of suspending the particles in the solvent, sonication (5 min) and retracting the particles from the solvent by the aid of the magnet. After the last washing step, the particles were dried in vacuum overnight and recovered as a black solid of 89 mg.

IR (KBr, cm<sup>-1</sup>)  $\nu$  3421, 2923, 2849, 1648, 1436, 1068.

Co-NH<sub>2</sub> conjugate **44**



*Turbobeads Amine* (200 mg, 0.1 mmol/g azide-loading, 0.01 mmol) were washed with degassed DMF (3x2 mL) and suspended in the same solvent (8 mL) by sonication (10 min) before **42** (90 mg, 0.20 mmol,) and TEA (6  $\mu$ L, 0.06 mmol) were added. The resulting slurry was sonicated for 36h at room temperature under a nitrogen atmosphere, then the nanoparticles were recovered from the reaction mixture with the aid of a neodymium based magnet and washed with DMF (2x5 mL), water (2x4 mL), EtOH (2x4 mL) and Et<sub>2</sub>O (2x4 mL) sequentially. Each washing step consisted of suspending the particles in the solvent, sonication (5 min) and retracting the particles from the solvent by the aid of the magnet. After the last washing step, the particles were dried in vacuum overnight and recovered as a black solid of 180 mg.

IR (KBr, cm<sup>-1</sup>)  $\nu$  3832, 3737, 3433, 2922, 2645, 1650, 1560, 1507, 1399, 1253, 1102.

### 5.3.2 Chain-breaking antioxidants activity

The chain-breaking antioxidant activity of the title compounds was evaluated by studying the inhibition of the thermally initiated autoxidation of styrene in chlorobenzene. Styrene was percolated twice on an alumina column before use, AIBN was recrystallized from methanol and stored at -20 °C. Solvents of the highest purity grade were used as received. Autoxidation experiments were followed by measuring the O<sub>2</sub> consumption by using a gas-uptake recording apparatus. In a typical experiment, an air-saturated mixture of styrene in chlorobenzene (50% v/v) containing AIBN (25 mM) was equilibrated with the reference solution containing also an excess of butylhydroxytoluene (BHT) in the same solvent at 30°C. After equilibration, a concentrated solution of the antioxidant was injected into the sample flask, and the oxygen consumption in the sample was measured. In the case of the experiments on CoNPs, the procedure was slightly modified, because of the impossibility to inject the magnetic CoNPs dispersions. A known amount of NPs was put in the sample vessel, and was dispersed in PhCN by sonication for 5 minutes. Then, after the addition of a concentrated AIBN solution and of styrene, the vessel was rapidly connected to the pressure recorder. The concentration of the antioxidant in the case of CoNPs-TOH was

derived from that of the  $-N_3$  or  $NH_2$  moieties in CoNPs- $N_3$  and CoNPs- $NH_2$  (0.1 mmol/g) respectively. From the slope of the oxygen consumption during the inhibited period,  $k_{inh}$  values were obtained by using the equation [1], while the  $n$  coefficient was determined by the length of the inhibited period ( $T_{inh}$ ) by using the equation [2] and [3].<sup>55</sup>

$$\Delta[O_2]_t = -k_p/k_{inh} [\text{styrene}] \ln(1-t / T_{inh}) \quad [1]$$

$$n = R_i T_{inh} / [\text{antioxidant}] \quad [2]$$

$$R_i = 2 [\text{BHT}] / T_{inh} \quad [3]$$

The  $k_p$  values (the propagation rate constant of the oxidizable substrate) of styrene at 303° is 41  $M^{-1} s^{-1}$ . The value of  $R_i$  (the speed in the production of radicals by the initiator) was determined by using BHT ( $n=2$ ) as a reference.

### 5.3.3 Stability tests on THF

The semi-quantitative determination of the hydroperoxides formation in THF was done using commercially available test strips with the trademark QUANTOFIX® Peroxide 25. In the presence of hydroperoxide in concentration between 0.5 and 25 mg/L, the colour of these strips turns from white to blue and a semi-quantification can be done by comparison to a colour scale.<sup>176</sup>

The evaluation of the hydroperoxides development in test solutions of THF containing the CoNPs-AntiOx was done using two different concentrations of the nanostructured antioxidants for each sample, 50 and 250 ppm. As references were also used a THF sample without stabilizers and two containing respectively 50 and 250 ppm of the molecular antioxidant BHT, corresponding to the range of concentration of the stabilizer in the commercial products. Each THF sample was stored in a 25 mL clear glass bottle closed with a screw top and exposed to the light in order to speed up the autooxidation of THF. Because the nanostructured antioxidants were not well dispersed in the solvent, each day their samples were manually stirred for about 30 seconds in order to facilitate the contact with the hydroperoxides in solution. In Table 4 is reported the composition of each bottle used for the test.

**Table 4:** Composition of THF samples used for the test stability with antioxidant functionalized Co-NPs.

Bottle	Stabilizer	Amount (mg)	mmol
1	-	-	-
2	BHT	0.5	$2.3 \times 10^{-3}$ (50 ppm)
3	BHT	2.5	$11.5 \times 10^{-3}$ (250 ppm)
4	Turbobeads Click	23	$2.3 \times 10^{-3}$ (50 ppm)

5	<i>Turbobeads Click</i>	115	$11.5 \times 10^{-3}$ (250 ppm)
6	<i>Turbobeads Amine</i>	23	$2.3 \times 10^{-3}$ (50 ppm)
7	<i>Turbobeads Amine</i>	115	$11.5 \times 10^{-3}$ (250 ppm)
8	<b>36a</b>	23.8	$2.3 \times 10^{-3}$ (50 ppm)
9	<b>36b</b>	23.8	$2.3 \times 10^{-3}$ (50 ppm)
10	<b>36b</b>	111	$11.5 \times 10^{-3}$ (250 ppm)
11	<b>37</b>	23.5	$2.3 \times 10^{-3}$ (50 ppm)
12	<b>43</b>	23.9	$2.3 \times 10^{-3}$ (50 ppm)
13	<b>44</b>	23.6	$2.3 \times 10^{-3}$ (50 ppm)
14	<b>44</b>	115	$11.5 \times 10^{-3}$ (250 ppm)

For determining the amount (in weigh) of CoNPs-AntiOx to add in order to obtain a content of antioxidant moiety of 50-250 ppm a simplification was done. We considered that the yield of the functionalization was 100% then, because the functional loading of the commercial nanoparticles is known (0.1 mmol/g), it was possible to calculate the corresponding amount of antioxidant moieties (in mmol).

## 5.4 References

- (1) Horikoshi, S.; Serpone, N. In *Microwaves in Nanoparticles Synthesis: Fundamentals and Applications*; Horikoshi, S., Serpone, N., Eds.; Wiley-VCH Verlag GmbH & Co. KGaA: Weinheim, Germany, 2013; pp 1–24.
- (2) Roduner, E. *Chem. Rev.* **2006**, *35*, 583–592.
- (3) De Morais, M. G.; Martins, V. G.; Steffens, D.; Pranke, P.; da Costa, J. A. V. *J. Nanosci. Nanotechnol.* **2014**, *14*, 1007–1017.
- (4) Contado, C. *Front. Chem.* **2015**, *3*, doi: 10.3389/fchem.2015.00048.
- (5) Mcnamara, K.; Tofail, S. A. M. *Adv. Phys. X* **2017**, *2*, 54–88.
- (6) Nel, A. E.; Mädler, L.; Velegol, D.; Xia, T.; Hoek, E. M. V.; Somasundaran, P.; Klaessig, F.; Castranova, V.; Thompson, M. *Nat. Mater.* **2009**, *8*, 543–557.
- (7) Hedayatnasab, Z.; Abnisa, F.; Wan Daus, W. M. A. *Mater. Des.* **2017**, *123*, 174–196.
- (8) De Jong, W. H.; Borm, P. J. A. *Int. J. Nanomedicine* **2008**, *3*, 133–149.
- (9) Gun'ko, Y. K. *Nanomaterials* **2016**, *6* (105), 1–3.

- (10) Wu, C.; Yang, Y.; Hsu, Y.; Wu, T.-C.; Hung, C.-F.; Huang, J.-T.; Chang, C.-L.-. *Oncotarget* **2015**, *6*, 26861–26875.
- (11) Holzinger, M.; Le Goff, A.; Cosnier, S. *Front. Chem.* **2014**, *2* (63), doi: 10.3389/fchem.2014.00063.
- (12) Donaldson, K.; Stone, V.; Tran, C. L.; Kreyling, W.; Borm, P. J. A. *Occup. Environ. Med.* **2004**, *61*, 727–728.
- (13) Oberdörster, G.; Oberdörster, E.; Oberdörster, J. *Environ. Health Perspect.* **2005**, *113*, 823–839.
- (14) Li, N.; Xia, T.; Nel, A. E. *Free Radic. Biol. Med.* **2008**, *44*, 1689–1699.
- (15) Kovacic, P.; Somanathan, R. *J. Nanosci. Nanotechnol.* **2010**, *10*, 7919–7930.
- (16) Nel, A.; Xia, T.; Madler, L.; Li, N. *Science (80-. )*. **2006**, *311*, 622–627.
- (17) Xia, T.; Kovochich, M.; Liong, M.; Madler, L.; Gilbert, B.; Shi, H.; Ye, J. I.; Zink, J. I.; Nel, a. E. *ACS Nano* **2008**, *2*, 2121–2134.
- (18) Fu, P. P.; Xia, Q.; Hwang, H.-M.; Ray, P. C.; Yu, H. *J. Food Drug Anal.* **2014**, *22*, 64–75.
- (19) Khanna, P.; Ong, C.; Bay, B. H.; Hun Baeg, G. *Nanomaterials* **2015**, *5*, 1163–1180.
- (20) Gonzalez, L.; Lison, D.; Kirsch-Volders, M. *Nanotoxicology* **2008**, *2*, 252–273.
- (21) Grabinski, C.; Hussain, S.; Lafdi, K.; Braydich-Stolle, L.; Schlager, J. *Carbon N. Y.* **2007**, *45*, 2828–2835.
- (22) Li, X.; Liu, W.; Sun, L.; Aifantis, K. E.; Yu, B.; Fan, Y.; Feng, Q.; Cui, F.; Watari, F. *J. Biomed. Mater. Res. - Part A* **2015**, *103*, 2499–2507.
- (23) Manke, A.; Wang, L.; Rojanasakul, Y. *Biomed Res. Int.* **2013**, *2013*, 15.
- (24) Sarkar, A.; Ghosh, M.; Sil, P. C. *J. Nanosci. Nanotechnol.* **2014**, *14*, 730–743.
- (25) Yildirim, L.; Thanh, N. T. K.; Loizidou, M.; Seifalian, A. M. *Nano Today* **2011**, *6*, 585–607.
- (26) Elswaifi, S. F.; Palmieri, J. R.; Hockey, K. S.; Rzigalinski, B. A. *Infect. Disord. Drug Targets* **2009**, *9*, 445–452.
- (27) Celardo, I.; Pedersen, J. Z.; Traversa, E.; Ghibelli, L. *Nanoscale* **2011**, *3*, 1411–1420.
- (28) Heckman, K. L.; Decoteau, W.; Estevez, A.; Reed, K. J.; Costanzo, W.; Sanford, D.; Leiter, J. C.; Clauss, J.; Knapp, K.; Gomez, C.; Mullen, P.; Rathbun, E.; Prime, K.; Marini, J.; Patchefsky, J.; Patchefsky, A. S.; Hailstone, R. K.; Erlichman, J. S. *ACS Nano*

**2013**, 7, 10582–10596.

- (29) Nelson, B.; Johnson, M.; Walker, M.; Riley, K.; Sims, C. *Antioxidants* **2016**, 5 (15), 1–21.
- (30) Kwon, H. J.; Cha, M. Y.; Kim, D.; Kim, D. K.; Soh, M.; Shin, K.; Hyeon, T.; Mook-Jung, I. *ACS Nano* **2016**, 10, 2860–2870.
- (31) Kang, D.-W.; Kim, C. K.; Jeong, H.-G.; Soh, M.; Kim, T.; Choi, I.-Y.; Ki, S.-K.; Kim, D. Y.; Yang, W.; Hyeon, T.; Lee, S.-H. *Nano Res.* **2017**, 10, 2743–2760.
- (32) Zhang, L.; Laug, L.; Münchgesang, W.; Pippel, E.; Gösele, U.; Brandsch, M.; Knez, M. *Nano Lett.* **2010**, 10, 219–223.
- (33) Stress, O.; Mencho, C.; Apostolova, N.; Victor, V. M.; Mercedes, A.; Garci, H. *ACS Nano* **2010**, 4, 6957–6965.
- (34) Chompoosor, A.; Saha, K.; Ghosh, P. S.; Macarthy, D. J.; Miranda, O. R.; Zhu, Z.-J.; Arcaro, K. F.; Rotello, V. M. *Small* **2010**, 6, 2246–2249.
- (35) Tedesco, S.; Doyle, H.; Redmond, G.; Sheehan, D. *Mar. Environ. Res.* **2008**, 66, 131–133.
- (36) Han, J. W.; Gurunathan, S.; Jeong, J.-K.; Choi, Y.-J.; Kwon, D.-N.; Park, J.-K.; Kim, J.-H. *Nanoscale Res. Lett.* **2014**, 9, 459.
- (37) Liu, G.; Gao, J.; Ai, H.; Chen, X. *Small* **2013**, 9, 1533–1545.
- (38) Huerta-garcía, E.; Pérez-arizti, J. A.; Márquez-ramírez, S. G.; Delgado-Buenrostro, N. L.; Irasema Chirino, Y.; Gutiérrez Iglesias, G.; López-Marure, R. *Free Radic. Biol. Med.* **2014**, 73, 84–94.
- (39) Buffet, P.-E.; Zalouk-Vergnoux, A.; Poirier, L.; Lopes, C.; Risso-de Faverney, C.; Guibbolini, M.; Gilliland, D.; Perrein-Ettajani, H.; Valsami-Jones, E.; Mouneyrac, C. *Environ. Toxicol. Chem.* **2015**, 34, 1659–1664.
- (40) Zhang, T.; Hu, Y.; Tang, M.; Kong, L.; Ying, J.; Wu, T.; Xue, Y.; Pu, Y. *Int. J. Mol. Sci.* **2015**, 16, 23279–23299.
- (41) Shvedova, A. A.; Pietroiusti, A.; Fadeel, B.; Kagan, V. E. *Toxicol. Appl. Pharmacol.* **2012**, 261, 121–133.
- (42) Guo, C.; Xia, Y.; Niu, P.; Jiang, L.; Duan, J.; Yu, Y.; Zhou, X.; Li, Y.; Sun, Z. *Int. J. Nanomedicine* **2015**, 10, 1463–1477.
- (43) Patil, U. S.; Adireddy, S.; Jaiswal, A.; Mandava, S.; Lee, B. R.; Chrisey, D. B. *Int. J. Mol. Sci.* **2015**, 16, 24417–24450.
- (44) Griffitt, R. J.; Weil, R.; Hyndman, K. A.; Denslow, N. D.; Powers, K.; Taylor, D.; Barber, D. S. *Environ. Sci. Technol.* **2007**, 41 (23), 8178–8186.



- (45) Tiwari, D. K.; Jin, T.; Behari, J. *Toxicol. Mech. Methods* **2011**, *21*, 13–24.
- (46) Rahman, M. F.; Wang, J.; Patterson, T. A.; Saini, U. T.; Robinson, B. L.; Newport, G. D.; Murdock, R. C.; Schlager, J. J.; Hussain, S. M.; Ali, S. F. *Toxicol. Lett.* **2009**, *187*, 15–21.
- (47) Trouiller, B.; Reliene, R.; Westbrook, A.; Solaimani, P.; Schiestl, R. H. *Mol. Biol. Pathobiol. Genet.* **2009**, *69*, 8784–8789.
- (48) Morry, J.; Ngamcherdtrakul, W.; Yantasee, W. *Redox Biol.* **2017**, *11*, 240–253.
- (49) Finkel, T.; Holbrook, N. J. *Nature* **2000**, *408*, 239–247.
- (50) Cui, H.; Kong, Y.; Zhang, H. *J. Signal Transduct.* **2012**, *2012*, 1–13.
- (51) Uttara, B.; Singh, A. V.; Zamboni, P.; Mahajan, R. T. *Curr. Neuropharmacol.* **2009**, *7*, 65–74.
- (52) Guo, D.; Zhu, L.; Huang, Z.; Zhou, H.; Ge, Y.; Ma, W.; Wu, J.; Zhang, X.; Zhou, X.; Zhang, Y.; Zhao, Y.; Gu, N. *Biomaterials* **2013**, *34*, 7884–7894.
- (53) Ahamed, M.; Akhtar, M. J.; Siddiqui, M. A.; Ahmad, J.; Musarrat, J.; Al-Khedhairy, A. A.; AlSalhi, M. S.; Alrokayan, S. A. *Toxicology* **2011**, *283*, 101–108.
- (54) Posgai, R.; Cipolla-McCulloch, C. B.; Murphy, K. R.; Hussain, S. M.; Rowe, J. J.; Nielsen, M. G. *Chemosphere* **2011**, *85*, 34–42.
- (55) Fukui, H.; Iwahashi, H.; Endoh, S.; Nishio, K.; Yoshida, Y.; Hagihara, Y.; Horie, M. *J. Occup. Health* **2015**, *57* (2), 118–125.
- (56) Sarkar, A.; Sil, P. C. *Food Chem. Toxicol.* **2014**, *71*, 106–115.
- (57) Aaroön Emmanuel, G.-E.; Claudia Lisset, C.-N.; Fermin Paul, P.-M.; Genaro Gabriel, O.; Fernando, J.-J.; Ana Rosa, R.-S. *Toxicol. Mech. Methods* **2015**, *25*, 166–175.
- (58) Worthington, K. L. S.; Adamcakova-Dodd, A.; Wongrakpanich, A.; Mudunkotuwa, I. A.; Mapuskar, K. A.; Joshi, V. B.; Allan Guymon, C.; Spitz, D. R.; Grassian, V. H.; Thorne, P. S.; Salem, A. K. *Nanotechnology* **2013**, *24*, 395101.
- (59) Shukla, S.; Jadaun, A.; Arora, V.; Sinha, R. K.; Biyani, N.; Jain, V. K. *Toxicol. Reports* **2015**, *2*, 27–39.
- (60) Yu, M.; Huang, S.; Yu, K. J.; Clyne, A. M. *Int. J. Mol. Sci.* **2012**, *13*, 5554–5570.
- (61) Stevanović, M.; Bračko, I.; Milenković, M.; Filipović, N.; Nunić, J.; Filipič, M.; Uskoković, D. P. *Acta Biomater.* **2014**, *10*, 151–162.
- (62) Nie, Z.; Liu, K. J.; Zhong, C.-J.; Wang, L.-F.; Yang, Y.; Tian, Q.; Liu, Y. *Free Radic. Biol. Med.* **2007**, *43*, 1243–1254.
- (63) Du, L.; Miao, X.; Jiang, Y.; Jia, H.; Tian, Q.; Shen, J.; Liu, Y. *Nanotoxicology* **2013**,

7, 294–300.

- (64) Du, L.; Suo, S.; Wang, G.; Jia, H.; Liu, K. J.; Zhao, B.; Liu, Y. *Chem. - A Eur. J.* **2013**, *19*, 1281–1287.
- (65) Viglianisi, C.; Di Pilla, V.; Menichetti, S.; Rotello, V. M.; Candiani, G.; Malloggi, C.; Amorati, R. *Chem. - A Eur. J.* **2014**, *20*, 6857–6860.
- (66) Pham-Huy, L. A.; He, H.; Pham-Huy, C. *Int. J. Biomed. Sci.* **2008**, *4*, 89–96.
- (67) Firuzi, O.; Miri, R.; Tavakkoli, M.; Saso, L. *Curr. Med. Chem.* **2011**, *18*, 3871–3888.
- (68) Hollman, P. C. H.; Van Trijp, J. M. P.; Buysman, M. N. C. P.; Martijn, M. S.; Mengelers, M. J. B.; De Vries, J. H. M.; Katan, M. B. *FEBS Lett.* **1997**, *418*, 152–156.
- (69) Wachtel-Galor, S.; Siu, P. M.; Benzie, I. F. F. In *Aging: Oxidative Stress and Dietary Antioxidants*; Preedy, V. R., Ed.; Academi Press: Oxford, 2014; pp 81–91.
- (70) Cerecetto, H.; Lopez, G. *Mini-Reviews Med. Chem.* **2007**, *7*, 315–338.
- (71) Chichirau, A.; Flueraru, M.; Chepelev, L. L.; Wright, J. S.; Willmore, W. G.; Durst, T.; Hussain, H. H.; Charron, M. *Free Radic. Biol. Med.* **2005**, *38*, 344–355.
- (72) Singh, D. K.; Jagannathan, R.; Khandelwal, P.; Abraham, P. M.; Poddar, P. *Nanoscale* **2013**, *5*, 1882–1893.
- (73) Wu, T.-H.; Yen, F.-L.; Lin, L.-T.; Tsai, T.-R.; Lin, C.-C.; Cham, T.-M. *Int. J. Pharm.* **2008**, *346*, 160–168.
- (74) Ahmad, N.; Umar, S.; Ashafaq, M.; Akhtar, M.; Iqbal, Z.; Samin, A.; Ahmad, J. F. *Protoplasma* **2013**, *250*, 1327–1338.
- (75) Du, L.; Chen, C.; Liu, Y. *Free Radic. Biol. Med.* **2014**, *48*, 1061–1069.
- (76) Mathew, A.; Fukuda, T.; Nagaoka, Y.; Hasumura, T.; Morimoto, H.; Yoshida, Y.; Maekawa, T.; Venugopal, K.; Kumar, D. S. *PLoS One* **2012**, *7*, e32616.
- (77) Doggui, S.; Kaur Sahni, J.; Arseneault, M.; Dao, L.; Ramassamy, C. *J. Alzheimer's Dis.* **2012**, *30*, 377–392.
- (78) Sonaje, K.; Italia, J. L.; Sharma, G.; Bhardwaj, V.; Tikoo, K.; Ravi Kumar, M. N. V. *Pharm. Res.* **2007**, *24*, 899–908.
- (79) Lu, X.; Xu, H.; Sun, B.; Zhu, Z.; Zheng, D.; Li, X. *Mol. Pharm.* **2013**, *10*, 2045–2053.
- (80) Al Shaal, L.; Shegokar, R.; Müller, R. H. *Int. J. Pharm.* **2011**, *420*, 133–140.
- (81) Zhou, L.; Chen, M.; Tian, L.; Guan, Y.; Zhang, Y. *ACS Appl. Mater. Interfaces* **2013**, *5*, 3541–3548.

- (82) Ing, H.; An, C.; SUn, Y.; Hou, Z.; Hong, Y.; Hu, B.; Zeng, X. *J. Agric. Food Chem.* **2008**, *56*, 7451–7458.
- (83) Peres, I.; Rocha, S.; Gomes, J.; Morais, S.; Pereira, M. C.; Coelho, M. *Carbohydr. Polym.* **2011**, *86*, 147–153.
- (84) Huang, S.-J.; Sun, S.-L.; Chiu, C.-C.; Wang, L.-F. *J. Biomater. Sci. Polym. Ed.* **2013**, *24*, 315–329.
- (85) Han, L.; Du, L.; Kumar, A.; Jia, H.-Y.; Liang, X.-J.; Tian, Q.; Nie, G.-J.; Liu, Y. *Biomaterials* **2012**, *33*, 8517–8528.
- (86) Behl, G.; Sharma, M.; Sikka, M.; Dahiya, S.; Chhikara, A.; Chopra, M. *J. Biomater. Sci. Polym. Ed.* **2013**, *24*, 865–881.
- (87) Pattni, B. S.; Chupin, V. V.; Torchilin, V. P. *Chem. Rev.* **2015**, *115*, 10938–10966.
- (88) Karewicz, A.; Bielska, D.; Gzyl-Malcher, B.; Kepczynski, M.; Lach, R.; Nowakowska, M. *Colloids Surfaces B Biointerfaces* **2011**, *88*, 231–239.
- (89) Takahashi, M.; Uechi, S.; Takara, K.; Asikin, Y.; Wada, K. *J. Agric. Food Chem.* **2009**, *57*, 9141–9146.
- (90) Rashidinejad, A.; Birch, E. J.; Sun-Waterhouse, D.; Everett, D. W. *Food Chem.* **2014**, *156*, 176–183.
- (91) Chen, Y.-P.; Chen, C.-T.; Hung, Y.; Chou, C.-M.; Liu, T.-P.; Liang, M.-R.; Chen, C.-T.; Mou, C.-Y. *J. Am. Chem. Soc.* **2013**, *135*, 1516–1523.
- (92) Shaji, J.; Varkey, D. *J. Pharm. Investig.* **2013**, *43*, 405–416.
- (93) Gao, X.; Hu, G.; Qian, Z.; Ding, Y.; Zhang, S.; Wang, D.; Yang, M. *Polymer (Guildf)*. **2007**, *48* (25), 7309–7315.
- (94) Deligiannakis, Y.; Sotiriou, G. A.; Pratsinis, S. E. *ACS Appl. Mater. Interfaces* **2012**, *4*, 6609–6617.
- (95) Yang, X. C.; Samanta, B.; Agasti, S. S.; Jeong, Y.; Zhu, Z. J.; Rana, S.; Miranda, O. R.; Rotello, V. M. *Angew. Chemie - Int. Ed.* **2011**, *50*, 477–481.
- (96) Kim, C. K.; Ghosh, P.; Pagliuca, C.; Zhu, Z.-J.; Menichetti, S.; Rotello, V. M. *J. Am. Chem. Soc.* **2009**, *131*, 1360–1361.
- (97) Bajaj, A.; Miranda, O. R.; Kim, I.-B.; Phillips, R. L.; Jerry, D. J.; Bunz, U. H. F.; Rotello, V. M. *Proc. Nail. Acad. Sci.* **2009**, *106*, 10912–10916.
- (98) Dykman, L.; Khlebtsov, N. *Chem. Soc. Rev.* **2012**, *41*, 2256–2282.
- (99) Daniel, M.-C.; Astruc, D. *Chem. Rev.* **2004**, *104*, 293–346.
- (100) Tiwari, P. M.; Vig, K.; Dennis, V. A.; Singh, S. R. *Nanomaterials* **2011**, *1*, 31–63.

- (101) Yeh, Y.-C.; Creran, B.; Rotello, V. M. *Nanoscale* **2012**, *4*, 1871–1880.
- (102) Fratoddi, I.; Venditti, I.; Cametti, C.; Russo, M. V. *Nano Res.* **2015**, *8*, 1771–1799.
- (103) Fard, J. K.; Jafari, S.; Eghbal, M. A. *Adv. Pharm. Bull.* **2015**, *5*, 447–454.
- (104) Kim, S. T.; Saha, K.; Kim, C.; Rotello, V. M. *Acc. Chem. Res.* **2013**, *46*, 681–691.
- (105) Khlebtsov, N.; Dykman, L. *Chem. Soc. Rev.* **2011**, *40*, 1647–1671.
- (106) Brust, M.; Walker, M.; Bethell, D.; Schiffrin, D. J.; Whyman, R. *J. Chem. Soc. Chem. Commun.* **1994**, 801–802.
- (107) Brust, M.; Fink, J.; Bethell, D.; Schiffrin, D. J.; Kiely, C. *J. Chem. Soc. Chem. Commun.* **1995**, 1655–1656.
- (108) Giersig, M.; Mulvaney, P. *Langmuir* **1993**, *9*, 3408–3413.
- (109) Seo, D.; Song, H. In *Gold Nanoparticles for Physics, Chemistry and Biology*; Louis, C., Pluchery, O., Eds.; Imperial College Press: London (UK), 2012; pp 103–138.
- (110) Mout, R.; Moyano, D. F.; Rana, S.; Rotello, V. M. *Chem. Soc. Rev.* **2012**, *41*, 2539–2544.
- (111) Devid, E. J.; Martinho, P. N.; Kamalakar, M. V.; Prendergast, Ú.; Kübel, C.; Lemma, T.; Dayen, J.; Keyes, T. E.; Doudin, B.; Ruben, M.; Molen, S. J. Van Der. *Beilstein J. Nanotechnol.* **2014**, *5*, 1664–1674.
- (112) Lei, H.; Atkinson, J. *J. Org. Chem.* **2000**, *65*, 2560–2567.
- (113) Peng, H. M.; Webster, R. D. *J. Org. Chem.* **2008**, *73*, 2169–2175.
- (114) Bianchini, R.; Catelani, G.; Cecconi, R.; D'Andrea, F.; Guazzelli, L.; Isaad, J.; Rolla, M. *European J. Org. Chem.* **2008**, 444–454.
- (115) Boksanyi, L.; Liardon, O.; sz. Kovats, E. *Helv. Chim. Acta* **1976**, *59*, 717–727.
- (116) Lee, B. Y.; Oh, J. S. *J. Organo* **1998**, *552*, 313–317.
- (117) Cho, H. J.; Park, S. J.; Kim, J. W.; Lee, S.-M.; Lee, Y.-S. *Synlett* **2013**, *24*, 20–23.
- (118) Belser, T.; Stöhr, M.; Pfaltz, A. *J. Am. Chem. Soc.* **2005**, *127*, 8720–8731.
- (119) Kalgutkar, A. S.; Crews, B. C.; Marnett, L. J. *J. Med. Chem.* **1996**, *39*, 1692–1703.
- (120) Khoukhi, M.; Vaultier, M.; Benalil, A.; Carboni, B. *Synthesis (Stuttg.)* **1996**, 483–487.
- (121) Rudzinski, D. M.; Kelly, C. B.; Leadbeater, N. E. *Chem. Commun.* **2012**, *48*, 9610–9612.

- (122) Nahm, S.; Weinreb, S. M. *Tetrahedron Lett.* **1981**, *22*, 3815–3818.
- (123) Cho, B. H.; Kim, J. H.; Jeon, H. B.; Kim, K. S. *Tetrahedron* **2005**, *61*, 4341–4346.
- (124) Kulkarni, M. G.; Thopate, S. R. *Tetrahedron* **1996**, *52*, 1293–1302.
- (125) Quéléver, G.; Kachidian, P.; Melon, C.; Garino, C.; Laras, Y.; Pietrancosta, N.; Sheha, M.; Kraus, J. L. *Org. Biomol. Chem.* **2005**, *3*, 2450–2457.
- (126) Tarascou, I.; Barathieu, K.; André, Y.; Pianet, I.; Dufourc, E. J.; Fouquet, E. *European J. Org. Chem.* **2006**, 5367–5377.
- (127) Miyamoto, K.; Sei, Y.; Yamaguchi, K.; Ochiai, M. *J. Am. Chem. Soc.* **2009**, *131*, 1382–1383.
- (128) Liu, Y.; Cornella, J.; Martin, R. *J. Am. Chem. Soc.* **2014**, *136*, 11212–11215.
- (129) Mizuno, M.; Kanai, M.; Iida, A.; Tomioka, K. *Tetrahedron* **1996**, *53*, 10699–10708.
- (130) Banerjee, D. R.; Dutta, D.; Saha, B.; Bhattacharyya, S.; Senapati, K.; Das, A. K.; Basak, A. *Org. Biomol. Chem.* **2014**, *12*, 73–85.
- (131) Park, K. D.; Cho, S. J. *Eur. J. Med. Chem.* **2010**, *45*, 1028–1033.
- (132) Fukuhara, K.; Nakanishi, I.; Kansui, H.; Sugiyama, E.; Kimura, M.; Shimada, T.; Urano, S.; Yamaguchi, K.; Miyata, N. *J. Am. Chem. Soc.* **2002**, *124*, 5952–5953.
- (133) Hakamata, W.; Nakanishi, I.; Masuda, Y.; Shimizu, T.; Higuchi, H.; Nakamura, Y.; Saito, S.; Urano, S.; Oku, T.; Ozawa, T.; Ikota, N.; Miyata, N.; Okuda, H.; Fukuhara, K. *J. Am. Chem. Soc.* **2006**, *128*, 6524–6525.
- (134) Laurent, S.; Forge, D.; Port, M.; Roch, A.; Robic, C.; Vander Elst, L.; Muller, R. N. *Chem. Rev.* **2008**, *108*, 2064–2110.
- (135) Wu, W.; He, Q.; Jiang, C. *Nanoscale Res. Lett.* **2008**, *3*, 397–415.
- (136) Yee, C.; Kataby, G.; Ulman, A.; Prozorov, T.; White, H.; King, A.; Rafailovich, M.; Sokolov, J.; Gedanken, A. *Langmuir* **1999**, *15*, 7111–7115.
- (137) Sahoo, Y.; Pizem, H.; Fried, T.; Golodnitsky, D.; Burstein, L.; Sukenik, C. N.; Markovich, G. *Langmuir* **2001**, *17*, 7907–7911.
- (138) Mohapatra, S.; Pramanik, P. *Colloids an Surfaces A Physiochem. Eng. Asp.* **2009**, *339*, 35–42.
- (139) Benbenishty-Shamir, H.; Gilert, R.; Gotman, I.; Gutmanas, E. Y.; Sukenik, C. N. *Langmuir* **2011**, *27*, 12082–12089.
- (140) Wilén, C.-E.; Luttkhedde, H.; Hjertberg, T.; Näsman, J. H. *Macromolecules* **1996**, *29* (27), 8569–8575.

- (141) Xie, J.; Xu, C.; Xu, Z.; Hou, Y.; Young, K. L.; Wang, S. X.; Pourmand, N.; Sun, S. *Chem. Mater.* **2006**, *18*, 5401–5403.
- (142) Xie, J.; Xu, C.; Kohler, N.; Hou, Y.; Sun, S. *Adv. Mater.* **2007**, *19*, 3163–3166.
- (143) Lee, Y.; Lee, H.; Kim, Y. B.; Kim, J.; Hyeon, T.; Park, H.; Messersmith, P. B.; Park, T. G. *Adv. Mater.* **2008**, *20*, 4154–4157.
- (144) Chanana, M.; Jahn, S.; Georgieva, R.; Lu, J.-F.; Baumler, H.; Wang, D. *Chem. Mater.* **2009**, *21*, 1906–1914.
- (145) Basti, H.; Ben Tahar, L.; Smiri, L. S.; Herbst, F.; Vaulay, M.-J.; Chau, F.; Ammar, S.; Benderbous, S. *J. Colloid Interface Sci.* **2010**, *341*, 248–254.
- (146) Stefaniu, C.; Chanana, M.; Wang, D.; Novikov, D. V.; Brezesinski, G.; Mohwald, H. *Langmuir* **2011**, *27*, 1192–1199.
- (147) Dalaigh, C. Ó.; Corr, S. A.; Gun'ko, Y.; Connon, S. J. *Angew. Chemie - Int. Ed.* **2007**, *46*, 4329–4332.
- (148) Campelj, S.; Makovec, D.; Drogenik, M. *J. Magn. Magn. Mater.* **2009**, *321*, 1346–1350.
- (149) Kralj, S.; Drogenik, M.; Makovec, D. *J. Nanoparticles Res.* **2011**, *13*, 2829–2841.
- (150) Smolensky, E. D.; Park, H.-Y. E.; Berquó, T. S.; Pierre, V. C. *Contrast Media Mol. Imaging* **2011**, *6*, 189–199.
- (151) Yuen, A. K. L.; Hutton, G. A.; Masters, A. F.; Maschmeyer, T. *Dalt. Trans.* **2012**, *41*, 2545–2559.
- (152) Lee, H.; Dellatore, S. M.; Miller, W. M.; Messersmith, P. B. *Science (80-. )*. **2007**, *318*, 426–430.
- (153) Dardonville, C.; Fernandez-Fernandez, C.; Gibbons, S.-L.; Ryan, G. J.; Jagerovic, N.; Gabilondo, A. M.; Meana, J. J.; Callado, L. F. *Bioorganic Med. Chem.* **2006**, *14*, 6570–6580.
- (154) Luo, Y.; Sun, K.; Li, L.; Gao, L.; Wang, G.; Qu, Y.; Xiang, L.; Chen, L.; Hu, Y.; Qi, J. *ChemMedChem* **2011**, *6*, 1986–1989.
- (155) Dodo, K.; Minato, T.; Hashimoto, Y. *Chem. Pharm. Bull.* **2009**, *57*, 190–194.
- (156) Zhang, Q.; Raheem, K. S.; Botting, N. P.; Slawin, A. M. Z.; Kay, C. D.; O'Hagan, D. *Tetrahedron* **2012**, *68*, 4194–4201.
- (157) Xu, C.; Xu, K.; Gu, H.; Zheng, R.; Liu, H.; Zhang, X.; Guo, Z.; Xu, B. *J. Am. Chem. Soc.* **2004**, *126*, 9938–9939.
- (158) Boley, J.; Lalatonne, Y.; Haddad, O.; Letourneur, D.; Soussan, M.; Péerard-Viret, J.; Motte, L. *Nanoscale* **2013**, *5*, 11478–11489.

- (159) Gulley-Stahl, H.; Hogan II, P. A.; Schmidt, W. L.; Wall, S. J.; Buhrlage, A.; Bullen, H. A. *Environ. Sci. Technol.* **2010**, *44*, 4116–4121.
- (160) Chen, Y. H. *J. Alloys Compd.* **2013**, *553*, 194–198.
- (161) *Advances in Magnetic Materials: Processing, Properties and Performance*; Zhang, S., Zhao, D., Eds.; CRC Press: Boca Raton (FL, USA), 2017.
- (162) Grass, R. N.; Athanassiou, E. K.; Stark, W. J. *Angew. Chemie - Int. Ed.* **2007**, *46*, 4909–4912.
- (163) <http://www.turbobeads.com/science>.
- (164) Himo, F.; Lovell, T.; Hilgraf, R.; Rostovtsev, V. V.; Noodleman, L.; Sharpless, K. B.; Fokin, V. V. *J. Am. Chem. Soc.* **2005**, *127*, 210–216.
- (165) <http://www.organic-chemistry.org/namedreactions/click-chemistry.shtm>.
- (166) Lethu, S.; Matsuoka, S.; Murata, M. *Org. Lett.* **2014**, *16*, 844–847.
- (167) Starck, J.-P.; Nakatani, Y.; Ourisson, G. *Tetrahedron* **1995**, *51*, 2629–2638.
- (168) Grée, D.; Grée, R. *Tetrahedron Lett.* **2010**, *51*, 2218–2221.
- (169) Mansfield, E.; Tyner, K. M.; Poling, C. M.; Blacklock, J. L. *Anal. Chem.* **2014**, *86*, 1478–1484.
- (170) Shabany, H.; Pajewski, R.; Abel, E.; Mukhopadhyay, A.; Gokel, G. W. *J. Heterocycl. Chem.* **2001**, *38*, 1393–1400.
- (171) Kitano, Y.; Nogata, Y.; Matsumura, K.; Yoshimura, E.; Chiba, K.; Tada, M.; Sakaguchi, I. *Tetrahedron* **2005**, *61*, 9969–9973.
- (172) Bhattacharyya, S.; Pathak, U.; Mathur, S.; Vishnoi, S.; Jain, R. *RSC Adv.* **2014**, *4*, 18229–18233.
- (173) Matsubara, H.; Suzuki, S.; Hirano, S. *Org. Biomol. Chem.* **2015**, *13*, 4686–4692.
- (174) Aldrich, S. Solvent Stabilizer Systems.
- (175) *EH&S Guidelines for Peroxide Forming Chemicals*; 2011.
- (176) <http://www.mnnet.com/Testpapers/QUANTOFIXteststrips/QUANTOFIXPeroxid25/tabid/10334/language/en-US/Default.aspx>.

## 6. Conclusions

The aim of my PhD project is the design and synthesis of new antioxidant systems able to improve their effectiveness in terms of radical trapping capacity, bio-availability and polymer stabilization. A common strategy to enhance the antioxidant activity is the chemical modification of known natural or synthetic antioxidants with the purpose to enhance the stability of their radical counterparts and/or the improvement of their physical properties. Recently, our research group has investigated the enhanced antioxidant activity of sulfur-substituted phenolic antioxidants bearing the sulfur atom *ortho* to the phenolic OH and inserted in a benzoxathiine heterocyclic system of type **1**. Following up such research, we discovered that compounds with the sulfur atom part of an aromatic five-membered ring, as in benzo[*b*]thiophenes **2**, exhibit an excellent antioxidant activity in terms of  $k_{inh}$  (rate constant of the reaction with  $ROO^{\bullet}$ ). In particular **2** had a  $k_{inh}$ , up to three times higher than those of the corresponding dihydrobenzo[*b*]thiophenes **3**. This behavior was unexpected considering the related benzo[*b*]furanol **4** and dihydrobenzo[*b*]furanol **5**: the former exhibits a considerably lower antioxidant activity than its dihydro- analogue (Figure 1). In the latter compounds, this was justified considering that aromatization reduces the electron-donating ability of the endocyclic O atom hence its ability in stabilizing the phenoxyl radical.

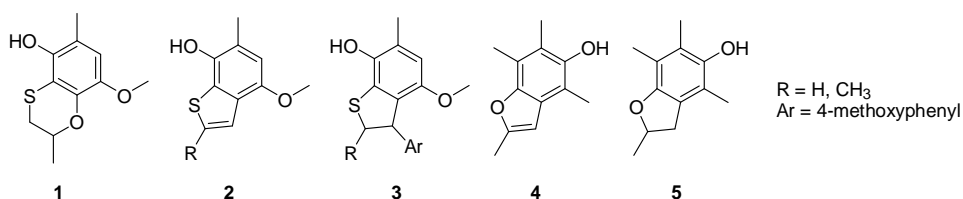
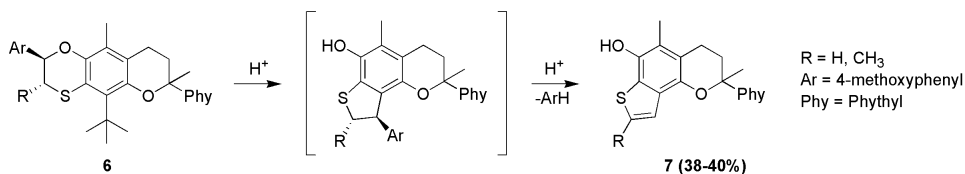


**Figure 1**

In the sulfur containing compounds, we hypothesized that this unforeseen behavior is related to the *ortho* position between sulfur and oxygen atoms. Indeed, analysis of the electrostatic potential surfaces showed the presence of a  $\sigma$ -hole on the S atom that points toward the phenoxyl oxygen, allowing the stabilization of the radical intermediate thanks to a non-covalent  $O\cdots S$  interaction. Moreover, in thiophenes, the  $\sigma$ -hole increases with aromatization, explaining the enhanced antioxidant activity of benzo[*b*]thiophenes compared to dihydro-analogues. We explored the insertion of the benzo[*b*]thiophene structural motif in the skeleton of  $\alpha$ -tocopherol, the main and most potent component of vitamin E. Using properly designed benzoxathiine derivatives **6**, desired benzo[*b*]thiophenes tocopherols **7** were obtained in an acid-mediated one-pot procedure consisting of a cascade of five electrophilic transformations that pass through a benzoxathiine-dihydrothiophene rearrangement (Scheme 1).

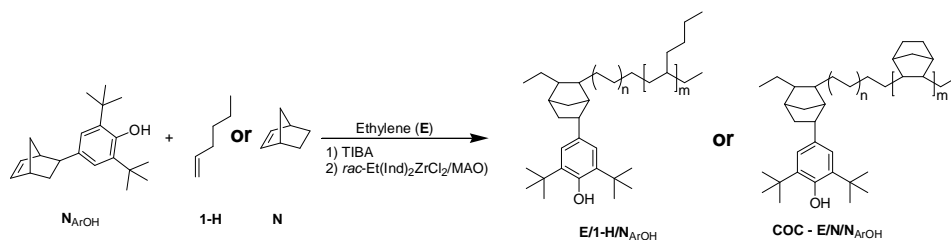




### Scheme 1

As expected, derivatives **7** showed an antioxidant activity higher than that of  $\alpha$ -tocopherol (up to three times) and dihydrobenzo[*b*]thiophenes and preserved the ability of  $\alpha$ -tocopherol of being recognized by the protein  $\alpha$ -TTP.

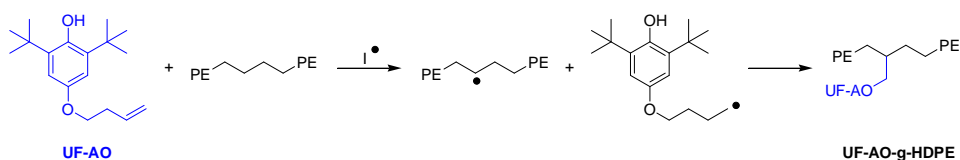
Another important research branch are polymeric antioxidants for the stabilization of synthetic polyolefins. An antioxidant derivative bearing a norbornene polymerizable function ( $N_{ArOH}$ ) was used as a comonomer in the terpolymerization with ethylene and 1-hexene (or norbornene), achieving an effective terpolymeric stabilizer. Since antioxidants efficiency depends not only on their chemical effectiveness but also on their miscibility with the polymeric matrix, the choice of the third comonomer is very important to provide macromolecular additives very similar to commercial polymeric matrices. In collaboration with the CNR-ISMAL institutions of Milano and Genova we prepared, characterized and tested the antioxidant performance of these ethylene-based terpolymers (Scheme 2).



### Scheme 2

The strong similarity of the microstructure of the terpolymeric additive with that of the polyethylene copolymer led to an excellent dispersion and a noticeable improvement of the protection capability using tiny amount of the antioxidant units.

During the third year of my PhD I spent a period of research in the group of professor S. Al-Malaika at the Aston University, Birmingham (UK), where we explored the preparation of polymer-bound antioxidants through the so-called reactive processing method. We used an antioxidant derivative bearing a terminal olefin function (**UF-AO**) that has been designed and prepared in Florence and used for a grafting reaction on HDPE catalyzed by a radical initiator (**I**) during a customary extrusion process (Scheme 3).



Scheme 3

The actual grafting of the antioxidant on the polymer was proved by evaluating the persistence of the stabilizing activity after Soxhlet extraction of the processed polymer using a solvent like dichloromethane able to extract all the unbound antioxidant. Thermal ageing of **UF-AO-g-HDPE** was done in order to evaluate its stabilizing performance compared with the same polymer simply mixed with a reference antioxidant, Irganox1076.

Immobilization of biologically active substances on macromolecular or supramolecular systems is one of the most important and rapidly developing trends in modern medicinal chemistry. Over the last few years nanoparticles (NPs) are increasingly being used for lots of biomedical applications because they act as very efficient support materials for the immobilization of biologically active compounds. Exploiting their amazing properties, we have paid our attention on the preparation of antioxidant decorated NPs with the aim to enhance the radical scavenger activity of capped ligands. Moreover, because ROS formation and oxidative stress induction are well-known drawbacks of NPs in their use in nanomedicine, antioxidant functionalization is a logical way to suppress their toxicity. During my PhD we prepared some antioxidant derivatives bearing an appropriate functionalization depending on the surface reactivity of each different metallic NP. Trolox, a hydrophilic analogue of  $\alpha$ -tocopherol, was functionalized with two linkers bearing a disulfide (**8**) and a catechol (**9**) respectively in order to exploit the affinity of gold NPs for thiols and of maghemite ( $\gamma$ - $\text{Fe}_2\text{O}_3$ ) NPs for catechols. Moreover, a disulfide analogue (**10**) with (+)-Catechin as antioxidant was prepared (Figure 2).

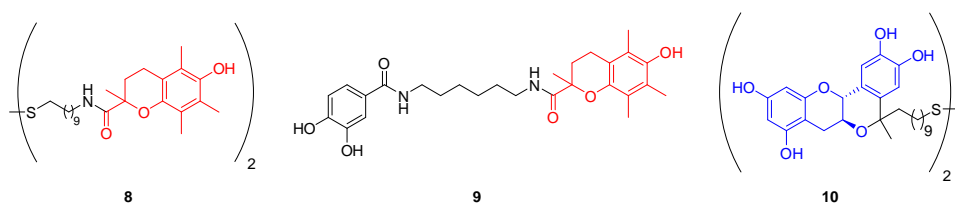
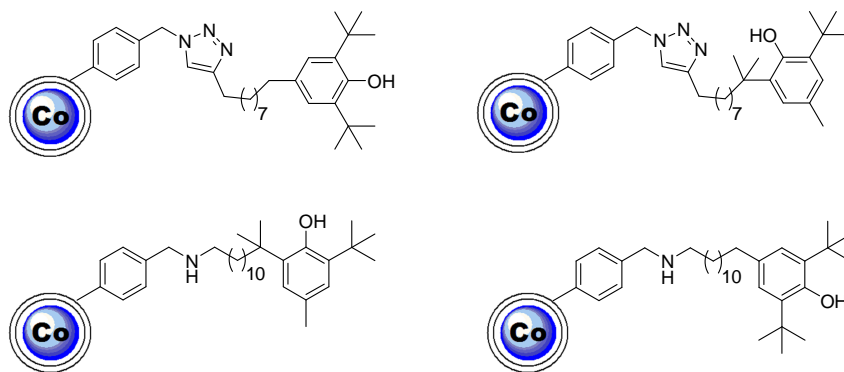


Figure 2

Four derivatives of BHT bearing a terminal alkyne and a terminal amine, respectively, were also prepared and used for the functionalization of cobalt nanoparticles (Figure 3).



**Figure 3**

These nanostructured systems proved to have a certain antioxidant activity, as demonstrated by the measurement of their reaction with alkylperoxyl radicals, and were tested as nanostructured antioxidant additives for the delay of hydroperoxides formation in ether solvents.